# THE ROLE OF CANNABINOID RECEPTORS IN THE DEVELOPMENT AND PROGRESSION OF DIABETIC NEUROPATHY

**Fan Zhang**

Thesis submitted in partial fulfilment of the requirements of
Napier University for the degree of Doctor of Philosophy

**December 2007**

## ABSTRACT

Diabetic neuropathy is characterised by neurodegeneration of peripheral sensory nerves, resulting in acute pain, sensory loss, and an increased risk of limb amputation. A clearer understanding of the mechanisms underlying the development and progression of diabetic neuropathy are likely to indicate new directions for the treatment of this complication of diabetes. A neuronal target for investigation is the endocannabinoid system. The aims of this project were to investigate whether the expression of cannabinoid ($CB_1$) receptors was decreased under hyperglycaemic conditions, which may contribute to the pathogenesis and progression of diabetic neuropathy, and whether altered $CB_1$ expression led to a decrease in $CB_1$ signalling.

In a rat pheochromocytoma (PC12) cell line *in vitro* model of diabetic neuropathy, we found a reduction in total neurite length induced by nerve growth factor (50ng/ml) at 20-50mM glucose on day 6 ($P<0.01$ versus 5.5mM; n=70-79 from 6 independent cultures). This effect was due to raised glucose levels, used to mimic diabetic conditions, rather than any hyperosmolality effects since mannitol (50mM) gave similar results to that of the physiological 5.5mM glucose control ($P=0.79$). High glucose was associated with increased oxidative stress and a dose-dependent increase in IL-6 production ($P<0.05$).

The expression of $CB_1$ receptors significantly decreased in PC12 cells cultured in hyperglycaemic conditions ($P<0.05$; n=5 for each) which corroborated with the results from an *in vivo* model showing a similar decline in $CB_1$ receptors in dorsal root ganglion neurons from diabetic rats ($P<0.01$; n=3 for immunohistochemistry, and n=5 for Western blot). Cell viability assays conducted in parallel on day 6 confirmed that the total cell numbers were not significantly different between the various glucose concentrations ($P=0.50$; n=6). These results suggest that high glucose concentrations are associated with decreased expression of $CB_1$ receptors in nerve cells.

We assessed $CB_1$ receptor function by measuring the inhibitory effect of the $CB_1$ receptor agonist HU210 on capsaicin-induced calcium influx in PC12 cells cultured in physiological and high glucose conditions. In fluo-4-loaded cells, capsaicin evoked an increase in fluorescence ($\approx[Ca^{2+}]_i$) in a concentration-dependent manner. Application of the $CB_1$ agonist HU210 (1μM) significantly inhibited capsaicin-induced calcium influx ($P<0.01$), and this inhibitory effect of HU210 was reversed by co-application of the $CB_1$ antagonist AM251 (1μM) but not the $CB_2$ receptor antagonist AM630 (1μM). At concentrations of HU210 below 1μM we observed a blunted inhibition of capsaicin-evoked calcium influx in cells cultured in high glucose. However, at concentrations ≥1μM HU210, the function of the $CB_1$ receptor was preserved, as evidenced by a similar degree of inhibition of capsaicin-evoked calcium influx in 5.5 and 50mM glucose conditions (61% versus 59%, respectively, n=30-50, from four independent cultures).

The synthetic $CB_1$ agonist, HU210 (0.03-30μM), was used in order to investigate $CB_1$ receptor-mediated 'neurite rescue' in PC12 cells. Addition of HU210 (0.03-3μM) had no significant effect on the total neurite length in PC12 cells cultured in 5.5mM glucose ($P=0.168$ versus the control/vehicle; n=148-220) while an increased total neurite length was found in cells cultured in 50mM glucose in a concentration-dependent manner. The HU210 (1μM)-mediated rescue of neurite outgrowth could be blocked by AM251 (1μM) ($P<0.05$) but not by AM630 (1μM), confirming the role of $CB_1$ receptors (n=131-208). In addition, HU210 significantly reduced high glucose-induced oxidative stress in PC12 cells via a $CB_1$-independent mechanism.

These results suggest that high glucose concentrations are associated with decreased expression, but preserved function of $CB_1$ receptors in nerve cells. Given the neuroprotective effect of cannabinoids, $CB_1$ receptors may be an appropriate therapeutic target in preventing the neurodegenerative process in diabetes.

## DECLARATION

I hereby declare that this submission is my own work and that, to the best of my knowledge and belief, it contains no material previously published or written by another person nor material which has been accepted for the award of any other degree or diploma of the university or other institute of higher learning, except where due acknowledgment has been made in the text.

Fan Zhang

## ACKNOWLEDGEMENTS

First of all, I would like to offer my deep and sincere gratitude to my supervisor Dr Paula Smith for her guidance, patience and inspiration. Paula has supported me throughout my PhD study, and her wide knowledge and logical thinking have been of great value for me.

I would like to thank my second supervisor Professor Vicki Stone for her valuable advice, understanding and encouragement. I wish to thank Dr David Mincher for his review and advice for my transfer and progression reports.

A special thanks goes to all the people in the Biomedicine Research Group. They provided a welcome environment to make me never feel away from home. Dr David Brown's technical help certainly facilitated my project. A warm thanks goes to my colleagues, especially Min Zhao and Helina Johnston, for their listening and understanding at good and bad times.

I would also like to thank Dr Shuangsong Hong at Michigan University for providing DRG samples and the advice for immunostaining, Dr David Wyllie and Dr Keith Finlayson at The University of Edinburgh for the use of an osmometer and the donation of PC12 cells, and Dr Edward Rowan at University of Strathclyde for the training of DRG dissection.

Finally, I would like to express my deep thanks to my family and friends, in particular, my parents for their never-ending support. I owe my loving thanks to my wonderful husband Haoying for always being there for me and believing in me. Without his encouragement and support, it would have been impossible to finish this work.

The financial support of Napier University and the Overseas Research Students Award Scheme is acknowledged.

## CONTENTS

## LIST OF FIGURES

## LIST OF TABLES

## LIST OF ABBREVIATIONS

| | |
|---|---|
| 2-ME | 2-mercaptoethanol |
| AA-DA | N-arachidonyl-dopamine |
| ACEA | Arachidonyl-2-chloroethylamide |
| AEA | Arachidonoylethanolamide |
| AGE | Advanced glycosylation end product |
| ATP | Adenosine-5'-triphosphate |
| ATPase | Adenosine triphosphatase |
| BSA | Bovine serum albumin |
| $Ca^{2+}$ | Calcium |
| cAMP | Cyclic adenosine monophosphate |
| $CB_1$ | Cannabinoid receptor 1 |
| CBD | Cannabidiol |
| cDNA | Cyclic deoxyribonucleic acid |
| CGRP | Calcitonin gene related peptide |
| CNTF | Ciliary neurotrophic factor |
| Cpu | Caudate putamen |
| CPZ | Capsazepine |
| CT-3 | 1', 1'-dimethylheptyl-$\Delta^8$-tetrahydrocannabinol-11-oic acid |
| CTLA-4 | Cytotoxic T lymphocyte antigen 4 |
| $dH_2O$ | Distlled water |
| DMEM | Dulbecco's modified eagles medium |
| DMSO | Dimethyl sulfoxide |
| DNA | Deoxyribonucleic acid |
| dNTPs | Deoxynucleotides |
| DRG | Dorsal root ganglion |
| DTT | Dithiothreitol |
| ECL | Enhanced Chemiluminescence |
| EDHF | Endothelium-derived hyperpolarising factor |
| EDTA | Ethylenediaminetetraacetic acid |

| | |
|---|---|
| ELISA | Enzyme Linked-Immuno-Sorbent Assay |
| ERK | Extracellular signal-regulated kinase |
| FITC | Fluorescein isothiocyanate |
| G protein | Guanine nucleotide binding proteins |
| GAPDH | Glyceraldehyde-3-phosphate dehydrogenase |
| GDP | Guanosine diphosphate |
| GSH | L-γ-glutamyl-L-cysteinylglycine, reduced from |
| GSSG | L-γ-glutamyl-L-cysteinylglycine, oxidised form |
| GTP | Guanosine triphosphate exchange |
| $H_2O_2$ | Hydrogen peroxide |
| HEPEs | N-Cyclohexyl-2-aminoethanesulfonic acid |
| HLA | Human leukocyte antigen |
| HRP | Streptavidin-horseradish peroxidase conjugate |
| HU-210 | Dexanabinol, Sinnabidiol |
| IL-1 | Interleukin-1 |
| IL-11 | Interleukin-11 |
| IL-6 | Interleukin-6 |
| JAK | Janus kinases |
| JNK | c-Jun N-terminal kinase |
| $K^+$ | Potassium ion |
| LDH | Lactate dehydrogenase |
| LIF | Leukaemia inhibitory factor |
| MAPK | Mitogen activated protein kinase |
| mRNA | Messenger ribonucleic acid |
| MTT | 3-(4,5-dimethylthiazol-2-yl)-2,5-diphenyltetrazolium bromide |
| NADH | Nicotinamide adenine dinucleotide (reduced) |
| NADPH | Nicotinamide adenine dinucleotide phosphate (reduced) |
| NEM | N-ethylmaleimide |
| NGF | Nerve growth factor |
| NO | Nitric oxide |
| NOS | Nitric oxide synthase |

| | |
|---|---|
| O-1057 | $\Delta^8$-tetrahydrocannabinod hydrochloride |
| OM | Oncostatin M |
| OPT | O-phthalaldehyde |
| PBS | Phosphate buffered saline |
| PBST | PBS Tween |
| PC12 | Pheochromocytoma cells |
| $PGI_2$ | Prostacyclin |
| PKC | Protein kinase C |
| PPAR | Peroxisome proliferator-activated receptor alpha |
| RAGE | AGE receptors |
| RIPA | RadioImmuno precipitation assay |
| ROS | Reactive oxygen species |
| RPMI | Roswell Park Memorial Institute medium |
| RT-PCR | Reverse transcription-polymerase chain reaction |
| RTX | Resiniferatoxin |
| SDS PAGE | Sodium dodecyl sulphate polyacrylamide gel electrophoresis |
| STAT | Signal transducer and activators of transcription |
| STZ | Streptozotocin |
| TBE | Tris-Borate-EDTA |
| $\Delta^9$-THC | Delta 9-tetrahydrocannabinol |
| TMB | Tetramethylbenzidine |
| TNF-α | Tumour necrosis factor-α |
| UV | Ultraviolet-Visible |
| VMH | Entromedial hypothalamus |
| VR1/TRPV1 | Vanilloid receptor-1 or transient receptor potential vanilloid 1 |

# CHAPTER 1

# INTRODUCTION

## 1.1 Diabetes mellitus

### 1.1.1 The prevalence of diabetes

Over past few decades, diabetes has become one of the major public health burdens worldwide. The enormous economic growth in developing countries is associated with the greatest increase in the occurrence of diabetes (Amos, 1997; King and Rewers, 1993). Globally, the number of adults with diabetes is estimated to rise from 171 million in 2000 to 366 million in 2030, and men and woman are at equal risk of diabetes (Wild *et al.,* 2004). Surprisingly, in developing countries, the number of young people with diabetes (24-44 years) is estimated to increase to more than double in the next 30 years, which is the same as the growth rate in older people with diabetes (45-64 and >65 years). In contrast, in developed countries, the diabetic prevalence is mainly in people > 45 years old, and the majority of those with diabetes are >64 years of age (Wild *et al.*, 2004). In the UK, at least 2.3 million people have been diagnosed with diabetes (Diabetes UK website http://www.diabetes.org.uk).

### 1.1.2 Types of diabetes

Diabetes mellitus is a group of metabolic disorders characterized by a high blood glucose level (hyperglycemia), which results from absent or insufficient production of, or response to, insulin. Insulin is the principal hormone produced by beta cells in the pancreas in response to rising levels of glucose in the blood, as occurs after a meal. Under normal conditions, insulin regulates uptake of glucose from blood into cells by promoting the translocation of glucose transporter proteins (e.g. GLUT4) into the plasma membrane, which facilitate the diffusion of glucose into the insulin-responsive cells of muscle, liver and adipose tissue (Watson and Pessin, 2001). Once inside the cell, glucose

undergoes cellular respiration to produce ATP, or is converted to other useful molecules, such as glycogen. If the pancreas no longer produces insulin, or cells stop responding to insulin, the excessive glucose cannot be removed from blood, resulting in persistent hyperglycemia, poor protein synthesis and metabolic disarrangement (Mathur *et al.,* 2005).

There are two types of diabetes mellitus, type 1 and type 2. Type 1, also called juvenile diabetes mellitus, is most commonly diagnosed in childhood and adolescence with a fairly abrupt onset. In this type of diabetes, the pancreas produces little or no insulin because the insulin-producing β cells in the islet of Langerhans are destroyed by an autoimmune response. These patients may require several insulin injections during the day to keep blood glucose level normal (Campbell *et al.,* 2005). The genetic susceptibility is associated with human leukocyte antigen (HLA) on chromosome 6, shorter forms of a variable number tandem repeat of insulin gene on chromosome 11, and cytotoxic T lymphocyte antigen 4 (CTLA-4) (Ueda *et al.,* 2003). All these important susceptibility genes for type 1 diabetes facilitate the presentation of pro-insulin antigen to T cells and result in T cell activation (Gillespie, 2006). In addition, increasing environmental pressure is also identified to impact on genetic susceptibility for type 1 diabetes. For instance, virus infection could put infants at very high risk of type 1 diabetes, exposure to microbes and other pathogens in early life has been shown to promote innate immune response and development of atopic and autoimmune disorders (Gillespie, 2006).

Type 2 is the most common form of diabetes mellitus, typically affecting adults over 40 years. The symptoms are milder than that of type 1 because of its slow onset, so that type 2 may not be noticed for years in patients before diagnosis

(Votery *et al.,* 2005). This form of diabetes mellitus is characterized by 'insulin resistance' as cells respond inappropriately to the insulin produced, combined with reduced insulin secretion. The level of insulin receptors expressed on cell membranes is certainly related to the defective responsiveness of body tissue to insulin (Michael *et al.,* 2000, Trischitta *et al.,* 1997). Since insulin is still produced at the early stage, type 2 diabetes can be controlled by improving insulin sensitivity and reducing glucose production by the liver, using drugs such as thiazolidinediones and metformin (Bolen *et al.,* 2007). However, as a consequence of uncontrolled type 2 diabetes, insulin injection becomes necessary. Central obesity is a common cause of insulin resistance: 90% of type 2 diabetics have the problem of obesity (McTernan *et al.,* 2002). Although both type 1 and type 2 diabetes are partially inherited, those with type 2 family histories are believed to have a higher chance of developing type 2 diabetes (Stumvoll *et al.*, 2005).

## 1.2 Diabetic neuropathy

### 1.2.1 Types of diabetic neuropathy

Diabetic neuropathy is a common complication of diabetes, resulting from sustained hyperglycaemia. It virtually affects every type of neuron fibre in the body, including sensory, autonomic and motor neurons, and causes significant morbidity and mortality in diabetic patients (Duby *et al.,* 2004). A comprehensive collection of epidemiological studies reveals that diabetic neuropathy affects 50% of diabetic patients and occurs at same frequency in type 1 and type 2 diabetes; this percentage approaches 100% if subclinical non-symptomatic neuropathy is included (Vinik *et al.,* 2006).

Diabetic neuropathy is classified by the nerve fibre affected, and includes peripheral sensory neuropathy, autonomic neuropathy and focal neuropathy (Vinik, 2004; Duby *et al.*, 2004). Distal symmetrical sensory polyneuropathy is the most common form of diabetic neuropathy, affecting both large and small afferent nerve fibres. It is characterized by neurodegeneration of peripheral sensory nerve endings ("dying-back" of distal axons), which results in acute pain and eventual sensory loss, impairment of warm thermal perception, and attenuated skin blood flow in diabetic patients (Said *et al.,* 1983; Said, 2007). Sensory impairment can result in injurious tissue damage, for example to the sole of the foot, which, when coupled with peripheral vascular disease and reduced blood flow, creates an ulcer which easily becomes infected. Gangrenous foot ulcers are associated with a high risk of limb amputation (Jeffcoate and Harding, 2003). In the UK, more than 5000 people with diabetes have amputation per year and people with diabetes are 15% more likely to have amputation than those without diabetes (NHS Diabetes foot guide http://www.diabetes.nhs.uk/downloads/NDST_Diabetic_Foot_Guide.pdf).

Diabetic autonomic neuropathy is a serious and key cause of morbidity and mortality in diabetes. Cardiovascular autonomic neuropathy occurs in 15% of type 1 and 20% of type 2 diabetic patients (Vinik *et al.,* 2006). The mortality rate in diabetic patients with cardiovascular complications is 22% higher than those without cardiovascular complications in 10 years scope (Ziegler, 1999). Cardiovascular autonomic neuropathy affects both the sympathetic and parasympathetic innervation of the heart and coronary vessels, resulting in cardiovascular dysfunction, myocardial infarction, orthostatic hypotension and sudden death. In addition, diabetic autonomic dysfunction also affects the entire gastrointestinal and genitourinary system. The people with these two

types of autonomic neuropathy may suffer sever constipation, diarrhoea, faecal incontinence, sexual dysfunction and urinary incontinence, which significantly influence quality of life (Duby *et al.,* 2004).

Focal and multifocal neuropathy is less common compared to other forms of neuropathy in diabetic patients, and is usually seen in elderly people with type 2 diabetes (Vinik *et al.,* 2006). It is characterized by sensorimotor deficit in territories of one or several nerve trunks, roots and plexus, leaving the muscle weak or in pain. Diabetic focal neuropathy affects cranial, limb, truncal and proximal nerves, causing inability of focus, double vision, aching behind the eye, limit of mobility, paralysis and pain throughout the body (Said, 2007; Vinik *et al.,* 2006).

Diabetic neuropathy is associated with high risk factors for macrovascular and microvascular complications, such as poor metabolic control, dyslipidaemia, smoking, microalbuminuria and retinopathy, due to their physiological co-dependency. Blood vessels depend on neural regulation to maintain their functions, and neurons depend on blood vessels to obtain nutrients. Early in diabetic neuropathy, the balance between vasodilatation and vasoconstriction is altered in favour of the latter, resulting in decreased blood flow and increased vascular permeability. This is reflected by the vulnerable vascular endothelium and deficit of major vasodilators, nitric oxide (NO), endothelium-derived hyperpolarising factor (EDHF) and prostacyclin ($PGI_2$). Hyperglycaemia may also cause decreased neurotrophic support. Taken together, all these changes lead to hypoxia, reduced nerve blood flow and ischaemia in the nervous system, contributing to the progression of diabetic neuropathy (Cameron *et al.*, 2001; Brownlee, 2001).

### 1.2.2 Diabetic Neuropathy and Sensory Neurons

Among these diabetic complications, sensory neurons are likely to be involved first. Unfortunately, loss of sensory neurons may become irreversible at later stages of the complication. The early sign of sensory neuropathy is pain in the toes and in the fingers, which are innervated by the longest sensory nerves in the body; the longer the nerve axon, the more likely it, and its terminals, will be targeted by hyperglycemic insults. In addition, the damaged perikaryon (the cell body of a neuron) fails to supply structural components to the most distal terminals (Toth *et al.*, 2004).

Sensory nerves can be divided into several subpopulations based on their neurochemistry, anatomy, and physiology. The majority of small diameter unmyelinated C-fibres and thinly myelinated Aδ-fibres are nociceptive, and constitutively express the neuropeptides, calcitonin gene related peptide (CGRP) and substance P, as well as the nerve growth factor (NGF) receptors, trkA and p75 (Lawson, 2002). The cell bodies of these fibres are located in the dorsal root ganglion (DRG), with central terminals in laminae I and II of the superficial dorsal horn and peripheral terminals in tissues (e.g. muscle, joint and skin). In diabetic patients small fibre (C and Aδ) neuropathy is responsible for the early hyperalgesia (excessive sensitivity to pain caused by noxious stimuli) and allodynia (exaggerated pain caused by non-noxious stimuli), and the late hypoalgesia (decreased sensitivity to pain stimuli), impairment of warm thermal perception and skin blood flow. C-fibres are thought to be the initial class of nerves to be affected in diabetic neuropathy: a study in patients with type 2 diabetes found axon-reflex mediated vasodilatation to be impaired at an earlier stage of diabetes than autonomic nerve and endothelial dysfunction (Stansberry *et al.*, 1999).

### 1.2.3 Models of diabetic neuropathy

Intensive research has focused on studying the pathogenesis of diabetic neuropathy using *in vivo* models. Experimental diabetes is commonly induced by injecting adult rats or mice with the beta-cell toxins, alloxan or streptozotocin, to destroy the function of insulin production, thus creating a hyperglycaemic condition (Calcutt, 2004). In non-diabetic human, normal blood glucose levels are between 4 and 7mM before meals (fasting levels), and less than 10mM after meals. Diabetes is typically diagnosed when fasting blood glucose levels are 7mM or higher (www.netdoctors.co.uk). In contrast, the rat diabetic model showed a 5-fold elevation in plasma glucose compared to controls, and these levels would fluctuate throughout the animals' lives. Others have reported plasma glucose levels in the STZ-diabetic rat range from 25 - 50mM (mean 34.5 ± 3.05mM) compared to controls (5.91 ± 0.54mM) (Purves *et al.,* 2001).

The sustained blood glucose level eventually triggers the occurrence of peripheral neuropathy, which is expressed as hypersensitivity to painful or non-painful sensory stimuli (Cole, 2007). Behavioural tests are the most commonly used screening methods: e.g., measuring the time for withdrawal of a limb, such as the tail or a paw, from a noxious heat or a non-noxious light touch by von Frey filaments (Calcutt, 2004). A shorter latency in the diabetic models illustrates hyperalgesia or allodynia, which is manifest in diabetic patients. In these *in vivo* models of diabetic neuropathy, hyperglycaemia is demonstrated to slow nerve conduction velocity (Malone *et al.,* 1996), decrease axonal transport of structure protein (Jakobsen and Sidenius, 1980) and initiate neuronal apoptosis (Barber *et al.*, 1998; Russell and Feldman, 1999; Vincent *et al.*, 2002).

Numerous *in vitro* cell models have been previously used to study the cellular mechanisms involved in the pathophysiology of diabetes, such as cultured vascular endothelial cells (Baumgartner-Parzer *et al.;* 1995; Doyle *et al.*, 1997), fibroblasts (Reenstra *et al.*, 1999; Atkin *et al.*, 1996) and kidney cells (Ortiz *et al.,* 1997). In these cell models of diabetes, hyperglycemia is simulated by addition of glucose to the culture medium. Most notably, cultured DRG is one of few neuronal cell models which have been used to study the effect of hyperglycaemia on neuronal functions. Some studies have reported that hyperglycaemia (0-300mM above controls 25-30mM) reduces neurite extension in cultured rat DRG neurons which is correlated with increased oxidative stress and apoptosis (Russell and Feldman, 1999, Sotelo *et al.*, 1991; Vincent *et al.*, 2005 ). Human neuroblastoma SH-SY5Y cells have also been used as an *in vitro* model to test the effect of hyperglycaemia on nerve function. Li *et al.* (2003) reported that administration of insulin/C-peptide can significantly stimulate cell proliferation and prevent apoptosis in SH-SY5Y cells cultured in the presence of high glucose (100mM versus control 25mM) (Li *et al.,* 2003). Recently, the neural-crest derived pheochromocytoma cells (PC12) was established as an *in vitro* cell model of diabetic neuropathy by Lelkes and colleagues (Lelkes *et al.,* 2001). With the most similarity to primary neurons, undifferentiated PC12 cells proliferate like embryonic neurons. However, in the presence of nerve growth factor (NGF), the attached PC12 cells cease their proliferation and start extending neurite branches like adult neurons. In addition, the nature of neurotransmitter secretion such as catecholamines makes PC12 cells an ideal neuronal cell model to study neuronal differentiation and neurotransmitter release. In the study by Lelkes *et al.* (2001) the high glucose (25mM versus the control 5mM) treated PC12 cells reproduced some of the phenomena of diabetic neuropathy: impaired neurite extension, increased

oxidative stress, apoptosis and upregulated neurotransmitter release, which are all implicated in contributing to the pathogenesis of diabetic neuropathy.

### 1.2.4 Potential Mechanism of Diabetic Neuropathy

The pathogenesis of diabetic neuropathy is complex and involves multiple pathways (Skundric and Lisak, 2003). The oxidative stress resulting from hyperglycaemia is believed to be a major factor involved in the development and progression of macro- and micro-vascular complications associated with diabetes, including peripheral neuropathy (Feldman, 2003).

Oxidative stress occurs in a cell or tissue when antioxidants such as glutathione (GSH) fail to deplete excessive free radicals generated. Free radical species are normally produced in the body during metabolic activity, such as superoxide ($O_2^-$), hydrogen peroxide ($H_2O_2$) and nitric oxide (NO). These three reactive oxygen species (ROS) are essential for maintaining normal physiology. However, they are also believed to be the mediators of aging and cellular degeneration in diabetic and other diseased states by producing highly active singlet oxygen (O-), hydroxyl radicals (HO-), and peroxynitrite (ONOO-) (Lee *et al.*, 2003; Vincent *et al.*, 2004). The products of these ROS can damage protein, lipid and DNA, resulting in decreased biological functions including loss of energy metabolism, transport, cell signalling and other major functions. Accumulation of such injuries eventually leads to cell loss through necrotic or apoptotic pathways (Vincent *et al.,* 2004). For example, the individual $O_2^-$ and NO can attack iron-sulphur centres of enzymes and other proteins, and consequently inhibit protein/enzyme activity. Furthermore, when they interact, the product of the highly reactive peroxynitrite attacks and inhibits proteins and lipids. Many proteins involved in the

mitochondrial electron transport chain, aconitase of the trichloroacetic acid cycle, and biotin synthase are extremely sensitive to this type of inhibition (Brown and Borutaite, 1999; Andersson *et al.*, 1998 ). End products of lipid peroxidation (malondialdehydes) can be toxic to cells and require removal by GSH that has dramatically decreased under chronic hyperglycaemic conditions (Hayes and McLellan, 1999; Dave and Kalia, 2007). In addition, accumulation of modified protein accounts for the decreased axonal transport, leading to impaired delivery of nerve growth factor and intermediates from tissue to cell bodies, resulting in induction of nerve degeneration and apoptosis (Metodiewa and Koska, 2000). Gene expression is tightly regulated in healthy cells. Oxidative modification of transcription factors can cause the imbalance between control protein and stress protein expression, leading to decreased apoptosis inhibition factors such as complex I, and increased apoptotic proteins such as c-Jun N-terminal kinase (JNK kinase) (De La Monte *et al.*, 2000; Conn *et al.*, 2001; Paschen *et al.*, 2001; Pugazhenthi *et al.*, 2003 ).

Recent studies on measurement of oxidative stress in sensory neurons as well as neuronal protection by antioxidants provide evidence that increased cellular oxidative stress mediated by hyperglycaemia is a unifying mechanism of nervous system injury in diabetes (Russell *et al.,* 2002). Animal and *in vitro* studies have suggested four pathways of glucose metabolism are implicated in the development of diabetic neuropathy (Feldman, 2003). These include increased polyol pathway activity; H-redox imbalances; increased formation of advanced glycation end-products (AGEs); protein kinase C (PKC) activation; and increased hexosamine pathway flux. ROS are overproduced through the hyperglycaemia-mediated pathways (Feldman, 2003). Figure 1.1 outlines the details of each pathway, which accounts for burdens of ROS.

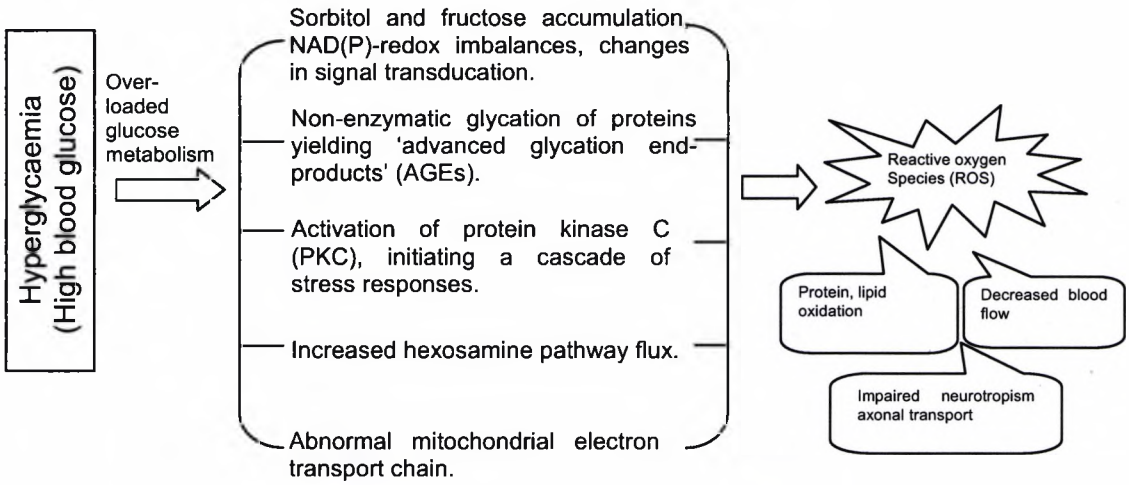


**Figure 1.1** Metabolic pathways of hyperglycaemia underlying oxidative stress. (Adapted from Feldman, 1999)

The first derivation of oxidative stress by glucose is via the polyol pathway. Under normal conditions the enzyme aldose reductase converts toxic aldehydes to inactive alcohols. Despite glucose being a poor substrate for aldose reductase, at high concentrations this enzyme converts glucose to sorbitol, initiating the polyol pathway of glucose conversion to fructose. NADPH is an essential factor to coordinate aldose reductase as well as GSH reductase enzyme. Therefore, excessive activation of the polyol pathway depletes cytosolic NADPH and subsequently inhibits GSH formation. With a deficit of antioxidant, the cell becomes vulnerable to ROS produced during normal cellular functions such as electron transfer. In addition, accumulation of sorbitol itself causes osmotic stress that also generates oxidative stress (Vincent *et al.*, 2004). Recent human genetic and biochemical data suggest polymorphisms of the aldose reductase gene and elevated tissue levels of this enzyme strongly increase risks for diabetic complications (Obara *et al.*, 2004).

The second pathway is advanced glycosylation end product (AGE)-mediated ROS formation. Glucose at elevated concentrations undergoes non-enzymatic reaction to form glycated residues called Amadori products that subsequently are converted to stable covalent adducts known as AGEs. These reactions are catalysed by transition metal ions. Reduced ability in diabetic patients to chelate transition metals may exacerbate AGE formation (Thornalley, 2002). AGE receptors (RAGE) are then activated by binding of AGE, initiating a cascade of signal transduction events involving $p^{44}/p^{42}$ microtubule affinity regulating kinases (MARKs), nuclear factor-$\kappa$Bm $p^{21}$ Ras, and other intermediates (Lander *et al.*, 1997; Wautier *et al.*, 1994). Interaction of AGEs with RAGE induces the production of ROS through a mechanism involving a key role for activated NADPH oxidase. In neuronal cell lines, application of AGEs depletes GSH and alters intracellular protein function (Feldman, 2003; Vincent *et al.*, 2004).

The next fate of glucose is activation of PKC pathway. PKC has several unique structural features that facilitate its regulation according to redox status. Prooxidants can stimulate PKC activity by reacting with its regulatory domain, but antioxidants inhibit its activity by the reaction with the catalytic domain of PKC. PKC becomes activated either directly by glycolytic intermediates or indirectly by stress hormones, which contribute to diabetic neuropathy through the effect of increased vascular disease, inflammation, and oxidative stress. Once activated, PKC stimulates the phosphorylation of transcription factors and alters the balance of gene expression, such as NF-$\kappa$B and NADPH oxidase, inducing ROS (Feldman, 2003; Vincent *et al*, 2004). This is evidence for the role of PKC in hyperglycaemia. In endothelial cells, NF-$\kappa$B was activated by

high glucose, leading to ROS formation and cellular activation; this effect was prevented in the presence of PKC inhibitor (Srivastava, 2002).

The final pathway involved in ROS generation is increased hexosamine pathway flux and impaired mitochondrial respiration. Overloaded glucose causes the accumulation of glycolytic intermediates and leads to escape of fructose-6-phosphate undergoing hexosamine pathway. The increased hexosamine pathway leads to vascular disease and formation of ROS. In addition, overloading and slowing of the election transport chain causes escape of reactive intermediates to produce ROS in mitochondria and activation of NADH oxidase generating ROS (Feldman, 2003).

These metabolic pathways induced by hyperglycaemia directly or indirectly produce ROS. In the nervous system, the oxidative stress triggers decreased blood flow, protein and lipid oxidation, and inflammation, leading to impaired neurotropism, axonal transport and gene expression, and loss of neural function. In the long term, oxidative stress can mediate apoptosis of neurons and supporting cells including Schwann cells, the glial cells of the peripheral nervous system (Brownlee, 2001; Feldman, 2003).

### 1.3 The role of cytokines (Interleukin-6)

Oxidative stress stimulates transcription of proinflammatory cytokines, such as interleukin-1 (IL-1), interleukin-6 (IL-6), and tumour necrosis factor-α (TNF-α), resulting in an inflammatory response. Cytokines possess multifunctional protein modulating activities on individual cells and tissues have been found to modulate neurological function (Viviani *et al.,* 2004). The precise of these cytokines in the nervous system is complex and incompletely understood.

IL-6 for example, which is secreted by e.g. macrophages, lymphocytes and epithelial cells, is an important cytokine displaying diverse biological functions (Jain *et al.,* 2003). In addition to modulation of inflammatory and immune response in the periphery, it also induces growth and differentiation of cells in the immune and hematopoietic systems (Gruol and Nelson, 1997). IL-6 belongs to the neuropoietic class of cytokines which include ciliary neurotrophic factor (CNTF), leukaemia inhibitory factor (LIF), oncostatin M (OM) and interleukin-11 (IL-11). This cytokine family shares a common tertiary structure giving rise to a very similar three-dimensional shape. Most importantly, they all act via receptors linked to gp130 signal transducing units to stimulate a kinase-signalling cascade (Alonzi et al., 2001; Taga and Kishimoto, 1997).

IL-6 displays both neurotrophic and neurodegenerative effects in the nervous system: low concentrations of IL-6 are neuroprotective, however, sustained or excessive IL-6 causes neuron degeneration (Gadient and Otten, 1996; Gruol and Nelson, 1997). IL-6 has been found to be expressed in sympathetic and sensory ganglia of adult rats (Gadient and Otten, 1996) and rapidly accumulates following nerve injury, which exacerbates functional nerve regeneration (Marz *et al.,* 1999). On the other hand, elevated levels of IL-6 in the central nervous system have been found in several neurological disorders, such as Alzheimer's disease (Gruol and Nelson, 1997). Therefore, the disrupted IL-6 signalling might contribute the development and progression of diabetic neuropathy.

IL-6 can promote the progression of diabetic neuropathy through interaction with nerve growth factor (NGF). As seen in Figure 1.2, IL-6 binds to the water-soluble IL-6 receptor linked to gp130 signal transducing unit, stimulating a

cytoplasmic signalling cascade to activate Janus kinases (JAK)/signal transducer and activators of transcription (STAT) pathway, leading to the IL-6 specific element transcription (Heinrich *et al.,* 2003 ). IL-6 in synergism with NGF can promote completely opposite actions on neurons, triggering neuron survival, or neuron degeneration and death (Otten *et al.,* 2000). At low concentrations of IL-6, NGF acts on trkA (high-affinity tyrosine kinase receptor), stimulating extracellular signal-regulated kinase (ERK)/mitogen activated protein kinase (MAPK) kinase cascade. This activation leads to neuroprotection. At high concentrations of IL-6, NGF binds to p75 (low-affinity glycoprotein) (Averill *et al.,* 1995)), activating JNK kinase cascade. This activation leads to neurodegeneration. Diabetic patients have already elevated blood levels of cytokines (Hussain *et al.*, 1996; Targher *et al.*, 2001) and further increases in circulating cytokines could exacerbate neurological complications in persons with pre-existing neuropathy.

Thus, IL-6 is a critical mediator in diabetic neuropathy since elevated levels could contribute to nerve degeneration and death. Although the mechanism of IL-6 and the correlation with other factors is complex, it is very important in understanding the pathogenesis of diabetic neuropathy.

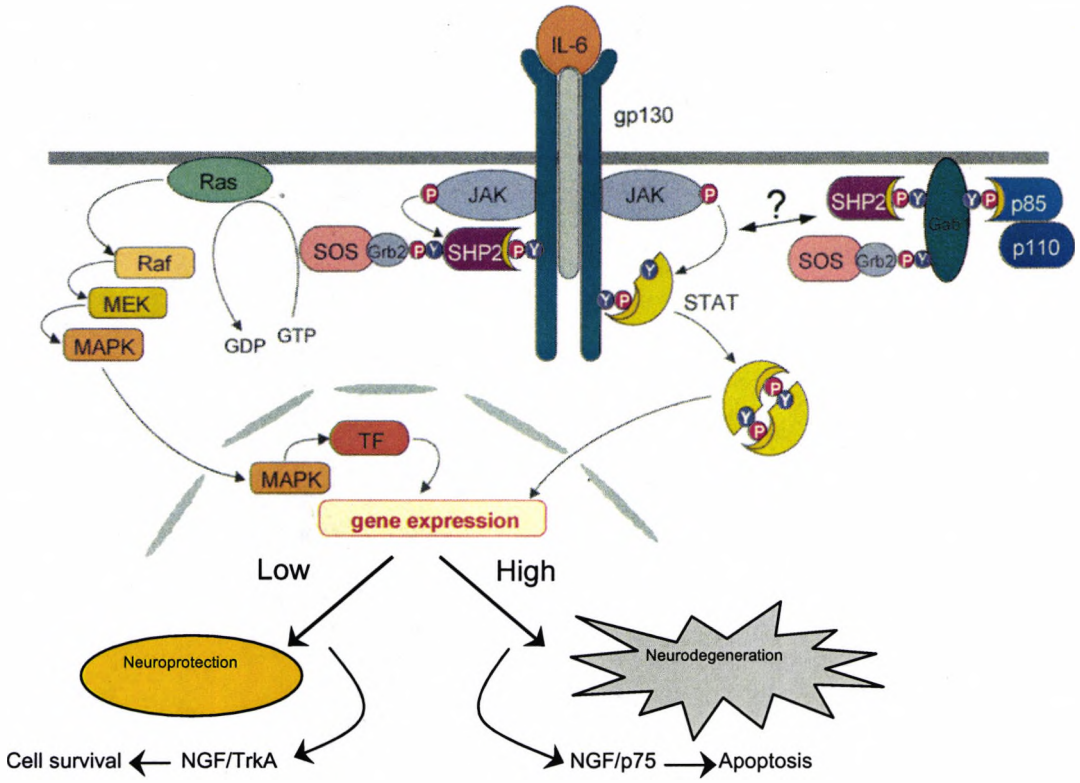


**Figure 1.2** The effects of neuroprotection and neurodegeneration induced by IL-6 signal transduction in synergism with NGF. (Adapted from Heinrich *et al.*, 2003)

## 1.4 The role of vanilloid receptors (TRPV1)

### 1.4.1 General introduction of TRPV1 receptors

Before the discovery of the vanilloid receptor (VR1 or transient receptor potential vanilloid 1, TRPV1), capsaicin (Figure 1.3 A), a main ingredient of chilli pepper, was found to excite a subset of primary sensory neurons in dorsal root ganglia (DRG) DRG or trigeminal ganglia. These capsaicin-sensitive neurons are generally peptidergic, small diameter neurons giving rise to unmyelinated C fibres (Holzer, 1991). However, not all small diameter neurons response to capsaicin, and, actually, the large diameter Aδ fibre neurons are also capsaicin-responsive (Ikeda *et al.,* 1997). Summarising from much research focused on capsaicin activity, three strong evidences indicate the existence of a specific capsaicin recognition site: capsaicin-mediated activity requires strict structure-activity relations (Szolcsanyi *et al.,* 1975; Szolcsanyi and Jancso-Gabor, 1976); only specific neuron tissues are sensitive to capsaicin (Holzer, 1991); and response to capsaicin is species-selective (Buck and Burks, 1986). In 1990, Szallasi and Blumberg demonstrated a specific binding of resiniferatoxin (RTX) (Figure 1.3 B), a capsaicin analogue, at rat DRG membrane (Szallasi and Blumberg, 1990), providing the first direct evidence for the existence of TRPV1 receptors. In 1997, Caterina and colleagues first cloned rat TRPV1 receptors which contain 838 amino acids with a molecular mass of 95KDa (Caterina *et al.,* 1997). The development of capsazepine (Figure 1.3 C) provides the first and only commercially available competitive TRPV1 antagonist (Walpole and Wrigglesworth, 1993). Capsazepine has been found to effectively inhibit both capsaicin (Lee and Lundberg, 1994; Lalloo *et al.*, 1995) and RTX responses (Ellis and Undem,

1994; Wardle *et al.*, 1996; Wardle *et al.*, 1997), and it has become an essential tool for studying neuronal functions.

The TRPV1 receptor, present on small diameter C- and Aδ- sensory nerve fibers, is defined as a non-selective cation channel, with high permeability of $Ca^{2+}$, sensitive to the pungent vanilloid capsaicin (Caterina *et al.,* 1997). Structurally, it spans six transmembrane domains and contains a possible pore-loop between the fifth and sixth membrane-spanning regions (Figure 1.4). The fact that the capsaicin binding site is intracellular comes from Humphrey H. Rang's study (Spring Pain Conference, Grand Cayman, BWI, 1998) showing that lower capsaicin concentrations are required to activate the cells from inside. This concept was further confirmed by Jung and co-workers in 1999 (Jung *et al.,* 1999).

It has been found TRPV1 exists in various brain regions and is highly expressed in DRG (Sanchez *et al.,* 2001). In addition to capsaicin, TRPV1 receptors are also activated endogenously by noxious heat (>42°C), acidic PH (<6.0), and the endocannabinoid, anandamide (arachidonoylethanolamide; AEA; Figure 3D), (Smith and McQueen, 2001; Zygmunt *et al.*, 1999). Inflammatory mediators including bradykinin, histamine, serotonin, and prostaglandin $E_2$ (Kress *et al.,* 1997), and proinflammatory cytokines such as TNF-α, IL-1 and IL-6 (Nicol *et al.,* 1997) have also been demonstrated to be able to enhance capsaicin sensitivity of rat DRG neurons.

When pungent vanilloids, like capsaicin, bind to TRPV1 receptors, the channel pore opens, leading to massive $Ca^{2+}$ influx (Marsh *et al.,* 1987). The $Ca^{2+}$ influx generates an action potential which is propagated along the entire length of the

excited neurons, causing central and peripheral release of the neuropeptides substance P and calcitonin gene-related peptide (CGRP). As well as giving rise to the perception of pain, these neuropeptides are important mediators of neurogenic inflammation, and induce production of proinflammatory cytokines by macrophages, lymphocytes and lung epithelial cells (Veronesi *et al.*, 1999).

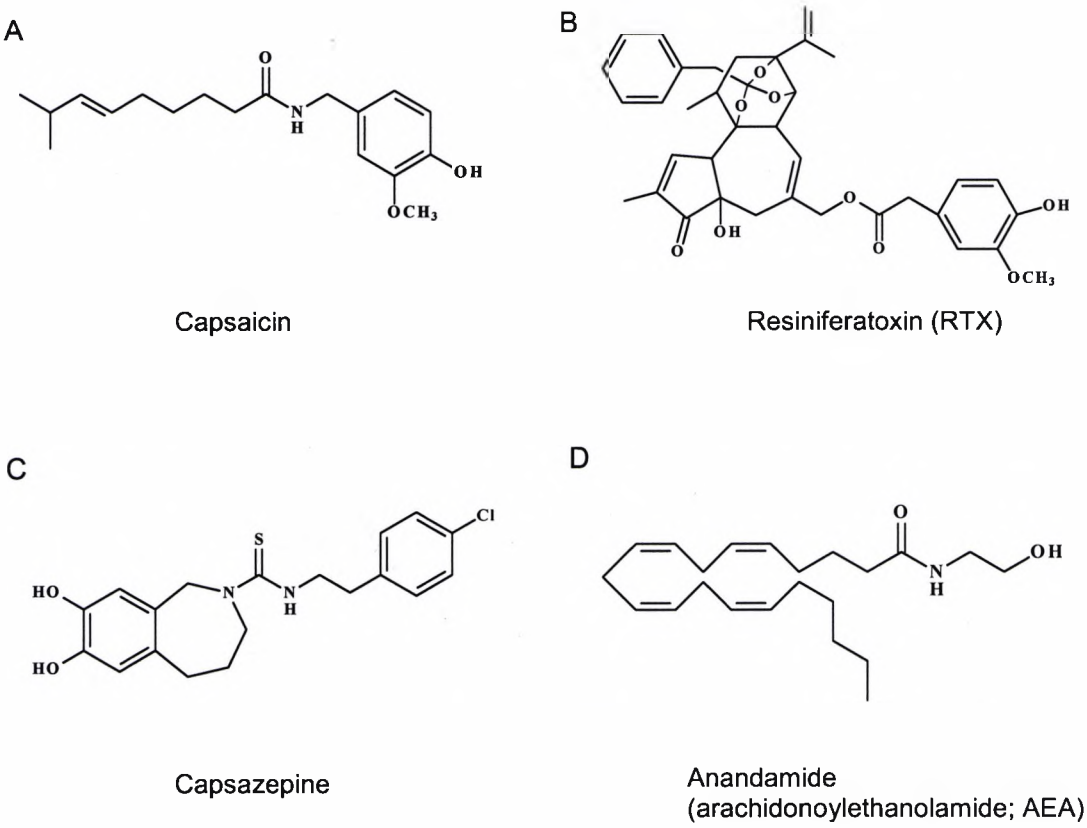


**Figure 1.3** Vanilloid structures: capsaicin, resiniferatoxin and anandamide are TRPV1 receptor agonists; capsazepine is a TRPV1 receptor antagonist.

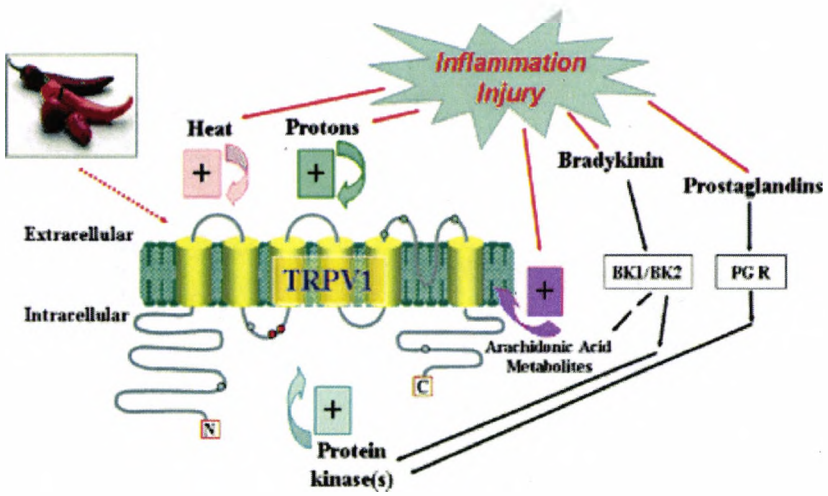


**Figure 1.4** TRPV1 functions as an integrator of noxious stimuli. (Adapted from Cortright and Szallasi, 2004)

### 1.4.2 The role of TRPV1 receptors in diabetic neuropathy

There is some evidence suggesting the activation of TRPV1 receptors plays a role in painful neuropathy. Hyperalgesia (excessive sensitivity and pain response to noxious stimuli) and allodynia (pain evoked from non-noxious stimuli) are two common types of neuropathic pain occurring frequently in diabetic patients. Kamei and colleagues have reported that the thermal hyperalgesia and allodynia observed in diabetic mice is due to sensitisation of TRPV1 receptors (Kamei *et al.,* 2001). Also, Hong and Wiley (2005) have shown that the TRPV1 receptor is highly sensitised on DRG from diabetic rats (Hong and Wiley, 2005)

As a cation channel, TRPV1 is regulated by phosphorylation and dephosphorylation processes. This sensitisation can occur via protein kinase C (PKC)-mediated phosphorylation of TRPV1, which lowers the activation threshold for proton and heat-induced currents (Premkumar and Ahern, 2000; Hong and Wiley, 2005; Numazaki *et al.*, 2002). Indeed, a PKC activator has been shown to block TRPV1 desensitisation on DRG neurons from diabetic rats; this effect is reversed by a PKC inhibitor (Hong and Wiley, 2005). PKC activation in diabetes could result from the enhanced release of chemical mediators under ischaemic conditions, following hyperglycaemia-induced oxidative stress as described earlier: bradykinin is one such example (Walker *et al.,* 1995). Bradykinin-induced sensitisation of TRPV1 occurs not only through PKC-mediated phosphorylation, but also via the displacement of membrane lipids from an inhibitory site on TRPV1 (Sugiura *et al.,* 2002). In addition to PKC, the activation of Erk/MAPK may also be involved in the sensitisation of TRPV1 receptors (Dai *et al.,* 2002). Taylor and colleagues have shown capsaicin prevents retrograde axonal transport in rat sensory neurons

by depriving sensory nerves of nerve growth factor (Taylor *et al.*, 1985), and excess TRPVR1 stimulation may therefore lead to axonal degeneration in diabetic neuropathy.

Capsaicin-evoked CGRP release from sensory neurons is inhibited by anandamide (Richardson *et al.*, 1998a). This effect is mediated by cannabinoid $CB_1$ receptors. Cannabinoid receptors ($CB_1$), belonging to the G protein-coupled receptor superfamily, are co-expressed with TRPVR1 in DRG neurons, and central and peripheral terminals of nociceptive afferents (Hohmann and Herkenham, 1999; Ahluwalia *et al.*, 2002).

## 1.5 History of cannabis in medical use

*Cannabis sativa* (cannabis) (Figure 1.5) has been recorded in medical use in China, India and Africa for thousands of years. The archeological and historical evidence shows that the earliest use of the cannabis plant was found in China. The ancient Chinese cultured cannabis for its fibres since 4,000 B.C., which can be made into strings, ropes, textiles and even paper (Li and Lin, 1974). The cannabis fruits were used as food until the beginning of the Christian Era when the new cultures were introduced (Touw, 1981; Zuardi, 2006).

More importantly, the seeds of cannabis were recorded in the world's oldest pharmacopoeia of China, as the main piece utilized in medicine to cure a variety of diseases, such as rheumatic pain, intestinal constipation, disorders of the female reproductive system and malaria (Touw, 1981). About 2000 years ago, Hua T'o, a famous Chinese physician, discovered the anaesthetic function of cannabis, and soon after performed the surgery with the aid of its anaesthesia (Li and Lin, 1974; Zuardi, 2006).

In India, the utilization of cannabis in surgery appeared around 1000 years B.C. (Mikuriya, 1969). Since the religion assigned sacred virtues to the plant, cannabis was applied both as a medicine and a recreational drug. As a significant extension, more parts of the cannabis plant, such as dry leaves, hairs and solitary resin glands, were found to have pharmacological activities, and subsequently adopted as remedies in the clinic. Probably due to the better preparation method of cannabis that was believed to effectively protect the activities of cannabinoid compounds, the psychoactive effects of the cannabis were well-known in India. Meanwhile, the medical use of the plant in India was

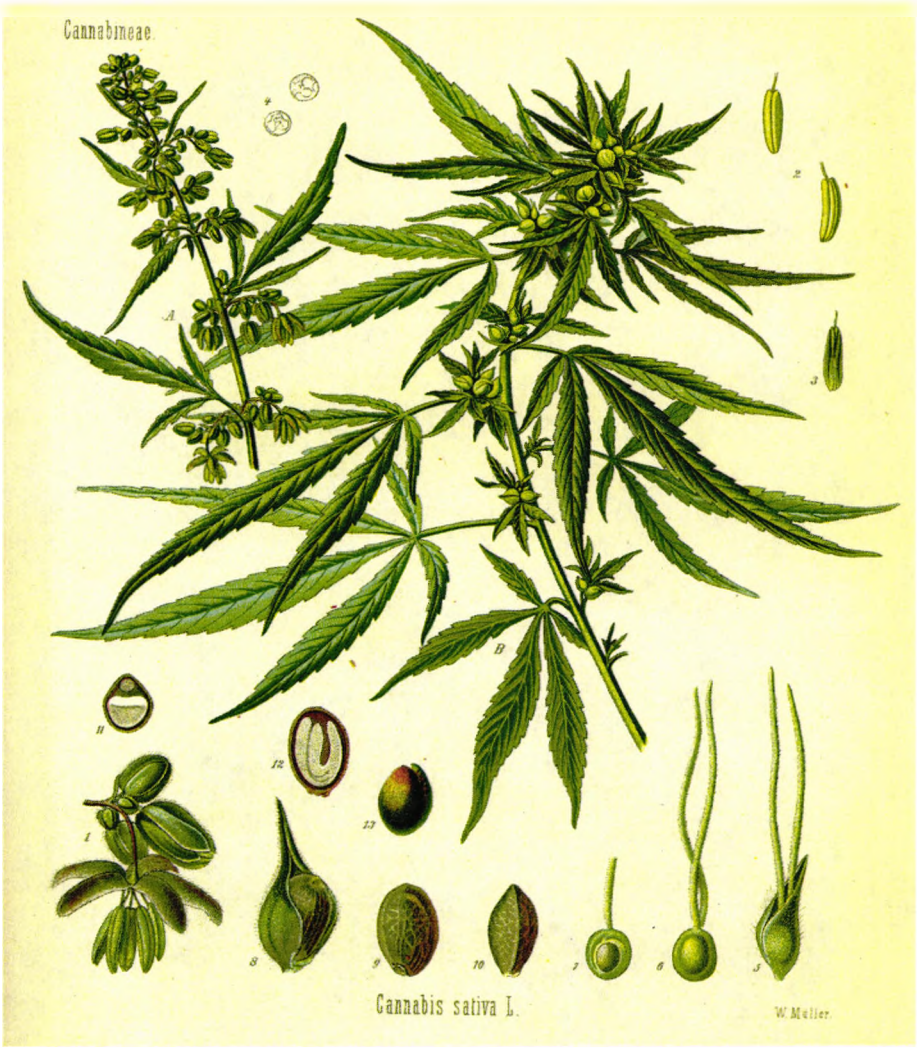


**Figure 1.5** Cannabis sativa which contains chemicals called cannabinoids which produce the "high" effect / mental + physical effects when utilized.
(Downloaded from http://www.cannabis.com/faqs/about_cannabis_FAQ/index.html)

numerous, such as analgesic (neuralgia, headache, and toothache), anticonvulsant (epilepsy, tetanus, and rabies), hypnotic, tranquilizer (anxiety, mania, and hysteria), anaesthetic, anti-inflammatory (rheumatism and other inflammatory diseases), and antibiotic (topical use on skin infections, erysipelas, tuberculosis) (Aldrich, 1997; Mikuriya, 1969; Touw, 1981; Zuardi, 2006). In the 15th century, cannabis was introduced into Africa by Arab traders, and the connection with India was evidenced by the similarity of the term for preparing the plants in Africa and in India (Du Toit, 1980). Today, we know the female flowers contain the highest concentration of psychoactive chemicals, the leaves less, and the seeds none.

In the 19th century, William B. O'Shaughnessy, an Irish physician, and Jacques-Joseph Moreau, a French psychiatrist, effectively brought cannabis into western medicine. O'Shaughnessy described various successful human experiments using cannabis in his book titled "On the Preparations of India Hemp, or Gunjah" (Mikuriya, 1969; Fankhauser, 2002). Moreau systematically experimented different cannabis preparations on himself and his students, and found the remarkable therapeutic effects of cannabis, especially on mental diseases which were recorded in his book titled "Du Hachisch et de l'Alienation Mentale: Etudes Psychologiques" (Brill and Nahas, 1984; Moreau, 1845). Because of their great contributions on improving the applications of cannabis, the use of this plant in medical fields spread rapidly from England and France to all other European countries. In the late 19th century and early 20th century, the applications of cannabis in medical fields reached a climax, which was mainly in three areas: sedative or hypnotic; analgesic; other uses to improve appetite and digestion (Fankhauser, 2002; Brill and Nahas, 1984). However, later on, in the 20$^{th}$ century, the use of cannabis experienced decline and

rediscovery. In the first decades, the active component of cannabis had not been isolated and the raw extracts were used to make drugs. Due to the varying efficacy of different samples of the plant, it was very difficult to obtain replicable effects (Fankhauser, 2002). In addition, the registration and tax payment were required for using cannabis. All these factors restricted the therapeutic exercises and experimentation of cannabis in western countries (Fankhauser, 2002; Zuardi, 2006).

With better knowledge of cannabis including identifying the chemical compositions and separating the pure active compounds, for instance, $\Delta^9$-tetrahydrocannabinol ($\Delta^9$-THC) was isolated in 1964 (Gaoni and Mechoulam, 1964), cannabis was once again brought back into scientific interest. In the early 1990's, cannabinoid receptors and an endocannabinoid system were discovered in the nervous system, stimulating extensive research activity into the relevant therapeutic effects (Martin *et al.,* 1999). Currently, more accurate scientific methods have been developed to elucidate the structures of chemical compounds extracded from cannabis, to clarify the mechanisms of the pharmacological functions, and to prove the effectiveness, efficacy and safety (Zuardi, 2006). A cannabimemetic drug, Sativex, containing $\Delta^9$-THC together with cannabidiol, was approved in UK in November 2005.

## 1.6 The molecular biology of cannabinoid receptors

### 1.6.1 The discovery of cannabinoid receptors

$\Delta^9$-tetrahydrocannabinol (THC) is the main constituent responsible for the psychoactive effects of *Cannabis sativa*. In terms of chemical structures, (-)-$\Delta^9$-THC produced more psychoactive effect by interacting more potently with artificial membrane containing only cholesterol and phospholipid than its nonpsychotropic enantiomer, (+)-$\Delta^9$-THC (Pertwee, 1988). It was initially believed that the psychoactivity of cannabinoids was through disordering neuronal cell membrane lipids by fitting into asymmetric components of the hydrocarbon matrix rather than binding into specific receptors (Pertwee, 1988).

In 1990, Matsuda and colleagues first cloned cannabinoid receptors ($CB_1$) from rat cortex (Matsuda *et al.,* 1990). Radioligand-binding studies showed that the brain distribution of $CB_1$ mRNA was highly overlapped with radio-labelled cannabinoids, which revealed the $CB_1$ receptor as the specific binding site for cannabinoids (Devane *et al.*, 1988; Herkenham *et al.*, 1990).

A few years later, a second type of the cannabinoid receptor ($CB_2$) was identified and cloned from rat spleen (Munro *et al.,* 1993). Compared to the $CB_1$ receptor which has been found to be widely present in the central nervous system, peripheral nervous system and haematopoietic cells (Munro *et al.,* 1993), the $CB_2$ receptor is mainly expressed on immune cells. In addition, $CB_1$ receptors are highly conserved in mice, rat and human, The $CB_2$ receptor, however, is more divergent. Rat $CB_2$ receptors have only 93% homology with mice and 81% with human (Griffin *et al.*, 2000; Shire *et al.*, 1996a; Munro *et al.*, 1993). Although the overall homology between human $CB_1$ and $CB_2$ receptor is

only as low as 42%, most of the plant-derived, endogenous, synthetic cannabinoids have similar affinities for both of the receptors (Showalter *et al.,* 1996).

As mentioned above, the $CB_1$ receptor is extensively expressed in central and peripheral nervous systems, and is believed to be the analgesic receptor responsive to cannabinoids. Whilst $CB_2$ receptors were thought to have immunosuppressive and anti-inflammatory activity due to their primary expression on immune cells, recent studies have revealed additional localization of $CB_2$ receptors in the pain pathway including A/C fibres, DRG and the dorsal horn, indicating a possible analgesic role involved in pain control (Beltramo *et al.,* 2006). Additional receptor types have been identified for cannabinoids, for example peroxisome proliferator-activated receptor alpha (PPAR$\alpha$) (Sun *et al.,* 2007)and the orphan receptor GPR55 (Ryberg *et al.,* 2007). In this thesis, the $CB_1$ receptor is the major target, to be studied regards its neuroprotective role in diabetic neuropathy.

### 1.6.2 The structure of $CB_1$ receptors

The diagrammatical structure of the human $CB_1$ receptor is illustrated in Figure 1.6. The $CB_1$ receptor was recognized by translated cDNA as a 473-amino-acid protein, and similarly to other members of G protein coupled receptors, has seven hydrophobic domains, and contains numerous residues which are highly conserved residues (Mukhopadhyay *et al.*, 2002; Matsuda *et al.*, 1990). The extracelluar loops of $CB_1$ receptors have high affinity for ligands such as $\Delta^9$-THC and anandamide, and subsequently trigger signal transduction. The intracellular loops are there to mediate G protein signalling (Joy *et al.,* 1999).

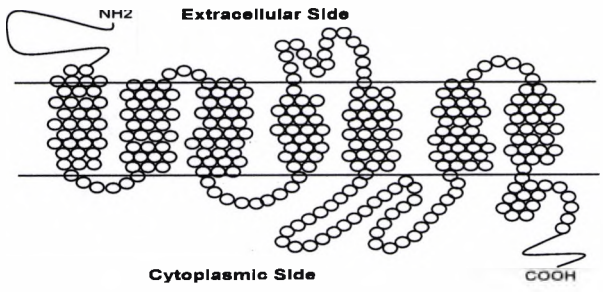


**Figure 1.6** Two-dimensional structure of the human hCB1 receptor. Three extracellular and intracellular regions are represented. (Adapted from Mukhopadhyay *et al.*, 2002)

### 1.6.3 The distribution of $CB_1$ receptors

The $CB_1$ receptor is believed to be the most abundant receptor in the brain and has been investigated by use of various bio-techniques including receptor autoradiography, immunohistochemistry, and in situ hybridization histochemistry (Walker and Huang, 2002). Its existence has been demonstrated in the brain of rat (Egertova and Elphick, 2000; Hajos *et al.*, 2000; Moldrich and Wenger, 2000), mouse (Marsicano and Lutz, 1999; Hermann *et al.*, 2002), bird (Soderstrom and Johnson, 2000), primate (Ong and Mackie, 1999), and, most importantly, human (Katona *et al.*, 2000; Mailleux and Vanderhaeghen, 1992).

The high densities of $CB_1$ in the central nervous system, such as basal ganglia, cerebellum, neocortical and hippocampus, account for the effect of $CB_1$ agonists on locomotor activity, cognition and memory performance. In other parts of the central nervous system, the expression of $CB_1$ receptors was found in spinal cord and DRG subpopulations, mostly on medium and small DRG neurons (Farquhar-Smith *et al.,* 2000; Hohmann and Herkenham, 1998), from which it is transported and assembled on central and peripheral terminal

afferents in the peripheral nervous system. This fact may be connected to the analgesic effect produced by spinal and/or peripheral administration of cannabinoid agonists (Herkenham *et al.*, 1991; Hohmann and Herkenham, 1998; Hohmann and Herkenham, 1999). Further evidence revealed the localization of $CB_1$ receptors on nerve endings, indicating the presynaptic inhibition of neurotransmitter release (Herkenham *et al.*, 1991; Mailleux and Vanderhaeghen, 1992; Tsou *et al.*, 1997). This presynaptic inhibition can directly cut the output of a neuron and subsequent communication to other neurons, by which the signal transduction is preliminarily hindered and analgesia is produced (Reviewed in Walker and Huang, 2002). These brains, spinal, and peripheral distributions of $CB_1$ receptors provide the strong anatomy basis to the $CB_1$-mediated antinociception.

### 1.6.4 The mechanism of G protein-coupled $CB_1$ receptor action

As a member of the G protein coupled receptor superfamily, the $CB_1$ receptor activates signal transduction through an adapter guanine nucleotide binding protein, G protein (Figure 1.7). The interaction of an agonist-stimulated $CB_1$ receptor and G protein causes the replacement of guanosine diphosphate (GDP) by guanosine triphosphate (GTP), via phosphate exchange, which subsequently stimulates the dissociation of the α, β and γ subunits. These subunits realize the signal transduction by regulating effectors of proteins including adenylyl cyclases, ion channels, phosphoinositide 3-kinase, and phospholipases (Diaz-Laviada and Ruiz-Llorente, 2005). The activated signal transduction returns to a resting state by the hydrolysis of GTP to GDP, and then the three subunits become reassociated (Feldman and Quenzer, 1984).

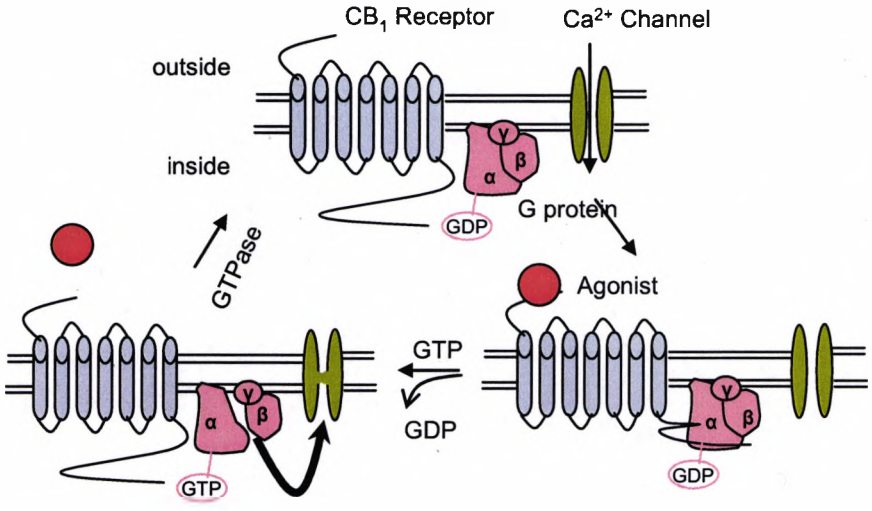


**Figure 1.7** The mechanism of G protein-coupled receptor action. (Adapted from Sinauer association Inc. Feldaman Fundamentals of Neuropsychopharmacology Figure 6.23)

### 1.6.5 The signal transduction of $CB_1$ receptors

The binding of a $CB_1$ agonist to the $CB_1$ receptor generates a series of signal transduction events. $CB_1$ receptors are linked to $G_{i/o}$ proteins, resulting in the inhibition of adenylyl cyclase, leading to decreased level of cAMP. As a second messenger, cAMP transmits information originating from the cell membrane to the cell's interior, so that the reduction of cAMP significantly hinders the cell response to exterior stimulation, for example, reduced $Ca^{2+}$ entry into noradrenergic nerve terminals, leading to decreased neurotransmitter release. Also, the decreased adenylyl cyclase influences the activity of protein kinase A, causing the reduction of phosphorylation of potassium channels which eventually increases the efflux of potassium (Azad *et al.,* 2001). Thus, the activation of the $CB_1$ receptor inhibits N and Q-type of $Ca^{2+}$ channels, and activates $K^+$ conductance via $G_{i/o}$. This cAMP-dependent mechanism eventually decreases $Ca^{2+}$ entry and increase $K^+$ efflux (Mackie and Hille, 1992; Mackie *et al.*, 1995; Twitchell *et al.*, 1997). Considering the findings that $CB_1$ receptors

*al.*, 1995; Twitchell *et al.*, 1997). Considering the findings that $CB_1$ receptors localize on presynaptic terminals (see above), neurotransmitter-positive neurons and nerve fibres (Hohmann and Herkenham, 1999; Dvorak *et al.*, 2003), these signalling pathways modulated by the $CB_1$ receptor may all account for the general inhibition of neuropeptide release.

The activities of the $CB_1$ receptor can also be desensitized by phosphorylation. Like other G protein-coupled receptors, the $CB_1$ receptor is primarily desensitized by phosphorylation of serine/threonine kinases and by interaction with beta-arrestins, a family of uncoupling proteins, which can form a complex to mediate the desensitization (Ferguson, 2001; Pierce *et al.*, 2001). Stimulation of protein kinase C was also found to disrupt cannabinoid-mediated activation of an inwardly rectifying potassium current ($K_{ir}$ current) and depression of P/Q-type calcium channels in $CB_1$ receptor-transfected AtT-20 cells, by phosphorylating a single serine (S317) of a fusion protein incorporating the third intracellular loop of $CB_1$ (Diaz-Laviada and Ruiz-Llorente, 2005; Garcia *et al.,* 1998).

The activation of $CB_1$ receptors also promotes the process of neurite outgrowth through the $G_{i/o}$ protein-mediated signal transduction. The regulation of neurite outgrowth is a tightly controlled process and requires the coordination of signals coming from outside and inside of cells. This function is based on the growth cone at the elongation of axonal and dendrites, which is believed to recognize and transduce such information into directed movement (Strittmatter and Fishman, 1991). $G\alpha_o$ protein is highly expressed in growth cone membrane (Strittmatter *et al.,* 1990). The evidence of its functional significance comes from the study showing that the expression of constitutively active $G\alpha_o$ results

in better neurite outgrowth in both neuroblastoma and PC12 cells (Strittmatter *et al.,* 1994).

The $CB_1$ receptor/$G_{o/i}$ signalling network in the regulation of neurite outgrowth (Figure 1.8) has been intensively studied in Neuro2A cells. Jordan and colleagues first demonstrated that the endogenous $G\alpha_{o/i}$–coupled $CB_1$ receptor in Neuro2A cells activated a small G protein, Rap1, to induce neurite outgrowth by regulating the proteosomal degradation of Rap1GAPII, a GTPase activating protein for Rap1. HU210, a $CB_1$ agonist, indeed, stimulated neurite outgrowth in Neuro2A cells, which was reversed by the inhibition of Rap1 and proteasomal degradation (Jordan *et al.,* 2005). Ral was later reported by He and coworkers (2005) to be activated by HU210 via Rap1 and involved in the signalling transduction of neurite outgrowth (He *et al.,* 2005). Furthermore, $G\alpha_{o/i}$ was proved to activate the Src-Stat pathway though Rap1 and Ral. The evidence showed that Rap1 and Ral activated $CB_1$-induced Src phosphrylation was inhibited by dominant negative of Rap1 and Ral. The dominant negative of Ral was observed to block $G\alpha_o$-induced Stat3 activation, but not to Src-induced activation, indicating that $CB_1$ receptor, through $G\alpha_{o/i,}$ mediates sequential activation of Rap1-Ral-Src-Stat3 in Neuro-2A cells (He *et al.,* 2005). Stat3 is indicated to be a key molecule in signalling neurite outgrowth through $CB_1$ receptors. The Rac-JNK pathway was also demonstrated to stimulate $CB_1$-mediated Stat3 activation by the evidence showing that the phosphorylation of JNK by HU210 was blocked by dominant negative of Rac, and the application of the JNK inhibitor (SB-202190) significantly inhibited HU210-induced Stat3 activation (He *et al.,* 2005).

It was found that the $CB_1$ receptor stimulates both the tyrosine and serine/threonine phosphorylation of Stat3. Based on the two divisions of signalling pathways, Src is likely to mediate the tyrosine phosphorylation and Rac-JNK is involved in the serine/threonine phosphorylation of Stat3. Therefore, the $CB_1$ receptor, through $G\alpha_{o/i,}$ triggers neurite outgrowth via the activation of two signalling pathways: Src and JNK that converge at Stat3 (He *et al.*, 2005).

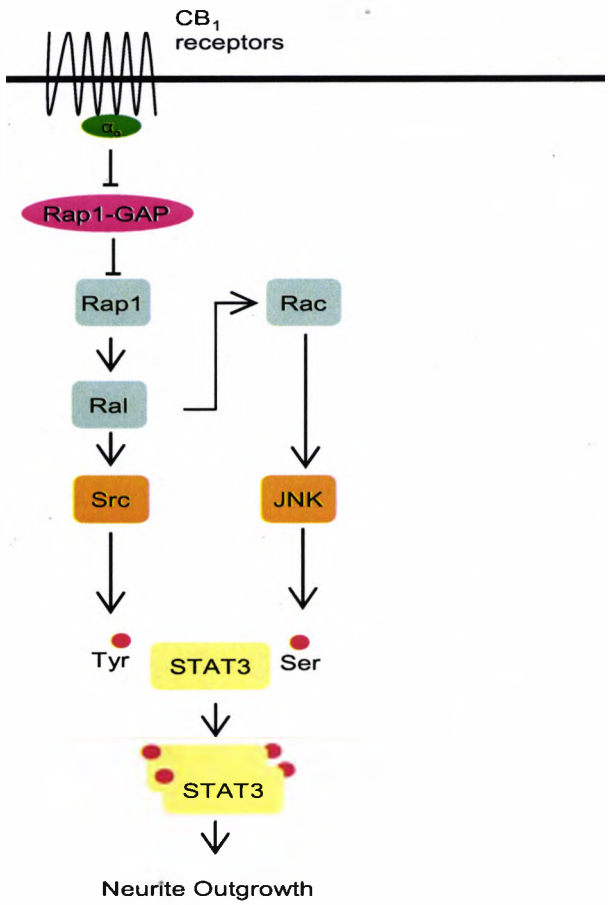


**Figure 1.8** The signalling pathways emanating from $CB_1/G\alpha_{i/o}$.

(Adapted from He *et al*, 2006)

### 1.6.6 The neuroprotective role of $CB_1$ receptor in nerve injury

The abundant distribution of $CB_1$ receptors throughout the whole nervous system has indicated its neuroprotective role in neuropathic diseases. In peripheral large myelinated fibres and small unmyelinated fibres, $CB_1$ receptors exist on CGRP-positive neurons (Stander *et al.,* 2005). Domenici revealed $CB_1$ receptors are expressed on presynaptic axon terminals of glutamatergic neurons (Domenici *et al.,* 2006). This evidence provides a molecular basis which contributes to the inhibition of neuropeptide release by $CB_1$ receptors. This theory is further verified in an animal study, which reported a significant increased in levels of substance P, dynorphin, enkephalin, and glutamic acid decarboxylase in $CB_1$-knockout mice (Steiner *et al.,* 1999).

Overloaded intracellular $Ca^{2+}$ breaks homeostasis in cells, causing excitotoxcity and leading to neuronal cell death. The deregulated intracellular homeostasis has been implicated in the pathogenesis of central nervous disorders, such as Alzheimer's and Parkinson's diseases (Annunziato *et al.,* 2003). Oxidative stress can be one of the causes of increased intracellular $Ca^{2+}$ concentration. Some studies have shown that free radicals cooperate with $Ca^{2+}$ ion to induce cell injury in glutamate induced cell death (Bridges *et al.,* 1991), or induces intracellular $Ca^{2+}$ concentration leading to the activation of endonucleases which degrades DNA, and eventually causing cell death (Cantoni *et al.,* 1989). Other findings have demonstrated that the overproduced free radicals can prevent $Ca^{2+}$-ATPase, causing imbalanced homeostasis and cell death (Chan and Mattson, 1999). Although oxidative stress does not always induce cell injury by the mechanism of deregulating intracellular $Ca^{2+}$ concentration, for instance, Rata and colleagues (1994) have reported that oxidative stress can directly induce immature cortical neurons (Ratan *et al.,* 1994), the evidences

have supported that the $Ca^{2+}$ dependent mechanism can be still significant when considering neuron injury. Furthermore, other evidence suggests that the activation of $Ca^{2+}$ channels/TRPV1 receptors can also cause imbalance of intracellular homeostasis by generating excessive $Ca^{2+}$ influx, leading to neuronal cell death. It was reported that capsaicin can kill cultured adult sensory neurons in a TRPV1 receptor-dependent pathway (Winter, 1987). This action can be prevented when removing extracelluar calcium, or blocking the calcium influx by ruthenium red (Chard *et al.*, 1995; Winter *et al.*, 1990).

The enhancement of intracellular $Ca^{2+}$ is suggested to cause thermal allodynia and hyperalgesia in diabetic mice, from the behavioural studies in which increased tail-flick latencies were found after increasing intracellular $Ca^{2+}$ in non-diabetic mice (Ohsawa and Kamei, 1999b). As mentioned before, the activation of $CB_1$ receptors results in a decrease in $Ca^{2+}$ influx, which well correlates with the therapeutic aspect of $CB_1$ receptors in pain relief. Consistently, synthetic and endogenous $CB_1$ receptor agonists (WIN 55212-2 and anandamide) have shown dose-dependent inhibition of $Ca^{2+}$ uptake in rat synaptosomes, which was reversed by a $CB_1$ receptor antagonist (SR 141716A). This study suggests that $CB_1$ receptor activation and the opening of voltage-sensitive $K^+$ channels inhibit $Ca^{2+}$ uptake of rat brain nerves (Yoshihara *et al.,* 2006). In some studies, stimulation and/or blockage of $CB_1$ receptors have been used to examine the function of the $CB_1$ receptor in models of neuropathic pain. Agonist stimulation of $CB_1$ receptors decreases the response to noxious stimuli in nociceptive neurons (Martin *et al.,* 1996). The reverse study showed blockage of $CB_1$ with selective antagonists produces hyperalgesia, and also blocks the analgesia produced by electrical stimulation in rats (Strangman *et al.,* 1998). Taken together, these data strongly suggest

that the activated $CB_1$ receptor is a neuroprotective mediator of neuropathic pain prevention and relief, and its activators, cannabinoid receptor agonists, act as antinociceptive agents through stimulation of $CB_1$ receptors.

## 1.7 Cannabinoids and pain control

### 1.7.1 The evidence of therapeutic effects of cannabinoids

Anandamide (N-arachidonoylethanolamide) was identified as an endogenous agonist at the $CB_1$ receptor in 1992 (Devane *et al.,* 1992) (Fig 1.3D). Anandamide can either inhibit or stimulate sensory neurotransmission, via the $CB_1$ or TRPV1 receptor respectively. These two receptors are highly co-expressed. These opposing actions of anandamide are concentration-dependent: low dose of anandamide inhibits the release of neurotransmitter via $CB_1$ receptors, while high dose increases the release of peptides via TRPV1 (Morisset *et al.,* 2001; Ralevic, 2003). As the TRPV1 binding site is intracellular (Kamei *et al.,* 2001b), anandamide firstly has to be taken up into the neuron via a membrane transporter before it can activate the TRPV1 receptor, thus providing a further level of discrimination between $CB_1$ versus TRPV1 activation. In untreated mice, intrathecal injection of a $CB_1$ antagonist, SR141716A, evoked a significant thermal hyperalgesia (Strangman *et al.,* 1998). Anandamide also attenuated hyperalgesia induced by the chemical damage in peripheral tissue through activating $CB_1$ receptors (Calignano *et al.,* 1998; Richardson *et al.,* 1998). These results suggest that endocannabinoids naturally modulate endogenous pain. The unbalanced endogenous system could trigger certain types of chronic.

With the isolation and structure-elucidation of pure cannabinoid compounds, many synthetic cannabinoids have also been used into animal studies to prove the antinociceptive effect both in central and peripheral nervous systems. It is recognised that cannabinoids relieve chronic pain both via $CB_1$-independent and $CB_1$-dependent mechanisms.

Oxidative stress has been implicated in the pathogenesis of neurodegenerative diseases, including diabetic neuropathy (Cameron *et al.,* 1993; Kamei *et al.,* 2001a; Karasu *et al.*, 1995; Van Dam *et al.*, 1995), and peripheral neurons are particularly vulnerable (Romero *et al.,* 1991). The phenolic moiety of the *Cannabis sativa* derivatives, $\Delta^9$-THC (Fig 1.9A) and cannabidiol (CBD; Fig 1.9B), acts as an electron donor and direct free-radical scavenger. This antioxidant property is fully independent of the $CB_1$ activation and confers neuroprotective properties to cannabinoids against oxidative stress (Chen and Buck, 2000; Hampson *et al.*, 1998; Marsicano *et al.*, 2002).

In addition to non-$CB_1$-mediated antioxidant effects, cannabinoids evoke neuroprotective effects via $CB_1$ receptor activation. The application of cannabinoid receptor agonists has an inhibitory effect on glutamatergic responses from forebrain presynaptic neurons (Domenici *et al.,* 2006). The inhibition by WIN55, 212-2 (Fig 1.9C) is absent in mice lacking $CB_1$ receptors in forebrain neurons (Domenici *et al.,* 2006). In brain injury, WIN55, 212-2 prevents neuron loss from global and focal ischaemia in rats through $CB_1$ activation (Nagayama *et al.,* 1999). These studies strongly suggest that cannabinoid suppresses excitatory synaptic transmission and vasodilatation by activating $CB_1$ receptors expressed on presynaptic axon terminals in the brain (Domenici *et al.*, 2006; Nagayama *et al.*, 1999). The cannabinoid HU210

(Dexanabinol, Sinnabidiol; Fig 1.9D) showed attenuation of capsaicin-stimulated $Ca^{2+}$ influx and substance P release in rat DRG cells (Oshita *et al.*, 2005). In a rat model of chronic neuropathic pain, WIN55, 212-2 effectively produced a $CB_1$-dependent reversal of mechanical and thermal hyperalgesia, and tactile allodynia (Herzberg *et al.*, 1997; Fox *et al.*, 2001). In the same model, another two cannabinoids HU210 and CP-55,940 (Fig 1.9E) were also studied and the inhibitory effect on mechanical hyperalgesia was similarly displayed (Fox *et al.*, 2001).

In an *in vitro* study, ACEA (arachidonyl-2-chloroethylamide; Fig 1.9F), a $CB_1$ agonist, significantly attenuated capsaicin evoked $Ca^{2+}$ response in DRG neurons from neuropathic rats, and this response was reversed by pre-treatment with the selective $CB_1$ antagonist, SR141716A (Fig 1.9G) (Kelly and Chapman, 2001). A subsequent *in vivo* study further proved that spinal administration of ACEA significantly inhibited the mechanically evoked responses of dorsal horn neurons, which was also antagonised by SR141716A (Kelly and Chapman, 2001). These studies have demonstrated the inhibitory effect of $CB_1$ agonists on evoked response of DRG neurons and dorsal horn neurons in neuropathic rats and strongly suggest cannabinoids are likely to attenuate chemical and mechanical-evoked hyperalgesia in rats and also cause anti-hyperalgesia in a model of neuropathic pain via a $CB_1$-mediated mechanism.

Peripherally, ACEA and WIN55, 212-2 both showed the $CB_1$ receptor-mediated therapeutic effects. The injection of peripheral ACEA inhibited innocuous and noxious mechanically evoked responses of spinal neurons, which was reversed by co-administration of SR141716A (Kelly *et al.*, 2003). These results suggest

peripheral $CB_1$ receptors mediate both innocuous (Aβ fibre) and noxious (Aδ and C fibres) stimulation. Dogrul and colleagues (2004) have firstly reported that topical administration of cannabinoid WIN 55,212-2 showed an anti-nociceptive effect through peripheral $CB_1$ receptors (Dogrul *et al.,* 2004). Also, an antinociceptive synergy between peripheral and spinal cannabinoid action was suggested by the findings that combining topical with spinal administered WIN 55,212-2 potentiated the analgesic effect (Dogrul *et al.,* 2003). This study indicates that topically administrated cannabinoids could avoid side effects mediated by actions in the central nervous system, such as hypoactivity, motor dysfunction and hypotermia hypothermia (Dogrul e*t al.,* 2003)

There are a number of recent papers reporting the generation of novel cannabinoid receptor ligands with antinociceptive properties. Different from the hydrophobic nature of other cannabinoids, the newly synthesised O-1057 ($\Delta^8$-tetrahydrocannabinol hydrochloride; Fig 1.9H) is a water soluble cannabinoid receptor agonist (Pertwee *et al.,* 2000). O-1057 has shown the ability to suppress cAMP production *in vitro*, reduce mouse spontaneous activity and rectal temperature, and induce antinociceptive activity in the tail flick test when given intravenously or even through inhalation, all of which were blocked by SR141716A (Pertwee *et al.*, 2000; Lichtman *et al.*, 2000). Two well established cannabinoid receptor agonists, $\Delta^9$-THC and CP-55,940, were compare with O-1057, and the more potent cannabimimetic properties of O-1057 were shown in the *in vivo* study, indicating the great clinical potential as an analgesic (Pertwee *et al.,* 2000). Another novel cannabinoid, AA-DA (N-arachidonyl-dopamine; Fig 1.9I) behaves as a $CB_1$ agonist and exhibits the analgesic effect along with other actions including hypothermia, hypo-locomotion, catalepsy in mice (Bisogno *et al.,* 2000).

With the high demand on producing analgesic agents with reduced side effects, a novel analogue of metabolites of $\Delta^9$-THC, CT-3 (1', 1'-dimethylheptyl-$\Delta^8$-tetrahydrocannabinol-11-oic acid; Fig 1.9J), has shown the potential to achieve this goal, which is under development by Atlantic Pharmaceuticals as an anti-inflammatory and analgesic drug (Dajani *et al.,* 1999). CT-3 induces marked analgesia both in rat and mice as assessed by tail flick and hot plate tests (Dajani *et al.,* 1999). Furthermore, in behavioural models of chronic neuropathic pain in the rat, CT-3 produced up to 60% reversal of mechanical hyperalgesia and allodynia by activating the $CB_1$ receptor, and was devoid of cannabis-like adverse events that usually develop in other cannabinoid treatment (Dyson *et al.,* 2005). This finding is in agreement with results from clinical trials of CT-3 in patients with neuropathic pain (Karst *et al.,* 2003; Mitchell *et al.,* 2005). With its superior therapeutic index, CT-3 shows promise to become a novel analgesic drug.

A

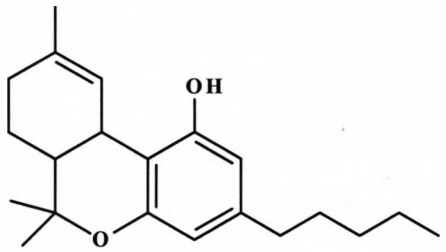


$\Delta^9$-THC
(Delta 9-tetrahydrocannabinol)
Affinity $CB_1$>$CB_2$; a $CB_1$ partial agonist

B

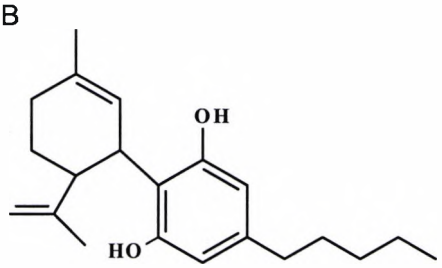


CBD
(cannabidiol)
Affinity $CB_1$>$CB_2$; a $CB_1$ partial agonist

C

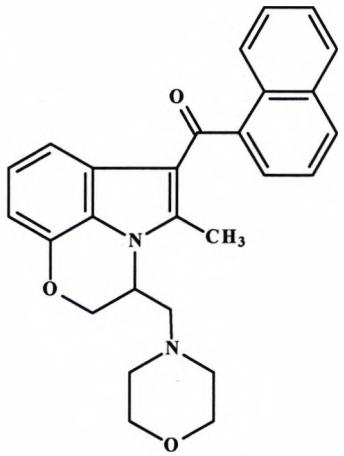


WIN 55, 212-2
Affinity $CB_1$~$CB_2$; a $CB_1$/ $CB_2$ agonist

D

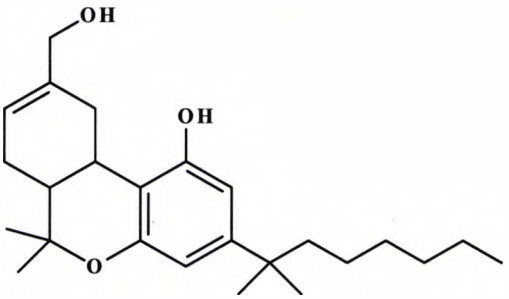


HU-210
(Dexanabinol, Sinnabidiol)
Affinity $CB_1$>$CB_2$ (Concentration ≤1μM); a $CB_1$ agonist

E

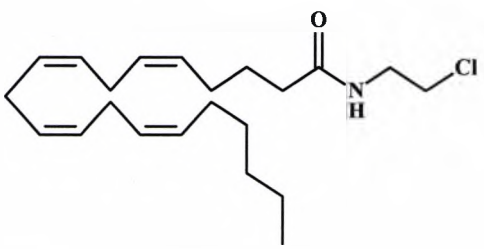


ACEA
(Arachidonyl-2-chloroethylamide)
Affinity $CB_1$>$CB_2$; a $CB_1$-selective agonist

F

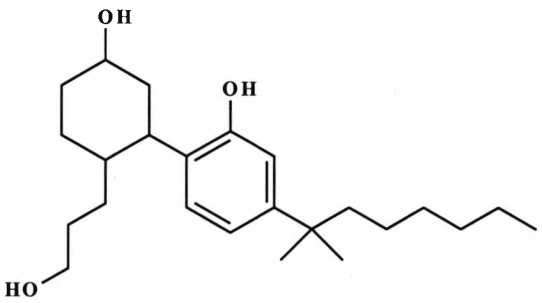


CP-55,940
Affinity $CB_1$~$CB_2$; a $CB_1$/$CB_2$ agonist

G

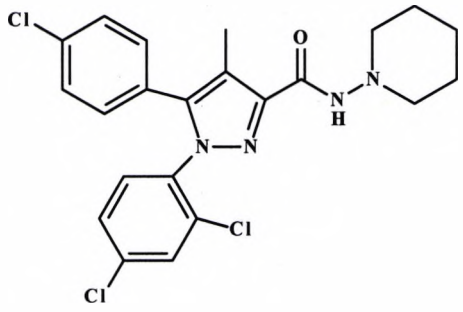

SR141716A
(Rimonabant)
Affinity $CB_1$>$CB_2$; a $CB_1$ selective antagonist

H

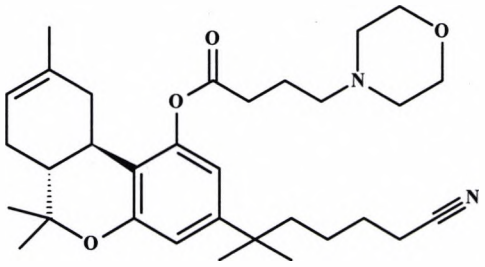

O-1057
($\Delta^8$-tetrahydrocannabinol hydrochloride)
Affinity $CB_1$~$CB_2$; a $CB_1$/$CB_2$ agonist

I

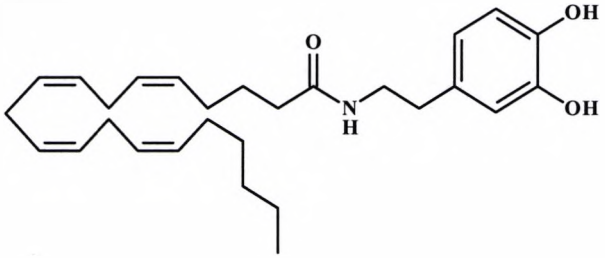

AA-DA
(N-arachidonyl-dopamine)
Affinity $CB_1$>$CB_2$; a $CB_1$ agonist

J

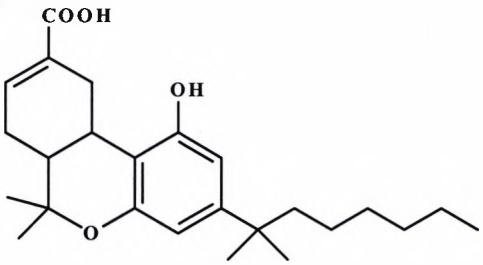

CT-3
(1', 1'-dimethylheptyl-$\Delta^8$-tetrahydrocannabinol-11-oic acid)
Affinity $CB_1$>$CB_2$; a $CB_1$ partial agonist

**Figure 1.9** Cannabinoid structures: $\Delta^9$-THC, CBD, WIN 55, 212-2, HU-210, ACEA, CP-55,940, SR141716A, O-1057, AA-DA, CT-3.

### 1.7.2 Commercially available cannabinoids

As the therapeutic value of cannabinoids is controversial, most of these cannabinoid agents have not broken through the limitation for marketing. Currently, three cannabinoid agonists are available on the international market, however, under tight regulation. They are dronabinol, nabilone, and a cannabis medicinal extract (Sativex™). Dronabinol, a synthetically manufactured THC, is available in the US as a Schedule III controlled substance which is mainly use to stimulate appetite in patients with HIV or suppress chemotherapy-induced nausea and vomiting (Burns and Ineck, 2006). Nabilone is available in Switzerland, the UK, and Canada. This THC analogue is indicated only for themotherapy-induced nausea and vomiting, but its successful use for multiple sclerosis-associated pain and spasticity has been reported (Hamann and di Vadi, 1999). However, these older cannabinoid drugs have considerable drawbacks of producing adverse effects, such as anxiety, confusion, dizzy, and sleepless. Most recently, Sativex™ received the approval (unlicensed) of its medical use in the UK as adjunctive treatment for symptomatic relief of neuropathic pain in adults with multiple sclerosis (Perras, 2005). It is a 1:1 THC:CBD sublingual whole-plant extract. CT-3, or ajulemic acid, is currently under development (Burns and Ineck, 2006). The dramatic therapeutic effects on anti-inflammation and analgesia with tolerable side effects, as discussed above, have made it a promising cannabinoid drug on the near future market. In July 2006, the cannabinoid antagonist Acomplia™ (rimonabant, also known as SR141716) was approved for use as an anti-obesity drug (Pi-Sunyer *et al.*, 2006). Cannabinoid agonists and antagonists are currently being examined as potential treatments for a plethora of additional clinical conditions (Table 1.1).

| | |
|---|---|
| agonists: | |
| – suppression of muscle spasm in MS | (Smith, 2002; Vaney *et al.*, 2004; Williamson and Evans, 2000) |
| – relief of chronic pain | (Herzberg *et al.*, 1997; Tsou *et al.*, 1996) |
| – glaucoma | (Porcella *et al.*, 2001; Stamer *et al.*, 2001) |
| – asthma | (Kasserra *et al.*, 2004, Lunn *et al.*, 2006) |
| – anxiety | (Moreira *et al.*, 2007; Pacher *et al.*, 2006) |
| – anti-emetic | (Sanger and Andrews, 2006; Sharkey *et al.*, 2007) |
| – anti-cancer | (Gustafsson *et al.*, 2006; Joseph *et al.*, 2004) |
| antagonists: | |
| – appetite suppressants/obesity treatment | (Bronander and Bloch, 2007, Sink *et al.*, 2008) |
| – schizophrenia | (Meltzer *et al.*, 2004) |
| – disorders of cognition and memory | (Wise *et al.*, 2007) |
| – addiction | (Filip *et al.*, 2006; Le Foll and Goldberg, 2005) |

**Table 1.1** Cannabinoids as novel therapeutic agents.

## 1.8 Regulation of the $CB_1$ receptor expression in neurodisorders

Mounting evidence demonstrates cannabinoids act as $CB_1$ agonists to produce neuroprotective effects. Attention has been focused on the changes of $CB_1$ receptor expression in various neurodisorders which may vary the expected therapeutic effect of cannabinoids. $CB_1$ receptor regulation caused by pharmacological treatment, pathological condition, and/or genetic modification does not necessarily follow a similar pattern.

In glucocorticoid-deprived rats, the $CB_1$ level was up-regulated by 50% in the caudate putamen(Mailleux and Vanderhaeghen, 1993). Increased $CB_1$ mRNA was observed in a rat model of chronic neuropathic pain (Siegling *et al.*, 2001). Intestinal inflammation has been found to upregulate $CB_1$ mRNA levels (Izzo *et al.*, 2001). Furthermore, cerebral artery occlusion-induced experimental stroke was found to enhance the $CB_1$ protein level in the ischemic tissue within a short term (Jin *et al.*, 2000). In a human study, patients with schizophrenia showed increased levels of $CB_1$ mRNA in the dorsolateral prefrontal cortex (Hakak *et al.*, 2001). From these findings the expression of $CB_1$ is likely enhanced in an effort to deal with degenerated biological function.

However, a down-regulation of $CB_1$ expression has been demonstrated in other cases. Chronic alcohol exposure leads to decreased $CB_1$ level in mice, indicating the involvement of $CB_1$ in alcohol tolerance and dependence (Basavarajappa *et al.*, 1998). Studies in patients diagnosed with Huntington's disease which is characterised by motor dysfunction, personality changes, dementia and premature death showed a reduction in cannabinoid receptor ligand binding in basal ganglia output nuclei and the substantia nigra pars reticulata compared to the neurologically normal controls prior to the

development of other identifiable neuropathology (Richfield and Herkenham, 1994; Glass *et al.*, 1993; Glass *et al.*, 2000). Consistent with the findings from human studies, mouse models of Huntington's disease exhibit reduced $CB_1$ receptor in basal ganglia (Glass *et al.*, 2004) and decreased $CB_1$mRNA in the subset of neurons, the lateral striatum, cortex and hippocampus (Denovan-Wright and Robertson, 2000). The observation of the loss in $CB_1$mRNA was also extended to another neurological disorder in the striatum of a rat model of Parkinson's disease (Silverdale *et al.,* 2001). In nitric oxide synthase (NOS)-knockout animals, a low level of $CB_1$mRNA was found in the ventromedial hypothalamus (VMH) and the caudate putamen (Cpu) which are the regions involved in cannabinoid-induced thermoregulation and decrease of locomotion (Azad *et al.,* 2001). These findings suggest that decreased $CB_1$ receptors may account for the pathogenesis and progression involved in neurodegenerative diseases.

At the outset of this thesis, no-one had previously examined the level of $CB_1$ receptor expression in diabetes. Two studies published in 2004 demonstrated the anti-nociceptive action of a mixed cannabinoid $CB_1/CB_2$ receptor agonist is preserved in diabetic mice (Dogrul *et al.,* 2004) and rats (Ulugol *et al.,* 2004). A clearer understanding of the role of $CB_1$ receptor in a model of diabetic neuropathy would be valuable for potentially relieving and reversing this complication of diabetes.

## 1.9 The role of $CB_1$ and its regulation with TRPV1

There is some evidence to suggest that the balance of $CB_1$- versus TRPV1-mediated responses is tipped unfavourably towards TRPV1 in diabetes. As described earlier, several studies have shown that TRPV1 is sensitised by PKC in diabetics. Interestingly, PKC disrupts $K^+$ current to downregulate $CB_1$ activation, while it sensitises TRPV1 receptors (Garcia *et al.,* 1998). Ellington and colleagues (2002) examined anandamide-induced inhibition of capsaicin-evoked CGRP release in rat paw skin from control and diabetic rats (Ellington *et al.,* 2002). They found anandamide inhibited CGRP release only in skin from non-diabetic animals, and furthermore, actually stimulated CGRP release in skin from diabetic rats when tested at higher concentrations. These data suggest anandamide action at TRPV1 receptors overcomes the inhibitory action mediated by $CB_1$ receptors in diabetes. Even if TRPV1 activation evokes synthesis and release of anandamide, as has been demonstrated in cultured DRG (Ahluwalia *et al.,* 2003), this will only serve to enhance TRPV1 signalling under conditions where $CB_1$ receptors are down-regulated. A differential regulation of TRPV1 versus $CB_1$ receptors remains to be determined, but there are clear implications of a decreased $CB_1$ action and/or increased TRPV1 action in the pathogenesis of neuropathy.

Therefore, the actions of TRPV1 and $CB_1$ receptors are relevant to mechanisms of neurodegeneration and neuroprotection, and their regulation needs to be explored, the understanding of which will be helpful for improvement of analgesic drugs.

## 1.10 Aims and Hypothesis

At the outset of this thesis it was hypothesised that, firstly, a decline in $CB_1$ receptor expression contributes to the neurodegenerative process observed in diabetic neuropathy. Secondly, a decrease in $CB_1$ receptor expression could result in attenuated nerve cell responses to a $CB_1$ agonist under hyperglycaemic conditions.

The specific aims arising from the above hypotheses were:

1. To validate PC12 as an *in vitro* cell model of diabetic neuropathy;
2. To examine $CB_1$ receptor expression in the *in vitro* model of diabetic neuropathy, at the mRNA and protein level, and compare this to expression in neurons from diabetic rats.
3. To investigate the function of $CB_1$ receptors and $CB_1$-mediated neuroprotective effects in the in vitro model of diabetic neuropathy.

# CHAPTER 2

# MATERIALS AND METHODS

## 2.1 Introduction

This chapter details all the methods and materials which have been used in this project. A variety of molecular biology and toxicology techniques were carried out in order to investigate the effect of hyperglycemia on expression and function of cannabinoid $CB_1$ receptors, and the neuroprotective effect of cannabinoid $CB_1$ receptor agonists.

In this project, the rat pheochromacytoma PC12 cell line was validated and used as an *in vitro* model of diabetic neuropathy to study the expression and function of $CB_1$ receptors regulated by high glucose. Diabetic rat doorsal root ganglion (DRG) neurons obtained from Michigan University in USA were used as *in vivo* model to confirm the findings from PC12 cells.

## 2.2 PC12

PC12 (purchased from European Collection of Animal Cell Cultures) is a rat cell line derived from pheochromacytoma which is a tumour of the adrenal gland. PC12 is a commonly used neuronal model in terms of its ability to differentiate into a neuronal phenotype with nerve growth factor (NGF) stimulation. PC12 cells were grown as non-adherent cells in RPMI 1640 medium (Sigma) supplemented with 10% foetal calf serum, 1% penicillin/streptomycin antibiotic mixture and 1% L-glutamine solution (all purchased from Invitrogen, UK). They were maintained at 37°C in a humidified atmosphere of 5% carbon dioxide in air, and split once or twice per week. The cells were collected by centrifugation at 2500g for 5 minutes and the pellet was then suspended in fresh medium.

## 2.3 Experimental Animals

Male Sprague-Dawley rats were housed in the animal facility of the University of Michigan Unit for Laboratory Animal Medicine, which was maintained at 22 °C, 55% relative humidity, with an automatic 12-h light/dark cycle. The animals received a standard laboratory diet and tap water *ad libitum*. All experiments were approved by the University of Michigan Committee on Use and Care of Animals according to the National Institutes of Health guidelines. Diabetes mellitus was induced by a single intraperitoneal injection of streptozotocin (STZ, 45 mg/kg) to 180–200g rats that had been fasted overnight to maximize the effectiveness of STZ treatment. STZ solution was prepared fresh by dissolving it in 0.1M citrate buffer, pH 5.5. Age matched control rats were injected with citrate buffer alone. The diabetic condition was assessed by glucose levels greater than 300mg/dl (16.7mM). Rats meeting this criterion were used experimentally 4–8 weeks after STZ induction. (Performed by Dr Shuangsong Hong, University of Michigan).

## 2.4 Preparation of varying glucose solution

As an *in vitro* model of diabetic neuropathy, glucose (Sigma, UK) was used to simulate hyperglycaemic conditions. Glucose solution stocks of 45,145,245,345,445mM were prepared in sterilised water, and then autoclaved. 10% of these glucose solutions were added to supplement dulbecco's modified eagles medium (DMEM; Sigma, UK) containing 5.5mM glucose (Sigma, UK) to achieve final glucose concentrations of 5.5 (physiological glucose level), 10,20,30,40,50mM.

## 2.5 Preparation of NGF solution

NGF (0.1mg; Sigma, UK) was diluted to 5ng/µl in DMEM medium and stored in aliquots at -20°C.

## 2.6 Plating PC12 cells

Prior to use, 6-well or 24-well plates were coated with poly-L-lysine (0.02%; Sigma, UK) which creates an adhesion surface for cells. Poly-L-lysine was left for 30 minutes and removed. The plates were then rinsed by $dH_2O$ and left to dry overnight under UV light. The following day, PC12 cells were seeded in 6-well or 24-well plates at density of $1x10^5$ cells/ml (2ml or 1ml per well in total, respectively). The cells were quantified by haemocytometer counts and the viability was determined using 2% trypan blue solution (Sigma, UK). With the exception of glucose 5.5mM (achieved by DMEM medium only), 10% of each glucose concentration (200µl) was added to each well and then supplemented by 10% FCS (200µl) and 50ng/ml NGF (20cl of 5ng/µl NGF). DMEM medium was finally added to bring the total volume to 2ml in each well. The plates were labelled as shown below and then incubated at 37°C in a humidified atmosphere of 5% carbon dioxide in air.

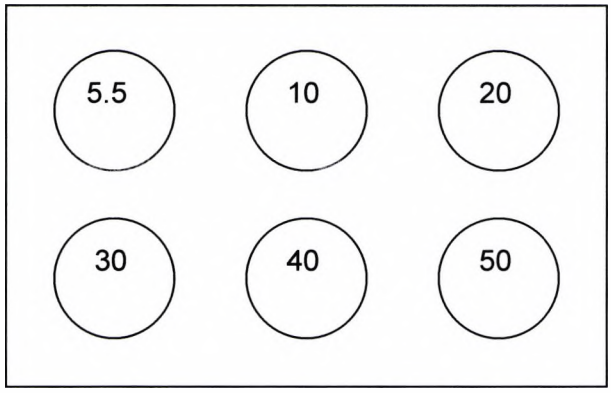


The medium and factors were changed every two days.

## 2.7 Morphology study (measurement of neurite length)

Neurite outgrowth of PC12 cells was examined at increasing glucose concentrations 5.5 to 50mM and osmotic controls (mannitol 30 and 50mM). The neurite outgrowth of PC12 cells was apparent after 4 days of treatment with NGF. Photographs were taken from three random fields from each well using a digital camera (SONY) installed to a light microscope (Zeiss Axiovert 25). The neurite length and cell body diameter in each picture was measured using the Metamorph™ programme (Universal Imaging Corporation) and analysed in ExcelTM.

Example photograph

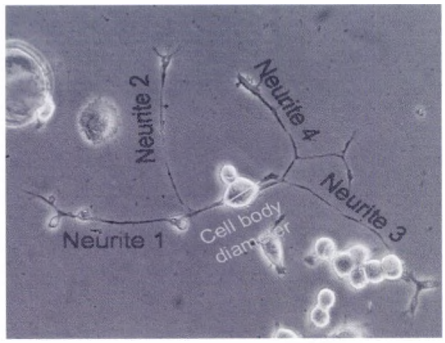


Metamorph™

The total neurite length was expressed as sum (length of each individual neurite) / cell body diameter to exclude the influence of magnification. The

longest neurite length was expressed as length of longest neurite of individual cell / cell body diameter.

## 2.8 Oxidative stress study (GSH/GSSG estimation)

### 2.8.1 Introduction

The method of Akerboom and Sies (1981) was adopted to examine oxidative stress in the cell model. Reduced glutathione (GSH) is a major natural antioxidant in human tissues, protecting the body by reduction of free radicals. Oxidised glutathione (GSSG) is then recycled into GSH by glutathione reductase and NADPH. However, excessive oxidative stress will disturb the balance and result in decreased GSH/GSSG ratio as a consequence of GSSG accumulation. Therefore, GSH/GSSG ratio is a significant indicator to estimate oxidative stress (Hissin and Hilf, 1976). PC12 treated with 5.5-50mM glucose, as described in section 2.6, were used to investigate the oxidative stress introduced by hyperglycaemia.

### 2.8.2 Cell extraction

Medium was removed from wells, which were then washed with 2ml of ice cold PBS before adding 250ml of 9mM ice cold EDTA/perchloric acid (75.2mg $Na_2EDTA$ dissolved in 20ml 14% perchloric acid). After the cells were lifted using a scraper, the plates were then incubated on ice for 15 minutes. The mixture from each well was transferred to separately labelled eppendorf tubes and centrifuged at 10,000g for 5 minutes at 4°C; 170µl of supernatant was transferred to clean eppendorfs and then filled up with 125µl neutralizing solution (1M KOH+1M $KHCO_3$). Extensive foam was formed by tapping the

bottom of the tubes. After full neutralization, the eppendorfs were centrifuged at 10,000g for 5 minutes at 4°C. The supernatant was transferred to clean eppendorfs and then placed on ice for assay on same day or stored at –80°C.

### 2.8.3 GSH assay

GSH stock (0.5mM; Sigma, UK) was made up in sodium phosphate/EDTA buffer (0.1M sodium dihydrogen orthophosphate ($NaH_2PO_4.2H_2O$) 0.005M EDTA pH8), from which a series of GSH standards were achieved: 0, 1.5625, 3.125, 6.25, 12.5, 25µM.

After 100µl of the samples were mixed with 1.8ml $NaH_2PO_4.2H_2O$/EDTA buffer, 100µl O-phthaldehyde (1mg/ml OPT in methanol; Sigma, UK) was added to the mixture. Following an incubation for 15 minutes at room temperature, 200µl of the mixture was then transferred into a white wall/clear bottom 96-well plate (Porvair, UK), in triplicate, which was read immediately in a fluorescence plate reader (BMG Lab Technologies, UK) at an excitation of 350nm and emission 420nm. The unknown samples were calculated from the constructed standard curve.

### 2.8.4 GSSG assay

In a similar procedure to the GSH assay, 0.5mM GSSG (Sigma, UK) was made up in 0.1M NaOH as the stock, from which GSSG standards were achieved: 0, 1.5625, 3.125, 6.25, 12.5, 25µM.

Different from the GSH method, 100µl of the samples were first mixed with 40µl prepared 0.04M N-ethyl-maleimide ((NEM) 0.05g NEM dissolved in 10ml $NaH_2PO_4$· EDTA buffer; Sigma, UK). Following 30 minutes of incubation at

room temperature, 100µl of the NEM treated extract was mixed with 1.8ml NaOH (0.1M) before adding 100µl of OPT. After a further 15 minutes incubation at room temperature, the samples were transferred and read immediately as described in GSH detection.

## 2.9 Lactase Dehydrogenase (LDH) assay

The LDH assay assesses cellular toxicity which is based on the theory that the soluble cytosolic enzyme (LDH) is released from cells into culture medium following loss of membrane integrity. Culture medium collected every two days from PC12 cells cultured in the presence of glucose (5.5, 30 and 50mM) with NGF (50ng/ml) was used to test LDH activities. After loading 10µl of the test supernatants to a 96-well plate in triplicate, 50µl of 1mg/ml NADH (diluted in 0.75mM sodium pyruvate; Sigma, UK) was added to the supernatant-containing wells, whilst 60µl of standard solutions with LDH activity (0-2000units/ml) were also included in the separate wells. Following exactly 30 minutes-incubation at 37°C, 50µl of 2,4-dinitrophenylhydrazine was added to each well and incubated for a further 20 minutes at room temperature. Diluted NaOH (4N) was finally added to all wells, and after 5 minute-incubation, the plate was read immediately at 540nM in a plate reader (Dynex spectrophotometer Revelation 4.25). The supernatant from Triton-X (0.1%)-treated cells was used as a positive control and considered as 100% cell lysis.

## 2.10 MTT assay

MTT assay measures cell viability and it is based on enzyme reduction of MTT (3-(4,5-dimethylthiazol-2-yl)-2,5-diphenyltetrazolium bromide) in living cells, since yellow MTT can be reduced to purple formazan only when mitochondrial reductase enzymes are active. The purple-coloured solution in DMSO is

measured colourimetrically, which is related to the viable cells.

PC12 cells ($1\times10^5$ cells/ml) were cultured in 24-well plates in the presence of glucose (5.5-50mM) and mannitol (30,50mM) under the stimulation of NGF for 6 days prior to this assay. MTT stock (5mg/ml; Sigma, UK) was prepared in PBS and filtered before use. To a 24-well plate, 100µl of the stock solution was added to each well containing cells and 1.0ml medium (final concentration=0.5mg/ml). Following a 4.5 hour incubation at 37°C, the wells were aspirated before 500µl of DMSO was added to each well and mixed to dissolve crystals. The mixture was incubated for 5 minutes at 37°C for a complete dissolution, from which 250 µl of the solution per well was finally transferred to a 96-well plate, and read in Dynex spectrophotometer at 550nm.

### 2.11 Measurement of osmolality

The increase in osmolality in PC12 culture medium caused by high glucose was assessed. A series of glucose/mannitol stocks was diluted 10 fold in DMEM to give a range of glucose concentrations (5.5, 10, 20, 30, 40, 50mM) and mannitol concentrations (30, 50mM). The osmolality was measured in an osmometer (model 3D3, Advanced Instruments Inc., USA; provided by Dr. David Wyllie, University of Edinburgh)

### 2.12 Measurement of glucose concentration

The glucose consumed by PC12 cells after 2 days of culture was determined by measuring the glucose concentration from aspirated culture medium from various glucose/mannitol treatments using a Glucose (GO) Assay Kit (Sigma; performed by Dr. Paula Smith, Napier University).

## 2.13 Bradford protein assay

The Bradford protein assay is a colourimetric assay based on the observation that the absorbance maximum for an acidic solution of Coomassie Brilliant Blue G-250 shifts from 465 nm to 595 nm when bound to arginine and hydrophobic amino acid residues present in protein. The absorbance is proportional to the protein concentration present in samples, so that the unknowns can be easily calculated according to standards set up in parallel.

The protein concentration was measured in PC12 cells cultured in various concentrations of glucose on day 6 of culture. After removal of culture medium, 320µl of Triton-X 100 (0.1%) was added into each well and then incubated for 5 minutes at room temperature. The cells were mixed into the solution and then transferred into eppendorfs. After centrifuging at 10,000g for 3 minutes, 10µl of supernatant of unknown samples was added into individual wells of a 96-well plate. A series of standards was made from BSA (1mg/ml; Sigma, UK) stock to give a range of 500, 250, 125, 62.5, 31.25, 15.6 mg/ml (i.e. 500µl of 1mg/ml stock and added to 500ul water, to give 500mg/ml solution, and so on). After 10µl of prepared BSA standards was pipetted into assigned wells of the same 96-well plate, all wells containing standard and samples were filled up with 200µl of diluted Bradford Reagent (1 Reagent+4 distilled $H_2O$). The plate was read immediately in a plate reader at 595nm (Dynex 3.04).

## 2.14 Enzyme Linked-Immuno-Sorbent Assay (ELISA)

### 2.14.1 Introduction

ELISA is a solid phase sandwich enzyme linked immuno-sorbent assay. Rat IL-6 is captured by the immobilized antibody that has been coated onto the wells

provided. A biotinylated antibody specific for rat IL-6 is added in order to bind to the captured rat IL-6 antigen. An enzyme is added, binding to the biotinylated antibody. A substrate solution is finally added to react with the enzyme, which produces colour. The intensity of coloured product indicates the concentration of rat IL-6 (Biosource International, UK).

### 2.14.2 Sample preparation

Samples were collected from the medium in which the PC12 cells were cultured with increasing glucose concentrations (5.5-50mM). The samples were placed on ice for use same day or stored at –80 °C.

### 2.14.3 IL-6 examination

The ELISA kit was purchased from Amersham Biosciences. Standard solutions were serially diluted from 10,000pg/ml reconstituted standards to 0, 31.2, 62.5, 125, 250, 500, 1000, 2000pg/ml in standard dilutant buffer.

50µl standards and samples were added to each well in duplicate after 50µl sample diluent buffer was added to each well. The plate was covered tightly by an adhesive plate cover and then incubated for 2 hours at room temperature. The plate was aspirated and washed three times with wash buffer (x1). Addition of 100µl of the biotinylated antibody reagent was applied to all wells. The plate was sealed again and left at room temperature for 1-hour incubation. During the incubation, Streptavidin-Horseradish Peroxidase Conjugate (HRP) solution was prepared as 3:2 dilution with streptavidin-HRP concentrate and buffer. After the incubation, the plate was aspirated and 100µl prepared streptavidin-HRP solution was then added. After 30 minutes incubation, 100µl of tetramethylbenzidine (TMB) substrate solution was pipetted into each well. A

blue colour was produced at room temperature for 30 minutes without plate cover. After 30 minutes incubation, 100µl of stop solution was finally added to each well, which allowed the blue colour to turn yellow. The absorbance was measured using a plate reader (Dynex 3.04) at 450nm.

### 2.15 RT-PCR for detection of mRNA expression

Conventional reverse transcription-polymerase chain reaction (RT-PCR) was performed to screen the mRNA expression of TRPV1 and $CB_1$ genes. PC12 cells were plated as described in section 2.6.

#### 2.15.1 RNA extraction

RNA was extracted from differentiated PC12 cells. Hyperglycaemic cells (differentiated) cultured in 6-well plates were lysed in TRI Reagent (0.5ml per well; Sigma, UK) for 5 minutes. The cells were lifted using a cell scraper and then transferred to eppendorfs for the next extraction.

The homogenate was supplemented with 0.2ml chloroform, followed by vigorous shaking for 15 seconds. The samples were then stored at room temperature for 2-15 minutes and centrifuged at 10,000g for 15 minutes at 4°C. After centrifugation, an upper aqueous phase was transferred and mixed with 0.5ml isopropanol. The samples were stored at room temperature for 5-10 minutes. A gel-like RNA precipitate was formed after centrifugation at 10,000g for 8 minutes at 4°C. The RNA pellet was washed with 70% absolute ethanol (BDH) and then sedimented by centrifugation at 7,500g for 5 minutes at 4°C. The washed RNA pellet was dried briefly and finally suspended in nuclease-free water. The RNA concentration was measured using a DU® 800 spectrophotometer (BECKMAN COULTER) at 260nm, and the purity was

expressed as the ratio 260/280nm. The yield of RNA was calculated using the equation below:

RNA (ng/µl) = Absorbance x 40ng/µl x Dilution Factor

The RNA samples were placed on ice to use on the same day or stored at -80°C.

### 2.15.2 Two step RT-PCR reaction

For the RT reaction, AMV reverse transcriptase, deoxynucleotides (dNTPs), Random Nonamer oligodeoxyribonucleotides and 2xAMV Buffer (final concentration, 50mM Tris-HCl (pH 8.3 at 25°C), 50mM KCl, 10mM $MgCl_2$, 0.5mM spermidine, 10mM DTT) were all purchased from Promega. An RT master mix was set up as outlined in the Table 2.1 by applying 1µg of prepared RNA for each reaction.

For the PCR reaction, each cDNA was added to a PuReTaqTM Ready-To-GoTM PCR Bead containing ~2.5U PuReTaq DNA polymerase, 200µM dNTPs, and Reaction Buffer (10mM Tris-HCl, (pH 9.0 at room temperature), 50mM KCl, 1.5mM MgCl2, stabilizers, and BSA), together with 125pmol specific primers for $CB_1$ (sense: 5'-ATGAAGTCGATCCTAGATGGCCTTG-3'; antisense: 5'-GTTCTCCCCACACTGGATG-3', Zhuang *et al.,* 1998) (MWG-Biotech AG, Germany) or rat β-actin (R&D Systems Europe Ltd.), to a final volume of 25µl. All the reagents were allowed to thaw at room temperature, spun down and placed on ice for use. A PCR master mix was set up as outlined in the Table 2.2. The tubes were gently mixed, spun down and then placed into a PCR thermal cycler (Thermo Scientific Hybaid PCR Sprint Thermal Cyclers). The RT and PCR programmes were optimised as described in Table 2.3.

| Reagents | × 1 | Master Mix |
|---|---|---|
| **Buffer** | 10 µl | **× samples+1** |
| **dNTP** | 1 µl | **× samples+1** |
| **Random Nonamers (2µM)** | 1 µl | **× samples+1** |
| **AMV Reverse Transcriptase (1U)** | 1 µl | **× samples+1** |
| **RNA** | 2-10ul | |
| **Nuclease-free $H_2O$** | x µl (adjust to 25µl) | |

**Table 2.1** The volume of reagents required to prepare one reaction and master mix for reverse transcription.

| Reagents | × 1 | Master Mix |
|---|---|---|
| **Sense primer (200nM)** | 1 µl | **× samples+1** |
| **Anti-sense primer (200nM)** | 1 µl | **× samples+1** |
| **PuReTaq™ Ready-To-Go™ PCR Beads** | 1 | |
| **cDNA** | 5 µl | |
| **Nuclease-free $H_2O$** | 18 µl (adjust to 25µl) | |

**Table 2.2** The volume of reagents required to prepare one reaction and master mix for PCR amplification.

**Two step RT-PCR thermal cycle programme:**

| | | | |
|---|---|---|---|
| **1)** | **RT Step for 1 cycle** | **Incubation** | **48°C for 45 minutes** |
| **2)** | **PCR step for 30 cycles** | **Hot start** | **95°C for 2 minutes** |
| | | **Denaturation** | **95°C for 30 seconds** |
| | | **Annealing** | **62°C for 1 minute** |
| | | **Elongation** | **68°C for 2 minutes** |
| **3)** | **Final elongation step** | | **68°C for 7 minutes** |
| **4)** | **Cooling for 1 cycle** | | **20°C for 1 minute** |
| | | | **4°C for 8 hours** |

**Table 2.3** Time and temperature scale for PCR thermal cycle reaction.

### 2.15.3 Examination of PCR products

The samples were analysed using gel electrophoresis. The amplified cDNA fragments migrated to different distances according to the different lengths, as monitored by a DNA marker (Roche). A 1.5% agarose gel (Bio-Rad) was prepared in 50µl of TBE buffer (×1) with addition of 1mg/µl of ethidium bromide (Sigma). 16µl of PCR products premixed with 4µl of loading buffer were loaded to the gel and then left to run at 100 volts for 45 minutes. 2µl of DNA marker was run in parallel. After the electrophoresis completed, the DNA bands were visualised under UV light and photographed using a digitalised gel documentation and analysis system (GeneSnap and Gene Tools from SynGene, Cambridge UK).

## 2.16 Real time PCR LightCycler

### 2.16.1 Introduction

The LightCycler system is a fluorescence-based method. Compared to conventional RT-PCR, real time PCR has the great advantage of monitoring the formation of products throughout the reaction. The fluorescent dye SYBR Green I binds to the double-stranded DNA and produces a detectable fluorescence. However, the unbound single stranded DNA exhibits very little fluorescence. Therefore, the more DNA amplified, the greater fluorescence obtained. The fluorescence is measured at the end of the elongation step to monitor the increasing amount of amplified DNA. A melting curve analysis is able to separate the signal for specific product from unspecific product. $CB_1$ was detected using a Roche LightCycler® 2.0 Instrument machine. Beta-actin was used as the reference gene to normalise the detected $CB_1$ mRNA expression.

### 2.16.2 Real time PCR reaction

The RNA samples and cDNA were prepared as described in section 2.15.1 and section 2.15.2. SYBR Green Taq ReadyMix™ containing 20mM Tris-HCl (PH 8.3), 100mM KCl, 7mM $MgCl_2$, 0.4mM each dNTP, stabilizers, passivator, 0.05unit/μl *Taq* DNA Polymerase, JumpStart Taq antibody, and SYBR Green I was purchased from Sigma. The specific primers for $CB_1$ and β-actin were purchased from SuperArray Bioscience. A PCR master mix was set up as described in Table 2.4, gently mixed and spun down. Each sample was transferred to a glass capillary tube and then spun down using a capillary centrifuge (Roche). The amplification of target DNA sequences was monitored using a PCR LightCycler system (Roche). The programme was optimised as described in Table 2.5. The PCR product was analysed using Roche LightCycler data analysis software.

| Reagents | × 1 | Master Mix |
|---|---|---|
| **SYBR Green Taq ReadyMix** | 10μl | **×samples +1** |
| **Primers (500nM)** | 1μl | **×samples +1** |
| **cDNA** | 5μl | |
| **Nuclease-free $H_2O$** | 4μl | |
| | (adjust to 20μl) | |

**Table 2.4** The volume of reagents used to prepare one reaction and a master mix for real time PCR

**PCR light cycler programme:**

| | |
|---|---|
| **Denaturation** | **Denaturation 94°C for 30 seconds** |
| **for 1 cycle** | **(Temperature transition rate 20°C/Sec)** |
| **Followed by** | |
| **PCR step for 58 cycles** | **Denaturation 94°C for 0 seconds** |
| | **(Temperature transition rate 20°C/Sec)** |
| | **Annealing 55/58°C for 5/10 seconds** |
| | **(for $CB_1$ and β-actin respectively)** |
| | **(Temperature transition rate 20°C/Sec)** |
| | **Elongation 72°C for 10/13 seconds** |
| | **(for $CB_1$ and β-actin respectively)** |
| | **(Temperature transition rate 20°C/Sec)** |
| **Followed by** | **95°C for 0 seconds** |
| **Melting curve for 1 cycle** | **(Temperature transition rate 20°C/Sec)** |
| | **60°C for 1 minute** |
| | **(Temperature transition rate 20°C/Sec)** |
| | **95°C for 0 second** |
| | **(Temperature transition rate 0.10°C/Sec)** |
| **Followed by** | |
| **Cooling for 1 cycle** | **40°C for 30 seconds** |
| | **(Temperature transition rate 20°C/Sec)** |

**Table 2.5** Time and temperature scale for PCR light cycler reaction.

## 2.17 Detection of expressed $CB_1$ and TRPV1 receptor protein in cultured PC12 cells

The expression of $CB_1$ and TRPV1 at the protein level was examined in differentiated PC12. Primary antibodies (rabbit anti-rat TRPV1 and goat anti-rat $CB_1$) and fluorochrome-conjugated secondary antibodies (FITC-anti-rabbit and Rhodamine-anti-goat) were all purchased from Santa-Cruz Biotechnology Ltd.

Confocal imaging and densitometric analysis of immunofluorescence were used to detect differences in protein expression between the groups with varying glucose concentrations. The cells were grown on sterilised glass coverslips at a density of $1\times10^5$ cells/ml in the presence of glucose as described in section 2.6.

The cultured cells were washed briefly with PBS mixture (PBS×1 with 0.3% BSA and 10mM EDTA) and then fixed with 4% paraformaldehyde (diluted in PBS×1) for 30 minutes. The specimens were incubated with 10% normal blocking serum (donkey serum in PBS mixture) for 20 minutes to suppress non-specific binding of IgG. After washing with PBS once, the specimens were incubated with 0.3μg/ml primary antibody (200μg/ml diluted in PBS mixture) for 2 hours, which was followed by washing with three changes of PBS mixture for 10 minutes each. The specimens were incubated again with fluorochrome-conjugated 0.3μg/ml secondary antibody (200μg/ml diluted in PBS mixture) and then washed with three changes of PBS mixture for 10 minutes each. The coverslips with specimens were mounted with mowoil on glass slides. The slides were examined using a confocal laser-scanning microscopy (Zeiss LSM-510) on the next day or stored in a dark location at room temperature for up to one week.

## 2.18 Detection of $CB_1$ receptor protein associated with C/Aδ fibres in diabetic and control DRG samples

The protein expression of $CB_1$ receptors alone or associated with C/Aδ nerve fibres was examined in formalin-fixed paraffin-embedded DRG tissue samples (supplied by Dr Shuangsong Hong, Michigan University, USA).

An antigen retrieval step was conducted prior to immunohistochemistry staining. The sample sections were deparaffinized in 3 changes of xylene for 5 minutes each, which was followed by rehydration in two changes of 100% alcohol and one change of decreasing concentration of alcohol (90%, 70%, 50%, 30%) for 5 minutes each. The sample section was kept in distilled water until the next step was ready.

Sodium citrate buffer comprised of tri-sodium citrate 0.294% (W/V), 0.2M hydrochloric acid solution 2.2% (V/V) in distilled water, and was adjusted to pH 6.0 using sodium hydroxide and hydrochloric acid. A microwaveable vessel containing the buffer solution and the sample slides was heated in a microwave (Proline) set to full power for 15 minutes after the solution came to boil. The buffer solution was then allowed to cool down for 20 minutes before the slides were washed in distilled water and once in PBS.

For immunohistochemistry staining, the sections were incubated in 0.3% Triton X-100 in PBS Tween (0.1%; PBST) for 2 hours and then briefly washed in PBST. 10% donkey serum (Sigma, UK) in PBST was used to block the sections to suppress non-specific binding for at least 4 hours. After being washed in one change of PBST and 2 changes of PBS for 5 minutes each, the sections were incubated with primary antibodies diluted in PBST: rabbit anti-rat $CB_1$ (1:300;

Sigma) alone or together with mouse anti-rat peripherin (1:500; Sigma), at 4°C overnight. The next day, the sections were washed in one change of PBST and two changes of PBS for 5 minutes each, and subsequently incubated with secondary antibodies: donkey anti-rabbit-rhodamine (1:80; Santa-Cruz Biotechnology Ltd) or together with goat-anti mouse-633 (1:400; Molecular Probes) for two hours in the dark. Again, the sections were washed in one change of PBST and two changes of PBS for 5 minutes each. Finally, mowoil and clean coverslips were mounted onto the sections to preserve fluorescence. The stained DRG sections were examined using a confocal microscope (Zeiss LCM-510) on the next day.

## 2.19 $Ca^{2+}$ influx study

### 2.19.1 Introduction

Fluo-3 AM/Fluo-4 AM is an acetoxymethyl ester derivative of fluo-3 which is a calcium probe. The AM form helps fluo-3 easily penetrate into cells by a certain time of incubation and then subsequently is cleaved off by hydrolysis. Fluo-3 is non-fluorescent in its free-ligand form, but the fluorescence increases more than 100 times on binding to calcium. Importantly, fluo-3 has an absorption spectrum compatible with excitation at 488nm by argon-ion laser sources, so that it has been widely used in conjunction with a confocal microscopy (Zeiss LCM-510).

### 2.19.2 Detection of intracellular $Ca^{2+}$ increase

Coverslips (42 mm) were pre-coated with poly-L-lysine, washed with $dH_2O$ and dried in petri dishes overnight before use. PC12 cells were plated at a density of $1\times10^5$ cells/ml (3ml in total) with or without the treatment of high glucose

(50mM), under the stimulation of NGF (50ng/ml) for 6 days.

As illustrated in Figure 2.1, on the $6^{th}$ day, the coverslip containing cells was washed using HEPEs buffer/saline three times and then incubated with 5μM fluo-3 AM or 3μM fluo 4-AM mixed with 0.02% pluronic F-68 for 40 minutes at 37°C.

To study TRPV1 receptor-mediated $Ca^{2+}$ entry, after washing off excessive dye, the coverslip containing cells was transferred to a confocal live imaging chamber and filled up with 500μl fresh HEPEs buffer saline. A confocal microscope (LSM Zeiss 510) with the filter sets: 488nm for excitation and 548nm for emission, was used for the fluorescence measurement. X-Y frame scan were adopted with the time series of 3.93 second intervals.

Firstly, a concentration-response curve to the TRPV1 receptor agonist capsaicin (1–700μM; Tocris Biosciences) was carried out in several control conditions. Capsaicin was added after 118 second-baseline scan and the capsaicin activation was monitored for a further 275 seconds. Subsequent experiments used a concentration of capsaicin which produced ~50% of the maximum response. To confirm that the capsaicin-evoked $Ca^{2+}$ influx was mediated by TRPV1 receptors, the effect of capsazepine (100μM; Tocris Biosciences), a competitive TRPV1 antagonist, was tested. To assess the potential for the $CB_1$ receptor agonist HU210 (Tocris Biosciences) to inhibit the capsaicin-evoked increase in $[Ca^{2+}]_i$, the response to capsaicin (300μM) alone or following 10 minutes pre-treatment with HU210 (0.03-30μM) was measured in separate experiments (to exclude possibility of TRPV1 desensitization) until

the fluorescence returned to baseline. The selective $CB_1$- and $CB_2$-receptor antagonists, AM251 (1μM) and AM630 (1μM) (both from Tocris Biosciences) respectively, were co-administered with HU210 in some experiments to establish the receptor subtype mediating the inhibitory action of HU210. KCl (70mM) was added at the end of each experiment to confirm cells were still viable. Only those cells responding to KCl were included in the analysis, and data expressed as a percentage of the KCl-evoked increase in fluorescence for each cell. All drugs were initially prepared as stock solutions in DMSO: fluo-3 AM/fluo-4 AM 1mM, capsaicin 50mM, capsazepine 100mM, HU210 100mM, AM251 100mM, AM630 100mM. HEPEs buffer/saline contains 120mM NaCl, 4.7mM KCl, 1.2mM $K_2HPO_4$, 1.2$MgSO_4$, 5.5mM D-Glucose, 10mM HEPE's and $CaCl_2$ 1.25mM/2.5mM.

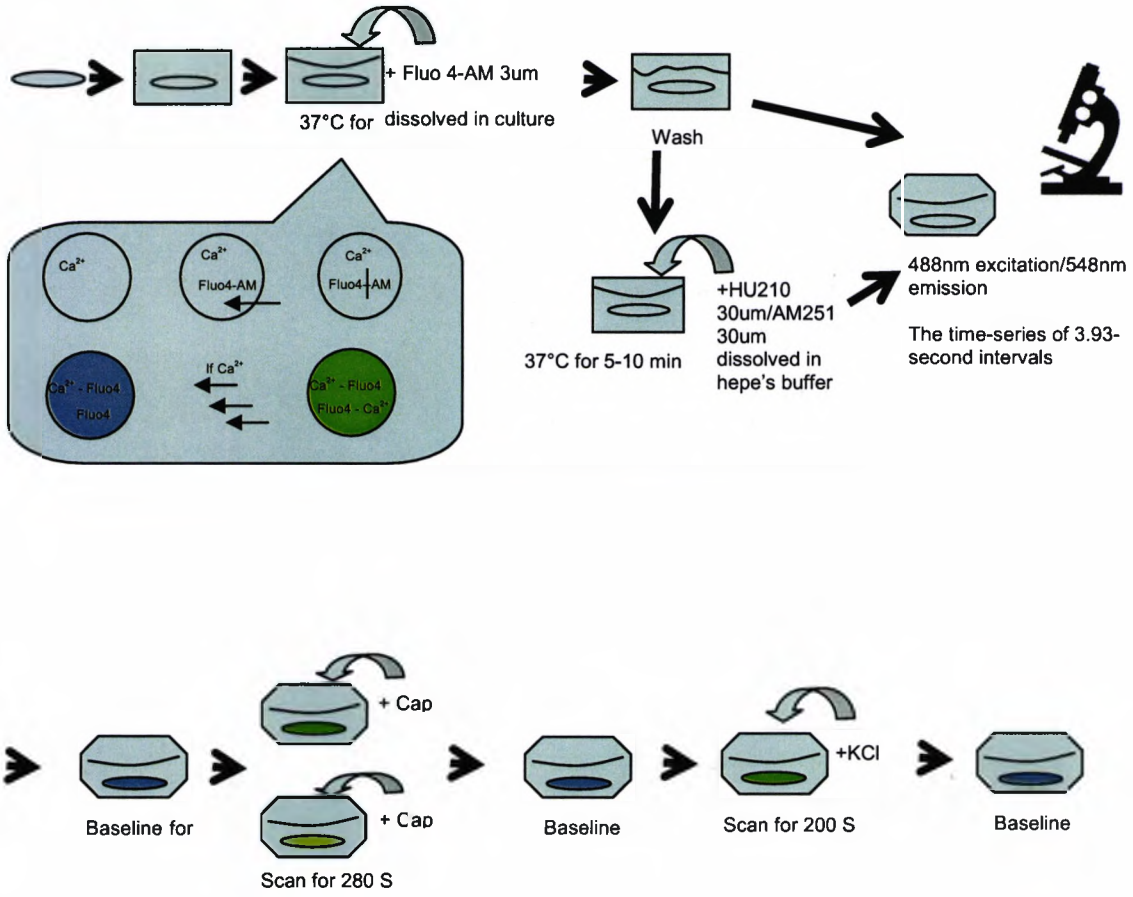


**Figure 2.1** Flow diagrams showing the procedure of $Ca^{2+}$ imaging study used to investigate the inhibitory effect of $CB_1$ agonists on $Ca^{2+}$ influx.

## 2.20 Western blotting: Preparation of cell lysate

PC12 cells were cultured for 6 days as described in section 2.6. The procedure was carried out restrictively on ice or in a cold room as protein starts to degrade as soon as lysis buffer is added; low temperature can dramatically slow down protein degradation and kinase reactions. PBS, eppendorfs, cell scrapers and radioImmuno precipitation assay (RIPA) buffer were all pre-cooled on ice before the experiment. The cell culture dishes containing PC12 cells were placed on ice and washed with PBS buffer before adding RIPA buffer and protease inhibitor cocktail. PC12 cells were scraped off and transferred to eppendorfs. The cell lysates were agitated for 30 minutes on ice, followed by a centrifugation at 10,000g for 20 minutes at 4°C. The supernatants were transferred to clean eppendorfs and placed on ice for use on the same day or stored at -80°C for delayed experiments. The supernatant was then assayed for total protein concentration using a Bradford Protein Assay (Bio-Rad, UK), with bovine serum albumin as a standard.

RIPA buffer 4x:
50mM Tris HCl PH8
150mM NaCl
1% NP-40 buffer
(20mM Tris HCl PH8; 137mM NaCl; 10% glycerol; 1% nonidet P-40 and 2mM EDTA)
0.5% Sodium Deoxycholate
0.1% SDS

Protease inhibitor cocktail:
1mM sodium orthovanadate
50mM sodium fluoride
1mM phenylmethylsulfonyl fluoride
2µg/ml aprotinin
10µg/ml leupeptin
10µg/ml antipain
1µg/ml pepstatin A

## 2.21 Immunoprecipitation

Protein A-Sepharose beads were purchased from Sigma as a powder. One hundred milligrams of the powder was allowed to hydrate in 1ml PBS (0.1M) for 1 hour, followed by a gentle centrifugation. The beads were aspirated and then incubated in 1ml PBS/BSA (1% w/v) for an hour to block non-specific binding. Following two rinses in PBS, the beads were preserved in 400µl of PBS with 0.1% azide (50% of slurry) and stored at 4°C.

On the day of use, the protein A beads slurry (50µl slurry for 500µg protein) was washed with cold lysis buffer three times in eppendorfs and collected by centrifugation at 10,000g for 30 seconds. At the end, the beads were re-suspended in cold lysis buffer to the original volume.

As illustrated in Figure 2.2, each protein sample with equal concentration and volume (1µg/µl and 500µl in total) was incubated on ice, with rabbit anti-rat $CB_1$ receptor antibody (1:500; Sigma) for 1 hour under agitation. The bead slurry was mixed well and carefully added to protein/antibody mixture. After the incubation at 4°C under rotary agitation overnight, the bead-protein-antibody complex was precipitated from solution and collected by a gentle centrifugation at 4°C. The sediment was washed three times in lysis buffer and then immersed in loading buffer (50µl for 50µl added slurry) after the supernatant was removed. Finally, the beads-protein-antibody complex was boiled at 95-100°C to release the protein from the beads and denature the protein. The supernatant was then collected by centrifugation and kept on ice for the use on same day or stored at - 80°C for a delayed experiment. The samples were run on SDS-PAGE and then subjected to Western blotting.

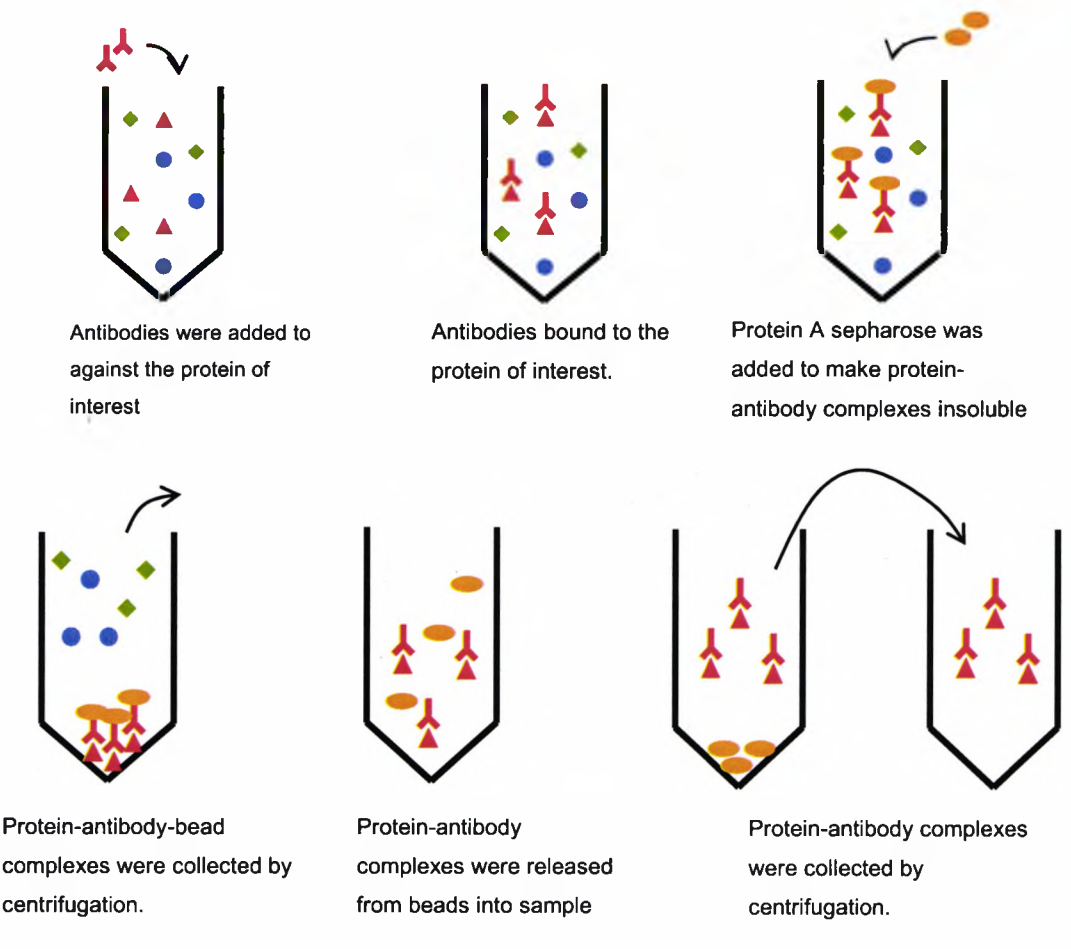


**Figure 2.2** Flow diagram showing the immunoprecipitation method used prior to western blotting to detect $CB_1$ receptor expression in PC12 cells.

## 2.22 Sodium dodecyl sulphate polyacrylamide gel electrophoresis (SDS PAGE)

Fifteen percent acrylamide separating gel was cast in a Hoefer dual gel caster unit (Amersham Biosciences). After 1 hour, a 5% acrylamide staking gel was laid on the top and left to dry for 45 minutes. Gel cassettes were transferred to a Hoefer TE 260 mini-vertical electrophoresis tank and immersed in electrophoresis buffer. Lysate samples were diluted 1:1 with sample buffer and then heated at 95°C for 5 minutes to denature protein. 20µl of each lysate/sample buffer mixture was loaded and migrated at 300V for 45 minutes. Biotinylated broad range molecular weight markers (Bio-Rad) and wide range colour markers (Sigma, UK) were prepared according to the manufacturer's instructions and run in parallel.

Separating gel in $H_2O$ (V/V)

| | |
|---|---|
| 15% | Acrylamide mix |
| 25.3% | 1.5M Tris (PH8.8) |
| 1.0% | 10% SDS |
| 1.0% | 10% Ammonium Persulphate (APS in $H_2O$) |
| 0.05% | (TMEM) |

Staking gel in $H_2O$ (V/V)

| | |
|---|---|
| 5.2% | Acrylamide mix |
| 12.6% | 0.5M Tris (PH6.8) |
| 1% | SDS+bromophenol blue |
| 1.0% | 10% Ammonium Persulphate (APS in $H_2O$) |
| 0.1% | (TMEM) |

Sample buffer in $H_2O$ (V/V)

| | |
|---|---|
| 12.5% | 0.5M Tris-HCl PH6.8 |
| 10% | Glycerol |
| 20% | 10%SDS |
| 5% | 2-mercaptoethanol (2-ME) |
| 2.5% | 0.05%Bromopherol-blue |

Electrophoresis buffer 5x in $H_2O$ (W/V)

| | |
|---|---|
| 1.5% | Tris base |
| 7.2% | Glycine |
| 0.5% | SDS |

## 2.23 Western Blotting

Transfer equipment was equilibrated in transfer buffer during electrophoresis. The protein on the gel was transferred to a nitrocellulose membrane (PerkinElmer) in a Hoefer TE 22 mini-tank transfer unit filled with transfer buffer. The transfer was completed after 90 minutes at a power of 100V. The membrane then was rinsed twice with washing buffer (0.25% Tween and 0.01% NP-40 in 1x PBS) and blocked with blocking buffer (5% non-fat milk powder or 3% BSA, 0.05% Tween, 0.1% NP-40 in 1x PBS) overnight at 4°C. The next day, after rinsing twice with washing buffer, the membrane was incubated with primary antibody (rabbit anti-rat $CB_1$ receptor 1:1000 or mouse anti-phosphorylated serine 1:1000 in PBST) on an orbital shaker for one hour at room temperature. Following a washing step which was three repeated washes with 5 minutes intervals, the secondary antibodies (horseradish peroxidase anti-rabbit IgG/horseradish peroxidase anti-mouse IgG, 1:1500 in PBST and streptavidin-horseradish peroxidase conjugate 1:2500 in PBST) were applied for a one hour incubation period on an orbital shaker at room temperature. The washing step was repeated again as described above after the antibody detection was completed. The membrane was then immersed in Enhanced Chemiluminescence (ECL) detection reagents (Amersham), spot dried and covered in cling-film. In the dark, the membrane was then exposed to a Hyperfilm (Amersham, UK) for 15sec after which the film was developed and fixed. The picture of the protein band on the film was taken under X-ray chamber (Syngene, Cambridge, UK), and the bands representing $CB_1$ receptor protein (60kDa) or phosphorylated $CB_1$ protein (60kDa) were quantified by densitometry using GeneTools™ (Syngene, Cambridge, UK).

## 2.24 Immuno-detection of $CB_1$ receptors in Rat DRG

**(Conducted by Dr Shuangsong Hong in Michigan University, USA)**

Plasma membrane proteins were extracted from rat DRGs using an aqueous twophase polymer system of dextran-polyethylene glycol as described previously (Hong & Wiley, 2005). Briefly, DRGs from control and diabetic rats were isolated and homogenized in ice-cold lysis buffer containing 50mM Tris, pH 8.0, 150mM NaCl, 1mM EGTA, 50mM NaF, 1.5mM MgCl2, 10% v/v glycerol, 1% v/v Triton X-100, 1mM phenylmethylsulfonyl fluoride, 1mM Na3VO4, and "Complete" protease inhibitor mixture (Roche Diagnostics). The DRG homogenates were then centrifuged at 100,000*g* for 30 minutes at 4°C, and the pellets containing proteins from both the plasma membrane and cellular organelle membranes were suspended and separated by using the two-phase polymer solutions. The plasma membrane was finally enriched by centrifugation at 100,000*g* for 20 minutes at 4°C. The enriched DRG membrane protein was separated by 4-15% Tris-HCl gel and transferred to nitrocellulose membrane. The nitrocellulose membrane was blocked with 5% non-fat dry milk for 4 hours and then incubated with anti-$CB_1$ antibody (Cayman Chemicals) overnight. The membrane was then probed with horseradish peroxidase-conjugated secondary antibodies for 1 h and developed using the West Dura Supersignal chemiluminescence kit (Pierce). The corresponding bands were scanned and quantified with ImageJ software (National Institutes of Health), and normalised to β-actin band intensity.

## 2.25 $CB_1$–mediated neuroprotection

PC12 cells were grown as described in section 2.6 for six days ± HU210 (0.03 - 3μM), in the presence or absence of selective $CB_1$- or $CB_2$- antagonists (AM251 and AM630, at 1 or 3μM).

**Neurite rescue study**

Neurite length was determined from photomicrographs taken on day 6 from three random fields/well, using MetaMorph™ software (Universal Imaging Corporation). The total neurite length measurement was conducted as described in section 2.7.

**The effect of HU210 on oxidative stress**

Levels of oxidative stress were measured using the glutathione assay as described in section 2.8.

**The effect of HU210/AM251/AM630 on cell viability**

Cell viability was examined by using the MTT assay as described in section 2.10, as well as the LDH assay as described in section 2.9.

All drugs were initially prepared in DMSO: HU210 100mM, AM251 100mM, AM630 100mM and then diluted in DMEM to achieve final concentrations.

## 2.26 Statistical analysis

Experiments were conducted in duplicate or triplicate. Data are presented as the mean ± standard error mean from at least three independent experiments, and analysed using MINITAB release 14. The immunoblot data were normalised as a percentage of control, and functional data were normalised as a percentage of KCl response. Multiple treatment data were analysed using one-way ANOVA with Fisher's pair wise comparison, whereas data between two groups were analysed by using Student's *t* test. Statistical significance was accepted at $P<0.05$.

# CHAPTER 3

# VALIDATION OF AN *IN VITRO* CELL MODEL OF DIABETIC NEUROPATHY

## 3.1 Introduction

Distal symmetrical polyneuropathy, the most common form of diabetic neuropathy, is characterized by neurodegeneration of peripheral nerve endings, resulting in acute pain, sensorimotor deficits, and an increased risk of limb amputation (Vinik *et al.,* 2006). Given the clinical observation that controlling blood glucose levels delays the onset of diabetic neuropathy, the elevated blood glucose (hyperglycaemia) is suggested as a main trigger to diabetic neuropathy. Some studies have demonstrated hyperglycaemia alters the nerve conduction velocity and causes sensory neuron loss in diabetic mice and rat models (Zaruba *et al.,* 2007; Malone *et al.,* 1996). The mechanisms underlying the pathophysiology are still unclear. Oxidative stress resulting from the over-loaded glucose metabolism is recognised as a unifying pathway, which causes protein and lipid oxidation in the nervous system (Russell *et al.*, 2002; Feldman, 2003). As consequences, mitochondrial dysfunction and apoptosis are preceded by the hyperglycaemia-induced oxidative injury in neurons, leading to neuronal dysfunction and cell death in diabetes (Schmeichel *et al.*, 2003; Russell *et al.*, 1999). The neuropoietic cytokine, IL-6, has dual functions contributing to either nerve degeneration or regeneration. At low levels, it facilitates neurite outgrowth and promotes recovery from injury, however, at high levels, it act as a pro-inflammatory factor. (Skundric and Lisak, 2003).

Previously, few *in vitro* models were established to investigate the hyperglycaemia-mediated neuronal cell dysfunctions. Cultured ganglionic neurons, developed as *in vitro* models of diabetes by Russell and colleagues, showed a high glucose-mediated neurite retraction which was ameliorated by the application of insulin growth factor I (Russell and Feldman, 1999; Russell *et al.*, 1999). PC12 cells derived from a rat adrenal pheochromacytoma were first

established as an *in vitro* cellular model of diabetic neuropathy by Lelkes and co-workers in 2001. Their study showed that PC12 cells displayed similar features of diabetes- related nerve disorders: decreased neurite outgrowth, increased oxidative stress and accelerated apoptosis, when cultured in elevated glucose (Lelkes *et al.*, 2001). The aim of this chapter was to validate PC12 cells as a cell culture model of diabetic neuropathy by culturing cells in physiological glucose (5.5mM) as well as serial elevated glucose concentrations (10-50mM). To exclude the possibility of increased osmolality causing observed differences, mannitol (30 and/or 50mM) was used as an osmotic control, whereby the osmolality of the solution would be the same as glucose, but the cells would be unable to utilize mannitol. The effect of glucose on morphology changes was determined by comparing neurite length in different glucose treatments. Oxidative stress, IL-6 production, and cell viability were also tested.

## 3.2 Determination of the time length for optimum neurite outgrowth of PC12 cells

To obtain the length of time for optimum neurite outgrowth, the measurement of neurite length in PC12 cells cultured in variety concentrations of glucose (5.5-50mM) and mannitol (10-30mM) was conducted on day 4, 6 and 8 of culture, using Metamorph$^{TM}$ computer software. Longest neurite length and total neurite length were both adopted to compare neurite outgrowth in cells, and expressed as percentage of cell body diameter.

As shown in Figure 3.1, both the longest neurite length (Figure 3.1 A) and total neurite length (Figure 3.1 B) data from all the treatment groups, including glucose and mannitol, followed a bell-shaped pattern, showing a maximal

neurite outgrowth on day 6 of culture. It also can be seen that the high glucose (20, 30, 40 and 50mM), but not mannitol (30 and 50mM), attenuated the neurite outgrowth compared with the control glucose (5.5mM) on day 6 and 8. In contrast, no clear difference on neurite outgrowth was observed among the treatment groups on day 4 of culture, especially from the result of total neurite length, which may due to the early stage of neurite outgrowth is not being sensitive enough to identify differences in neurite extension affected by glucose. Thus, day 6 of culture is suggested to be the optimal time point for neurite outgrowth studies, taking advantage of maximal neurite differentiation and sensitive identification of the effect of glucose on neurite extension.

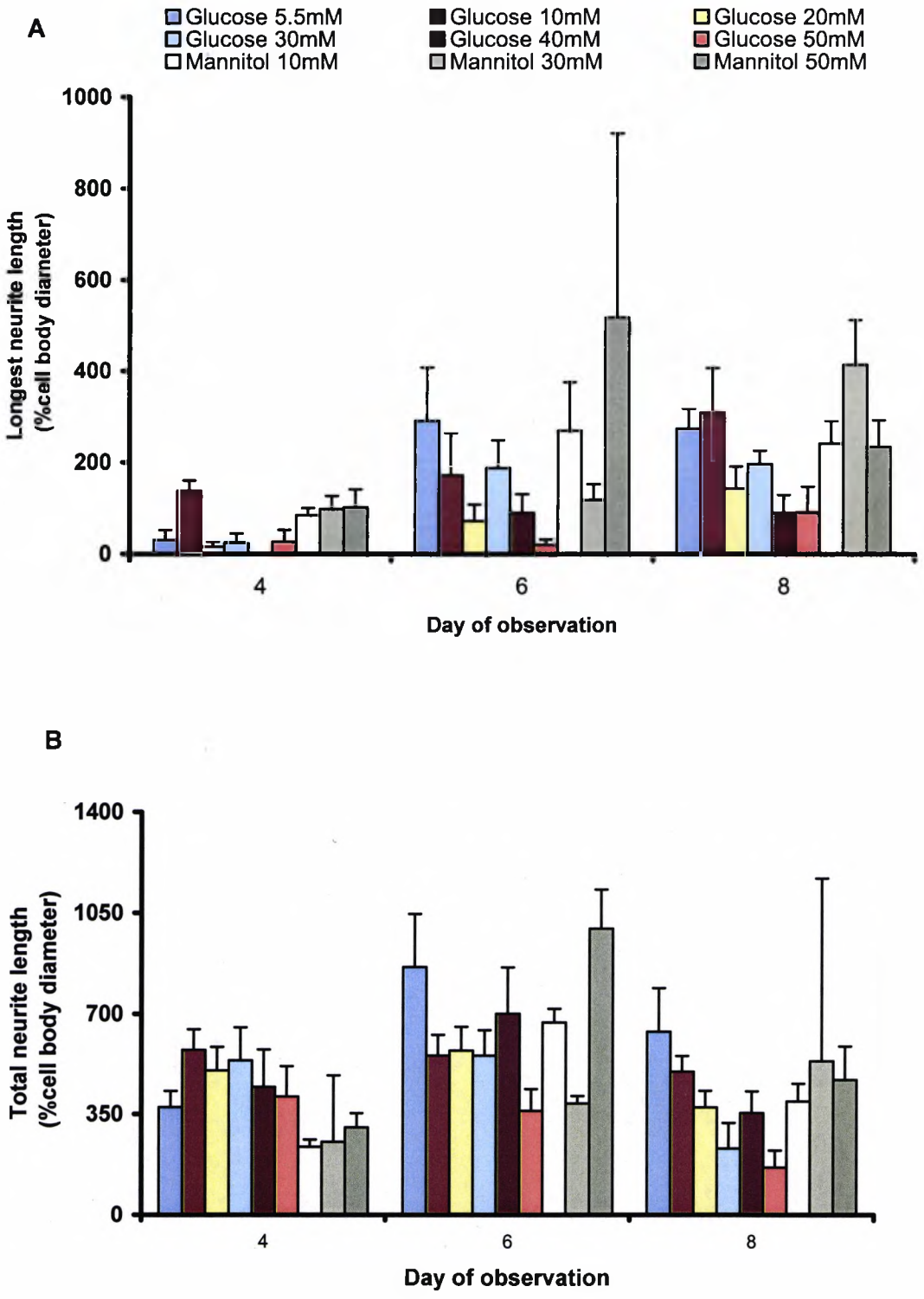


**Figure 3.1** The effect of glucose on neurite outgrowth in PC12 cells in the presence of nerve growth factor (50ng/ml) on day 4, 6, 8. The neurite outgrowth in each cell was analysed using digital quantitative analysis software (Metamorph™), and expressed as percentage of cell body diameter. **A** represents longest neurite length and **B** represents total neurite length (n≥10 for each condition).

### 3.3 Validation of Metamorph™ methods on measuring neurite length

Metamorph™ quantitative digital analysis software (Universal Imaging Corporation) provides a fast method of neurite outgrowth study. To validate Metamorph™ measurement methods, a manual measurement was conducted on more than 10 cells to compare with the digital measurement. Figure 3.2 shows the correlation between the two measurement methods. It was found that the results of neurite length measured using Metamorph™ and manual measurement methods correlated highly ($R^2$=0.9771), suggesting Metamorph™ is a valid method in morphology studies.

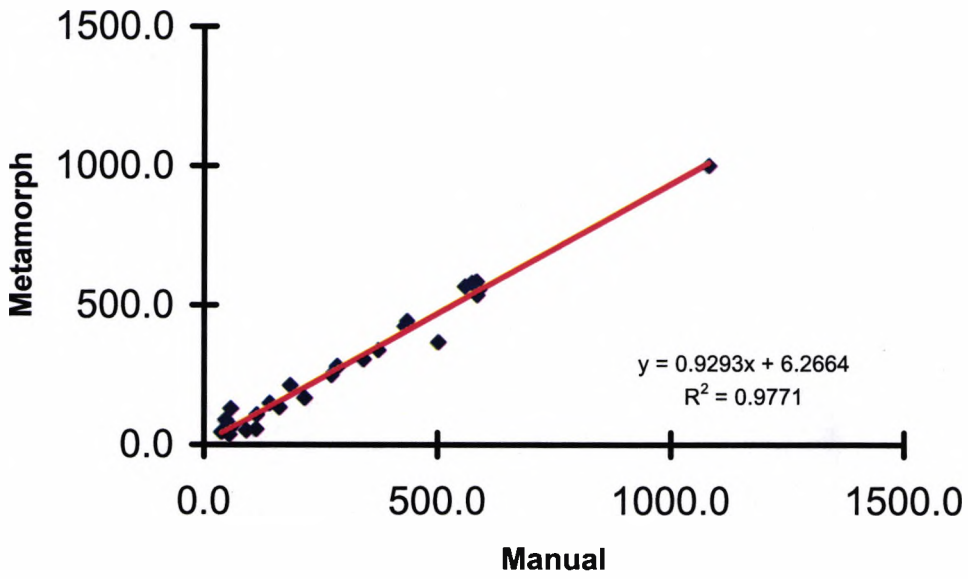


**Figure 3.2** The correlation between manual measurement and digital quantitative analysis software measurement on neurite outgrowth in PC12 cells growth in the presence of nerve growth factor (50ng/ml) on day 6 (n=24 and regression $R^2$=0.9771).

### 3.4 Effects of glucose on neurite outgrowth in PC12 cells

To study the effect of glucose on NGF-induced neurite outgrowth, the morphology study was conducted in PC12 cells cultured in DMEM supplemented with increasing concentrations of glucose (5.5-50mM) with the stimulation of NGF (50ng/ml) for 6 days.

Figure 3.3 shows the photomicrographs illustrating neurite outgrowth of PC12 cells cultured in each condition. It was observed that cells were highly differentiated in 5.5 and 10mM of glucose (Figure 3.3 A and B); with increasing glucose concentration, the differentiation rate declined. The shortest neurite length was observed in cells cultured in 40 and 50mM glucose (Figure 3.3 E and F). Mannitol (30 and 50mM; Figure 3.3 G and H) gave a comparable neurite outgrowth to 5.5mM glucose in PC12 cells.

The measurements from over seventy cells were plotted in Figure 3.4 A. The plotter graph (Figure 3.4 A) illustrates the distribution of longest or total neurite length from each condition, showing the neurite length of majority cells stays in higher Y axis in 5.5 or 10mM glucose, and it moves downwards with the glucose concentration increasing (20-50mM glucose). It indicates that 5.5 or 10mM glucose is beneficial for neurite outgrowth in PC12 cells compared to the higher concentrations of glucose. Statistically, glucose with the concentrations more than 10mM (Figure 3.4 B) significantly inhibited neurite outgrowth in PC12 cells (versus the control 5.5mM of glucose; $P<0.01$). It was ~two-fold decrease in total neurite length in PC12 cells cultured in 30-50mM of glucose compared to that in the control glucose. In contrast, mannitol (30 and 50mM) gave similar results to that of the physiological 5.5mM glucose control ($P = 0.79$), indicating the inhibitory effect is due to raised glucose levels.

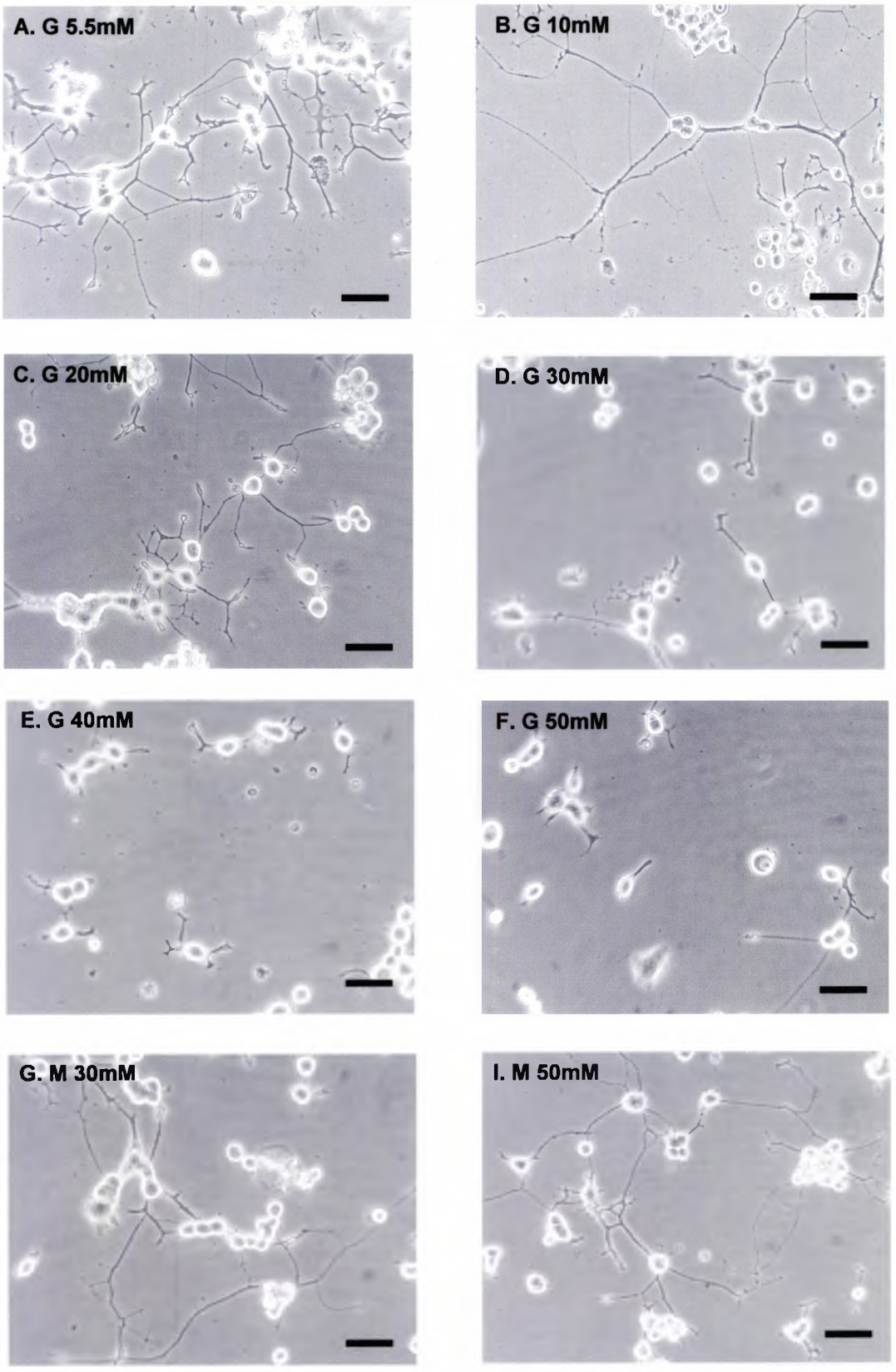


**Figure 3.3** Representative photomicrographs showing the effect of increasing glucose concentration on neurite outgrowth in PC12 cells grown in the presence of nerve growth factor (50ng/mL). **A-F** represent individual field observed under light microscopy (x40) in the increasing glucose concentration 5.5-50mM (G5.5-G50mM). **G-I** represent individual field observed in mannitol 30 and 50mM (M30 and 50mM). Scale bar = 25µm. x40 magnification.

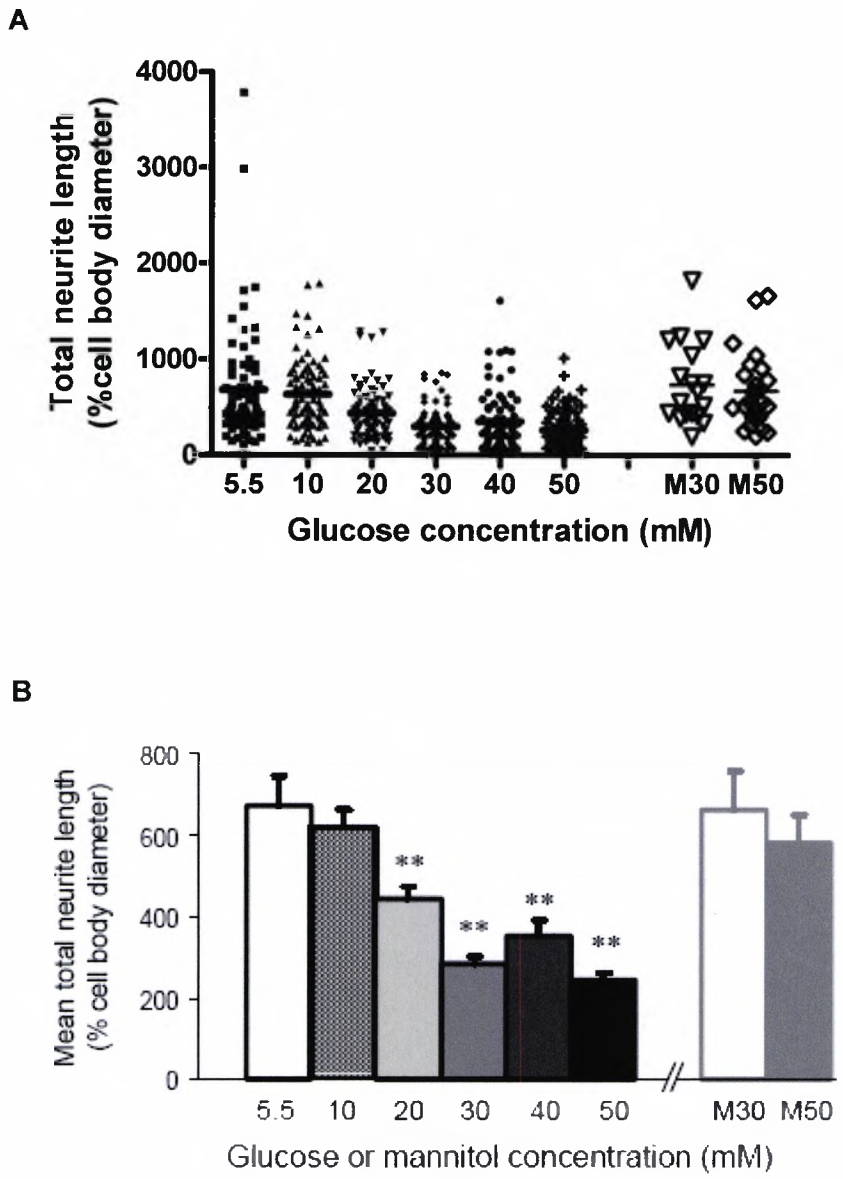


**Figure 3.4** The effect of glucose on neurite outgrowth in differentiated PC12 cells. From three random fields of view per well, the total length of individual neurites per differentiated cell was measured using quantitative digital analysis software (Metamorph™), and expressed as a percentage of cell body diameter. Data shown are mean ± s.e.mean, where n=70-79 cells per condition from six independent experiments (**, $P < 0.01$, versus 5.5 mM glucose: one-way ANOVA-Fisher's post-hoc analysis). Mannitol (30 and 50 mM) was included as an osmotic control (M30, M50). **A** is the scatter graph and **B** is the bar graph.

An osmolality measurement was conducted independently (Table 3.1), showing no significant difference between 30 and 50mM of glucose and mannitol (P =1.00 and 0.37 respectively), which further confirmed no hyperosmotic effects were involved in the inhibition of neurite outgrowth.

Figure 3.5 shows that the cell culture model is one of maintained elevated glucose concentrations. The average fall in glucose levels from aspirated medium is 3.1 ± 0.8mM across the concentration range after 2 days in cell culture, but there is not a severe peak-to-trough variation in glucose (Figure 3.5).

| Glucose (mM) | Osmolality (mOsm/kgH2O) |
|---|---|
| 5.5 | 290 ± 1 |
| 10 | 298 ± 1 |
| 20 | 309 ± 0 |
| 30 | 320 ± 1 |
| 40 | 332 ± 1 |
| 50 | 342 ± 1 |
| 5.5 + Mannitol 30mM | 320 ± 1 |
| 5.5 + Mannitol 50mM | 341 ± 0 |

**Table 3.1** Osmolality of cell culture medium. Osmolality of culture media was measured in an osmometer (model 3D3, Advanced Instruments Inc., USA) (average of three readings). No significant differences were observed between the 30 and 50mM glucose and mannitol osmotic controls ($P > 0.05$, unpaired Student's *t*-test).

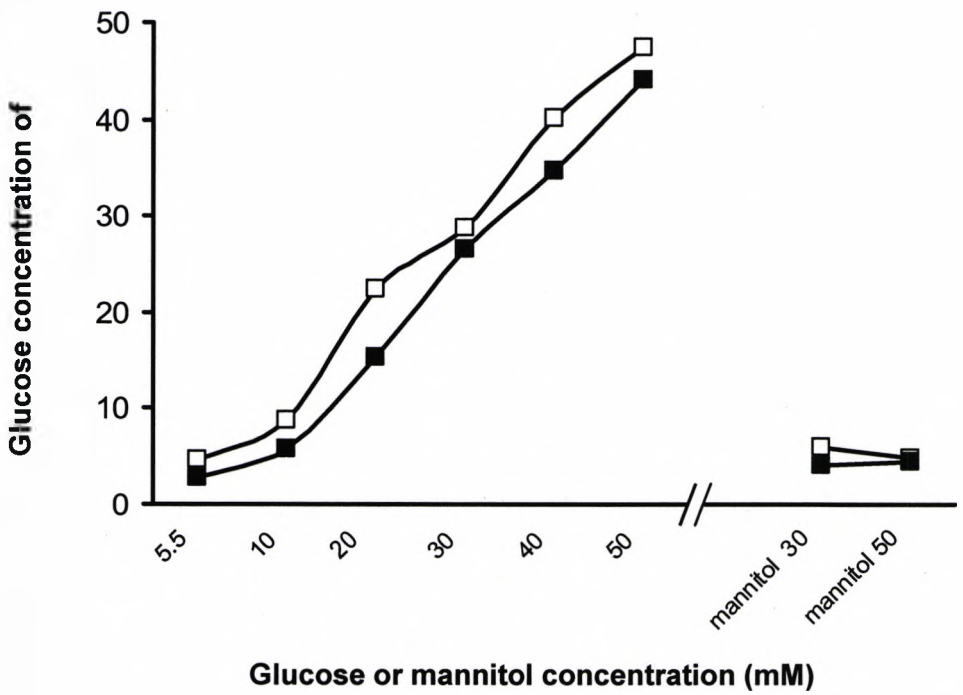


**Figure 3.5** Measurements of glucose concentrations in the aspirated medium following 2 days in culture, either in plates containing no cells, or those plated with $1x10^5$ PC12 cells/ml.

## 3.5 Effects of glucose on oxidative stress in PC12 cells

Oxidative stress was examined in PC12 cells cultured in increasing concentration of glucose (5.5, 30, 50mM) on day 6. The glutathione assay measures the level of the reduced form of glutathione (GSH) as well as the oxidized form of glutathione (GSSG), identifying the level of oxidative stress in cells. GSH acts as a natural body defence, scavenging free radicals by donating a free ion whilst turning itself into GSSG. The ratio of GSSG/GSH indicates the oxidative stress level in cell bodies. Figure 3.6 shows the effect of glucose on oxidative stress in PC12 cells. It was found that glucose produced oxidative stress in a concentration-dependent manner. The concentration of 30 and 50mM of glucose significantly increased oxidative stress compared with the control concentration (5.5mM) ($P<0.05$ and $P<0.01$) by ~two-and-three-fold, respectively. No significant change in oxidative stress was observed with mannitol treatment (50mM) ($P=0.98$) (versus the control 5.5mM), indicating there is no osmotic effect on oxidative stress levels found with high glucose treatment (30 and 50mM).

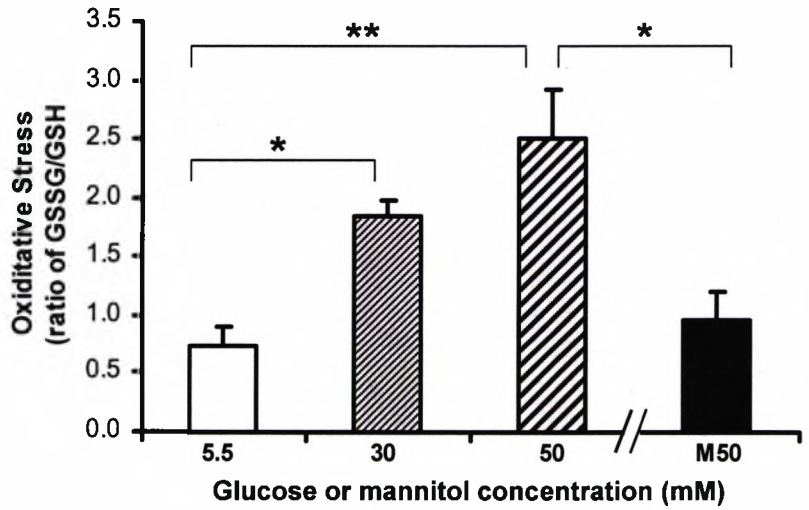


**Figure 3.6** The effect of glucose on oxidative stress in differentiated PC12 cells. An increased ratio of GSSG/GSH represents oxidative stress in PC12 cells cultured in the presence of NGF (50ng/ml) and increasing concentrations of glucose (5.5, 30, 50mM). Mannitol 50mM was used as an osmotic control (n=4; **, $P<0.01$; *$<P0.05$; one-way ANOVA-Fisher's post-hoc analysis).

### 3.6 Effects of glucose on cell viability in PC12 cells

Cell viability was examined in PC12 cells cultured in variety concentrations of glucose (5.5, 30 and 50mM) with the stimulation of NGF (50ng/ml) for 6 days by using the lactase dehydrogenase (LDH) assay and MTT assay. LDH serves as a general indicator to assess cell membrane integrity and the leakage of LDH from plasma into cell medium suggest cytotoxicity which may result from chemicals and environmental changes. Figure 3.7 shows LDH levels in culture medium of PC12 cells cultured in the presence of glucose (5.5-50mM) and mannitol (50mM) on day 2, 4 and 6 with the positive control from Triton-X (0.1%) treated cells. A similar trend of a flat line was found in LDH levels from all of the three time points and in contrast to the positive control value of 1800-2000unit/ml, LDH levels observed from other groups all remained below 500unit/ml. These data reveal that high glucose (30 and 50mM) did not cause significant LDH release in PC12 cells compared with the control LDH level (glucose 5.5mM) in all of the three time points. No significant change in LDH level was found in the mannitol (50mM) treatments when compared with the glucose treatments, which excludes the possibility of osmotic effects.

The MTT assay is a colourimetric method based on the ability of live cells to reduce a tetrazolium-based compound to a blue formazan product. Cell viability is expressed as absorption at 550 nm. Different from the LDH assay, the MTT assay was conducted in PC12 cells on day 6. As shown in Figure 3.8, there was no significant difference on cell viability within all the treatment groups, including mannitol treatments (P=0.86). The result is consistent with the finding from the LDH studies, suggesting glucose has no adverse impact on cell viability in PC12 cells.

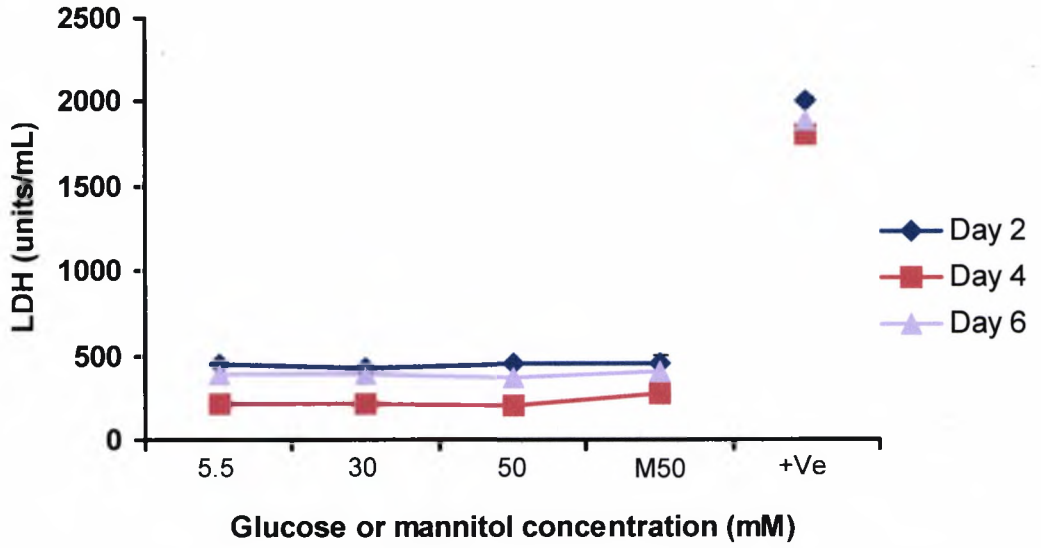


**Figure 3.7** Mean concentration of lactase dehydrogenase release from PC12 cells stimulated with NGF (50ng/ml) and in the absence/presence of high glucose (30 and 50mM) on day 2, 4 and 6 of culture. Mannitol (50mM) is the vehicle control to exclude an osmotic effect. +Ve is the positive control from Triton-X (0.1%)-treated cell lyses. Values represent mean ± SEM from 3 independent experiments (P >0.05, one-way ANOVA-Fisher's post-hoc analysis).

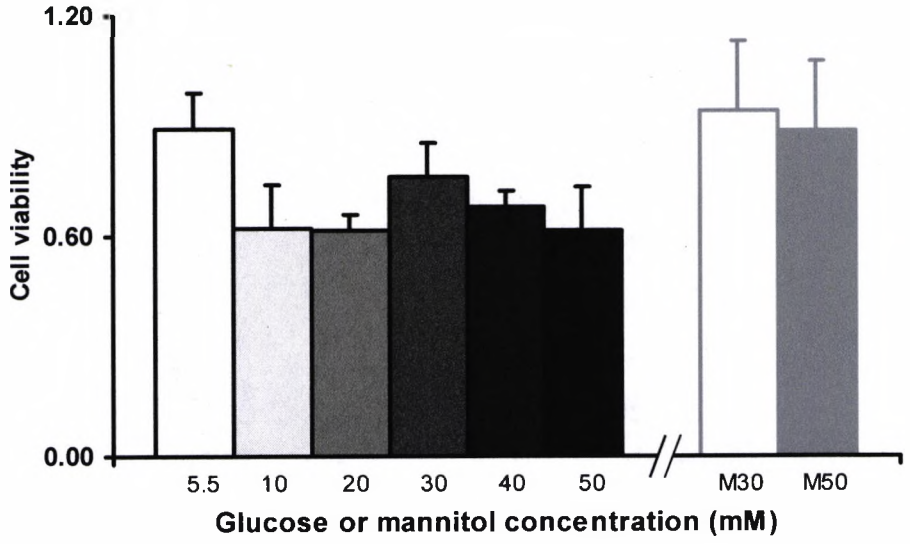


**Figure 3.8** Cell viability of PC12 cells cultured in an increasing concentration of glucose (5.5, 10, 20, 30, 40, 50mM) under the stimulation of NGF (50ng/ml) for 6 days. Mannitol (30 and 50mM) is an osmotic control. Data shown are mean ± s.e.mean, from n=12 independent experiments performed in duplicate (P >0.05 one-way ANOVA-Fisher's post-hoc analysis).

### 3.7 Effects of glucose on cell proliferation in PC12 cells

Protein concentration and cell density were also examined, along with cell viability assays, to assess the effects of glucose on cell proliferation. The Bradford protein assay determines protein concentration in relation to a standard albumin curve. Figure 3.9 shows protein concentrations in PC12 cells cultured in increasing concentrations of glucose (5.5-50mM). No significant difference was found within the glucose treatment groups, although there was a slight increase with higher concentrations of glucose (>10mM; P=0.72). The results from mannitol (30 and 50mM) treatments showed no osmotic effect was involved in cell proliferation.

The above result was further confirmed in the cell density assay. A random cell count (Figure 3.10) was conducted to compare the cell density in different concentrations of glucose (5.5, 30 and 50mM) and mannitol (50mM). Taking the control (5.5mM glucose) cell density as 100%, the result revealed a constant cell density in all the treatment groups, including mannitol (50mM), with a maximal 10% of variation. The results from both studies suggest glucose itself has no effect on cell proliferation in PC12 cells.

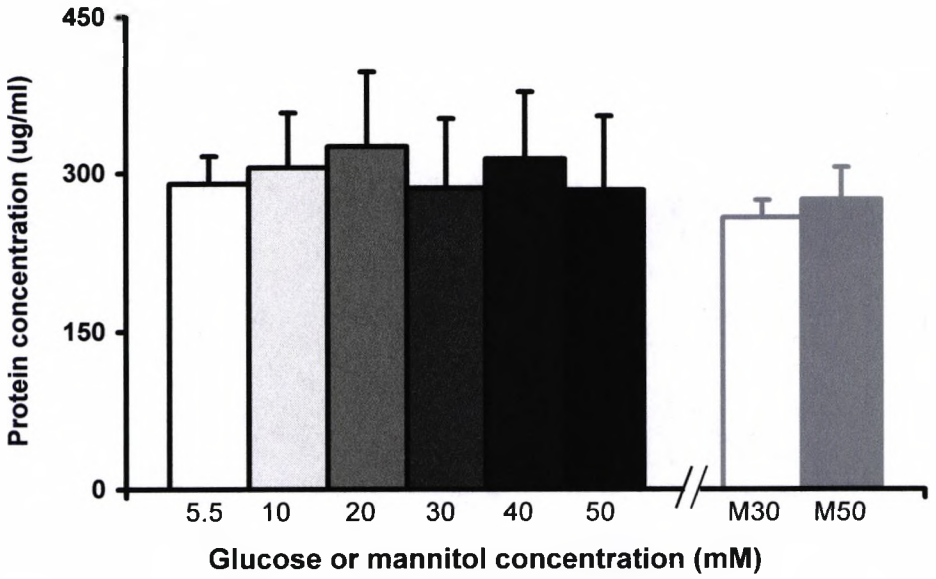


**Figure 3.9** The effect of glucose on cellular protein levels in PC12 cells. The Bradford protein assay was carried out in cells cultured for 6 days with nerve growth factor (50 ng/ml), in the presence of 5.5 – 50mM glucose. Mannitol (30 and 50 mM) was included as an osmotic control (M30, M50). Protein concentration is expressed as µg/ml, in relation to a standard curve (albumin). All values expressed as mean ± s.e.mean from 3 independent experiments performed in duplicate (P >0.05, one-way ANOVA-Fisher's post-hoc analysis).

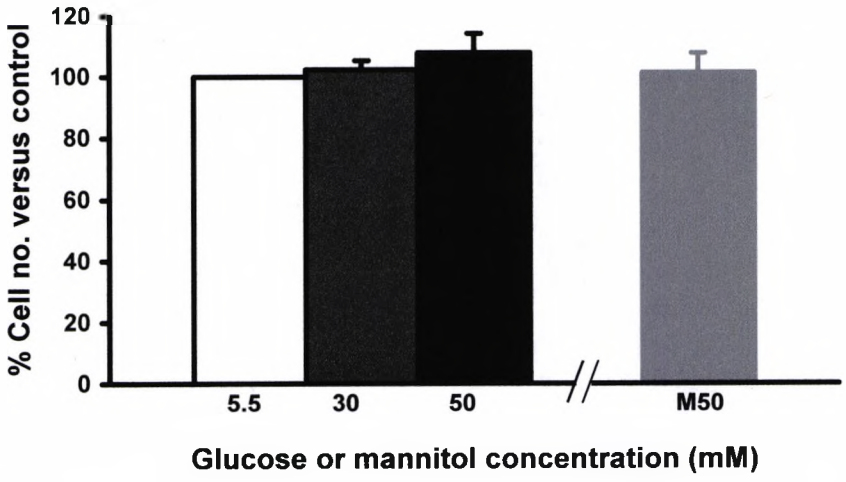


**Figure 3.10** The effect of glucose on cell density in PC12 cells. Cells were counted from three random fields in each well after 6 days of culture with nerve growth factor (50ng/ml), in the presence of 5.5, 30 and 50mM glucose. Mannitol (50 mM) was included as an osmotic control (M50). The cell number is expressed as percentage of the control (5.5mM glucose). All values expressed as mean ± s.e.mean from 3 independent experiments performed in duplicate (P >0.05, one-way ANOVA-Fisher's post-hoc analysis).

### 3.8 Effects of glucose on interleukin-6 (IL-6) production

Figure 3.11 shows the IL-6 production in PC12 cells cultured in control glucose (5.5mM) and high glucose (30, 50mM). The mean values from various treatments displayed that glucose has a tendency to increase the IL-6 production in PC12 cells in a dose-dependent manner, however, this failed to reach statistical significance (P=0.427).

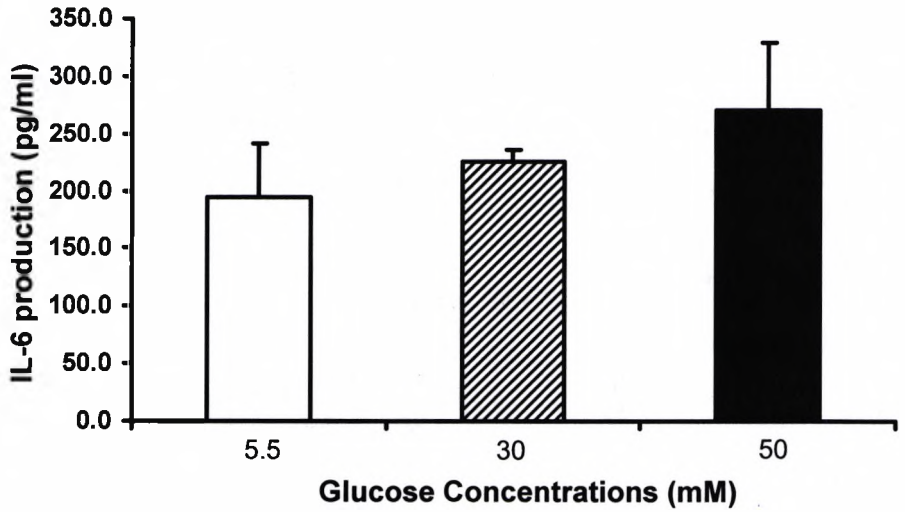


**Figure 3.11** The effect of glucose on interleukin-6 production. The level of IL-6 was measured in the culture medium of PC12 cells cultured in the absence or presence of high glucose (30, 50mM glucose) with the stimulation of NGF (50ng/ml) on day 6. All values expressed as mean ± s.e.mean from 3 independent experiments performed in duplicate (P >0.05, one-way ANOVA-Fisher's post-hoc analysis).

## 3.9 Discussion

Greene and Tischler first established the NGF responsive cell line, PC12, in 1976. Upon the stimulation of NGF, PC12 cells not only cease to multiply and begin to extend branching varicose processes, but also synthesise and store neurotransmitters, such as catecholamine and noradrenaline. The high similarity to cultured primary neurons suggests PC12 as a useful model system for neurobiological and neurochemical studies (Greene and Tischler, 1976). In the present study, we validated PC12 cells being an *in vitro* cell model of diabetic neuropathy, as previously established by Lelkes *et al.* (2001). Firstly, the optimum time length was investigated in the NGF stimulated PC12 cells. The neurite outgrowth of PC12 cells was studied at three time points: day 4, 6 and 8, under the stimulation of NGF (50ng/ml). Day 6 was found to be the optimum time when maximal neurite length and a distict neurite outgrowth were observed with increasing concentrations of glucose (5.5-50mM). This finding is in agreement with a previous study showing that PC12 cell differentiation and neurite growth induced by a similar dose of NGF (50ng/ml) reached a plateau after 6 days in culture (Das *et al.*, 2004). Ohuchi *et al.* (2002) compared the assay-based quantitative analysis (using protein and enzyme markers) with the neurite length measurement method to assess neurite outgrowth by stimulating PC12 cell differentiation with NGF for 5 days and the results showed a high correlation between these methods (Ohuchi *et al.*, 2002). Lelkes *et al.* (2001) studied the effect of high glucose on neurite outgrowth on day 6 of culture in PC12 cells with NGF (50ng/ml) present. During the process of cell model selection, human neuroblastoma SH-SY5Y cells were also tested with chronic high glucose treatments. However, unlike PC12 cells, SH-SY5Y cells multiplied very rapidly during the culture, making the assessment of, particularly, the

glucose related morphology change and the future neurite-rescue study impossible to carry out over a 6-day period.

The quantitative computer program, Metamorph™, provides an accurate and fast method for morphology studies, which has been widely used in analysing neurite outgrowth in many cell types, such as cultured rat hippocampal neurons (McCroskery *et al.*, 2006), cultured rat doosal root ganglion neurons (Li *et al.*, 2004; McCroskery *et al.*, 2006), neuroblastoma cells (Sheehan *et al.,* 2006) and PC12 cells (Shin *et al.*, 2006). Based on its diverse uses on assessment of neurite degeneration and regeneration, we adopted Metamorph™ to measure neurite length in NGF-stimulated PC12 cells, following a validation of the semi-automatic measurement method which proved to be highly correlated with the manual measurement method.

Hypersensitivity, such as hyperalgesia and allodynia, occurs in the early stages of diabetic neuropathy, followed by the late-stage loss of sensation (Vinik *et al.,* 2006). *In vitro*, many cell models have been used to examine the cellular mechanism involved in the pathophysiology of diabetic complications, such as endothelial cells (Baumgartner-Parzer *et al.*, 1995; di Wu *et al.*, 1999; Sheu *et al.*, 2005), but few neuronal cell models have been studied. We, therefore, following Lelkes and colleagues' (2001) study, set up PC12 cells as a neuronal cell model of diabetic neuropathy to investigate the effect of glucose on neurite outgrowth. The result from total neurite length showed glucose attenuated neurite outgrowth in PC12 cells in a concentration-dependent manner, and glucose concentrations higher than 20mM significantly inhibited neurite outgrowth which is in agreement with Lelkes *et al.* (2001) reporting 25mM glucose gave significant inhibitory effect on neurite outgrowth compared to the

control (5mM glucose) in the same cell model. The osmotic control (mannitol 30 and 50mM) gave a comparable neurite outgrowth to that of physiological 5.5mM control, suggesting the inhibitory effect is due to high glucose, mimicking hyperglycaemic conditions, rather than any hyperosmotic effect. This result is related to the clinical study showing loss of epidermal nerve fibers in skin biopsies from diabetic patients (Dyck *et al.*, 1986; Kennedy *et al.*, 1996) and the recent animal study reporting axonal atrophy in sensory neurons from experimental diabetic animal models (Zochodne *et al.*, 2001). In line with other *in vitro* models, high glucose was found to consistently inhibit neurite outgrowth in cultured sympathetic ganglion nerves (Semra *et al.,* 2004) and induce neurite degeneration in dorsal root ganglion neurons (Russell *et al.*, 1999). The inhibitory effect of hyperglycaemic conditions on neurite outgrowth in PC12 cells may appropriately reflect the impaired peripheral nerve regeneration process observed in diabetes (Kennedy and Zochodne, 2005). Of course, due consideration must be made when comparing "*in vitro* high glucose" and "*in vivo* diabetic" states, since we had a 9-fold difference in glucose levels between cell-treatment groups, which remained elevated during the culture (Figure 3.5), whilst the rat diabetic model showed a 5-fold elevation in plasma glucose compared to controls, and these levels would fluctuate throughout the animals' lives. Others have reported plasma glucose levels in the STZ-diabetic rat range from 25 - 50 mM (mean 34.5 ± 3.05mM) (Purves *et al.*, 2001), thus making the concentrations used in the present *in vitro* study reasonable.

Oxidative stress is considered as a crucial pathogenic factor in diabetic neuropathy. The excessive ROS generated by hyperglycemia damages DNA, protein and lipid, which accompanied by disrupted natural antioxidant defence characterised by reduced level of glutathione (GSH), glutathione peroxides in

peripheral nerve system, all contributing to alterations in cell signal transduction (Low *et al.*, 1997; McHugh and McHugh, 2004). In the present study, we examined the level of GSH and GSSG in PC12 cells cultured in high glucose to asses the level of oxidative stress. The result revealed high glucose (30 and 50mM) significantly induced oxidative stress in a concentration-dependent manner compared to the 5.5mM glucose control in this cell model system. This finding is consistent with other *in vitro* studies which demonstrated ROS was markedly increased by high glucose (45mM) in cultured DRG neurons, Schwann cells and neuroblastoma cells (Schmeichel *et al.*, 2003; Vincent *et al.*, 2002; Vincent *et al.*, 2005), which are well corroborated by *in vivo* studies showing high levels of oxidative stress are present in diabetic animals and human (Vincent *et al.,* 2002).

Following the observation of high glucose-induced oxidative stress, cell viability was also investigated in the absence or presence of high glucose by using the MTT and LDH assays. The results from both cell viability assays suggest high glucose did not significantly decrease cell viability in PC12 cells, which contradicts some studies suggesting high glucose triggers apoptosis in neuronal cells (Russell *et al.,* 1999). Two studies conducted by Lelkes *et al.* (2001) and Koshimuran *et al.* (2002) reported that high glucose induced mitochondrial dysfunction and programmed cell death in PC12 cells on day 7 of culture. In contrast, we found only a slight, non-significant decrease in mitochondrial related-cell viability measured using the MTT assay with glucose concentrations of 10-50mM compared to the controls (5.5mM glucose, and mannitol 30 and 50mM), and values from the LDH assay measuring cell membrane integrity were relatively constant before all treatments. In the view of Toth *et al.* (2004) and Sullivan and Feldman, (2005), the nerve terminal loss or

axonal atrophy is the feature of early diabetic neuropathy due to the longest 'exposed' length is more vulnerable (Sullivan and Feldman, 2005; Toth *et al.*, 2004). The finding of the morphology study in which high glucose significantly inhibited neurite outgrowth on day 6 of culture shares some common pathways when considering regeneration of nerves.

Later, the effect of glucose on proliferation of PC12 cells was tested by using both protein assay and cell counting. Both of the results indicate, on day 6 of culture, high glucose did not influence the NGF-stimulated PC12 cell growth and protein level, suggesting no net cell death is involved at this stage of high glucose exposure, which is consistent with the previous cell viability results. In fact, as mentioned before, NGF-treated PC12 cells cease to multiply and start growing neurites once attached to poly-L-lysine/collagen treated plates, which are highly similar to adult neurons. These findings support PC12 as a useful neuronal model in studying adult diabetic neuropathy.

Based on the dual role of the neuropoietic cytokines IL-6 in the nervous system, we measured the level of IL-6 in differentiated PC12 cells in the presence of high glucose. The results revealed a glucose concentration-dependent increase in IL-6 production, although the values did not reach statistical significance. Restricted to the nervous system, IL-6 rapidly accumulates following nerve injury, which is suggested to improve functional nerve regeneration (Marz *et al.*, 1999). In fact, two recent studies have shown that the administration of low dose IL-6 improved nerve function and attenuated the development of neuropathy in STZ-diabetic rats (Andriambeloson *et al.*, 2006; Cameron and Cotter, 2007). The dose-dependent increase in IL-6 level in the current study

may due to the stimulation of a 'self-rescue' mechanism in response to high glucose.

Collectively, in this chapter PC12 cells were validated as a cell culture model of diabetic neuropathy. On the optimum time length of 6 days in culture, elevated glucose levels significantly attenuate NGF induced neurite outgrowth, and are associated with increased levels of oxidative stress and IL-6 production in PC12 cells, thus reproducing some of the phenomena of diabetic neuropathy.

# CHAPTER 4

# AN INVESTIGATION OF THE CANNABINOID $CB_1$ RECEPTOR EXPRESSION IN HYPERGYCAEMIC PC12 CELLS AND DIABETIC RATS

## 4.1 Introduction

Cannabinoid $CB_1$ receptors are G-protein coupled receptors, which are expressed abundantly in central and peripheral nervous system. Activation of $CB_1$ receptors regulates $Ca^{2+}$ channels, suppressing neurotransmitter and neuropeptide release. It has been found that the declined $CB_1$ receptor expression contributes to central neurodegenerative process in Huntingson's diseases (Glass *et al.*, 2000; Glass *et al.*, 2004). TRPV1 receptors are non-selective cation channels, whch highly co-express with $CB_1$ receptors on nociceptive afferents. They are activated endogenously by noxious heat (>42°C), acidic pH (<6.0) and the endocannabinoid, anandamide (Zygmunt *et al.*, 1999; Smith & McQueen, 2001), causing central and peripheral release of substance P and calcitonin gene-related peptide (CGRP). Some evidence showing that, upregulated function and expression of TRPV1 receptors occur in the model of diabetic neuropathy (Rashid *et al.*, 2003; Hong and Wiley, 2005), may indicate the balance of $CB_1$- versus TRPV1–mediated responses is tipped unfavourably towards TRPV1 in diabetes.

We hypothesize that a decline in $CB_1$ receptor expression contributes to the neurodegenerative process observed in diabetic neuropathy. The aim of this chapter was to investigate whether the neuronal $CB_1$ receptor expression is down-regulated in hyperglycaemic conditions by using *in vitro* and *in vivo* models of diabetic neuropathy. We have previously found that the NGF-induced neurite outgrowth was reduced by high glucose in PC12 cells. In this chapter, the $CB_1$ receptor expression at gene and protein levels was then studied in PC12 cells in order to examine whether the impaired neurite outgrowth was associated with the decreased $CB_1$ expression. The *in vitro*

finding was further investigated in primary DRG neurons from diabetic rats to test the consistency.

## 4.2 $CB_1$ mRNA down-regulation induced by high concentration of KCl

A high concentration of potassium chloride (KCl, 25mM) was reported to downregulate $CB_1$ receptor expression in cerebellar granule neurons compared with the control concentration of KCl (5mM) by Vallano and colleagues in 2006 (Vallano *et al.,* 2006). In the current experiment, the high concentration of KCl treatment was employed in use of PC12 cells in order to ensure PC12 is a suitable neuronal cell line to study the regulation of $CB_1$ receptors.

The effect of KCl (25mM) on the expression of $CB_1$ mRNA and GAPDH in PC12 cells was investigated, and gel electrophoresis with EtBr staining was employed to determine the amount of gene expression in terms of the intensity of fluorescence signal (Figure 4.1). As seen in Figure 4.1 (B), the upper image shows the fluorescence signal of GAPDH, which were bright bands in both cases, suggesting the increase of KCl concentration in the medium had no great impact on the expression of GAPDH in PC12 cells. However, the fluorescence signal of $CB_1$ (the lower image) was noticeably decreased in the concentration of 25mM compared to that in the concentration of 5mM, indicating the gene expression of $CB_1$ mRNA in PC12 cells was considerably diminished as the concentration of KCl was augmented from 5mM to 25mM.

The intensities of $CB_1$ mRNA signal bands at 5mM and 25mM were quantified and normalized by those of GAPDH expressed at the same concentration of KCl respectively (Figure 4.1 A). Taking the normalised $CB_1$ band intensity with

KCl 5mM as 100%, the high concentration of KCl (25mM) significantly decrease the $CB_1$ mRNA expression by 60%. This result suggests that membrane depolarisation down regulates the expression of $CB_1$ receptors in PC12 cells and the PC12 cell line is appropriate to study the change of $CB_1$ receptor expression.

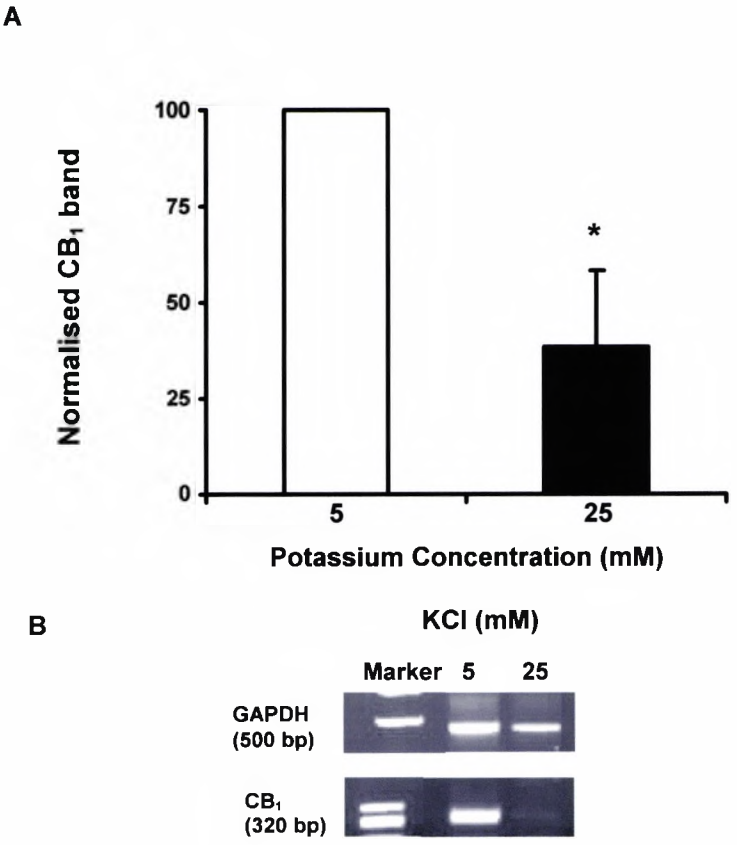


**Figure 4.1** Reverse transcription-PCR analysis of the effect of potassium choride on $CB_1$ cannabinoid receptor mRNA expression in PC12 cells. RT-PCR was performed on total RNA (2 µg) extracted from cells cultured for 6 days in the presence of 50 ng/ml nerve growth factor and 5 or 25mM KCl. **(A)** After gel electrophoresis and ethidium bromide staining, the intensity of the $CB_1$ bands was quantified by densitometry, and normalised relative to GAPDH and the positive control of KCl 5mM. Data is expressed as individual value from three independent experiments (*, $P < 0.05$, unpaired Student's *t*-test). **(B)** Representative gel of RT-PCR reactions: marker, ΦX174 RF DNA/*Hae*III fragments.

## 4.3 The effect of glucose on $CB_1$ gene expression in *an in vitro* cell model

### 4.3.1 Conventional RT-PCR

Figure 4.2 shows the gene expression of $CB_1$mRNA in PC12 cells cultured in varying concentration of glucose and its statistical analysis. The representative gel result is displayed in Figure 4.2 (B), showing that the strongest band of $CB_1$mRNA was observed in the positive control, rat brain. A strong enhancement in $CB_1$mRNA signal was observed when the glucose concentration was raised from 5.5mM (physiological glucose level) to 10mM. When the concentration of glucose was further increased to 20mM and 30mM, the gene expression of $CB_1$ appeared similar strength but had a reduction in comparison with that expressed in culture medium with 10mM glucose. The reduction of gene expression would be enhanced as the increase of glucose in the culture medium. The florescence signal attributed to the gene expression in 40mM and 50mM glucose levels dramatically declined in contrast with those expressed in 10mM glucose levels.

The GAPDH was employed as the reference gene due to its stable expression in cells cultured at any concentration of glucose. GeneSnap were used to quantify the density of the bands of both $CB_1$ mRNA and GAPDH. The data of signal density of $CB_1$mRNA normalized by that of GAPDH were plotted (Figure 4.2 A), and the means were then statistically explored (n=5). For the gene expression in any individual treatment where the concentration of glucose was constant, it was clearly shown that there was a wide range of data distribution in the similar range, and there was no significant difference of the expressed

$CB_1$mRNA in PC12 cells cultured with a wide range of glucose concentration. The reason causing variable results may due to the considerable amount of undifferentiated cell samples.

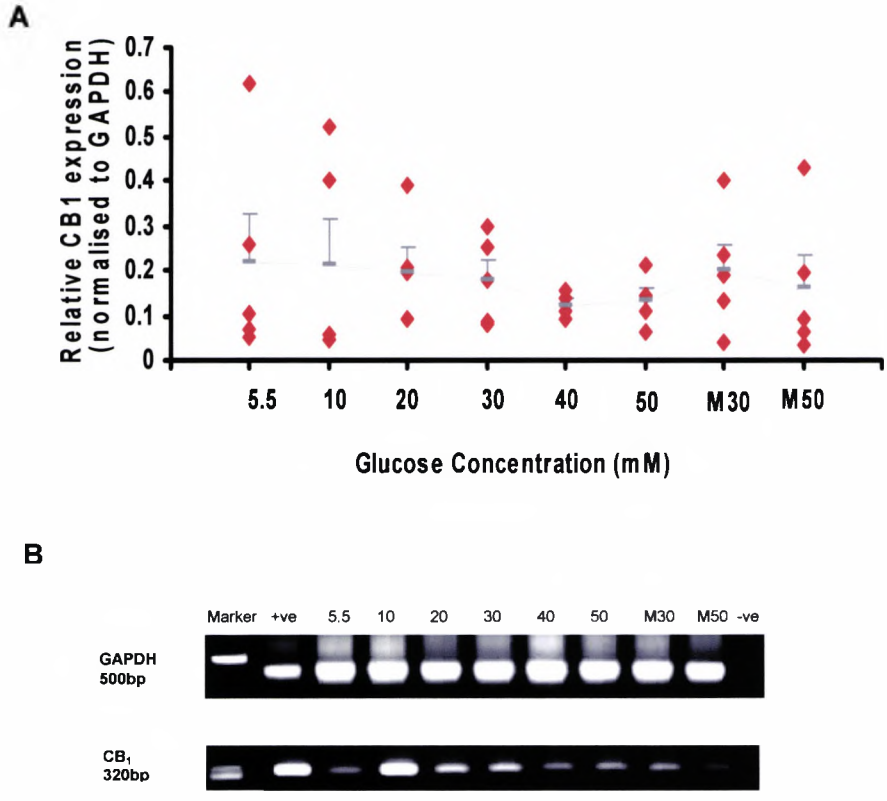


**Figure 4.2** Reverse transcription-PCR analysis of the effect of glucose on $CB_1$ cannabinoid receptor mRNA expression in PC12 cells. RT-PCR was performed on total RNA (2 µg) extracted from cells cultured for 6 days in the presence of 50ng/ml nerve growth factor, 5.5-50mM glucose and 30 or 50mM Mannitol. **(A)** After gel electrophoresis and ethidium bromide staining, the intensity of the $CB_1$ bands was quantified by densitometry, and normalised relative to GAPDH. Mannitol (30 and 50 mM) was used to exclude potential effects of increased osmolality (M30, M50). Data expressed as individual values from five independent experiments ($P > 0.05$one-way ANOVA-Fisher's post-hoc analysis). **(B)** Representative gel of RT-PCR reactions: –ve, the negative control (i.e. minus template); +ve, the positive control (mRNA extracted from rat brain); marker, ΦX174 RF DNA/*Hae*III fragments.

The RT-PCR detecting the $CB_1$ expression in 5.5 or 50mM glucose and 50mM mannitol was conducted again after optimising the plating method and purchasing new batch of NGF. The RNA was extracted from PC12 cells on 6 days of culture when a full differentiation was observed.

As shown in the representative image of gel results (Figure 4.3 B), it was observed that the density of $CB_1$ band at glucose 50mM was weaker than those at glucose 5.5mM and mannitol 50mM (the upper image). There was no obvious difference observed on the $CB_1$ bands at glucose 5.5mM and mannitol 50mM. Beta-actin was used here to replace GAPDH as the reference gene in order to exclude the influence of saturation. The lower image shows that the intensity of beta-actin bands was comparable among these three treatments.

The density of bands was measured and the results from four independent experiments are shown in Figure 4.3 (A). It was found that 50mM glucose significantly decreased $CB_1$mRNA expression ($P<0.05$) to 57% of the control level. The $CB_1$mRNA expression in mannitol 50mM was 110% of the control level, which was also significantly higher than that in glucose 50mM ($P<0.05$). The result excluded the effect of osmolality on the $CB_1$ expression, indicating that high glucose itself downregulates $CB_1$ mRNA expression.

A

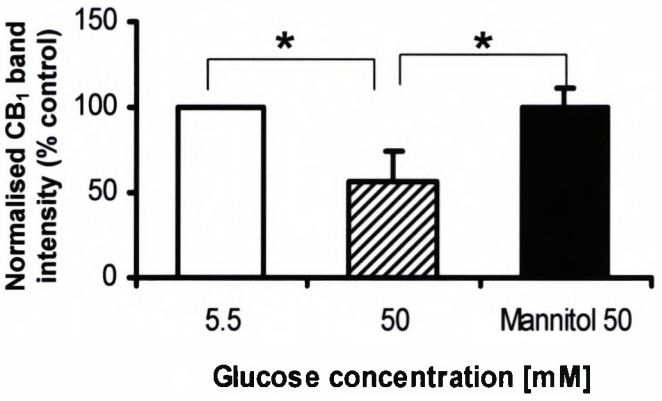


B

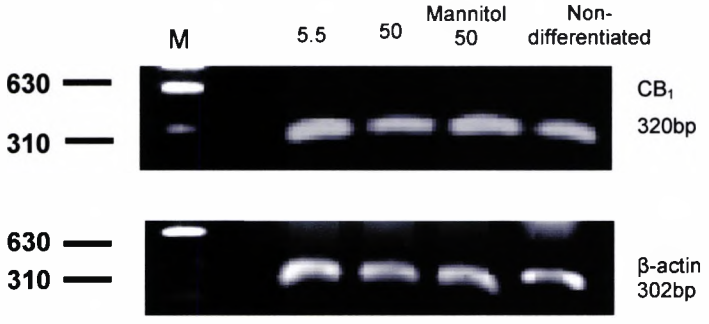


**Figure 4.3** Reverse transcription-PCR analysis of the effect of glucose on $CB_1$ receptor mRNA expression in PC12 cells. RT-PCR was performed on total RNA (2 µg) extracted from cells cultured for 6 days in the presence of 50 ng/ml nerve growth factor, 5.5 or 50 mM glucose and 50mM Mannitol. **(A)** After gel electrophoresis and ethidium bromide staining, the intensity of the cDNA for $CB_1$ (320bp) was quantified by densitometry, and normalised relative to β-actin (302bp). Data expressed as individual values from four independent experiments (*, $P < 0.05$: one-way ANOVA-Fisher's post-hoc analysis). The amount of $CB_1$ products was normalised to the corresponding beta actin and the control level of 5.5mM. **(B)** Representative gels of RT-PCR products. M = marker, ΦX174 RF DNA/HaeIII fragments.

### 4.3.2 Real time-PCR

The fluorescence dye, SYBR GREEN, binds to only double strand DNA, so that, more DNA template exists, greater fluorescence is generated. Therefore, the cDNA with most target products reaches the exponential phase first with lowest threshold cycles ($CT_{50}$).

As $CB_1$ receptors express abundantly in brain, rat brain RNA was used here to validate the real-time PCR conditions by applying a serial concentration of rat brain RNA template (0.04-0.68μg). The real time-PCR result (Figure 4.4 A) showed that the threshold cycles for the reactions were on a reverse-manner of the amount of RNA applied. The reaction with biggest amount of RNA (0.63μg) reached the exponential stage first with a lowest $CT_{50}$ and the reaction with lowest amount of RNA (0.04μg) reached exponential stage last with a highest $CT_{50}$.

The real-time PCR products were run on an agrose gel in order to assure the accuracy of SYBR GREEN-dependent $CB_1$ detection. The gel result (Figure 4.4 B) showed the intensities of $CB_1$ bands were on a template concentration-dependent manner, indicating the amount of final $CB_1$ products was on proportion to the amount of RNA templates. The gel result was consistent with the real-time result, suggesting the real-time conditions are optimised for detecting $CB_1$ expression in samples.

Figure 4.5 (A) shows representative traces of $CB_1$ expression in PC12 cells cultured in glucose 5.5, 50mM and mannitol 50mM with β-actin as the reference gene. It can be seen that the threshold cycle of $CB_1$ from glucose 50mM is much later than those of $CB_1$ from glucose 5.5mM and mannitol

50mM. In comparison, the traces of β-actin from all treatment stay very close. This result suggests less $CB_1$ target fragments in glucose 50mM. The melting curve of both $CB_1$ and β-actin (Figure 4.5 B) shows clean products above 80°C.

**A**

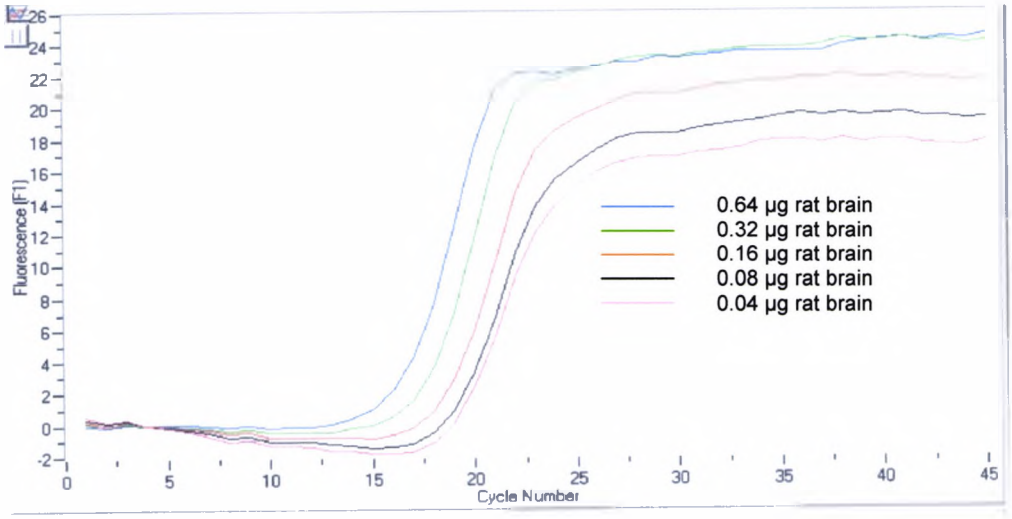


**B**

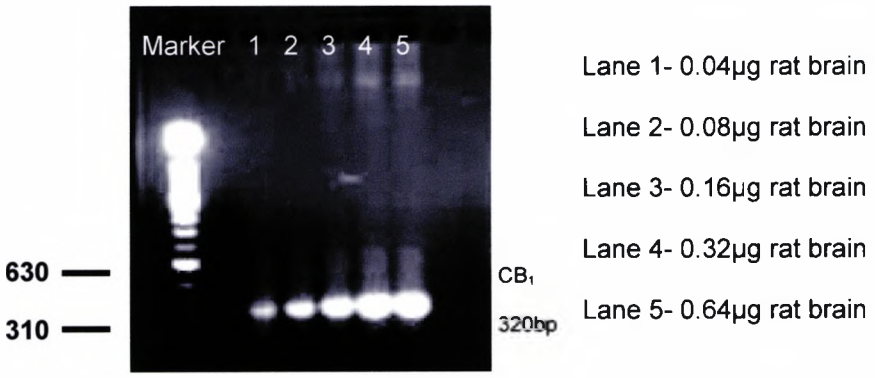


**Figure 4.4** Real time-PCR analysis of the $CB_1$ receptor mRNA expression in rat brain. **(A)** The fluorescence traces representing $CB_1$ amplification from rat brain 0.04, 0.08, 0.16, 0.32 and 0.64 µg. **(B)** The agrose gel result of real time-PCR products. Maker, ΦX174 RF DNA/HaeIII fragments.

A

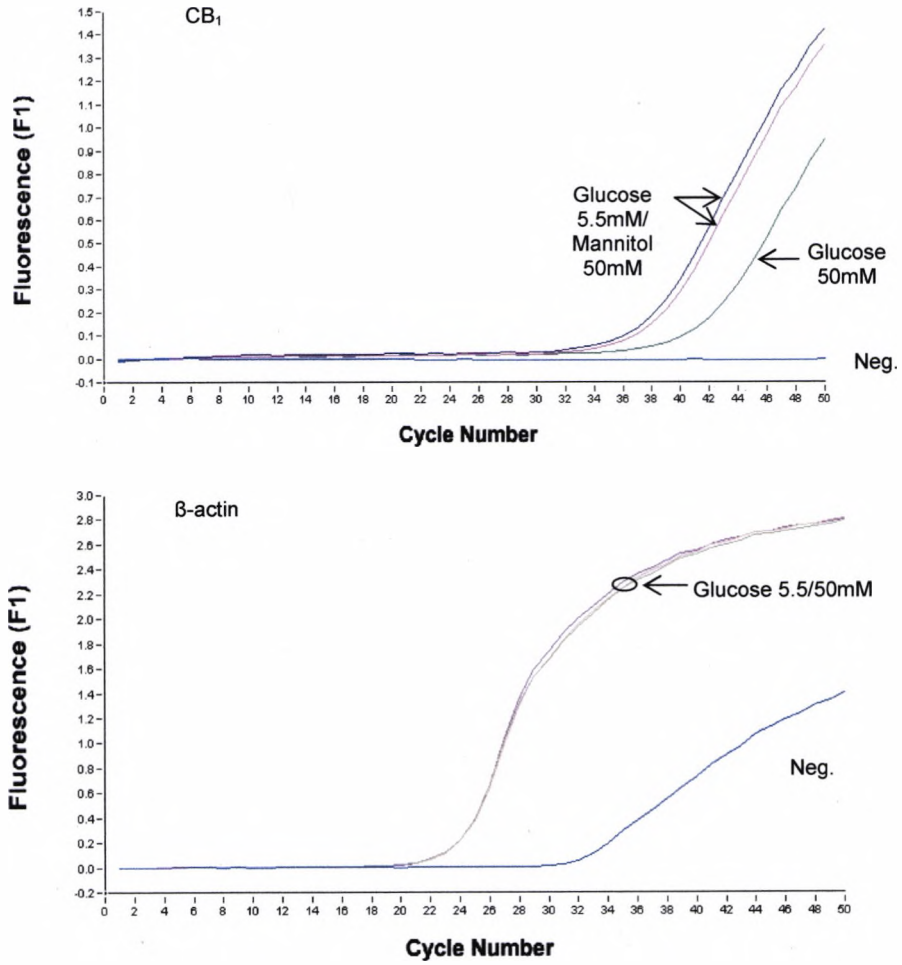


B

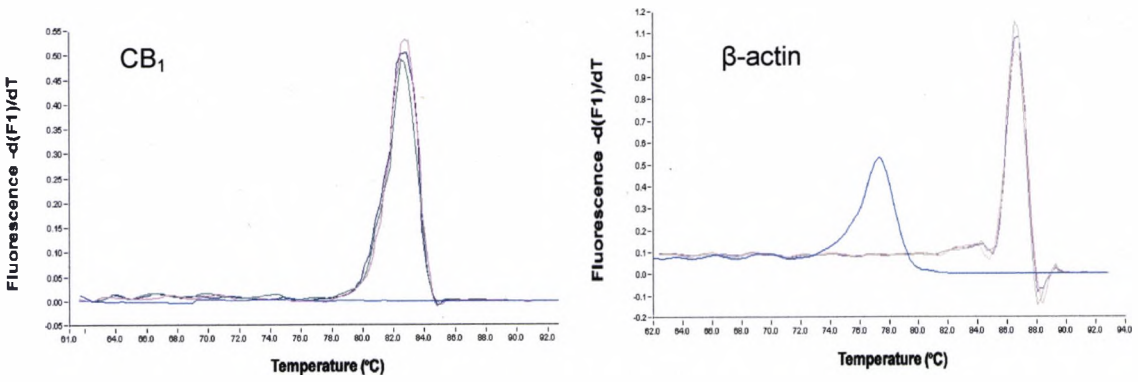


**Figure 4.5** Representative real time-PCR analysis of the $CB_1$ receptor mRNA expression in PC12 cells. **(A)** The fluorescence traces representing $CB_1$/β-actin amplification from PC12 cells cultured in glucose 5.5 and 50mM and mannitol 50mM. **(B)** The melting curves of real time-PCR products.

## 4.4 The cannabinoid $CB_1$ protein expression in hyperglycaemic PC12 cells and DRG neurons from diabetic rats

### 4.4.1 *In vitro* cell model

#### 4.4.1.1 Immunocytochemistry

The PC12 cells on day 6 of culture in 5.5mM and 50mM glucose conditions were stained by using $CB_1$ (red) and TRPVR1 (green) antibodies, and monitored by using confocal microscopy to investigate the expression level of $CB_1$ receptors. Figure 4.6 (A) shows a representative image displaying a fully differentiated cell cultured in 5.5mM glucose on day 6. As seen in Figure 4.6 (B and C), it was observed that the soma and neurite outgrowths of PC12 cells expressed $CB_1$ receptors, with immunofluorescence associated predominantly on the neurite tips and cell body membrane. The decreased immunofluoresence of $CB_1$ (red) was observed in cells cultured in 30mM and 50mM glucose levels (Figure 4.6 E and F) compared with the fluorescence in cells cultured in 5.5mM glucose levels (Figure 4.6 D), indicating downregulation of $CB_1$ protein in cells treated with high glucose (30 and 50mM). Meanwhile, the co-staining revealed TRPV1-postive immnofluoresence (green) in cells cultured in all of three conditions, suggesting the TRPV1 protein is not degraded in response to high glucose (30 and 50mM).

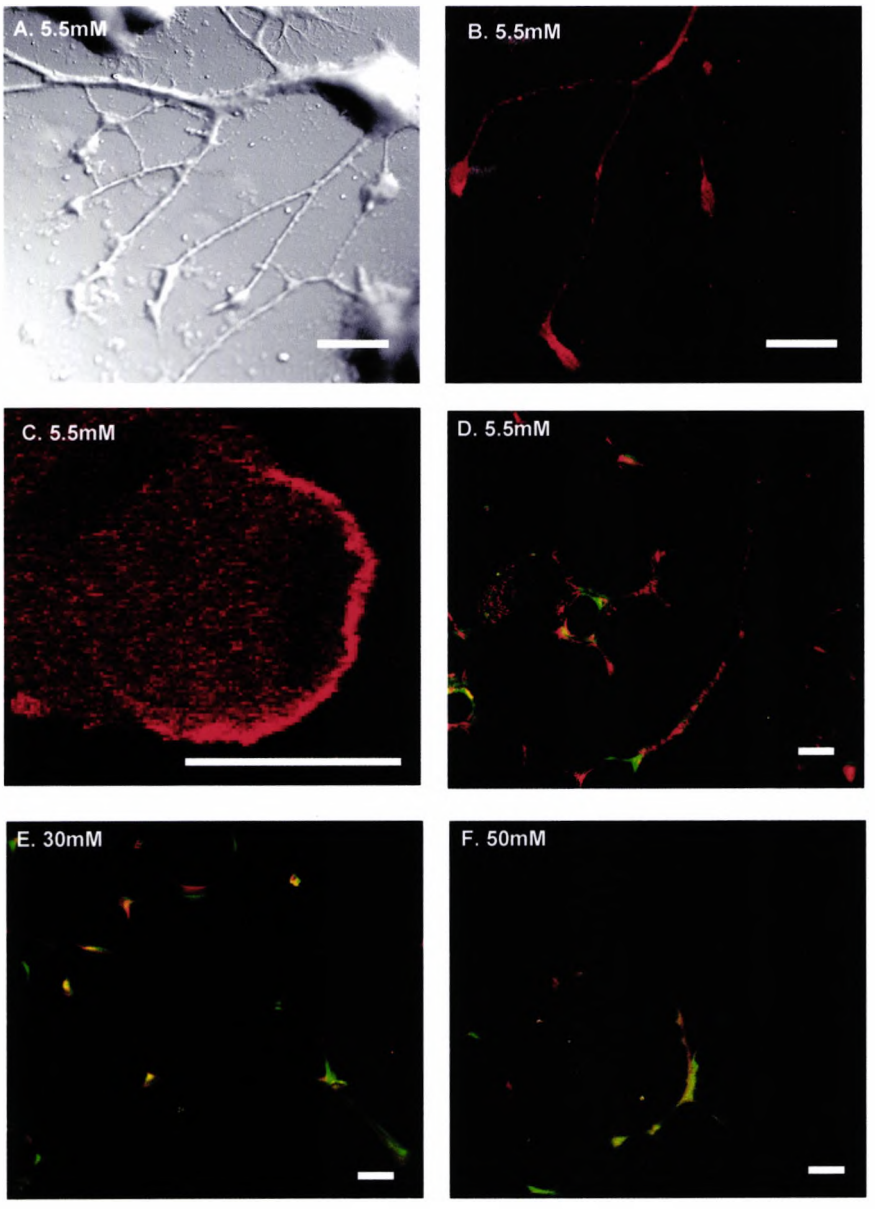


**Figure 4.6** Confocal and Western analysis of $CB_1$ receptor expression in differentiated PC12 cells cultured in variable glucose concentrations. Immunoreactivity (fluorescence) is associated with the soma and neurites: red corresponds to $CB_1$ receptor label (rhodamine) and green to TRPV1 receptor label (FITC). **(A), (B)** and **(C)** reveal highly differentiated PC12 cells, and the cellular location of $CB_1$ expression when cultured in 5.5 mM physiological glucose concentration (single staining for $CB_1$). **(D), (E)** and **(F)** represent the graded reduction of $CB_1$ receptor protein (red) expressed in PC12 cells cultured in glucose 5.5, 30, and 50 mM, respectively (dual-staining for $CB_1$ and $TRPV_1$). Representative images of six independent cultures. Scale bar = 10 µm. x40 magnification.

#### 4.4.1.2 Western blotting and immunoprecipitation

The $CB_1$ receptor expression was further confirmed by using Western blot and immunoprecipitation. The western blot result (Figure 4.7 A) showed there was a reduction of $CB_1$ protein in cells cultured in 50mM glucose compared with that in cells cultured in 5.5mM glucose although double bands appeared in each condition. In order to obtain highly specific bands and improve the initial protein concentration loaded into SDS gels, immunoprecipitation was adopted to detect $CB_1$ protein. The result (Figure 4.7 B) showed a very clear single band of $CB_1$ protein at 60kDa and a reduced density of $CB_1$ band in the lane of 50mM glucose compared to that in the lane of 5.5mM glucose, whilst the reference protein, beta-actin, remained unchanged.

The $CB_1$ bands from four independent experiments were measured by densitometry and analyzed as shown in Figure 4.7 (C). Taking $CB_1$ protein levels in 5.5mM conditions as 100%, the $CB_1$ receptor was significantly reduced in 50mM conditions by 40%. This indicates a downregulation of $CB_1$ protein expression in PC12 cells cultured in high glucose conditions (50mM).

As protein kinases disrupt $CB_1$ protein activities by phosphorylating $CB_1$-serine, the phosphorylation of $CB_1$ receptor was also studied by applying anti-phosphorylated serine antibody to the precipitated $CB_1$ protein. The result (Figure 4.8 A) showed that the phosphorylation level of $CB_1$ receptors was less in cells cultured in 50mM glucose than in cells culture in 5.5mM glucose (left panels). The $CB_1$ protein from same samples was conducted as controls (right panels). The bands were measured and normalised to control $CB_1$ protein levels from 5.5mM and 50mM glucose correspondingly. The result (Figure 4.8

B) showed phosphorylated $CB_1$ protein levels were relatively equal in 5.5mM and 50mM glucose conditions without significant differences.

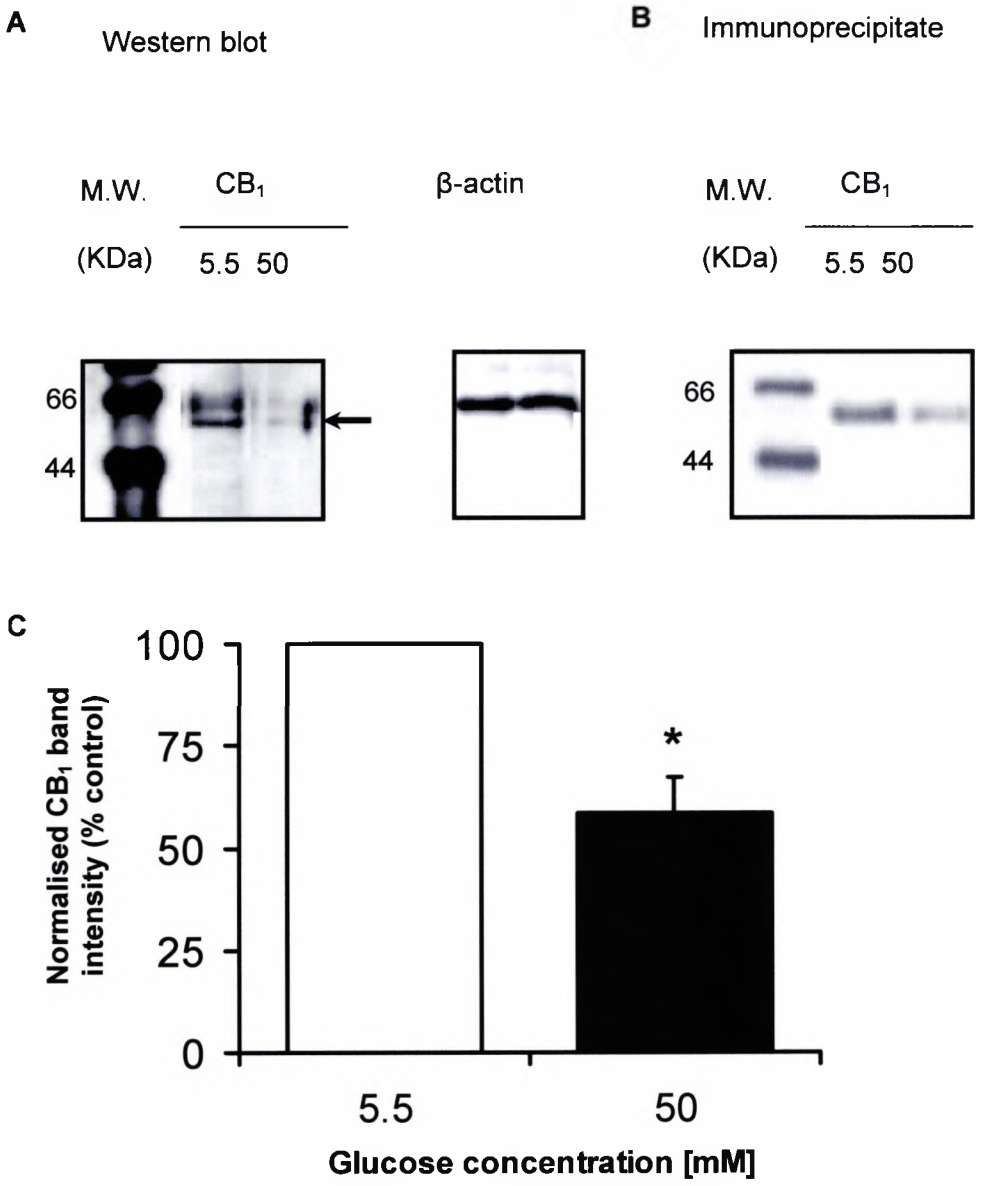


**Figure 4.7** Western blot analysis confirmed the reduction of $CB_1$ receptor protein in cells cultured in high glucose. **(A)** Representative image of western blot of $CB_1$ protein (60 kDa) in 5.5 or 50mM glucose levels. **(B)** Representative image of immunoprecipitate of $CB_1$ protein (60 kDa) in 5.5 or 50mM glucose levles. **(C)** The intensity of the band for $CB_1$ was quantified by densitometry and normalised to β-actin band intensity, and is expressed a percentage of the control level (5.5 vs. 50 mM glucose. *, $P < 0.05$: unpaired Student's *t*-test, n = 5 independent cultures).

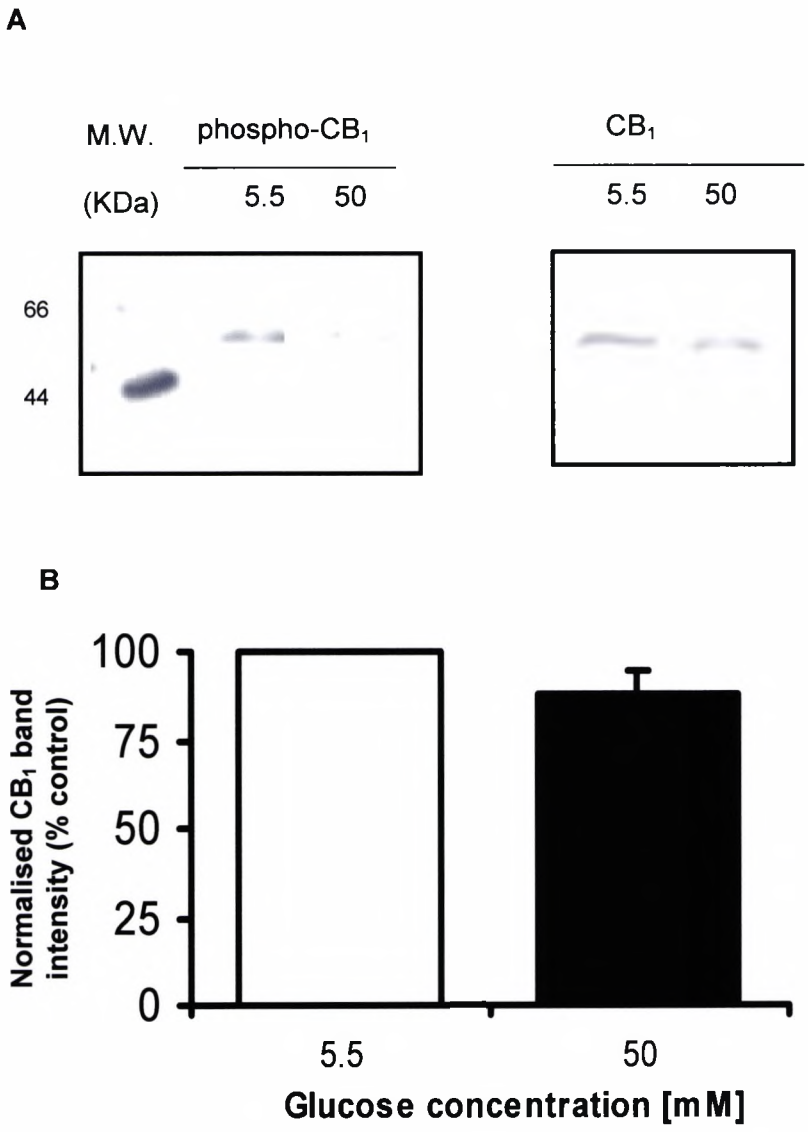


**Figure 4.8** Immunoprecipitate analysis of phosphorylation of $CB_1$ receptors in PC12 cells cultured in 50mM glucose versus controls (5.5mM). **(A)** Representative images of phosphorylation levels of $CB_1$ receptors (left panel) and $CB_1$ protein (right panel) in PC12 cells cultured in the control (5.5mM) and 50mM glucose. **(B)** The intensity of the bands for phosphorylated $CB_1$ receptors were quantified by densitometry and normalised to $CB_1$ band intensity, and is expressed a percentage of the control level (5.5 vs. 50mM glucose, $P > 0.05$, unpaired Student's *t*-test, $n = 4$ independent cultures).

### 4.4.2 *In vivo* model

#### 4.4.2.1 Optimisation of immunohistochemistry on formalin fixed paraffin embedded tissue samples

Paraffin fixation masks the antigenicity of tissue samples, so that an appropriate antigen retrieval procedure prior to immunostaining is very important to improve the signal of immunofluoresence by unmasking antigen. In the current experiment, human mid-brain tissue sections were employed as the abundant expression of $CB_1$ receptors and rich existence of A and C fibres.

A dual staining of $CB_1$ plus A/C fibres or A plus C fibres was conducted in order to examine the efficiency of antibodies, dual staining protocols as well as antigen retrieval techniques (stated in methods). The immunofluorescence of $CB_1$ protein, A and C fibres detected by the antibodies was all observed in the brain samples (Figure 4.9). Figure 4.9 (A) shows that $CB_1$ receptor was highly co-localised with C fibres, in contrast, there was only a partial co-localisation observed between $CB_1$ and A fibres (Figure 4.9 B). The dual staining of A and C fibres showed an interlocked distribution of these two type of fibres in human brain samples. The sensitive immunofluoresence and accurate detection indicates the antibodies, dual staining protocols and antigen retreiveal techniques are efficient to detect the expression and location of $CB_1$ receptors.

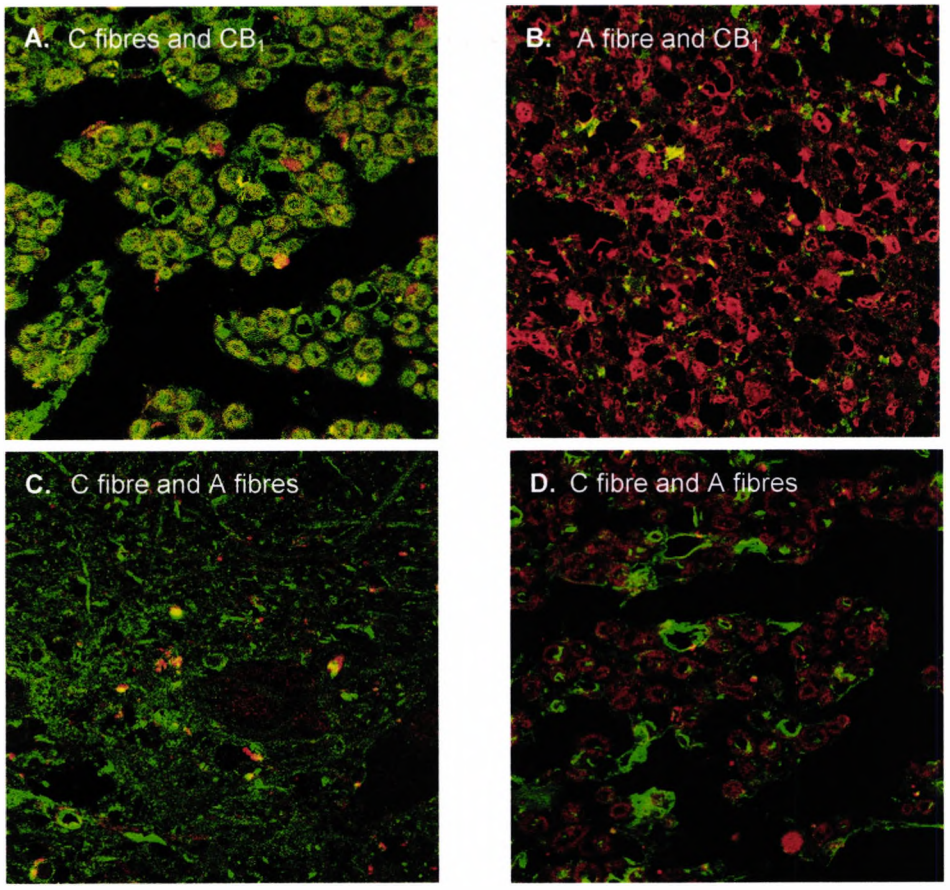


**Figure 4.9** Confocal detection of the colocalisation of cannabinoid $CB_1$ receptors, and A or C fibres in human mid-brain. **(A)** represents the colocalisation of $CB_1$ receptors and C fibres, red corresponds to C fibres and green to $CB_1$ receptors. **(B)** represents the colocalisation of $CB_1$ receptors and A fibres, red to A fibres and green to $CB_1$ receptors. **(C** and **D)** represent the colocalisation of A and C fibres, red to C fibres and green to A fibres.

#### 4.4.2.2 Immuno-detection of $CB_1$ protein expression in DRG neurons from control and diabetic rats

A single $CB_1$ staining was conducted in order to investigate the $CB_1$ expression in DRG neuron samples from control or diabetic rats. Figure 4.10 shows that the immunofluorescence of $CB_1$ protein (red) was mainly located on small and intermediate neurons, indicating $CB_1$ receptors predominately expressed on small and intermediate sized DRG neurons. The results revealed that a lower level of $CB_1$ receptors existed in DRG neurons from diabetic rats (Figure 4.10 B and D) when compared with those expressed in control DRG neurons (Figure 4.10 A and C). The positive $CB_1$ immunofluoresence was further confirmed by the negative control showing no clear immunofluoresence detected when omitting the first $CB_1$ antibody.

$CB_1$ positive neurons in each section were quantified as shown in Figure 4.10 (F). It was found that $CB_1$ positive neurons were 49% of total neurons from control rats and 26% of total neurons from diabetic rats. There was a significant reduction on $CB_1$ expression in DRG neurons from diabetic rats compared with controls.

The result was further confirmed by using Western blot. Figure 4.11 (A) shows that the intensity of $CB_1$ bands was observed to be decreased in the lane of diabetic rats compared to the intensity of $CB_1$ bands in the lane of control rats. The reference protein of beta-actin was detected to be unchanged in the same samples. The intensity of $CB_1$ bands were quantified and normalised to beta-actin. The results (Figure 4.11 B) showed that the $CB_1$ expression in diabetic DRG neurons was 38% of the control levels. This was a more than 2-fold reduction with significant difference ($P<0.01$) on $CB_1$ protein levels.

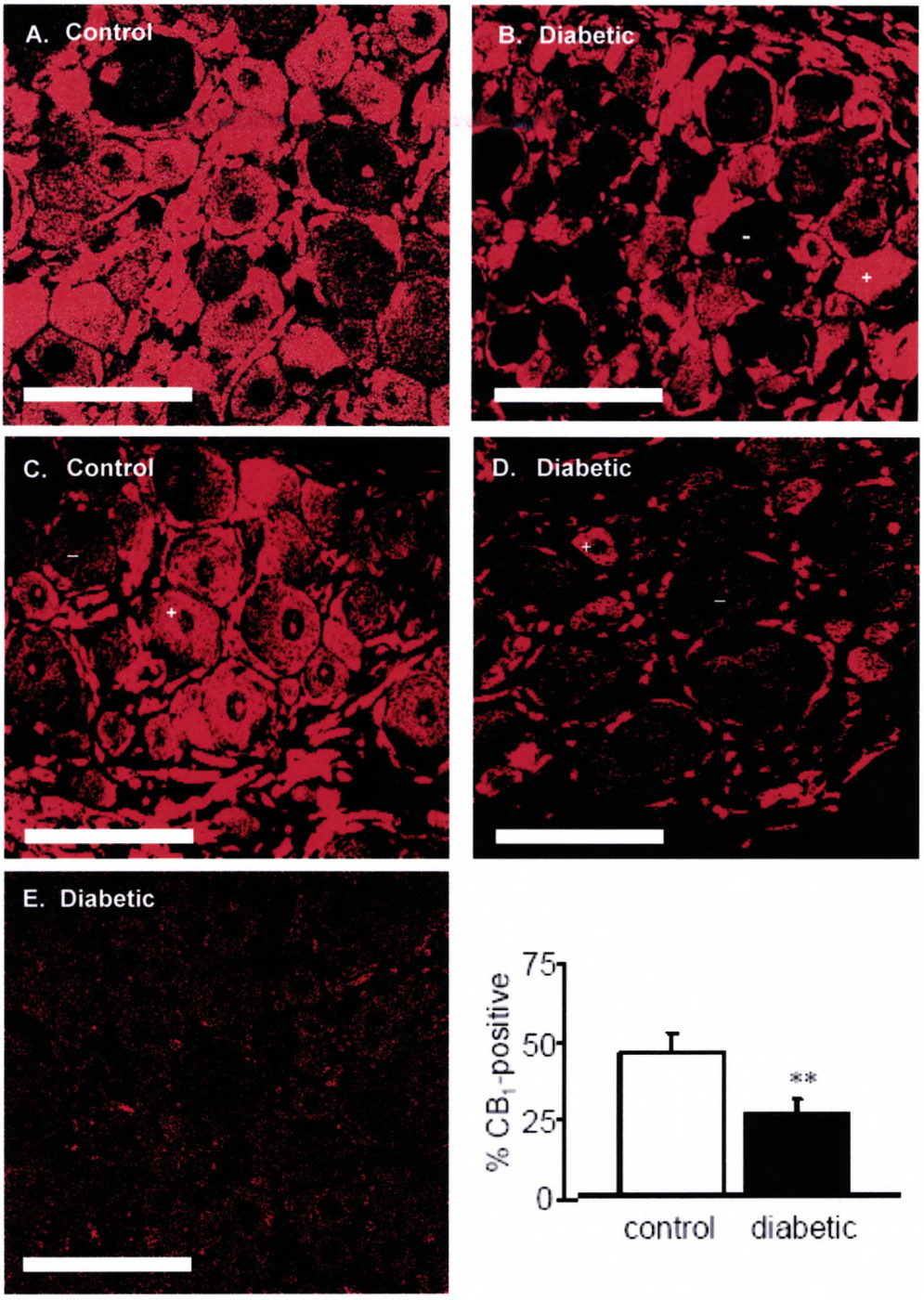


**Figure 4.10** Confocal analysis of $CB_1$ protein expressed in rat DRG. Immunoreactivity (fluorescence) is associated with the DRG neuron cell bodies: red corresponds to $CB_1$ receptor label (rhodamine) under x40 magnification. **(A** and **C)** represent $CB_1$ postive (+) and negative (-) DRG neurons in control rats. **(B** and **D)** represent $CB_1$ postive (+) and negative (-) DRG neurons in diabetic rats. **(E)** represents the negative control of $CB_1$ staining by omitting the first antibody. Scale bar = 50μm. When expressed as a percentage of total neuron count per section, **(F)** shows that experimental diabetes significantly decreased the number of $CB_1$-positive neurons (approximately twofold) in the 4-8 week diabetic animals compared to controls. Data shown are the mean ±29 s.e.mean of five animals in each group (**, P<0.01: unpaired Student's *t*-test).

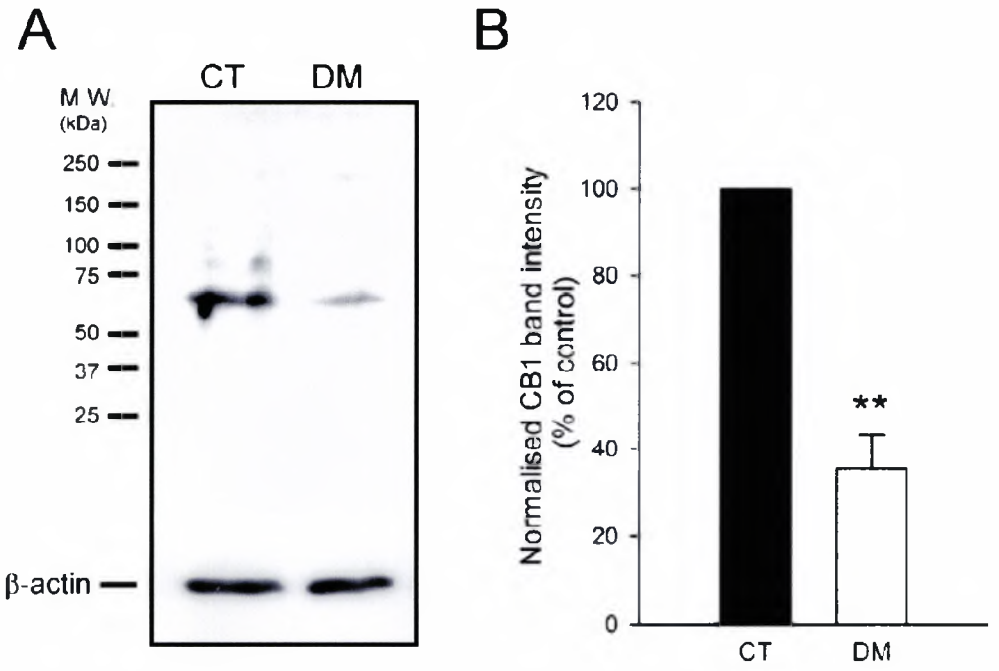


**Figure 4.11** Western blot analysis of $CB_1$ receptor expression in rat DRG. The expression level of $CB_1$ receptor protein markedly decreased on plasma membranes of DRG neurons from diabetic rats (DM) as compared with the controls (CT). The intensity of the band for $CB_1$ (60 kDa) was quantified by densitometry and normalised to β-actin band intensity, and is expressed a percentage of the control level (**, $P < 0.01$: unpaired Student's *t*-test, n = 3 per group).

#### 4.4.2.3 Immuno-detection of the co-expression of $CB_1$ receptors and C fibres in DRG neurons from control and diabetic rats

The degenerated small neuron fibres are believed to be mainly involved in the progression of painful neuropathy occurred in diabetic patients. The current experiment examined the $CB_1$ protein level in C and Aδ fibre-DRG neurons from diabetic rats in order to investigate whether loss of $CB_1$ receptor occurs on small fibre neurons in diabetic conditions.

Figure 4.12 shows the representative confocal images of dual $CB_1$ and C fibre immunoreacitivity in rat DRG neurons. The result revealed that the co-localisation (yellow) of $CB_1$ receptors (green) and C fibres (red) were less in diabetic DRG neurons (Figure 4.12 A and C) than that observed in control neurons (Figure 4.12 B and D), indicating a reduction of $CB_1$ expression on C and Aδ fibres in DRG neurons from diabetic rats compared with controls.

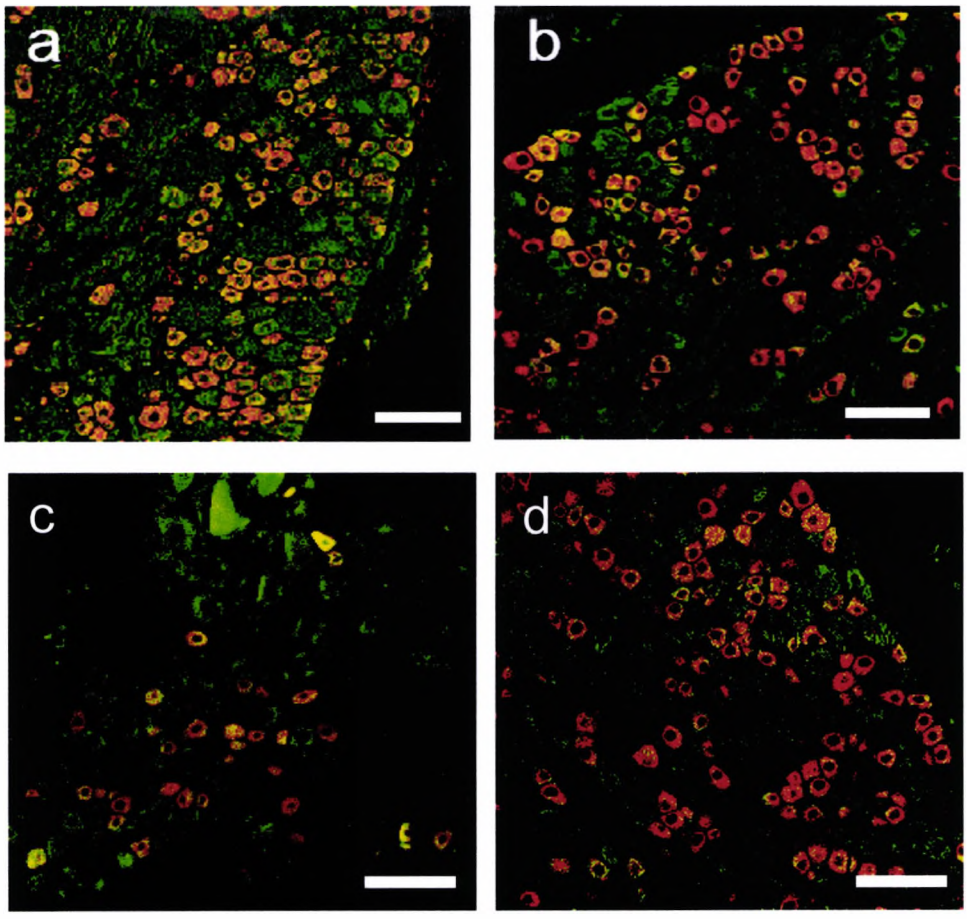


**Figure 4.12** Confocal analysis of co-localisation of $CB_1$ protein and C fibre in rat DRG neurons. Dual-staining for $CB_1$ (green fluorescence) and C- and Aδ-fibers (red fluorescence) associated with DRG cell bodies in **(A** and **C)** control and **(B** and **D)** diabetic rats under low magnification (x20); scale bar = 75μm.

## 4.5 Discussion

Based on the observation in the previous chapter, PC12 cells reproduced some of the phenomena of diabetic neuropathy when exposed to that chronic of high glucose. PC12 cells were chosen as an *in vitro* model of diabetic neuropathy to investigate the effect of glucose on expression of $CB_1$ receptors. Furthermore, these cells are known to express both $CB_1$ receptors (Bisogno *et al.*, 1998) and TRPV1 receptors (Someya *et al.*, 2004).

To our knowledage, this is the first study to investigate the role of $CB_1$ receptors in diabetic neuropathy by using PC12 cell model. We, therefore, decided to confirm that this cell line is capable of reflecting changes in $CB_1$ expression induced by exogenous stimuli. A previous study conducted by Vallano *et al.*, (2006) showed that depolarizing the cell membrane by increasing the KCl concentration from 5 to 25mM in culture medium down-regulates $CB_1$ expression in $CB_1$-rich cerebellar granule neurons, which subsequently alters down-stream signal transduction (Vallano *et al.*, 2006). By adopting the method in PC12 cells, the membrane depolarization was found to down-regulate $CB_1$ mRNA level by 60% on day 6 of culture. The consistent result strongly suggests PC12 is a valid neuronal cell line to study changes in $CB_1$ expression in an *in vitro* model of diabetic neuropathy.

The regulation of $CB_1$ gene expression was firstly studied in PC12 cells cultured in a range of glucose treatments (5.5, 10, 20, 30,40 and 50mM) under the stimulation of NGF (50ng/ml). It can be seen that the results were highly variable, although there is a trend towards decreased $CB_1$ expression, which may due to the unequal amount of differentiated cells, based on the observation that PC12 cells did not fully attach and were poorly differentiated

during the experiment. To address this issue, we compared the $CB_1$ gene expression in undifferentiated cells and NGF-induced differentiated cells, both cultured in physiological glucose (5.5mM), after optimising the plating method by extending the drying time of poly-L-lysine coated-plates and purchasing a new batch of NGF. The results show that, in 5.5mM glucose, NGF-induced differentiated cells had more $CB_1$mRNA than the raw cells, which suggests that the undifferentiated cells masked the effect of glucose on $CB_1$ expression in differentiated cells. The likelihood of NGF regulating $CB_1$ expression seems to be ruled out by evidence provided by Ahluwalia *et al*, (2002) showing that the number of $CB_1$ expressing DRG neurons did not decline without NGF supplement in culture (Ahluwalia *et al.,* 2002). However, in that study the existence of $CB_1$ receptors was only defined in the neuronal cell body by immunostaining (Ahluwalia *et al.,* 2002), the lack of quantitative measurement (eg. Western blot) and omission of axons and dendrites may have led to an inaccurate conclusion of NGF-related $CB_1$ expression.

By ensuring PC12 cells were optimally differentiated, high glucose was found to decrease the expression of $CB_1$ receptors at the RNA level by using both conventional RT-PCR (50% decrease) and real time PCR ($\Delta C_T$=4). Based on the evidence that $CB_1$ receptors are synthesised in the cell body and inserted to axonal terminals (Hohmann and Herkenham, 1998, Hohmann and Herkenham, 1999), the impaired neurite outgrowth induced by high glucose may related to the decreased $CB_1$mRNA expression.

Subsequently, the effect of high glucose on $CB_1$ receptors at the protein level was also examined. Immunocytochemical analysis revealed $CB_1$ receptors are located predominantly on the plasma membrane of the soma and neurite tips,

which may be related to the existence of $CB_1$ receptors on presynaptic terminals regulating neurotransmitter release (Domenici *et al.,* 2006). From the immunostaining images, an overt reduction in $CB_1$ receptor protein expression was seen with high glucose, whilst TRPV1 receptors, a nociceptive neuronal maker, were strongly expressed in PC12 cells at both glucose concentrations, which supports the hypothesis that the decreased $CB_1$ protein expression is involved in the pathogenesis of diabetic neuropathy. These results, together with the later Western blot analysis showing a 50% loss of $CB_1$ receptors in PC12 cells cultured in 50mM glucose, suggest that high glucose decreases $CB_1$ protein expression. It is known that neurotransmitters and neuropeptides transduce the cell signals from the painful stimuli to the central nervous system, and depletion of $CB_1$ receptors elevates neuropeptide release in mice (Steiner *et al.,* 1999). Combined with the findings showing that hyperglycaemia enhances neurotransmitter secretion from PC12 cells (Lelkes *et al.,* 2001), the results of decreased $CB_1$ expression in the current study may indicate that the enhanced neurotransmission induced by hyperglycaemia is due to the loss of $CB_1$ receptors.

These results were corroborated in DRG from diabetic rats, where the number of $CB_1$-positive neurons was decreased to approximately half that of control animals, and the density of $CB_1$ receptors was reduced by 60% in diabetic versus control DRG. Previous studies report 25-57% of DRG neurons are $CB_1$-positive in rats (Ahluwalia *et al.,* 2000; Bridges *et al.,* 2003). The decrease in number of $CB_1$-positive neurons might reflect a cessation of $CB_1$ synthesis in neurons that normally express $CB_1$ (a phenotypic switch), or simply that the level of expression was undetectable due to reduced receptor density. $CB_1$ receptors mediate, in part, the neuroprotectant properties of cannabinoids

(reviewed by van der Stelt & Di Marzo, 2005), and any decrease in expression is expected to contribute to the development and progression of the neurodegeneration associated with diabetes. A study recently published by Duarte *et al.* (2007) revealed decreased $CB_1$ mRNA expression in the hippocampus of diabetic rats, concomitant with an increase in $CB_1$ protein density. Whilst the mRNA data are in agreement with our findings, differences in neuronal $CB_1$ protein expression between hippocampus (↑ Duarte *et al.*, 2007) and DRG (↓ present study) from STZ-induced diabetic rats may reflect site-specific signalling pathways involved in mRNA translation, e.g. activation of the key rate-limiting translational pathway mTOR in hippocampal neurons (Duarte *et al.,* 2007).

Abnormal cell signalling induced by increased PKC activity is indicated in the pathophysiology of diabetes. PKC was reported to disrupt $CB_1$ activity by phosphorylating the receptors (Garcia *et al.,* 1998). We, therefore, examined the phosphorylation level of $CB_1$ receptors in the cell model of diabetic neuropathy. It was found that the phosphorylation level of $CB_1$ receptors was relatively equal in both glucose concentrations, suggesting the $CB_1$ activity is preserved. This result may be positively connected to two recent animal studies showing anti-nociceptive action of a mixed cannabinoid $CB_1/CB_2$ receptor agonist is preserved in diabetic mice (Doğrul A, *et al.*, 2004) and rats (Ulugol A, *et al.*, 2004). However, a $CB_1$ function study, investigating whether a decreased $CB_1$ receptor leads to a decreased function in this cell model, was warranted. The results of this study are presented in Chapter 5.

# CHAPTER 5

# AN INVESTIGATION OF THE EFFECT OF GLUCOSE ON CANNABINOID RECEPTOR FUNCTION

## 5.1 Introduction

This chapter investigates whether the function of $CB_1$ receptors is altered in PC12 cells cultured in high glucose, mimicking hyperglycaemic conditions, where we have previously found a decreased $CB_1$ expression. TRPV1 receptors are a non-selective cation channel sensitive to the pungent vanilloid capsaicin (Caterina *et al.,* 1997). Capsaicin-evoked CGRP release from sensory neurons is inhibited by the endocannabinoid, anandamide (Richardson *et al.,* 1998a). This effect is mediated by cannabinoid $CB_1$ receptors, which are co-expressed with TRPV1 in nociceptive afferents (Ahluwalia *et al.*, 2002; Ahluwalia *et al.*, 2003). Activation of $CB_1$ receptors suppresses neuropeptide release via inhibition of $Ca^{2+}$ channels and activation of $K^+$ conductance; *in vivo* and *in vitro* studies have shown that $CB_1$ agonists inhibit capsaicin stimulated-$Ca^{2+}$ entry into sensory neurons via a $CB_1$-dependent pathway (Kelly and Chapman, 2001; Oshita *et al.*, 2005). In the current studies, the $CB_1$ agonist, HU210, was used to assess $CB_1$-mediated inhibition of capsaicin-evoked $Ca^{2+}$ influx in the neuronal cell line, PC12. In 2005, Hong and Wiley demonstrated a greater $Ca^{2+}$ current in response to capsaicin occurred in sensory neurons from diabetic rats (Hong and Wiley, 2005). It is important to know whether a decreased $CB_1$ receptor expression leads to a decreased function, resulting in increased signal transduction towards TRPV1 receptors in the model of diabetic neuropathy.

The aims of this chapter were to determine 1) whether TRPV1 receptors were sensitised in differentiated PC12 cells cultured in high glucose mimicking hyperglycaemic conditions; 2) whether $CB_1$ receptors lost their function in response to high glucose in PC12 cells. In the experiments of this chapter,

PC12 cells were cultured in physiological glucose level (5.5mM) and high glucose level (50mM) under the stimulation of NGF (50ng/ml) for 6 days. A $Ca^{2+}$ imaging assay was used to assess the $CB_1$ receptor function in differentiated PC12 cells from both conditions. A considerate number of preliminary experiments were conducted to optimize the techniques. The optimal concentration of $Ca^{2+}$ indicator dye, duration of incubation, frequency of scanning, and the time point for the stimulation, were all very important to ensure the efficient capture of $Ca^{2+}$ influx by confocal microscopy. A concentration- response course was conducted to obtain the optimal concentration of capsaicin and HU210 response in differentiated PC12 cells. Having established the capsaicin response and inhibitory effect of HU210 on $Ca^{2+}$ influx, the selective $CB_1$ receptor antagonist, AM251, and the selective $CB_2$ receptor antagonist, AM630, were used to examine whether the inhibition of $Ca^{2+}$ influx was mediated by $CB_1$ receptors, and/or $CB_2$ receptors, respectively.

## 5.2 Optimization of parameters for $Ca^{2+}$ imaging assay with confocal microscopy

The parameters of $Ca^{2+}$ imaging were optimized in the preliminary studies. In these experiments, the applicability and efficacy of the optimized conditions was determined by stimulating intracellular $Ca^{2+}$ increase in PC12 cells by KCl (70mM; depolarizes cell membrane) and thapsigargin (10mM; releases $Ca^{2+}$ from intracellular stores), which was monitored by using a confocal microscope. PC12 cells were incubated with 5μM of fluo-3 AM, a calcium-sensitive fluorescence dye, for 40 minutes at 37°C before the stimulation.

In Figure 5.1, the upper panel of confocal images shows the fluorescence increase, indicating intracellular $Ca^{2+}$ concentration was induced by KCl (70mM). The lower panel of confocal images shows that thapsigargin stimulated a second rise of fluorescence which was due to release of intracellular $Ca^{2+}$ stores. Representative traces revealed that a rapid increase in $Ca^{2+}$ levels stimulated by KCl and the $Ca^{2+}$ level is maintained above baseline levels for more than 600 seconds, and the second stimulation with thapsigargin induced a further rise in intracellular $Ca^{2+}$, which was more transient in nature (Figure 5.1 B).

This result indicates that the concentration of fluo-3 AM and the time scale of the incubation with PC12 cells, as well as the continuous scan used in this experiment, were the optimal conditions, which could be used in further studies.

A

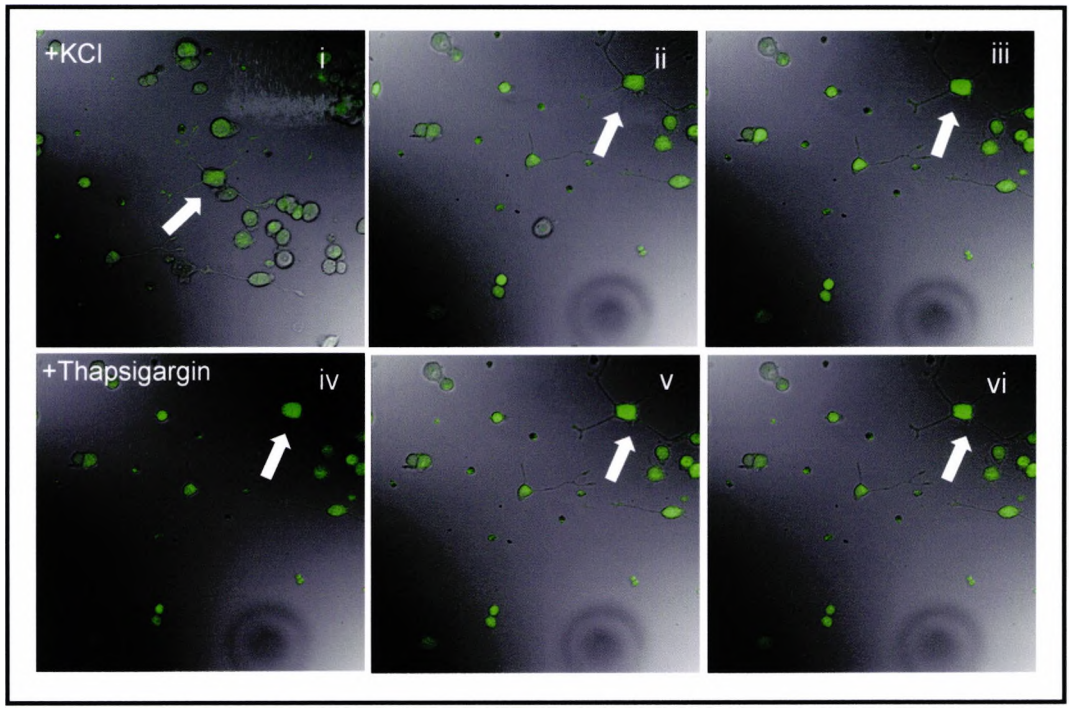


B

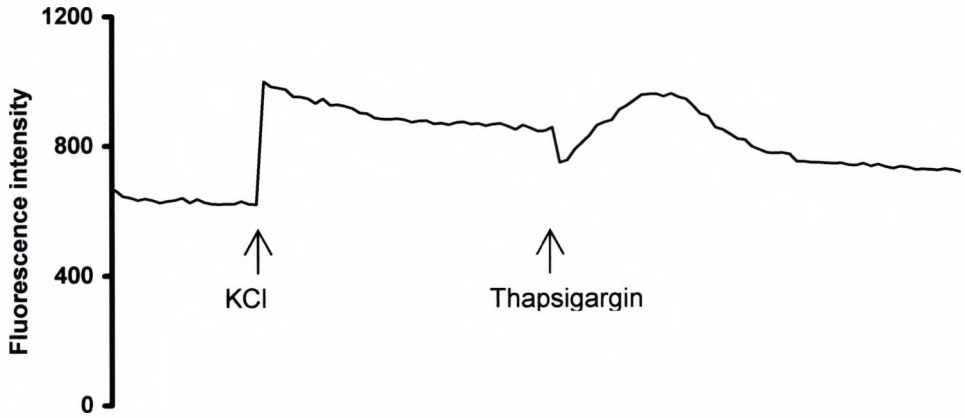


**Figure 5.1** $Ca^{2+}$ influx induced by the addition of KCl and Thapsigargin. **(A)** Upper Box: confocal images (i) before (ii) 300 seconds after (iii) 600 seconds after the stimulation of potassium chloride. Lower box: confocal images (iv) before (v) 300 seconds after (vi) 600 seconds after the stimulation of thapsigargin. **(B)** A representative trace of the intracellular $Ca^{2+}$ change stimulated by KCl and thapsigargin in a single PC12 cell (pointed out by the white arrow). The cell was exposed to potassium chloride (70mM) for 600 seconds followed by the addition of thapsigargin (10μM).

## 5.3 $Ca^{2+}$ influx triggered by Capsaicin (1μM)

Initial experiments were designed to test multiple treatments of capsaicin and HU210 in one sample. PC12 cells cultured in 50mM glucose were loaded with fluo-3 AM (5μM) for 40 minutes at 37°C. As shown in Figure 5.2 (A), in control levels, the addition of vehicle (HEPES buffer) caused a small amount of intracellular $Ca^{2+}$ fluctuation. The following treatment with capsaicin 1μM triggered a large $Ca^{2+}$ influx in the fluo-3 labelled PC12 cells. After $Ca^{2+}$ returned to baseline, HU210 (1μM) was added prior to capsaicin (1μM) in order to study the inhibitory effect of HU210 on $Ca^{2+}$ entry. This combination of HU210 (1μM) and capsaicin (1 μM) also induced a comparable amount of $Ca^{2+}$ influx, which did not show a dramatic decrease compared with the previous single exposure to capsaicin. After removing the HU210, the exposure to capsaicin again stimulated a large transient $Ca^{2+}$ influx, which proved the cells were not desensitised by the previous repeated application of capsaicin. At the end, a larger $Ca^{2+}$ influx was observed after the addition of the positive control, KCl (70mM). Statistically, the inhibitory capacity of HU210 in PC12 cells cultured in 50mM glucose is summarized in Figure 5.2 (B). It shows that the fluorescence intensity produced by capsaicin was 390.8±39.7 which is significantly higher than that produced by the combination of HU210 and capsaicin (278.4±53.1) ($P<0.05$). In other words, HU210 (1μM) inhibits the $Ca^{2+}$ influx triggered by 1μM of capsaicin by 29.77%.

The most common concentration of capsaicin used for the stimulation of $Ca^{2+}$ influx in primary neuronal cells, such as DRG cells is no more than 1μM (Dedov and Roufogalis, 1998, Khasabova et al., 2002, Winter, 1987). However, it is worth mentioning that in this study, only 5% of tested PC12 cells cultured in 50mM glucose were found to respond to capsaicin at 1μM. In fact, less than

5% of tested PC12 cells from control (5.5mM glucose) cells were found to have a detectable capsaicin response at 1μM. Therefore, a capsaicin concentration-response curve was needed to be conducted in order to find an appropriate concentration of capsaicin to obtain repeatable responses in this particular cell line.

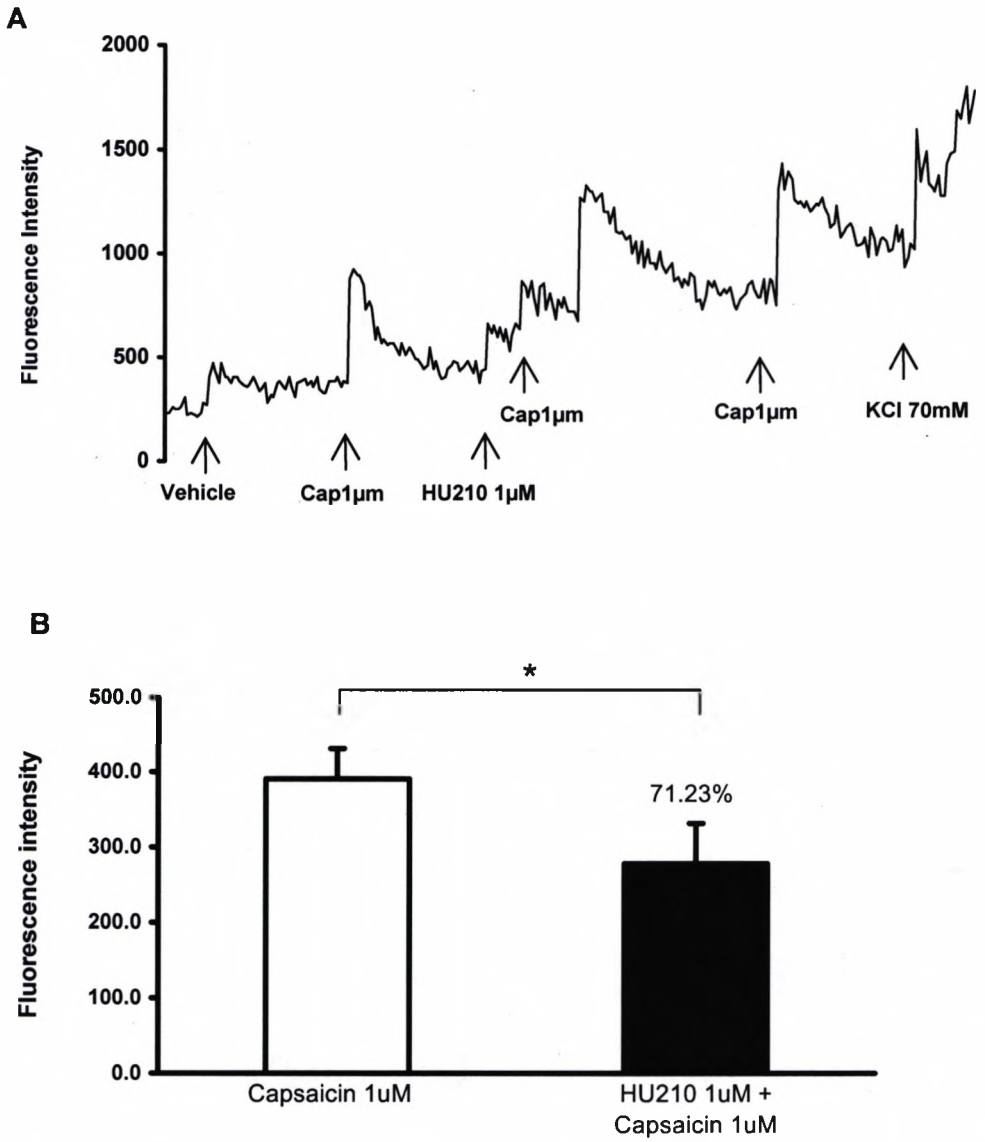


**Figure 5.2** Inhibition of the response of $Ca^{2+}$ influx to capsaicin in the presence of HU210 in PC12 cells cultured in 50mM glucose for 6 days. **(A)** is a representative trace monitoring fluorescence change in PC12 cells during treatments indicated. Firstly, cells were treated with vehicle and capsaicin (1 μM) without any inhibitor; then pre-incubated with HU210 (1 μM) for 3 min before addition of capsaicin; then, a third dose of capsaicin alone followed by KCl after the washout of capsaicin is the end. **(B)** shows the values which are expressed as the mean ± S.E. of the increased fluorescence above the basal fluorescence. The increase of fluorescence intensity in the PC12 cells treated with capsaicin (1 μM) was significantly different from HU210 1μM (pre-treatment for 3 min) plus capsaicin (n=8). (*, $P<0.05$ Student's paired *t*-test).

## 5.4 Capsaicin concentration-response curve

In these experiments, the $Ca^{2+}$ indicator, fluo-3 AM was replaced by its analogue, fluo-4 AM, since fluo-4 AM emits fluorescence brighter under the same wavelength. All the other preparation remained unchanged. In addition, a single treatment of capsaicin followed by KCl (70mM) was adopted in order to improve the applicability and remove the concern of TRPV1 desensitisation. Therefore, the capsaicin response was normalized to KCl response to exclude the influence of variable fluorescence baseline and response capacity from each individual cell.

In the capsaicin concentration-response study, a range of capsaicin concentrations (1- 700μM) were used to generate a $Ca^{2+}$ influx in differentiated PC12 cells. As shown in Figure 5.3, capsaicin above 50μM was able to stimulate $Ca^{2+}$ entry in PC12 cells, and the capsaicin response followed a concentration-dependent manner up to 700μM. The representative images in Figure 5.3 show the rapid $Ca^{2+}$ entry evoked by capsaicin. An application of KCl 70mM was used at 197 seconds after the recovered $Ca^{2+}$ level, which generated a second peak of $Ca^{2+}$ entry by depolarizing the cell membrane, and then allowed to return to baseline (images not shown). By the different mechanism of generation of $Ca^{2+}$ influx, only the cells responsive to KCl were included for analysis to ensure the viability of cells.

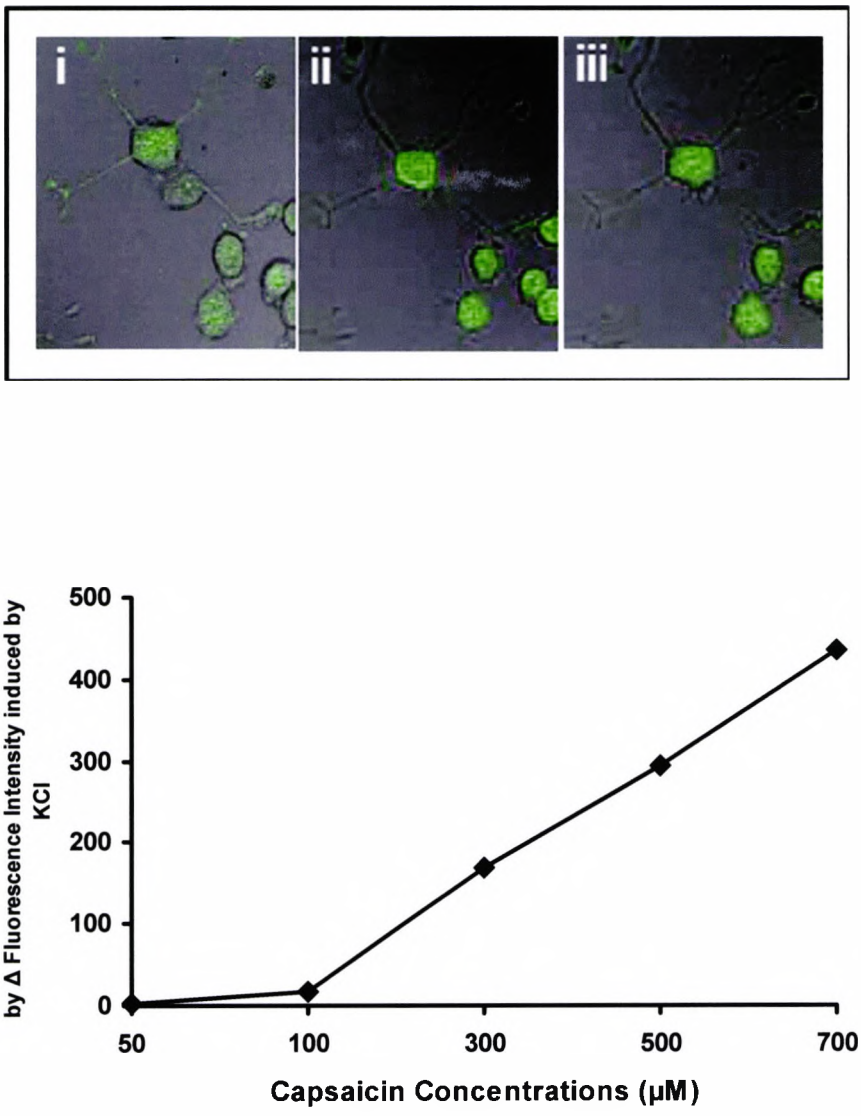


**Figure 5.3** Concentration-response curve to the TRPV1 receptor agonist capsaicin, expressed as the change in fluo-4 fluorescence (≈[Ca2+]i) as a percentage of the response to potassium chloride (70 mM); box: confocal images of fluo-4-loaded PC12 cells (i) before, (ii) 120 seconds after (peak), and (iii) 200 seconds after stimulation with 300μM capsaicin.

## 5.5 $Ca^{2+}$ influx triggered by capsaicin (300μM)

From the capsaicin concentration-response curve, a single concentration of 300μM capsaicin was adopted to compare the $Ca^{2+}$ influx in PC12 cells cultured in control and hyperglycaemic conditions. The representative traces in Figure 5.4 show that capsaicin evoked an overt $Ca^{2+}$ influx both in 5.5mM (A) and 50mM (B) conditions, followed by the second $Ca^{2+}$ peak induced by the addition of KCl 70mM. The vehicle of capsaicin (DMSO 0.6%) did not stimulate $Ca^{2+}$ increase in PC12 cells (C), which excluded the impact of DMSO on intracellular $Ca^{2+}$ increase. To confirm the increased intracellular $Ca^{2+}$ was caused by an influx from extracellular space rather than a release from intracellular $Ca^{2+}$ stores, $Ca^{2+}$-free buffer was adopted to replace normal buffer. As shown in Figure 5.4 (D), both capsaicin and KCl did not cause any intracellular $Ca^{2+}$ increase in PC12 cells present in $Ca^{2+}$- free buffer, suggesting that, in the previous experiments, the intracellular $Ca^{2+}$ increase caused by capsaicin and KCl was indeed from extracelluar space. As summarized in Figure 5.4 (E), after normalizing the capsaicin-evoked fluorescence (~ $[Ca^{2+}]i$) increase to the response to KCl, the maximal intracellular $Ca^{2+}$ level after the stimulation of capsaicin (300μM) in PC12 cells cultured in 50mM glucose was significantly greater than that in PC12 cells cultured in 5.5mM glucose ($P<0.05$). The magnitude of $Ca^{2+}$ influx in 50mM cells was 40% greater than in control cells. Considering that capsaicin is a TRPV1-receptor agonist (confirmed in the following experiment), the results suggest that the TRPV1 receptor was sensitized in PC12 cells cultured in hyperglycaemic conditions.

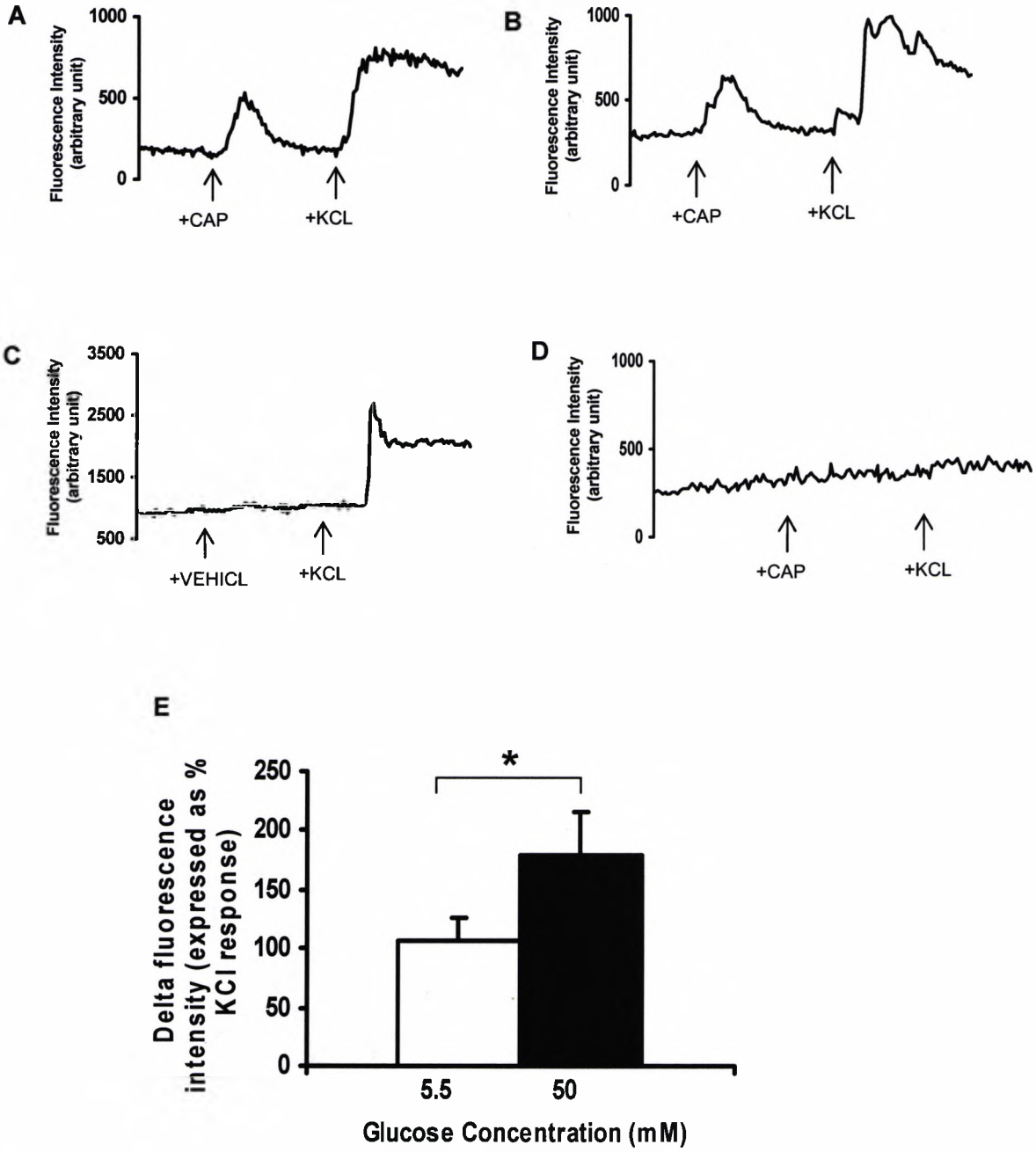


**Figure 5.4** Representative traces showing changes in fluo-4 fluorescence induced by capsaicin (Cap, 300 μM) and potassium chloride (KCl, 70mM). **(A)** represents the control (5.5mM glucose), **(B)** represents the high glucose condition (50mM glucose), **(C)** represents the fluorescence changes induced by vehicle (0.6% DMSO) and KCl (70mM), **(D)** represents the fluorescence changes in Calcium-free buffer. **(E)** shows that the magnitude of capsaicin-evoked fluorescence increase is significantly larger in 50mM cells than in 5.5mM cells (n=33-35). ( *, $P< 0.05$ Student's unpaired *t*-test).

## 5.6 The inhibitory effect of capsazepine on $Ca^{2+}$ influx induced by capsaicin

To confirm that the capsaicin-evoked $Ca^{2+}$ influx was mediated by TRPV1 receptors, capsazepine (CPZ), a TRPV1 receptor antagonist, was used to block the capsaicin-evoked $Ca^{2+}$ influx. The representative traces in Figure 5.5 showed that the co-application of CPZ with capsaicin prevented $Ca^{2+}$ influx; however, KCl was still able to induce $Ca^{2+}$ influx in PC12 cells cultured in either 5.5mM (A) or 50mM (B) glucose condition. As summarized in Figure 5.5 (C), compared with the $Ca^{2+}$ influx caused by capsaicin alone, the co-application of CPZ with capsaicin attenuated the effect of capsaicin on $Ca^{2+}$ influx by 90% in 5.5mM condition ($P<0.01$) and 85% in 50mM condition ($P<0.01$). The inhibition of capsaicin-evoked $Ca^{2+}$ influx by CPZ indicates that capsaicin stimulates $Ca^{2+}$ influx in PC12 cells via TRPV1 receptors.

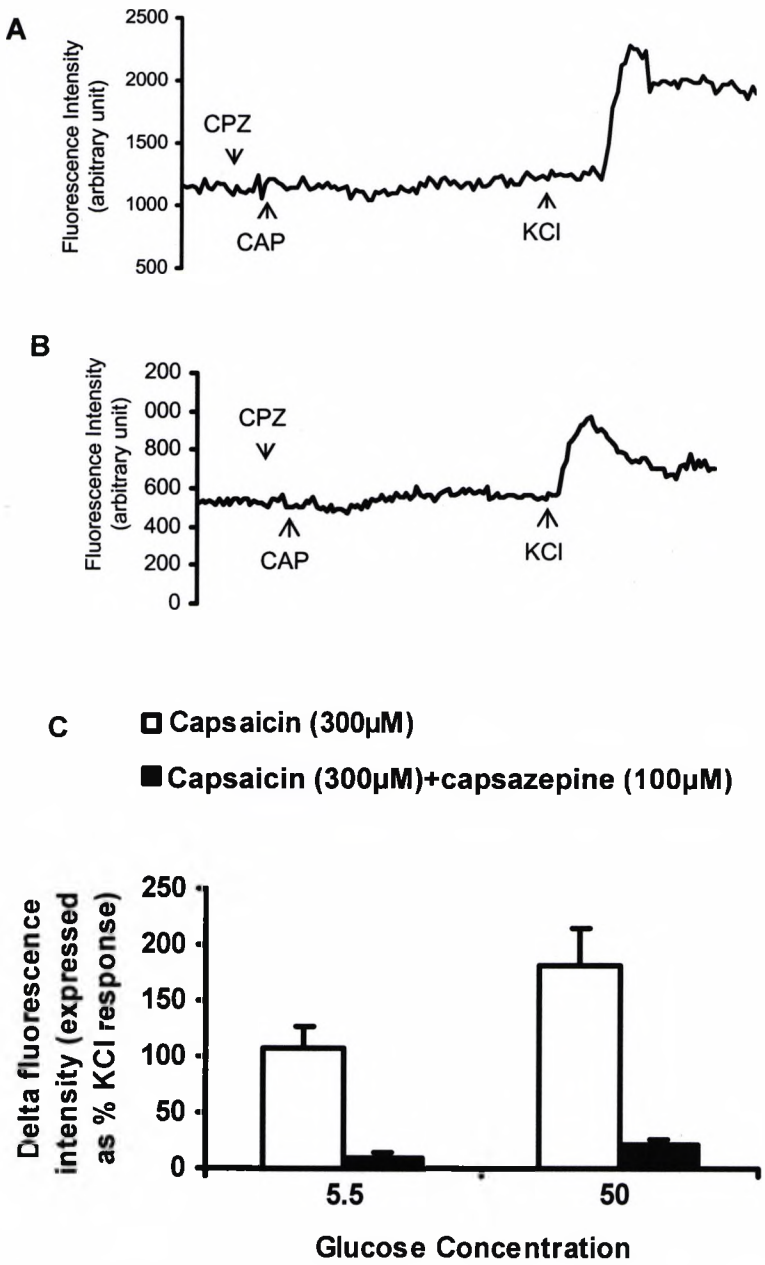


**Figure 5.5** Capsazepine blocks capsaicin evoked $Ca^{2+}$ entry in PC12 cells. **(A)** and **(B)** Representative traces showing the change in fluo-4 fluorescence induced by capsaicin (300μM) and potassium chloride (KCl 70mM) with co-application of capsazepine for 5.5mM (A) and 50mM (B) glucose conditions. **(C)** With the co-application of capsazepine, capsaicin response was reduced to 10% of control values in cells cultured in 5.5mM glucose (n= 18), and similarly to 15% of control values in cells cultured in 50mM glucose (n= 20). (**, P<0.001 Student's unpaired *t*-test).

## 5.7 Inhibitory effect of cannabinoid agonist HU210 on calcium influx is mediated by $CB_1$ receptors, not by $CB_2$ receptors

### 5.7.1 Concentration-response curve of inhibitory effect of HU210 on $Ca^{2+}$ influx

A wide range of HU210 concentrations from 0.03-30μM was used to study its inhibitory effect on capsaicin-evoked $Ca^{2+}$ influx. As shown in Figure 5.6, in PC12 cells cultured in 5.5mM glucose, HU210 showed a concentration-dependent inhibition (solid line), whereby, 0.03μM of HU210 did not inhibit capsaicin-evoked $Ca^{2+}$ influx, and seen as 0%; 30μM of HU210 gave maximal 85% inhibition.

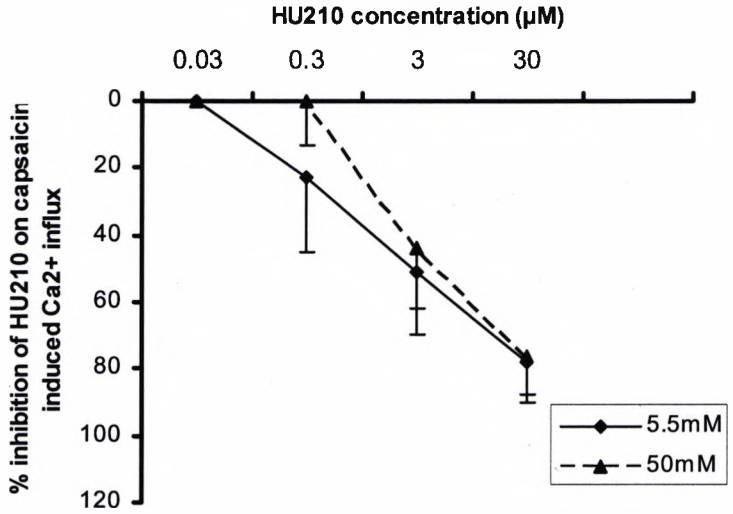


**Figure 5.6** Concentration-response curves of the inhibitory effect of HU210 on capsaicin evoked $Ca^{2+}$ influx in PC12 cells. HU210 (0.03-30 μM) was incubated with PC12 cells for 5-10min before the addition of capsaicin (300 μM). The solid line represents the % inhibition in control PC12 cells and the dashed line represents the % inhibition in PC12 cells cultured in hyperglycaemic conditions. The mean fluorescence increase from $Ca^{2+}$ influx induced by capsaicin 300 μM in the absence of HU210 is considered as 100%. The % inhibition of HU210 on capsaicin induced $Ca^{2+}$ influx is expressed as 100%-% $Ca^{2+}$ influx induced by capsaicin in the presence of HU210. n=15-31 cells.

In contrast, the HU210 concentration-response curve (shown in dashed line) in PC12 cells cultured in 50mM glucose is shifted to the right of the curve of 5.5mM conditions. It shows that neither 0.03 nor 0.3μM of HU210 inhibited the $Ca^{2+}$ influx and was thus seen as 0% of inhibition. However, 30μM of HU210 showed a similar maximal 84% inhibition to that in 5.5mM condition. At 3μM, HU210 blocked the $Ca^{2+}$ influx by 44% in 50mM glucose condition, compared to 51% in 5.5mM glucose condition.

### 5.7.2 The effect of a selective $CB_1$ receptor antagonist on HU210 responses

To examine whether the inhibitory effect of HU210 on $Ca^{2+}$ influx is mediated by $CB_1$ receptors, the selective $CB_1$ antagonist, AM251, was employed. HU210 (30μM) was chosen to give a maximal inhibition of capsaicin (300μM)-evoked $Ca^{2+}$ influx. Responses to capsaicin and KCl were tested in PC12 cells cultured in both 5.5mM and 50mM glucose in the presence of HU210 30μM only, or HU210 30μM+ AM251 .

In Figure 5.7, (A) represents that $Ca^{2+}$ influx in PC12 cells cultured in 5.5mM glucose. The trace on the left showed that capsaicin 300μM did not stimulate $Ca^{2+}$ influx in the presence of HU210 30μM, however, KCl 70mM did induce a rapid $Ca^{2+}$ entry in the same cells. In contrast, there was a small peak of $Ca^{2+}$ influx stimulated by capsaicin only when the combination of HU210 30μM and AM251 30μM was present. Similarly, in PC12 cells cultured in 50mM glucose (B), the trace on the left showed that capsaicin (300μM) was unable to induce a overt $Ca^{2+}$ influx in the presence of HU210 30μM and the trace on the right showed that capsaicin-evoked $Ca^{2+}$ influx was recovered in the presence of HU210 30μM and AM251 30μM. KCl-induced $Ca^{2+}$ entry were showed in both

of the traces. The effect of vehicle of HU210 and AM251 was also tested. As shown in trace C, in the presence of vehicle only, capsaicin did stimulate a considerable level of $Ca^{2+}$ entry.

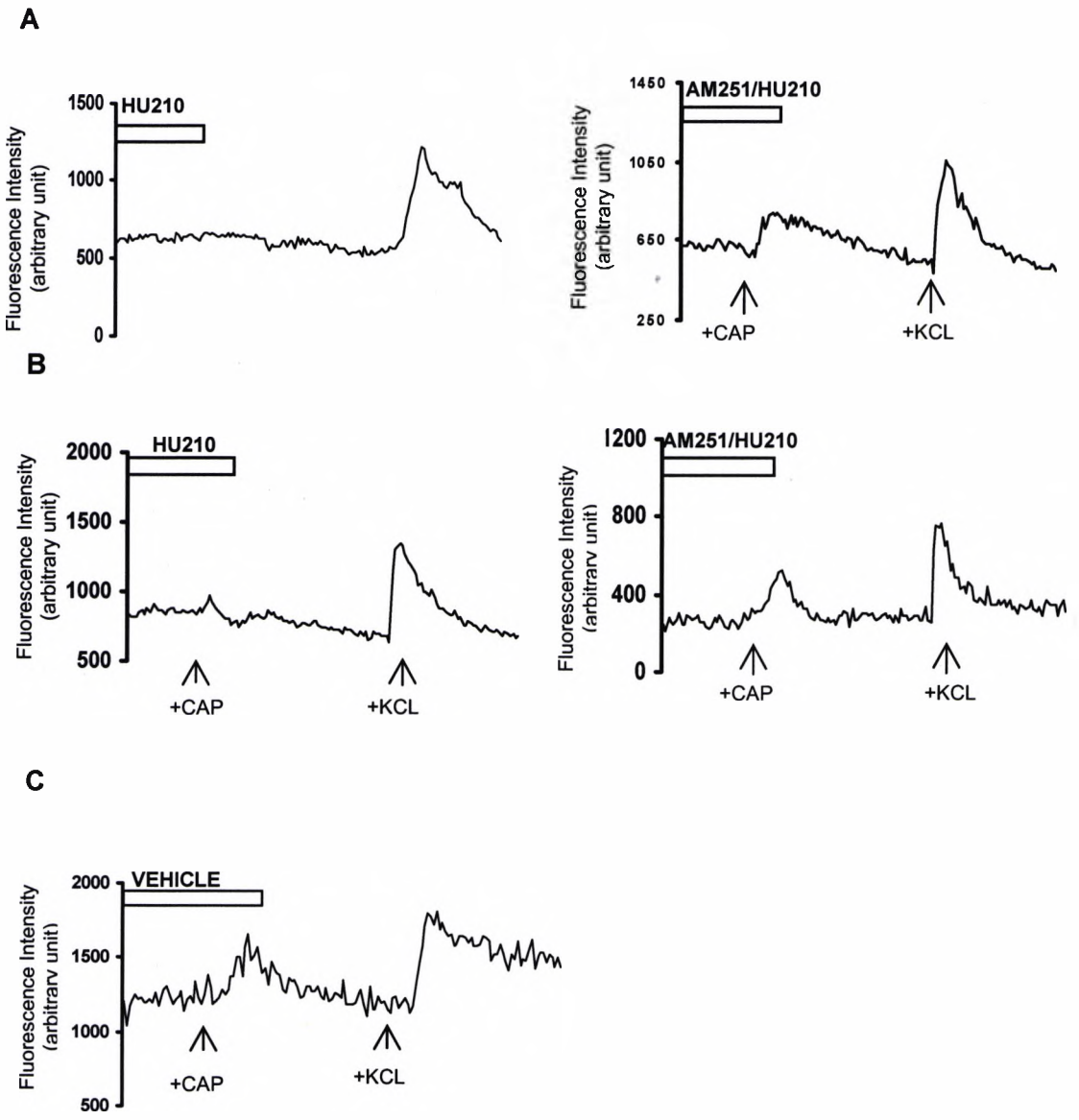


**Figure 5.7** Representative traces showing changes in fluo-4 fluorescence induced by capsaicin (Cap, 300μM) and potassium chloride (KCl, 70mM), in the presence (left panels) of HU210 (30 μM) or with the co-application of AM251 (30 μM) (right panels), in 5.5 mM glucose **(A)** and 50 mM glucose **(B)**. **(C)** shows the change in fluo-4 fluorescence induced by capsaicin and KCl in the presence of vehicle. Scale bar = 120 seconds.

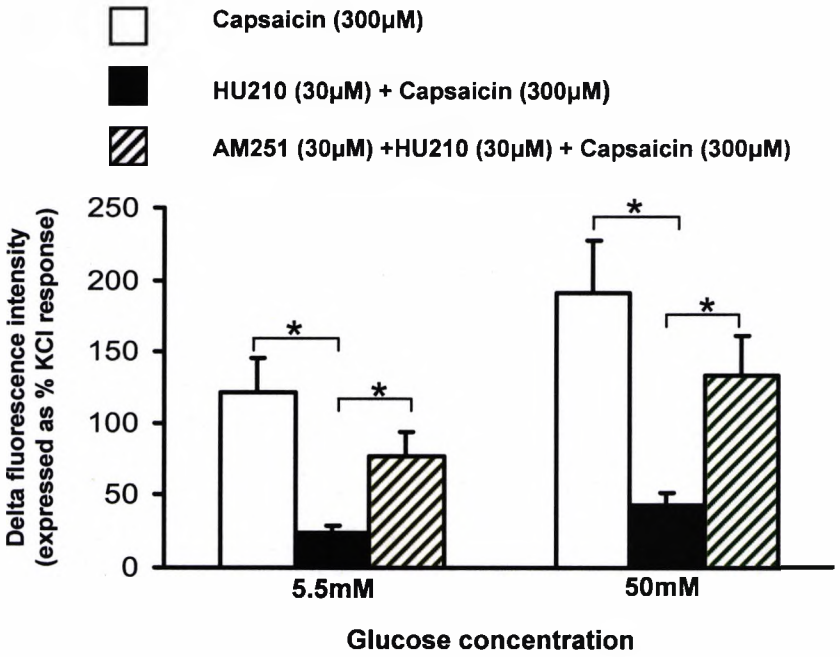


**Figure 5.8** HU210 inhibits capsaicin-evoked responses in PC12 cells In the presence of HU210 (30μM) the capsaicin response was reduced to 20% of control values in cells cultured in 5.5mM glucose, similarly to 23% of control in cells cultured in 50mM glucose (n = 29-42 cells per condition). The $CB_1$ receptor antagonist AM251 (30μM) was able to reverse the inhibitory response to HU210, confirming its effect was mediated via $CB_1$ receptors (n = 33-50 cells per condition). Data shown are the mean ± s.e.mean (*, P<0.05, unpaired Student's *t*-test).

As summarized in Figure 5.8 , in the presence of HU210 30μM, the capsaicin response was significantly reduced to 20% of control values in 5.5mM glucose condition and 23% of control values in 50mM glucose condition which means that HU210 30μM gave 80% and 77% of inhibition of $Ca^{2+}$ influx respectively. Meanwhile, AM251 (30μM) significantly reversed the inhibitory effect of HU210 (30μM) in both 5.5mM and 50mM glucose conditions by recovering the $Ca^{2+}$ peak back to 63% of control values and 69% of control values, respectively.

### 5.7.3 The inhibition of $Ca^{2+}$ influx by HU210 (1μM)

In the previous experiments, a high concentration of HU210 had been used. It is possible, at 30μM, HU210 may have been acting non-specifically, therefore, in further studies, we decided to examine lower concentrations. From the HU210 concentration- response curve shown above, a concentration of 1μM was adopted to study the inhibitory effect on capsaicin-evoked $Ca^{2+}$ influx. The selective $CB_1$ receptor antagonist, AM251 (1μM), was again used in order to confirm the inhibitory effect of HU210 was mediated by the $CB_1$ receptor. Representative traces are shown in Figure 5.9. Similar to earlier findings, in PC12 cells cultured in 5.5mM glucose, capsaicin stimulated a visible $Ca^{2+}$ influx in the presence of HU210, however, compared with the application of capsaicin alone, the $Ca^{2+}$ peak was much smaller. The co-application of AM251 and HU210 reversed the inhibitory effect of HU210 on $Ca^{2+}$ influx. The magnitude of $Ca^{2+}$ peak was comparable to the $Ca^{2+}$ peak induced by capsaicin alone. A second peak of $Ca^{2+}$ induced by KCl confirmed the cell viability in both traces.

In PC12 cells cultured in 50mM glucose (Figure 5.9 B), the traces showed a very similar trend to those from the control PC12 cells; HU210 showed an inhibition of capsaicin-evoked $Ca^{2+}$ influx, and co-application of AM251 reversed the HU210 inhibition. As a control, a single application of AM251 (1μM) was used to treat PC12 cells as shown in Figure 5.7 C demonstrating that AM251 itself did not induce any intracellular $Ca^{2+}$ change (via possible inverse agonist actions).

The $Ca^{2+}$ influx was quantified and is summarized in Figure 5.10. In PC12 cells cultured in 5.5mM glucose, HU210 (1μM) significantly inhibited the capsaicin-induced $Ca^{2+}$ by 43%, and the co-application of AM251 (1μM) reversed the

HU210 inhibition, bringing the $Ca^{2+}$ influx back to 100% when stimulated with capsaicin (300μM). In high glucose conditions, HU210 (1μM) also significantly attenuated the capsaicin-evoked $Ca^{2+}$ influx by 40%, and in the presence of AM251 (1μM)+HU210 (1μM), the $Ca^{2+}$ peak returned to 95% of the magnitude of the $Ca^{2+}$ peak stimulated with capsaicin alone.

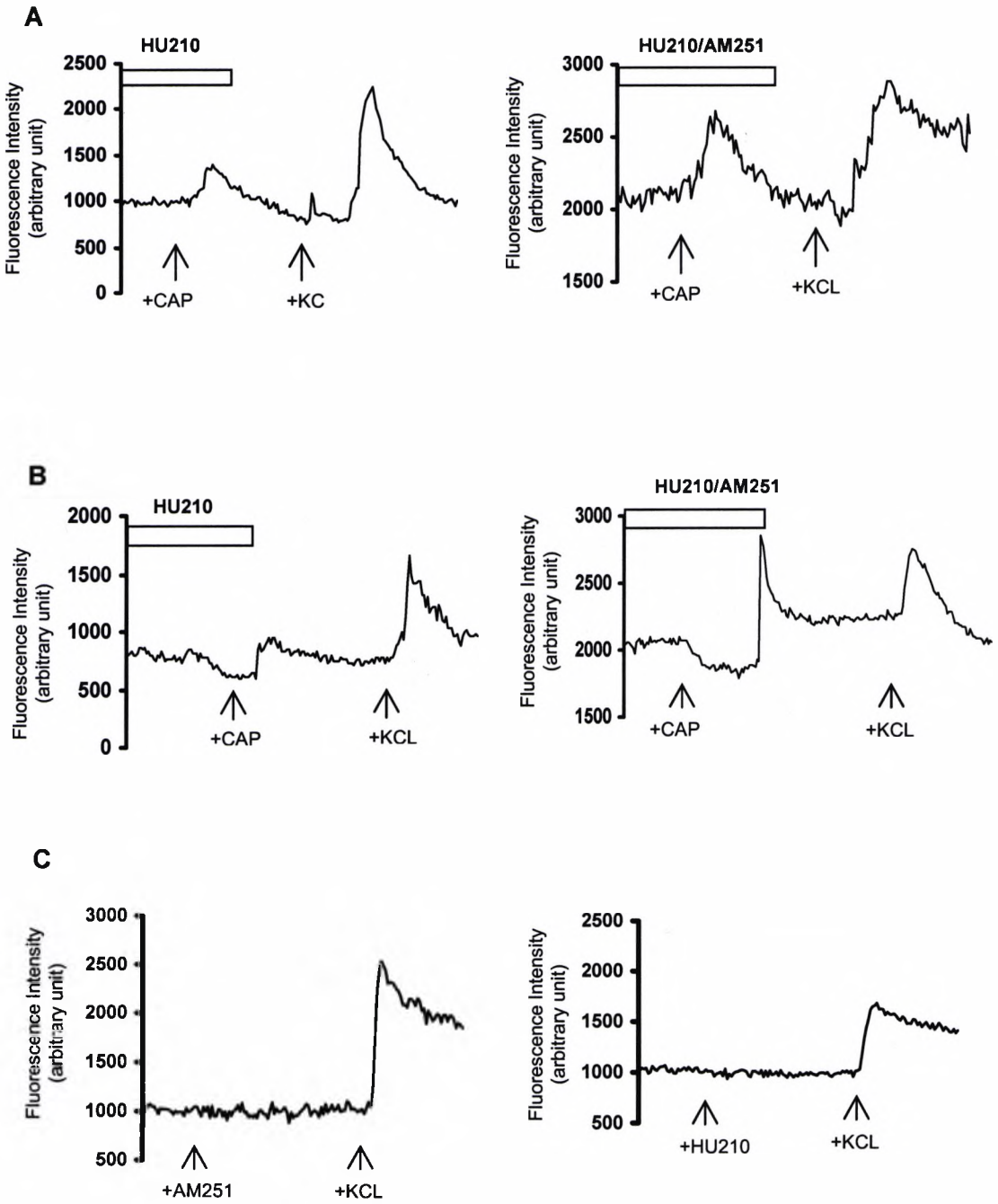


**Figure 5.9** Representative traces showing changes in fluo-4 fluorescence induced by capsaicin (Cap, 300μM) and potassium chloride (KCl, 70mM), in the presence (left panels) of HU210 (1μM) or with the co-application of AM251 (1μM) (right panels), for 5.5mM glucose **(A)** and 50mM glucose **(B).** The representative trace **(C)** showing changes in fluo-4 fluorescence induced by AM251 (1μM) or HU210 (1μM) alone followed by potassium chloride (KCl 70mM). Scale bar = 120 seconds.

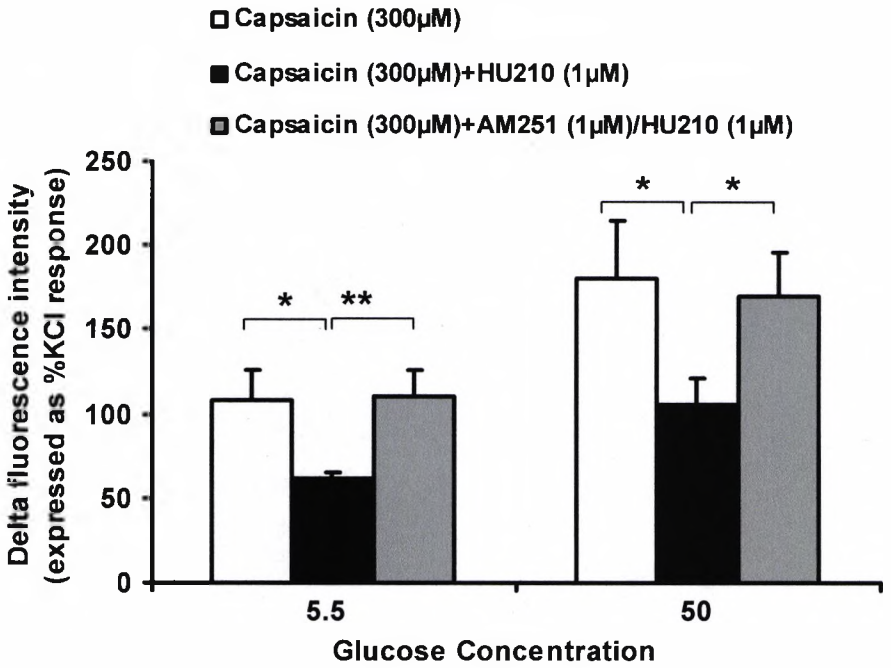


**Figure 5.10** HU210 inhibits capsaicin-evoked responses in PC12 cells. In the presence of HU210 (1µM) the capsaicin response was reduced to 57% of control values in cells cultured in 5.5.mM glucose, similarly to 60% of control in cells cultured in 50mM glucose (n = 29-42 cells per condition). The $CB_1$ receptor antagonist AM251 (1µM) was able to reverse the inhibitory response to HU210, confirming its effect was mediated via $CB_1$ receptors (n = 33-50 cells per condition). Data shown are the mean ± s.e.mean (*, P<0.05, **, P<0.01, unpaired Student's *t*-test).

### 5.7.4 The effect of a selective $CB_2$ antagonist on HU210 responses

AM630 is a selective $CB_2$ receptor antagonist. An equal concentration of AM630 (1μM) was used to replace AM251 in these experiments in order to exclude the possibility that HU210 inhibits capsaicin-evoked $Ca^{2+}$ influx by a $CB_2$-mediated mechanism.

The addition of AM630 (1μM) had no significant effect on the inhibitory response of HU210 (1μM) in PC12 cells cultured in 5.5 and 50mM glucose (Figure 5.11). Compared with the previous study showing that HU210 (1μM) produced 43% of inhibition of $Ca^{2+}$ influx in cells with 5.5mM glucose (Figure 5.10), HU210 (1μM) +AM630 (1μM) in this study gave a comparable 41% inhibition (Figure 5.11 D), At 50mM glucose, levels of HU210-mediated inhibition were 40% in the absence (Figure 5.10), versus 39% in the presence of AM630 (Figure 5.11 D).

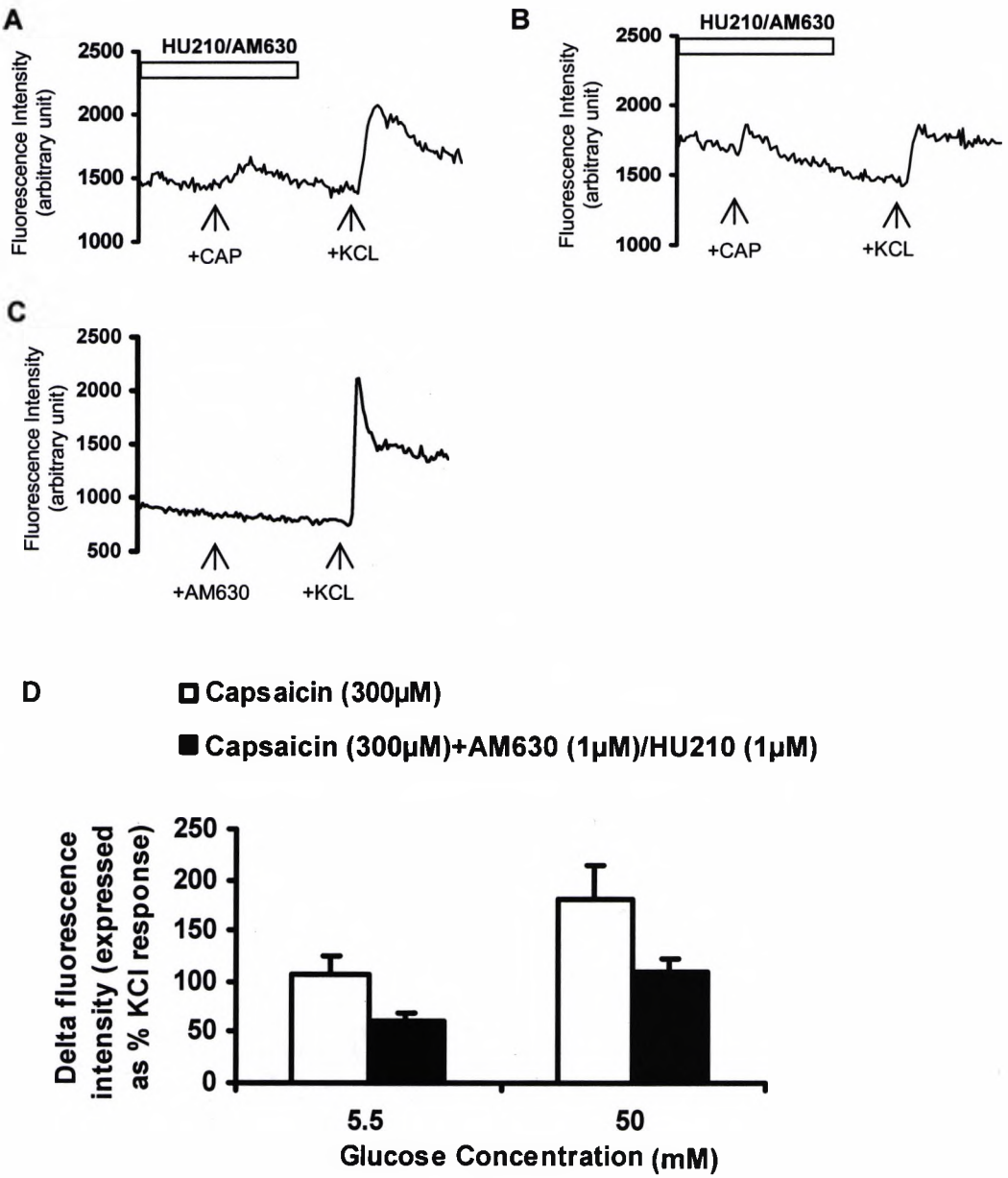


**Figure 5.11** The $CB_2$ antagonist AM630 is unable to reverse the inhibitory effect of HU210 on $Ca^{2+}$ influx triggered by capsaicin. **(A)** and **(B)** Representative traces showing changes in fluo-4 fluorescence induced by capsaicin (Cap, 300µM) and potassium chloride (KCl, 70mM), in the presence of HU210 (1µM) and AM630 (1µM) , for 5.5mM glucose (A) and 50mM glucose (B). **(C)** Representative trace showing changes in fluo-4 fluorescence induced by AM630 (1µM) and potassium chloride (KCl, 70mM), Scale bar = 120 seconds. **(D)** In the presence of HU210 (1µM) and AM630 (1µM), the capsaicin response was reduced to 59% of control values in cells cultured in 5.5.mM glucose, similarly to 61% of control in cells cultured in 50mM glucose (n = 29-42 cells per condition). The $CB_2$ receptor antagonist AM251 (1µM) was unable to reverse the inhibitory response to HU210, confirming its effect was mediated via $CB_1$ receptors (n = 33-50 cells per condition). Data shown are the mean ± s.e.mean (**, $P<0.01$: unpaired Student's t-*test*).

## 5.8 Discussion

$CB_1$ receptor stimulation suppresses TRPV1-mediated calcium influx and neurotransmitter release (Millns *et al.*, 2001; Oshita *et al.*, 2005). We therefore assessed $CB_1$ receptor function by measuring the inhibitory effect of HU210 on capsaicin-induced calcium influx in PC12 cells cultured in physiological and high glucose conditions.

Initial $Ca^{2+}$ imaging experiments using fluo-4 AM revealed that intracellular fluorescence could be stimulated by KCl (70mM) and thapsigargin (10μM) in PC12 cells. The intracellular $Ca^{2+}$ change caused by the two stimuli were through different mechanisms, indicating that the preparation procedure (3μM of fluo-4 with 0.04% of pluronic acid, 40 minutes loading incubation at 37°C, and 2.5mM calcium in HEPES buffer) and scanning frequency (3.93 second per scan) were optimal to detect the intracellular $Ca^{2+}$ change from either extracelluar $Ca^{2+}$ entry or release from intracellular $Ca^{2+}$ stores.

In DRG and other TRPV1 expressing or recombinant cells, 0.1 to 10μM of capsaicin stimulates TRPV1-mediated $Ca^{2+}$ influx (Oshita *et al.*, 2005; Vriens *et al.*, 2004), and the maximal concentration of 20μM gives a saturated response in DRG cells (Vellani *et al.,* 2001). To keep the consistence with primary neurons, a most commonly used concentration, 1μM of capsaicin, was firstly used into PC12 cells. At the outset, the $Ca^{2+}$ influx induced by capsaicin (1μM) and the inhibitory effect of HU210 (1μM) were studied in individual differentiated PC12 cell cultured in either control (5.5mM) or high glucose (50mM) conditions by applying multiple treatments. It was found that, in PC12 cells cultured in high glucose, the $Ca^{2+}$ influx induced by capsaicin (1μM) was detected in only 5% cells which responded to KCl (70mM), which was

significantly inhibited by HU210 (1μM). However, in PC12 cells cultured in control glucose levels, even less than 5% of KCl-responding cells responded to capsaicin (1μM). Such a small proportion of responsive cells cannot represent the function of TRPV1 or $CB_1$ receptors in a whole sample scale. In addition, the multiple treatments in one sample were found difficult to operate and the repeated exposure to capsaicin was at risk of desensitization of TRPV1 receptors (Dray *et al.*, 1989; Szolcsanyi, 1977; Piper *et al.*, 1999).

A single application of capsaicin followed by addition of KCl in one sample was adopted in subsequent studies in order to improve the applicability and efficiency of experiments. The capsaicin concentration-response study revealed that capsaicin (50 to 700μM) stimulated a transient $Ca^{2+}$ influx in a concentration-dependent manner, and only concentrations above 50μM were able to stimulate a reproducible $Ca^{2+}$ influx in the particular cell line. The concentration of capsaicin (300μM) which evoked half of maximal responses was applied to the subsequent studies. High glucose facilitated a greater capsaicin-evoked $Ca^{2+}$ influx in PC12 cells and the response was significantly blocked by capsazepine (100μM) in both normal and high glucose conditions, confirming the response is mediated by TRPV1 receptors. This *in vitro* result is positively correlated to the animal study showing the over-sensitised TRPV1 receptor was found in DRG neurons from diabetic rats (Hong and Wiley, 2005). The concentration of capsaicin required to evoke calcium entry into the cells was relatively high (300μM) compared to studies involving DRG neurons or TRPV1-transfected cell lines. However, Someya *et al.* (2004) have reported PC12 cells require concentrations above 100μM to evoke an increase in $[Ca^{2+}]i$, and equate this to low capsaicin-sensitivity in PC12 cells. Also, the results showing capsaicin failed to evoke cytosolic calcium increase in the cells when

calcium was omitted in buffer may reflect the previous expression study showing TRPV1 receptor was mainly expressed at cell membrane which is also demonstrated in study by Someya *et al.* (2004).

A wide range of HU210 (0.03, 0.3, 3, 30μM) was used to study the inhibition of capsaicin induced-$Ca^{2+}$ influx. The inhibition (%) curve generated from high glucose conditions shifted to the right compared with the control inhibition curve, indicating high glucose may slightly decrease $CB_1$ function. Focus down to the maximal concentration at 30μM used in order to pursue a maximal inhibition of calcium entry, HU210 significantly inhibited capsaicin-evoked calcium entry by 80% and 77% in control and high glucose respectively, which was reversed by the $CB_1$ antagonist, AM251 (30μM), indicating a $CB_1$-receptor mediated inhibition of calcium entry induced by capsaicin. However, the concern about the high concentration used is raised from other studies reporting that HU210 at 1-10μM inhibited TRPV1-mediated $Ca^{2+}$ entry in rat DRG neurons and human cells (Fischbach *et al.*, 2007; Wilkinson and Williamson, 2007; Oshita *et al.*, 2005), and AM251 at more than 1μM acted as an inverse agonists at $CB_2$ receptors in human cells (New and Wong, 2003).

Using the more pharmacologically relevant concentration, it was found that HU210 at 1μM inhibited capsaicin evoked-$Ca^{2+}$ influx in PC12 cells cultured in both control and high glucose levels by 43% and 40% correspondingly. The inhibitory effect was significantly reversed by the $CB_1$ antagonist, AM251 (1μM) but not by the $CB_2$ antagonist, AM630 (1μM), while HU210/AM251/AM630 did not have any effect of their own on PC12 cells. These results strongly suggest that the inhibitory effect of TRPV1-mediated calcium entry is mediated by $CB_1$, not $CB_2$ receptors, and there is no inverse agonist effect involved. This is the

first study to investigate $CB_1$ function in PC12 cells. The inhibitory effect of HU210 found in the current cell model is consistent with other studies of cannabinoid inhibition of capsaicin-induced response (calcium entry, neuropeptide release) in DRG neurons (Oshita *et al.*, 2005; Millns *et al.*, 2001), spinal cord (Winter *et al.*, 1988; Sarker *et al.*, 2000) and skin (Richardson *et al.*, 1998; Ellington *et al.*, 2002).

In conclusion, in the cell culture model of diabetic neuropathy, we for the first time demonstrate that TRPV1 receptors were over-sensitised in PC12 cells cultured in hyperglycaemic conditions. The $CB_1$ agonist, HU210, inhibited the capsaicin-evoked calcium entry at a similar level in both control and high glucose conditions through a $CB_1$-dependent pathway, indicating that the $CB_1$ function is still preserved in hyperglycaemic conditions.

# CHAPTER 6

# THE NEUROPROTECTIVE EFFECT OF A CANNABINOID $CB_1$ RECEPTOR AGONIST *IN VITRO*

## 6.1 Introduction

This chapter investigates the neuroprotective effect of the $CB_1/CB_2$ ($CB_1>CB_2$) agonist, HU210, in the cell model of diabetic neuropathy. There is considerable evidence showing cannabinoids improve neuron viability and protect neuron from insults, such as ischaemia, excitotoxicity, and oxidative stress *in vivo* and *in vitro* (Hampson *et al.*, 1998; Nagayama *et al.*, 1999; Shen and Thayer, 1998; van der Stelt *et al.*, 2001) through $CB_1$-dependent or $CB_1$-independent mechanism. Two recent studies have showed that the antinociceptive action of a mixed $CB_1/CB_2$ agonist is preserved in diabetic mice (Dogrul *et al.,* 2004) and rats (Ulugol *et al.,* 2004), indicating cannabinoids might be appropriate therapeutic agents on treating diabetic related-neurodegeneration. In fact, $CB_1$ activation promotes neurite outgrowth by activating $G_{i/o}$ protein–involved kinase cascade (He *et al.,* 2005). Considering the previous study showed the $CB_1$ function was preserved in PC12 cells cultured in hyperglycaemic conditions, we speculate $CB_1$ agonists may rescue the nerve degeneration caused by high glucose.

The aim of this chapter was to investigate whether HU210 can rescue the neurite outgrowth in PC12 cells cultured in hyperglycaemic conditions via $CB_1$ receptor-mediated mechanism. In the studies of this chapter, a dose response course of HU210 on cell viability was firstly conducted. A study done by Sarker and colleagues showed that exogenous stimulation of anandamide had no any effect on cell viability of PC12 cells with the dose no more than 5μM, whilst it induced apoptosis with the dose more than 10μM (Sarker *et al.,* 2000). Therefore, in order to study whether HU210 can protect neurite outgrowth from high glucose, an appropriate range of dose must be carefully determined.

Subsequently, NGF-induced neurite outgrowth in the presence of HU210 was studied in PC12 cells cultured in control or high glucose level. Neuroprotective effect of HU210 was assessed by the total length of neurites growing out of PC12 cells treated with HU210. The co-treatment of the $CB_1$ antagonist, AM251, and/or $CB_2$ antagonist, AM630, with HU210 was conducted in parallel in order to investigate whether $CB_1$ or/and $CB_2$ receptors were involved in the activation of HU210. Finally, the study examining the antioxidant property of HU210 in PC12 cells cultured in hyperglycaemic conditions was conducted to determine whether the neuroprotective effect of HU210 (if any) was independent of $CB_1$ receptors.

## 6.2 The treatment of PC12 cells with a cannabinoid receptor agonist

### 6.2.1 Concentration response - relationship of HU210 on cell growth

The cell viability of PC12 cells treated with a variety of concentrations of HU210 in the absence (5.5mM glucose) or presence of high glucose (50mM glucose) was determined by using a lactase dehydrogenase (LDH) assay and MTT assay. PC12 cells were cultured in DMEM medium supplemented with HU210 (0, 0.03, 0.3, 3, 30μM) for 6 days under the stimulation of NGF (50ng/ml). The supernatant was collected every two days and used to monitor LDH release from cytoplasm. The LDH assay determines cell membrane integrity and the leakage of LDH from cytoplasm suggests cellular toxicity. Figure 6.1 shows the concentration of LDH released from PC12 cells with HU210 treatment on day 2, 4 and 6, compared to the positive control which was determined from Triton-X (0.1%) induced cell lysis. The LDH curves either from 5.5mM or 50mM glucose on day 2, 4 and 6 were found to follow a very similar trend, showing a flat line from 0μM to 3μM of HU210, followed by a dramatic increase at 30μM of HU210 (Figure 6.1). For each time point studied, it was observed that HU210 up to 3μM did not induced any significant increase in LDH release from PC12 cells cultured in either 5.5mM or 50mM glucose, compared to the control (0μM HU210). In contrast, HU210 at 30μM to induced a significant increase in LDH release from PC12 cells cultured in both control and high glucose ($P<0.01$). The vehicle (DMSO: 0.6%) was not significantly different from the control. It can be seen from Figure 6.1 that the LDH release induced by 30μM HU210 was gradually increasing from day 2 to day 6, and at day 6, it was approximately equal to the level induced by the positive control (Triton-X: 0.1%).

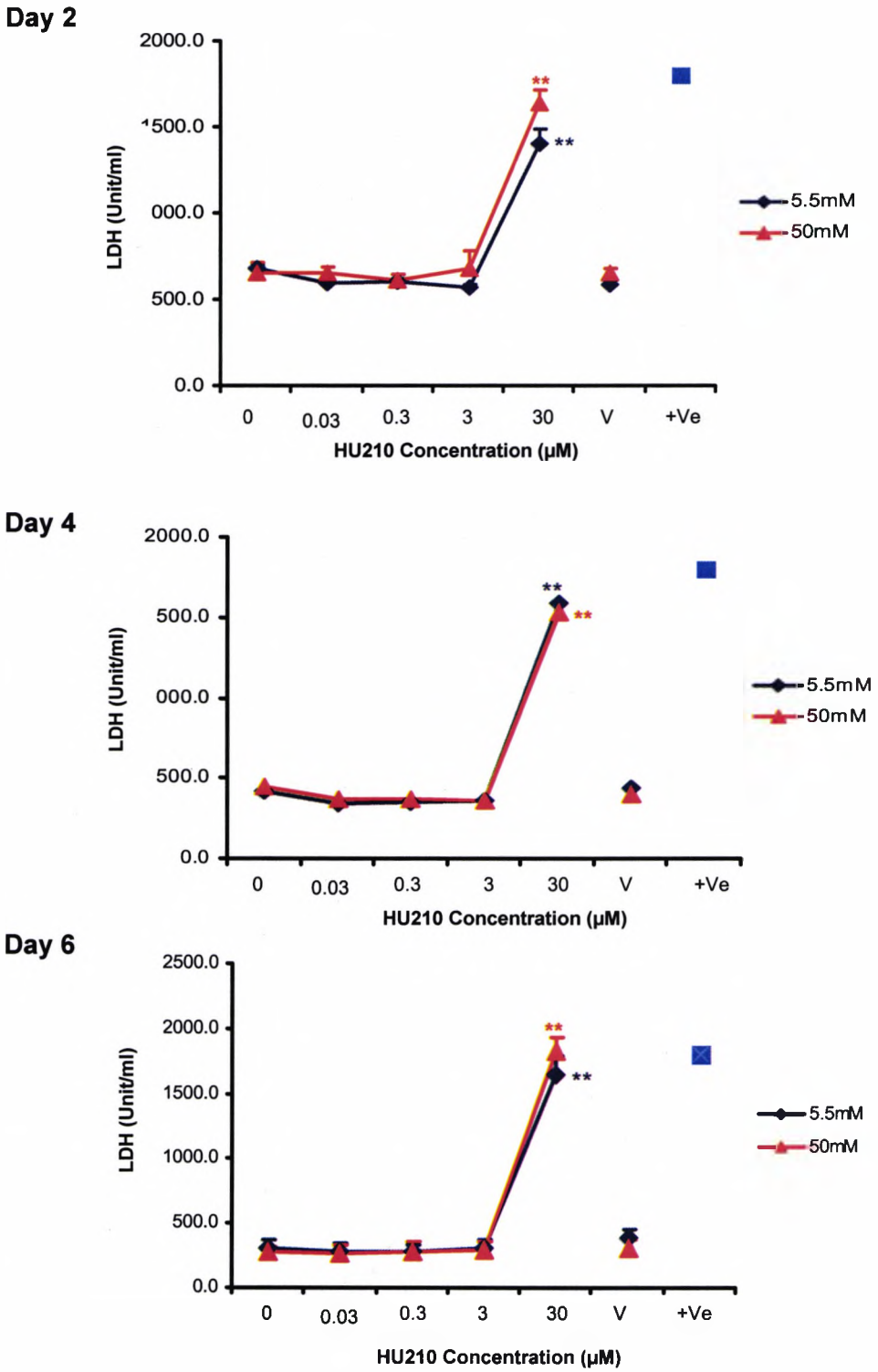


**Figure 6.1** Mean concentration of lactate dehydrogenase release from PC12 cells stimulated with NGF (50ng/ml) and in the absence/presence of high glucose (50mM) when treated with HU210 (0 – 30µM) on day 2, 4 and 6 of culture. V= vehicle (DMSO: 0.6%). +Ve= complete LDH release (from 0.1% Triton-treated cells). Values represent mean± SEM from 3 independent experiments. (**, P<0.01 compared to 0µM HU210 concentrations. one-way ANOVA-Fisher's post-hoc analysis).

Whilst the cell culture supernatants were used for the LDH assay, the actual PC12 cells were used as the sample for MTT assay preformed on day 6. The MTT assay is based on the mitochondria in living cells being able to convert yellow MTT to purple formazan, and the conversion, therefore, is directly related to the number of living cells. Figure 6.2 shows the cell viability related to the density of purple color detected in PC12 cells treated with HU210 (0.03 to 30μM). It was found that the treatment of HU210 from 0.03 to 3μM did not affect the cell viability of PC12 cells cultured in either 5.5mM or 50mM glucose when compared with the corresponding control (0μM HU210). In comparison, a 10-fold decrease in cell viability was observed in PC12 cells treated with 30μM HU210, in both 5.5 and 50mM glucose conditions ($P<0.01$). The vehicle treated cells showed equal cell viability to the control (0μM HU210).

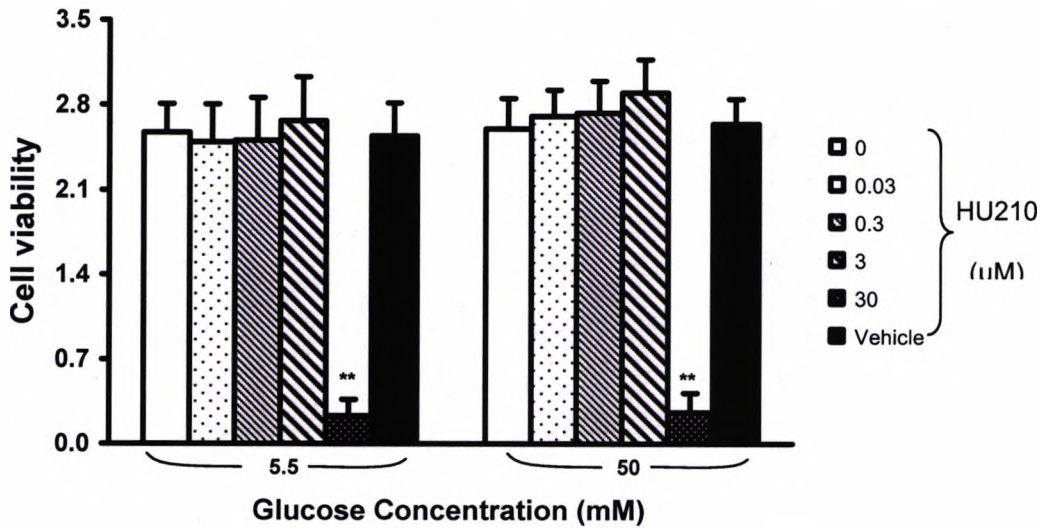


**Figure 6.2** Cell viability of PC12 cells treated with HU210 (0 – 3μM). PC12 cells were stimulated with NGF (50ng/ml) and in the absence/presence of high glucose (50mM) for 6 days. Values represent mean ± SEM from 3 independent experiments. (**, $P<0.01$ compared to the rest of concentrations. one-way ANOVA-Fisher's post-hoc analysis).

### 6.2.2 The effect of HU210 on neurite outgrowth

Neurite length was measured in PC12 cells on day 6 of culture in the presence of HU210 (0.03 to 3μM) and expressed as the percentage of cell body diameter. Representative photomicrographs of neurite outgrowth in PC12 cells cultured in 5.5mM and 50mM glucose in the presence of HU210 (0.03, 0.3, 3μM) are shown in Figure 6.3. The neurite length with increasing concentrations of HU210 did not shown an obvious difference when compared to the control (A) and the vehicle (E) in cells cultured in control glucose. However, in cells cultured in 50mM glucose, neurite grew longer in the presence of HU210, particularly with 0.3 and 3μM, when compared to the control (A) which had relatively shorter neurites. Vehicle (E) showed a very similar neurite outgrowth to the control.

The effect of HU210 on neurite outgrowth of PC12 cells cultured in control (5.5mM) and high glucose (50mM) is summarized in Figure 6.3. As previously observed (chapter 3), high glucose attenuate neurite outgrowth by approximately 2-fold in PC12 cells (data for 0μM HU210). Whilst HU210 had little effect on neurite outgrowth in the control glucose condition, at 50mM glucose conditions, it rescued neurite outgrowth impaired by high glucose in a concentration-dependent manner. The neurite length of PC12 cells in the presence of 0.3 and 3μM of HU210 was found to be significantly longer than the control ($P<0.01$). The vehicle from the highest concentration of HU210 did not affect neurite outgrowth compared with the control.

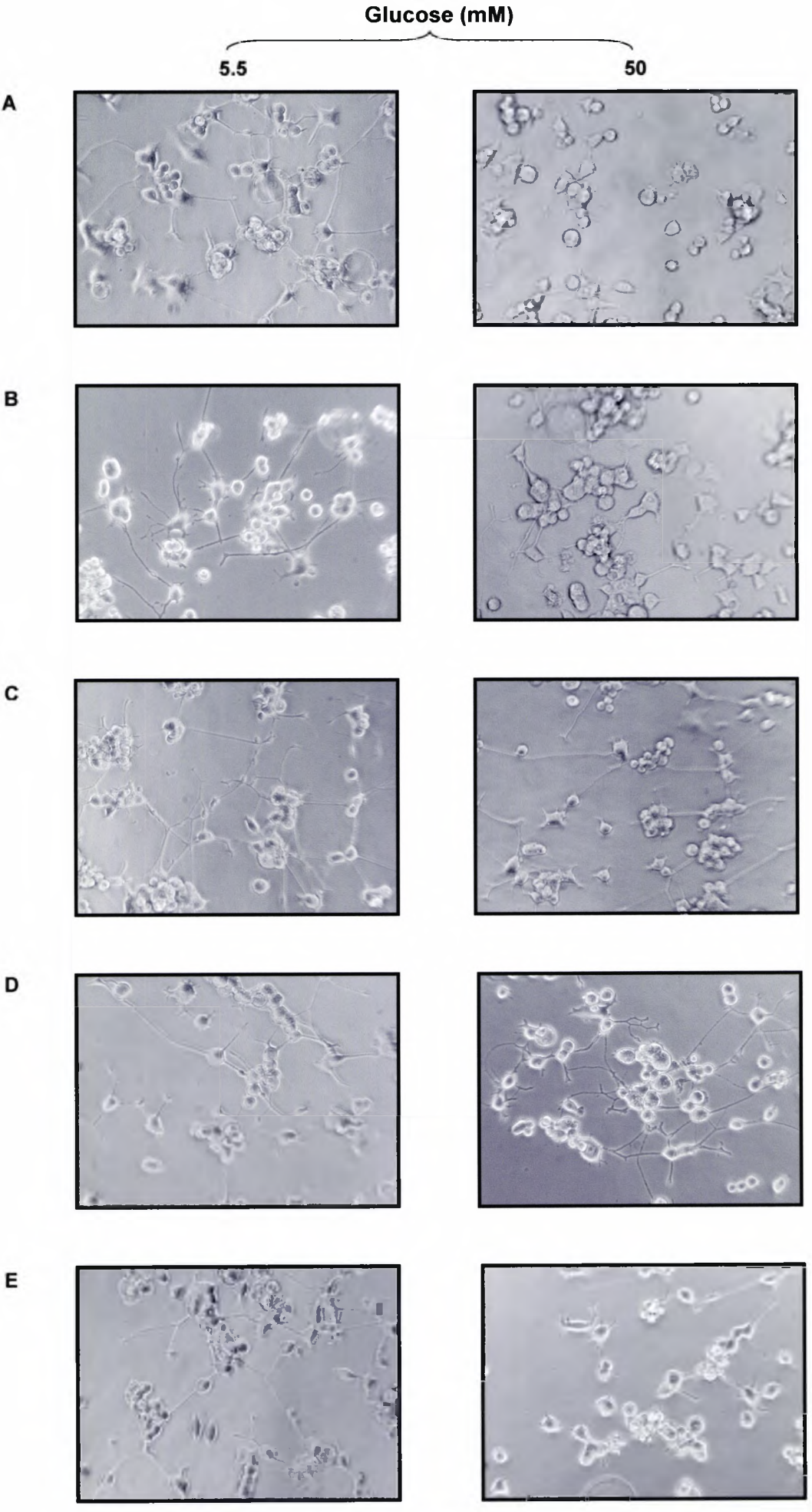
Glucose (mM)
5.5
50
A
B
C
D
E

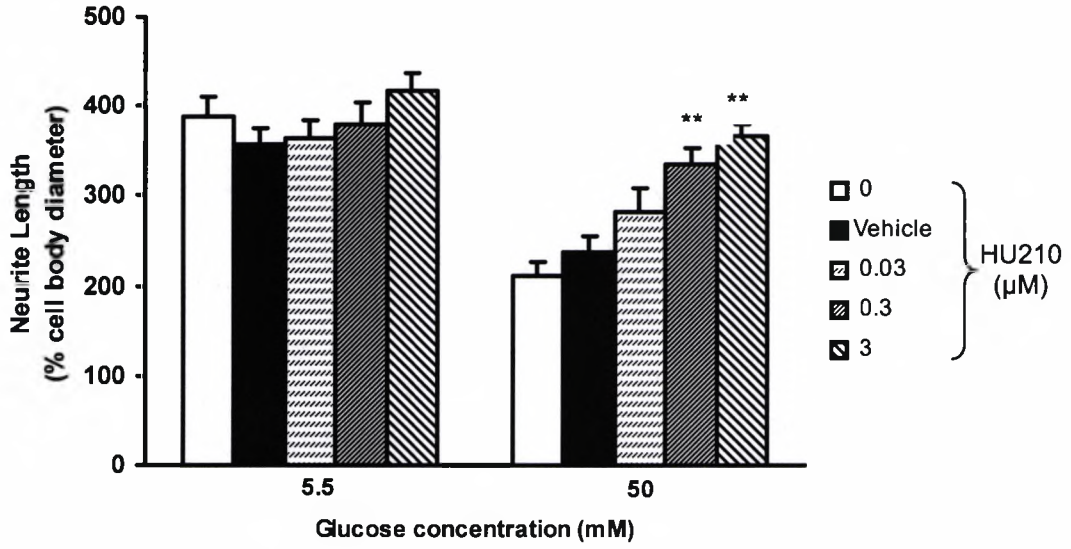


**Figure 6.3** $CB_1$ agonist treatment promotes neurite outgrowth in PC12 cells: the effect of HU210 (0.03-3μM) on neurite length (normalised to cell body diameter) of differentiated PC12 cells in control (n=148-220) and high glucose conditions (n=112-216). (**, P<0.01 vs. control (0μM HU210). one-way ANOVA-Fisher's post-hoc analysis). The representative photomicrographs A to E show the neurite outgrowth of PC12 cells cultured in 5.5 and 50mM glucose in the presence of HU210 (0, 0.03, 0.3, 3μM) or vehicle (DMSO: 0.6%).

### 6.2.3 The protective effect of HU210 on oxidative stress caused by high glucose

PC12 cells were cultured in DMEM supplemented with a variety of concentration of HU210 for 6 days in the absence or presence of high glucose. Cell lysates were collected to measure oxidative stress. The ratio of GSSG:GSH indicates relative amount of oxidized versus reduced glutathione content, and a higher ratio is considered as greater intracellular oxidative stress. It has been shown previously, in chapter 3, that higher oxidative stress is found in PC12 cells cultured in high glucose (50mM) compared with controls (5.5mM). Figure 6.4 shows the impact of HU210 treatment on oxidative stress in PC12

cells cultured in control and high glucose. In the 5.5mM glucose condition, all concentrations of HU210 were not found to have significant effect on oxidative stress when compared with the control. In the 50mM glucose condition, it appeared that less oxidative stress occurred in PC12 cells cultured in 0.03 and 0.3μM of HU210, but not in the highest concentration of HU210 (3μM) when compared with the control value. Thus, the reduction of oxidative stress by HU210 did not follow a concentration-dependent pattern and the difference were not statistically significant (P=0.978 for 5.5mM and P=0.346 for 50mM glucose). Vehicle gave comparable value to the control.

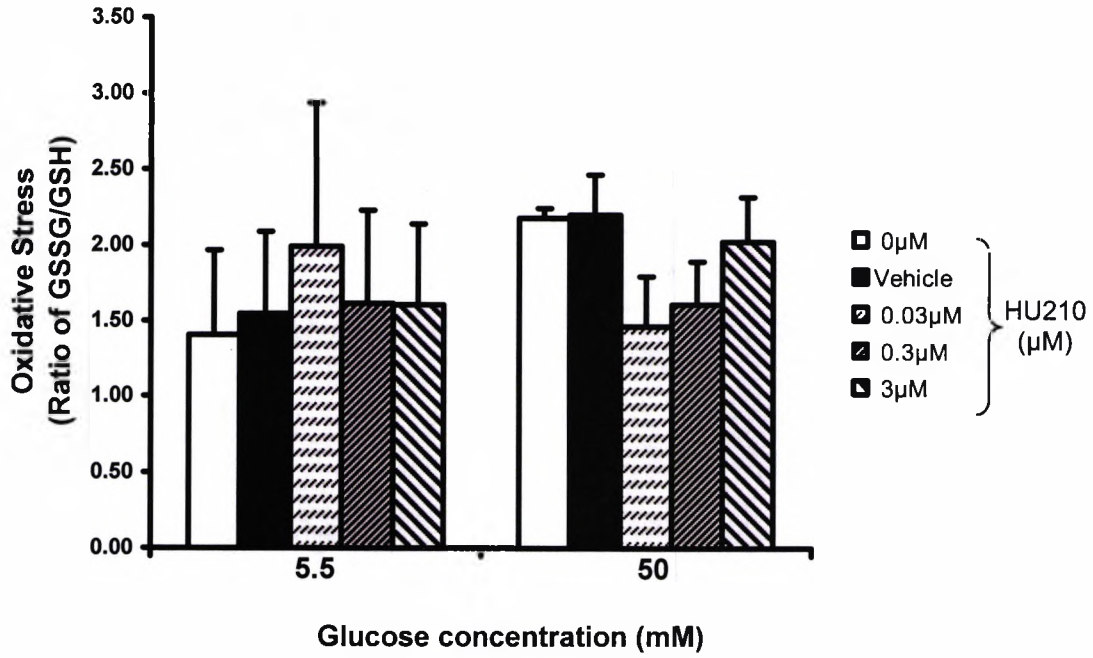


**Figure 6.4** A $CB_1$ agonist has no significant impact on oxidative stress in differentiated PC12 cells. The effect of HU210 treatment (0.03-3μM) on oxidative stress in differentiated PC12 cells at control (5.5mM) and high glucose level (50mM). Values represent mean± SEM from 3 independent experiments (P >0.05, one-way ANOVA-Fisher's post-hoc analysis).

## 6.3 The co-application of a selective cannabinoid $CB_1$ receptor antagonist

### 6.3.1 Concentration-response relationship of AM251 (3μM) on cell growth

The LDH assay and MTT assay were used to determine the cell viability of PC12 cells cultured with the co-application of AM251 (3μM) and HU210 (0-3μM) in the absence or presence of high glucose. Similar to HU210 treatment alone, the LDH release was tested in the supernatant on day 2, 4 and 6 of culture. A maximal LDH release by treating cells with Triton-X (100%) was used as the positive control. Figure 6.5 shows the LDH level released from PC12 cells with the treatment of AM251+ HU210 on day 2, 4 and 6. A similar pattern of a flat line was observed in the LDH release from the three time point studies. It was observed that the LDH level released from PC12 cells treated with the combination of AM251 3μM with each of HU210 concentration: 0, 0.03, 0.3, 3 was very similar to the control and vehicle values in both of 5.5mM and 50mM conditions. Compared to the positive control value of 1800 units/ml, the LDH values from the three time points all remained below 500units/ml.

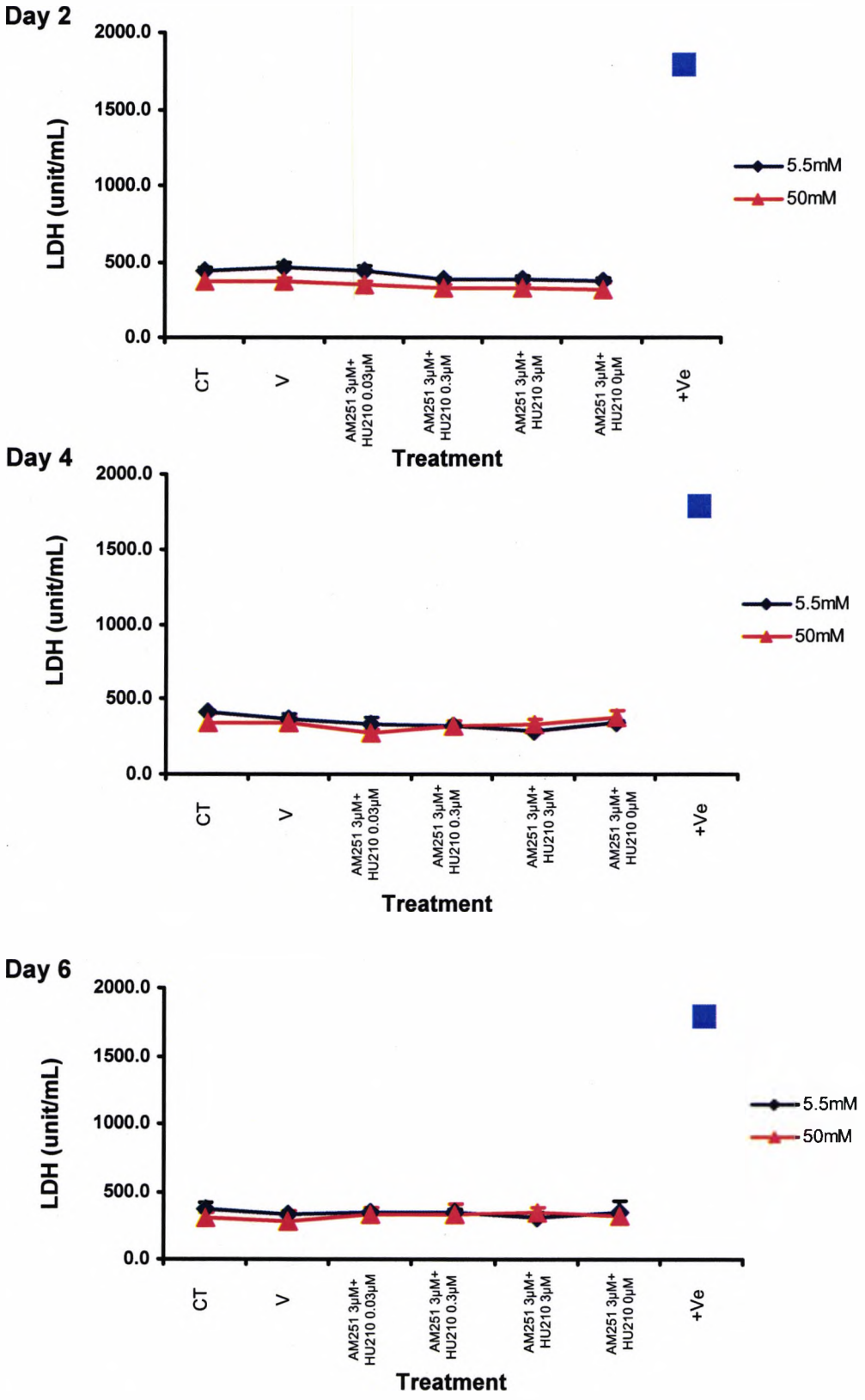


**Figure 6.5** Mean concentration of lactase dehydrogenase release from PC12 cells stimulated with NGF (50ng/ml) and in the absence/presence of high glucose (50mM) when treated with the combination of a $CB_1$ antagonist AM251 (3μM) and a selective $CB_1$ agonist HU210 (0 – 3μM) on day 2, 4 and 6 of culture. Values represent mean ± SEM from 3 independent experiments ($P>0.05$, one-way ANOVA-Fisher's post-hoc analysis).

The MTT assay was conducted on day 6 of cell culture to test the effect of the co-application of AM251 and HU210 on cell viability. Figure 6.6 shows the cell viability of PC12 cells cultured in the combination of AM251 (3μM) with each concentration of HU210 (0, 0.03, 0.3, 3μM) in the normal or high glucose concentrations. It was observed that, at 5.5mM glucose, the treatment of AM251 with each concentration of HU210 did not cause a significant change in cell viability when compared with the control. A similar result was found at 50mM glucose, showing constant cell viability in all groups of treatments. Both of the vehicle data were found to be comparable to the corresponding control. In addition, there was no obvious difference in cell viability with the various groups of treatments between 5.5mM and 50mM glucose.

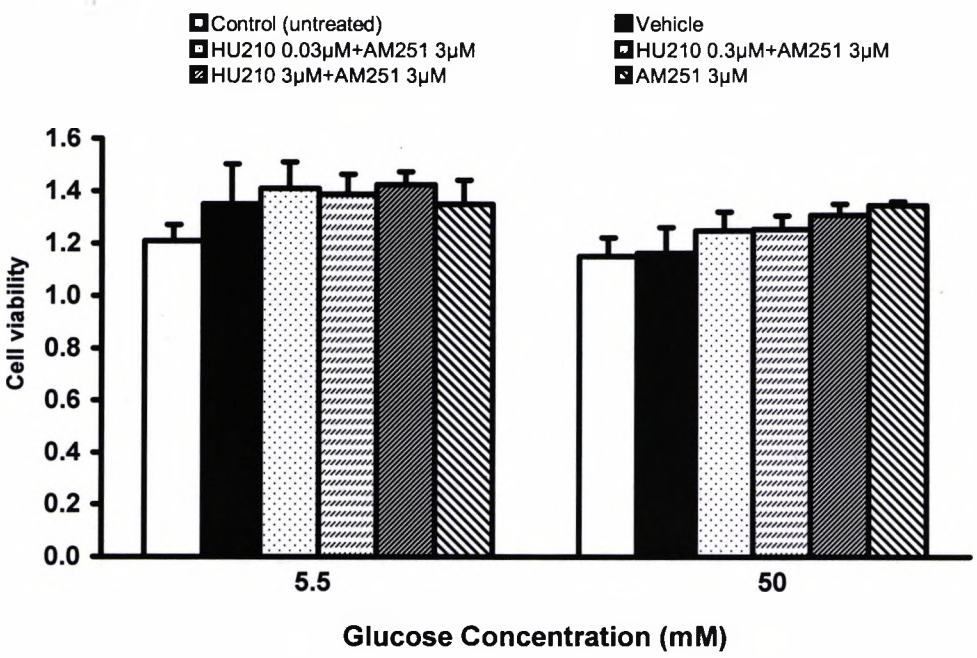


**Figure 6.6** Cell viability of PC12 cells treated with the combination of a selective $CB_1$ antagonist AM251 (3μM) with a $CB_1$ agonist HU210 (0 – 3μM). PC12 cells were stimulated with NGF (50ng/ml) and in the absence/presence of high glucose (50mM) for 6 days. Values represent mean ± SEM from 3 independent experiments. ($P > 0.05$, one-way ANOVA-Fisher's post-hoc analysis).

### 6.3.2 Neurite outgrowth affected by the co-application of AM251 (3μM) and HU210

The representative pictures of the neurite outgrowth of PC12 cells treated with the combination of AM251 (3μM) and HU210 (0-3μM) in the presence of high glucose are showed in Figure 6.7. It was observed that short neurites extended from the cell bodies cultured in control (50mM) and vehicle medium (A and B). The presence of AM251 3μM alone was not observed to affect the neurite length (C). In contrast, in the presence of the combination of AM251 3μM with each HU210 0.03, 0.3 and 3 μM (D, E and F), PC12 cells seemed to bear longer neurites, particularly in the co-application of AM251 3μM and HU210 0.03μM when compared with the control. The same treatments were also applied to PC12 cells cultured in control level of glucose. It was observed that the neurite outgrowth from each combination treatment appeared to be less advanced when compared with the control and vehicle (pictures not shown).

The result from analyzing 82 to 104 cells in each group from both control and high glucose conditions is showed in Figure 6.8. In PC12 cells cultured in 5.5mM glucose, each combination of AM251 3μM with HU210 (0, 0.03, 0.3, 3μM) was found to reduce neurite outgrowth compared with the control and vehicle, however, the reduction did not reach the significant difference ($P=0.168$). In PC12 cells cultured in 50mM glucose, the co-treatment of AM251 3μM and HU210 0.03μM showed a biggest increase on the neurite length reaching 272 (%cell body) among all the treatments compared with the control level of 212. This increase is consistent with the previous finding with HU210 0.03μM treatment only. Although the combination of AM251 3μM and HU210 0.3 and 3μM did promote a small increase on neurite outgrowth, there was no dose relation and significant difference ($P=0.089$) found within those treatments.

This result is opposite to the previous study with HU210 treatment only showing a dose-dependent neurite outgrowth increase in PC12 cells cultured in 50mM glucose with the significant increase found in the treatment of HU210 0.3 and 3μM.

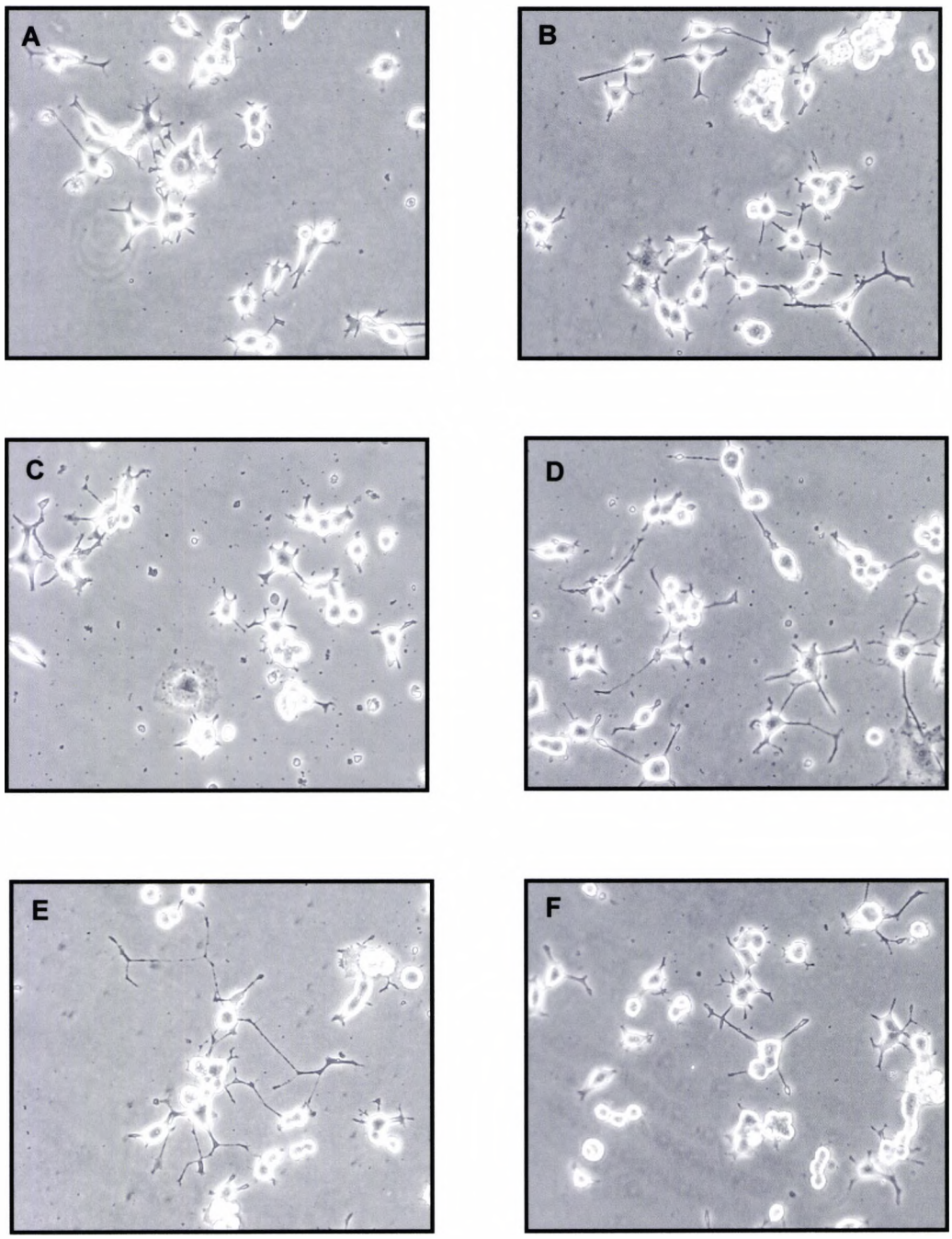


**Figure 6.7** The representative pictures showing the neurite outgrowth in PC12 cells cultured in combination of AM251 and HU210 in the presence of high glucose. **(A),** the control (50mM); **(B),** the vehicle; **(C),** AM251 3μM only; **(D),** AM251 3μM+HU210 0.03μM; **(E),** AM251 3μM+HU210 0.3μM; **(F),** AM251 3μM+HU210 3μM.

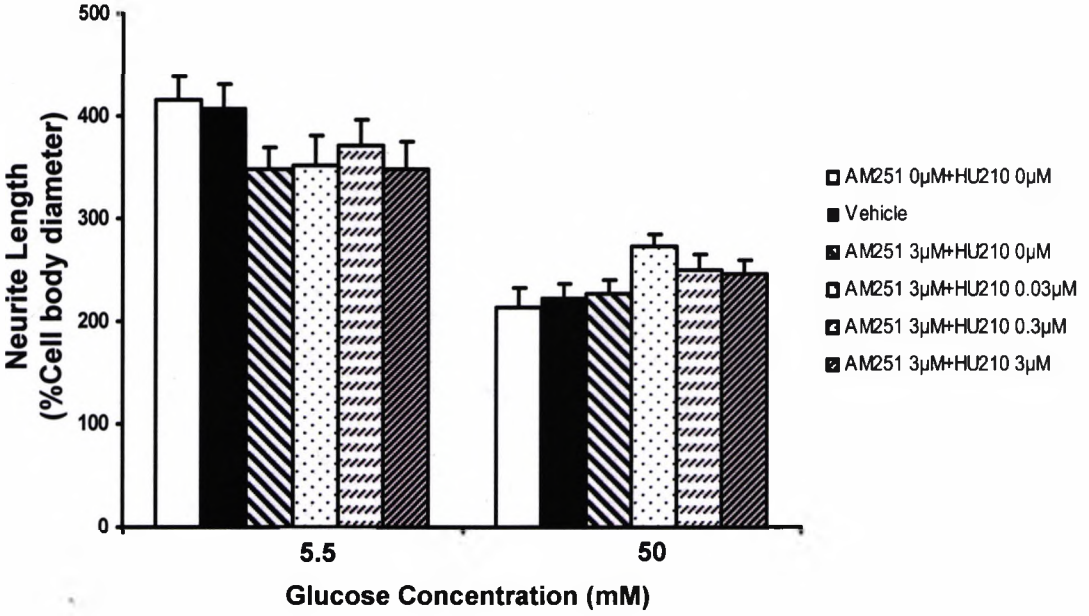


**Figure 6.8** The co-application of AM251 and HU210 affects neurite outgrowth in PC12 cells. The effect of AM251 (3μM) plus HU210 (0.03-3mM) on neurite length (normalised to cell body diameter) of differentiated PC12 cells in control (n=82-104) and high glucose conditions (n=86-104). Values represent mean from 3 independent experiment ± SEM. (P>0.05, one-way ANOVA-Fisher's post-hoc analysis).

### 6.3.3 The effect of the co-treatment of AM251 and HU210 on oxidative stress induced by high glucose

Oxidative stress was examined in PC12 cells treated with the combination of AM251 (3μM) + HU210 (0, 0.03, 0.3, 3μM) in the absence or presence of high glucose for 6 days as shown in Figure 6.9. In PC12 cells cultured in 5.5mM glucose, it was found that the co-application of AM251 with each concentration of HU210 did not cause any significant change on oxidative stress level versus the control group (P=0.978). In PC12 cells cultured in 50mM glucose, it was observed that treatment with AM251+ concentrations of HU210 at 0.03 and 0.3μM appeared to reduce oxidative stress when compared with the control value. In comparison, the oxidative stress in PC12 cells cultured with AM251+

3μM HU210 was very similar to the level of the control. Thus, the change in oxidative stress in PC12 cells cultured in the combination of AM251+ HU210 did not follow a concentration-dependent pattern, which was similar to the previous finding with HU210 treatment alone. It was also observed that the oxidative stress level with AM251 alone was less than the control level. However, there was no significant difference found between the groups, including the vehicle (P=0.346).

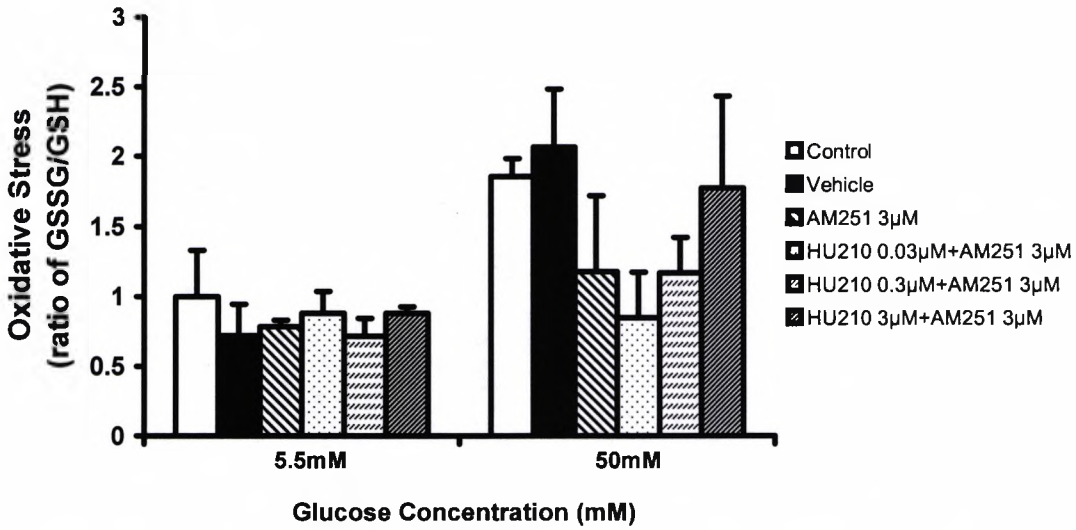


**Figure 6.9** The effect of $CB_1$ antagonists on oxidative stress in differentiated PC12 cells with/without HU210. Values represent mean± SEM from 3 independent experiments. (P>0.05, one-way ANOVA-Fisher's post-hoc analysis).

## 6.4 The co-application of a cannabinoid $CB_1$ antagonist AM251 (1μM) or/and a $CB_2$ antagonist AM630 (1μM)

### 6.4.1 Cell viability following treatment with AM251 (1μM) and/or AM630 (1μM) with HU210

PC12 cells were cultured in DMEM supplemented with different combinations of HU210, AM251 and AM630 in the presence of high glucose (50mM) for 6 days under the stimulation of NGF (50ng/ml). The samples were examined by MTT assay to assess the cell viability. Figure 6.10 shows the cell viability of PC12 cells treated with the co-administration of HU210 (0.3μM), HU210 (0.3μM) + AM251 (1μM), HU210 (0.3μM) +AM630 (1μM) and HU210 (0.3μM) +AM251 (1μM) +AM630 (1μM) as well as the control and vehicle groups in high glucose. No significant change in cell viability between any of the two groups was observed compared with the control value (one way ANOVA, P=0.089).

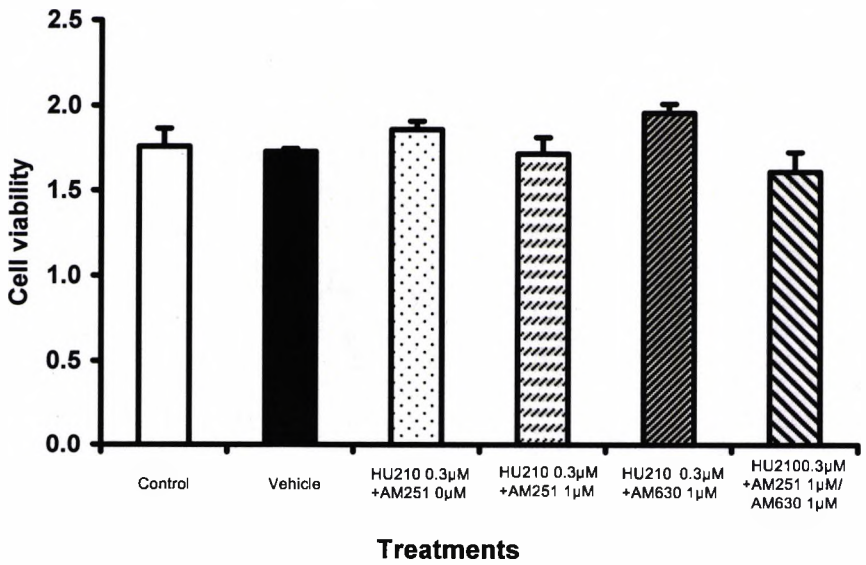


**Figure 6.10** Cell viability of PC12 cells treated with the combination of HU210 (0.3μM) with AM251 (1μM) or/and AM630 (1μM). PC12 cells were stimulated with NGF (50ng/ml) in the presence of high glucose (50mM) for 6 days. Values represent mean ± SEM from 3 independent experiments (P>0.05, one-way ANOVA-Fisher's post-hoc analysis).

### 6.4.2 Neurite outgrowth following the co-application with AM251 (1μM) and/or AM630 (1μM)

A lower concentration of the selective $CB_1$ antagonist, AM251 (1μM), and a selective $CB_2$ antagonist, AM630 (1μM), were both co-applied with HU210 (0.3μM) in order to examine whether the HU210-induced neurite outgrowth is mediated by $CB_1$ receptors or $CB_2$ receptors. PC12 cells were cultured in the following combinations: HU210 0.3μM only, HU210 0.3μM + AM251 1μM, HU210 0.3μM + AM630 1μM and HU210 0.3μM + AM251 1μM + AM630 1μM, as well as control and vehicle groups, for 6 days under the stimulation of NGF (50ng/ml). A representative photomicrograph of neurite outgrowth in PC12 cells cultured in control medium (50mM) is shown in Figure 6.11(A). The addition of vehicle to the culture medium had no effect on neurite outgrowth compared to the control (Figure 6.11 B). When HU210 (0.3μM) was added to the medium, the neurite length of PC12 cells was observed to be longer than in the control as shown in (Figure 6.11 C). The co-application of HU210 (0.3μM) + AM251 (1μM) appeared to reduce the neurite length in PC12 cells compared with the HU210 (0.3μM) treatment only (Figure 6.11 D). In contrast, longer neurite length was still observed in PC12 cells treated with the combination of HU210 0.3μM + AM630 1μM compared to the control (Figure 6.11 E). The extent of neurite outgrowth was similar to that observed in HU210 (0.3μM) treatment alone. Again, in the presence of AM251 (1μM) + HU210 (0.3μM) + AM630 (1μM), the neurite length in PC12 cells was observed to be shorter than that in the co-application of HU210 (0.3μM) + AM630 (1μM).

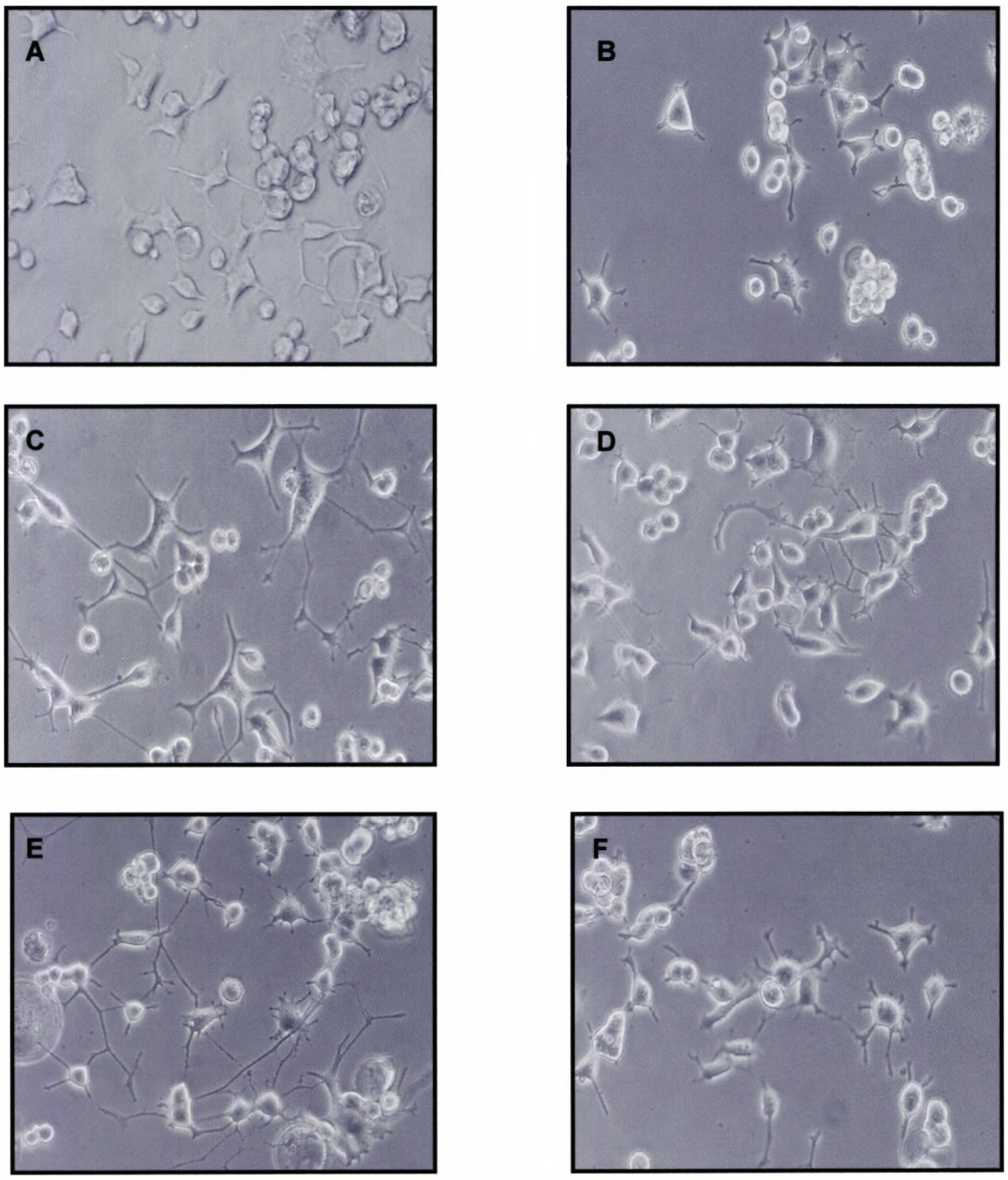


**Figure 6.11** The representative photomicrographs show the neurite outgrowth in PC12 cells cultured in control medium **(A)**, vehicle medium **(B)** and the medium supplemented with HU210 0.3μM **(C),** HU210 0.3μM+AM251 1μM **(D),** HU210 0.3μM+AM630 1μM **(E),** and HU210 0.3μM+AM251 1μM+AM630 1μM **(F).**

Figure 6.12 shows the total neurite length (expressed as % cell body diameter) measured from at least 130 individual cells from each group. In comparison to the control group, the addition of HU210 (0.3 μM) alone was found to significantly increase neurite outgrowth more than two-fold ($P<0.05$). The co-application of AM251 (1μM) but not AM630 (1μM), with HU210 (0.3μM) significantly reduced the neurite outgrowth compared to HU210 (0.3μM) treatment alone ($P<0.05$). The neurite length of PC12 cells cultured in AM251 (1μM) + HU210 (0.3μM) + AM630 (1μM) was significantly reduced compared with the neurite length in the HU210 (0.3μM) alone group and the co-treatment of HU210 (0.3μM) + AM630 (1μM) ($P<0.05$).

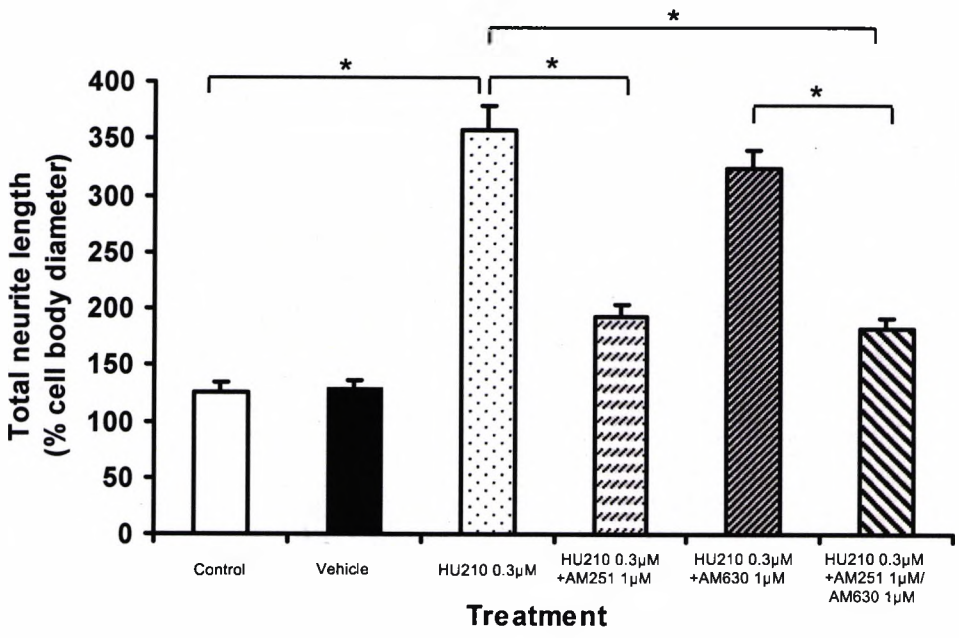


**Figure 6.12** HU210 promotes neurite outgrowth in a $CB_1$-dependent manner. It shows the total neurite length (expressed as the % of cell body diameter) of PC12 cells cultured in control media (50mM glucose) or the media supplemented with the $CB_1$ agonist, HU210 (0.3μM) +/- selective $CB_1$ antagonist, AM251 (1μM), and/or selective $CB_2$ antagonist AM630 (1μM) (n=131-208). Values represent mean from 3 independent experiment ± SEM. (*, $P<0.05$, one-way ANOVA-Fisher's post-hoc analysis).

## 6.5 Discussion

In Chapter 4 and 5, we have demonstrated that $CB_1$ receptors remained functional although the expression decreased in PC12 cells cultured in high glucose. We hypothesized that treatment with cannabinoids may rescue the impaired neurite outgrowth through $CB_1$ receptors. Cannabinoids are suggested to control the survival and death of neurons. Many *in vitro* and *in vivo* studies have reported that cannabinoids improve neuron viability and protect against toxic insults (Mechoulam *et al.,* 2002; van der Stelt *et al.,* 2002) whilst, in contrast, others have shown that cannabinoids can induce apoptosis in cultured neurons as well as other non-neuronal cells (Chan *et al.,* 1998; Guzman, 2003). The dual effect of cannabinoids may result from various experimental factors, such as *in vivo* or *in vitro* studies, culture conditions, and the range of doses used.

In this chapter, we firstly conducted viability assays in PC12 cells cultured in the medium supplemented with a range of HU210 concentration in the presence of control or high glucose, and under the stimulation of NGF for 6 days. Both LDH and MTT assays revealed that, apart from HU210 at 30μM where cells showed a significant death, the cell viability was not different in cells among other concentrations (0.03μM-3μM) in both normal and high glucose conditions compared with control and vehicle groups. This result is in agreement with the study by Sarker *et al,* (2000) reporting that the endocannabinoid, anandamide, dose-dependently caused the loss of cell viability of PC12 cells (Sarker *et al.,* 2000): no change in cell viability when the concentration was less than 7.5μM; loss of cell viability when the concentration reached 10μM. It was also reported in the study conducted by Hart *et al.,* (2004) that $\Delta^9$-THC and other cannabinoids at nanomolar levels accelerated cell

proliferation in glioblastoma cells, immune cells, whilst high concentrations of cannabinoids induced apoptosis (Hart *et al.,* 2004). The co-treatment with the $CB_1$ selective antagonist, AM251 (1μM /3μM) + HU210 (0.03μM-3μM) did not affect cell viability, indicating that $CB_1$ antagonism, at least at these two concentrations, had no impact on cell viability.

The neurite outgrowth study showed that the addition of HU210 (0.03μM-3μM) had no significant effect on the total neurite length in PC12 cells cultured in 5.5mM glucose, while an increased total neurite length was found in PC12 cells cultured in 50mM glucose in a HU210 concentration-dependent manner when compared with the controls. HU210 at 0.3μM and 3μM significantly rescued neurite outgrowth versus control which was reversed by the $CB_1$ antagonist, AM251 (3μM). To exclude the possibility of AM251 and AM630 acting at additional receptors at higher concentration (>1μM), a lower concentration (1μM) was chosen for use in subsequent experiments Although AM251 is described as a $CB_1$-selective antagonist, at high concentrations (above 1μM) it can also have effects on $CB_2$ receptors (New and Wong, 2003). Thus, we examined whether a lower, selective concentration of AM251 (1μM) had similar effects on $CB_1$ agonist-evoked inhibition of TRPV1 calcium responses. We found that, the lower concentration, 1μM of AM251, but not the $CB_2$ antagonist (AM630 1μM), also significantly attenuated the HU210 (0.3μM) mediated-neurite rescue. This result indicates that HU210 has a therapeutic potential in neurodegenerative diseases and it may restore neurite regeneration through activating $CB_1$ receptors. HU210 has been previously found to trigger neurite outgrowth in cultured Neuro-2A cells (Jordan *et al.,* 2005), where signalling through Gi/o-coupled $CB_1$ receptors causes activation of the small G protein, Rap1, and neurite outgrowth via a signal transducer and activator of

transcription (Stat)3-dependent convergent step (He *et al.,* 2005). In PC12 cells, activation of Rap1 and extracellular signal-regulated kinase (ERK) plays a critical role in neurite outgrowth (Vossler *et al.,* 1997), and $CB_1$ can selectively activate the ERK pathway in neurons (Derkinderen *et al.,* 2003, Graham *et al.,* 2006).

A recent study by Dagon *et al.,* (2007) found that HU210 ameliorates hyperglycaemia induced impaired neurite outgrowth in PC12 cells. However, they also observed increases in neurite outgrowth in the control ("normoglycaemic") group - we found only significant effects of HU210 in the hyperglycaemic group. There are several differences in the experimental design of Dagon and colleagues (2007) and our study. Firstly, we measure total neurite length of cells whereas Dagon *et al.* measured percentage of cells with neurites. Secondly, the concentrations of glucose used were different between each study: for the control/normoglycaemic group we used 5.5mM glucose compared to 25mM by Dagon *et al.*; for the high glucose/hyperglycaemic group we used 50mM compared to 150mM by Dagon *et al.*, (2007). It is possible neurite outgrowth was already impaired in their 25mM control group, such that HU210 would show an improvement. The higher glucose concentrations could also account for the hyperglycaemia-induced apoptotic cell death found by Dagon *et al.*, (2007). Finally, the concentrations of HU210 were higher in the Dagon study (ranging from 5-20μM) compared to ours (0.03-3μM). At 30μM HU210, we observed ~100% cell toxicity after 48 hour-exposure, and so for chronic (6 day) neuroprotective studies we used a maximum of 3μM. In the *in vivo* arm of the Dagon study, HU210 was shown to alleviate cerebral oxidative stress and cognitive impairment in diabetic mice, through a $CB_1$ receptor-independent mechanism(s) (Dagon *et al.,* 2007).

Oxidative stress has been implicated in the pathogenesis of neurodegenerative diseases, including diabetic neuropathy (Brownlee, 2001, Vincent *et al.,* 2004). The phenolic moiety of the *Cannabis sativa* derivatives, $\Delta^9$-tetrahydrocannabinol ($\Delta^9$-THC) and cannabidiol, acts as an electron donor and direct free-radical scavenger. This antioxidant property is fully independent of $CB_1$ activation and confers neuroprotective properties to cannabinoids against oxidative stress (Hampson et al., 1998, Marsicano et al., 2002). Reduced glutathione (GSH) is one of the major endogenous antioxidants in humans. We found that HU210 at 0.03 and 0.3μM reduced the levels of oxidative stress in hyperglycemic cells, as shown by a decrease in the ratio of oxidized to reduced glutathione (GSSG:GSH) and the addition of AM251 did not change the antioxidant property of HU210. Like Δ9-THC and cannabidiol, this antioxidant effect was receptor independent, and likely involves the phenol ring present in HU210's structure.

In summary, we have demonstrated in this chapter, that the synthetic cannabinoid HU210 treatment, reversed impaired neurite outgrowth and reduced oxidative stress in hyperglycaemic PC12 cells, through $CB_1$ receptor-dependent and-independent pathway, respectively.

# CHAPTER 7

# GENERAL DISCUSSION

## 7.1 General discussion

The population of people with diabetes is predicted to reach 366 million worldwide in 2030 (Wild *et al.,* 2004). Both type 1 and type 2 diabetic patients likely develop diabetic neuropathy, which is the most common complication associated with diabetes, however, the exact mechanisms remains at least understood (Sima, 2003; Vinik *et al.*, 2006). Distal symmetric polyneuropathy, the commonest type of diabetic neuropathy, is characterized by the degeneration of peripheral nerve endings, resulting in acute pain, sensorimotor deficits, and high risk of limb amputation (Vinik *et al.,* 2006). So far, the only effective way to prevent and slow diabetic neuropathy is the control of blood glucose itself. Failure to do this means that the damage resulting from hyperglycaemia is irreversible. The disrupted cellular glucose metabolism in hyperglycaemia induces over-production of free radicals and reduces natural antioxidant defences, causing oxidation of DNA protein, lipid and abnormal signal transductions (McHugh and McHugh, 2004; Vincent *et al.*, 2004). At tissue level, hyperglycemia not only reduces the production of NGF and impairs NGF transport, but it also slows blood flow and creates ischaemia, resulting in neuronal dysfunction (Siemionow and Demir, 2004). However, simply supplying antioxidant and NGF, as well as inhibiting other therapeutic targets such as protein kinase C or AGEs, have not been found to be successful in human clinical trials (Sullivan and Feldman, 2005). The development of a treatment that can delay the onset of neuropathy and slow its progression is urgently needed to improve the quality of life in patients with diabetes and reduce demands on health resources.

Since the revelation that cannabinoids exert their biological functions through binding to cannabinoid receptors ($CB_1$), which are abundantly expressed in the

central nervous system and peripheral nerves, cannabinoid signalling has been the focus of intensive research. Much of the research thus far has focused on cannabinoids' protective role in the central nervous system in response to chronic neurodegenerative diseases, including Alzheimer's disease and multiple sclerosis, or injury associated with stroke or brain trauma (reviewed by Bahr *et al.,* 2006). These studies demonstrated that both $CB_1$ receptor-independent (antioxidant) and -dependent mechanisms (inhibition of $Ca^{2+}$ influx, reduced glutamate release and excitotoxicity, vasodilatation, increased NGF production and neurotrophic support, hypothermia) are involved in the neuroprotectant effect. Peripherally, the activation of $CB_1$ receptors has been proved to attenuate the release of neurotransmitters and neuropeptides (Ralevic, 2003), producing analgesic effects. The loss of $CB_1$ receptors has been demonstrated in a number of neurodegenerative diseases, including Huntington's disease (Denovan-Wright & Robertson 2000; Glass *et al.*, 2004) and Parkinson's disease (Silverdale *et al.*, 2001). Moreover, Denovan- Wright & Robertson (2000) found the decrease in $CB_1$ mRNA occurred before the onset of the motor-related Huntington's disease-like symptoms in mice and preceded neural degeneration, suggesting abnormalities in cannabinoid signalling play a significant pathogenetic role. At the outset of this PhD project, no one had previously studied the cannabinoid signalling in diabetic neuropathy. To our knowledge, this project is the first to investigate the role of $CB_1$ receptors in the pathogenesis of diabetic neuropathy, and the neuroprotective role of cannabinoids in experimental diabetes.

Numerous *in vitro* models have previously been used to examine the cellular mechanisms involved in the pathophysiology of diabetic complications, including human SH-SY5Y neuroblastoma cells (Shindo *et al.*, 1996), and rat

dorsal root ganglia (DRG) (Russell *et al.,* 1999). In the chapter 1, our initial experimental design (Figure 7.1) involved setting up two *in vitro* cell models of diabetic neuropathy: rat PC12 cells and human SH-SY5Y neuroblastoma cells, which would be corroborated with animal studies. The results from both *in vitro* and *in vivo* studies have the potential to lead to a therapeutic indication in human clinical trails.

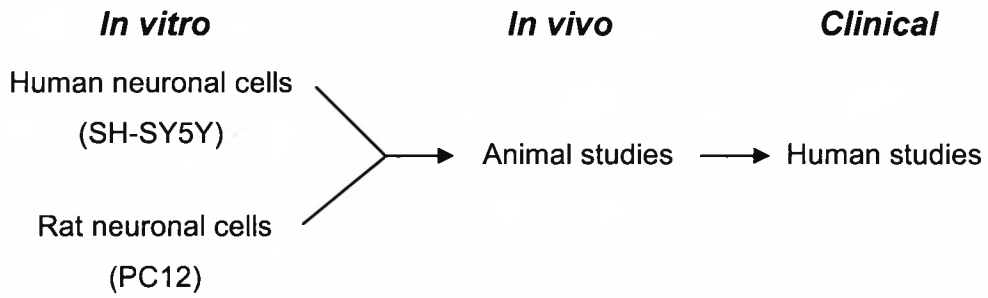


**Figure 7.1** The route of the experimental design.

However, as mentioned in Chapter 3, SH-SY5Y cells remain indefinitely dividing, which makes the morphological assessment from a chronic study difficult. Most importantly, the lack of TRPV1 receptors in this cell line makes the study on inhibitory effect of $CB_1$ receptors on capsaicin (a TRPV1 agonist)-induced $Ca^{2+}$ influx impossible to conduct. Therefore, use of SH-SY5Y cells does not fit with the experimental design on the model of small sensory neurons which are mainly responsible for painful diabetic neuropathy, based on the fact that TRPV1 receptors are present on small sensory neurons and share more than 80% of localization with $CB_1$ receptors (Ahluwalia *et al.,* 2000). Unlike SH-SY5Y cells, PC12 cells are similar to cultured DRG neurons, in that they express both TRPV1 and $CB_1$ receptors. Therefore, we discontinued use of SH-SY5Y cells, and set up PC12 cells in this study as the *in vitro* model of

diabetic neuropathy, after establishment by Lelkes and colleagues (Lelkes *et al.,* 2001). To validate this cell model, we cultured PC12 cells with increasing concentrations of glucose to mimic hyperglycaemic conditions and stimulated neurite outgrowth with NGF. This cell model reproduced some of the phenomenon of diabetic neuropathy: high glucose attenuated NGF-induced neurite outgrowth, which was associated with oxidative stress, and caused dose-dependent increase in IL-6 production.

Many animal and *in vitro studies* have suggested various pathway of glucose metabolism in the initiation and progression of diabetic neuropathies. They include: increased polyol pathway activity; formation of advanced glycation end-products; activation of protein kinase C; and impaired mitochondrial electron transfer chain (Yagihashi *et al.,* 2007). These pathways all directly or indirectly produce excessive ROS and promote oxidative stress. Indeed, type 1 diabetics with high serum levels of ROS have more severe peripheral neuropathy (Pop-Busui *et al.,* 2004). Oxidative stress is likely to be the unifying mechanism triggering the onset of deteriorative processes. Kaur *et al,* (2005) have reported that oxidative stress can disrupt NGF signalling by blocking activation of STAT kinase activation which is essential for neurite extension, causing neuronal damage observed in neurodegenerative diseases (Kaur *et al.,* 2005). Oxidative stress-induced mitochondrial dysfunction and apoptosis has been widely found in various neuronal cells (Vincent *et al.*, 2002; Schmeichel *et al.*, 2003). In the current study, we observed impaired neurite outgrowth caused by high glucose occurs before overall cell death. Although not an exact model of the "dying-back" axonopathy observed in diabetic neuropathy, it provides a basis for examination of neuroprotective agents.

In parallel with our finding in Chapter 3, high levels of IL-6 have been found in plasma and monocytes isolated from diabetic patients, suggesting an inflammatory process induced by hyperglycaemic conditions (Giulietti *et al.,* 2007; Targher *et al.,* 2001; Jain *et al.,* 2003), In the nervous system, IL-6 has both physiological and pathophysiological functions. Otten *et al.,* (2000) suggests an interaction between cytokines and neurotrophins in normal and diseased states, which comes from evidence showing that IL-6 and neurotrophinsare co-expressed at the site of nerve injury. Rapid accumulation of IL-6 after nerve injury indicates the 'neuron-rescue' role of IL-6. The neuron-protective action may be achieved through directly or indirectly signalling the binding of neurotrophin with TrkA receptors, triggering the pathway of neuronal protection (Otten *et al.,* 2000). On the other hand, sustained high levels of IL-6 can promote completely opposite on neurons by triggering degeneration of neurons after nerve injury. A study from Campbell *et al,* (1993) reported that transgenic mice over-expressing IL-6 in astrocytes showed a marked neurodegeneration and the recovery process was hindered by neurotrophin-mediated scar formation (Campbell *et al.*, 1993). This study implicates the interaction between IL-6 and neurotrophins: sustained high levels of IL-6 may promote neurotrophin binding to, the low-affinity receptor , p75, inducing neuronal apoptosis (Otten *et al.,* 2000). In addition, numerous clinical studies have shown increased synthesis of IL-6 in brain tissue at post-mortem from patients with various neurological disorders, including Alzheimer's, Parkinson's, multiple sclerosis and epilepsy, infection, injury, inflammation and stroke (Rothwell and Relton, 1993). However, it is unclear that the increased production of IL-6 is directly involved in the pathogenesis of neurodgeneration or the increase is only secondary to nerve damage.

In 2005, Bierhaus and colleagues have reported that loss of pain perception, indicative of a long-standing diabetic neuropathy, was remarkably reversed in mice lacking the receptor of advanced glycation end products (associated with sustained activation of NF-κB), indicating RAGE play a central role in sensory neuronal dysfunction. In this study, AGE dysregulated the activation of NF-κB and NF-κB-IL-6 expression in peripheral nerves of diabetic mice though binding to RAGE (Bierhaus *et al.,* 2005). The association between RAGE and activation of NF-κB was further confirmed by the evidence that NF-κB activation was blunted in the absence of RAGE. In the view of Bierhaus *et al.,* (2005), the initial pulse of NF-κB activation and subsequent IL-6 expression has cytoprotective properties in response to oxidative stress. However, more sustained NF-κB activation, leading to sustained over-expression of IL-6, might have deleterious consequences for neuronal properties. Although AGE-RAGE mediated signal transduction involving sustained over-expression of pro-inflammatory cytokines is not the only factor inducing neuron damage, it, at least partially, contributes to the development and progression of diabetic neuropathy (Bierhaus *et al.,* 2004).

Chapter 4 investigated the regulation of $CB_1$ expression in *in vitro* and *in vivo* models of diabetic neuropathy. In agreement with our hypothesis, $CB_1$ receptor protein appears to be down-regulated in nerve cells grown in conditions mimicking hyperglycaemia and in neurons from diabetic rats, which may contribute to the neurodegenerative process observed in diabetic neuropathy. Whilst data from *in vitro* studies involving animal cells cannot be directly extrapolated to human disease, the fact we also demonstrated reduced $CB_1$ expression in DRG neurons of a rat model of diabetes *ex vivo* adds credence to our findings. Of course, due consideration must be made when comparing "*in*

*vitro* high glucose" and "*in vivo* diabetic" states, since we had a 9-fold difference in glucose levels between cell-treatment groups, which remained elevated during the culture, whilst the rat diabetic model showed a 5-fold elevation in plasma glucose compared to controls, and these levels would fluctuate throughout the animals' lives. Others have reported plasma glucose levels in the STZ-diabetic rat range from 25 - 50 mM (mean 34.5 ± 3.05 mM) (Purves *et al.*, 2001), thus making the concentrations used in our *in vitro* study reasonable.

The pathogenesis of diabetic neuropathy is multifactorial. Extending from our findings, Figure 7.2 illustrates the possible downstream mechanisms derived from hyperglycaemia-induced oxidative stress, which may be involved in the development and progression of diabetic neuropathy.

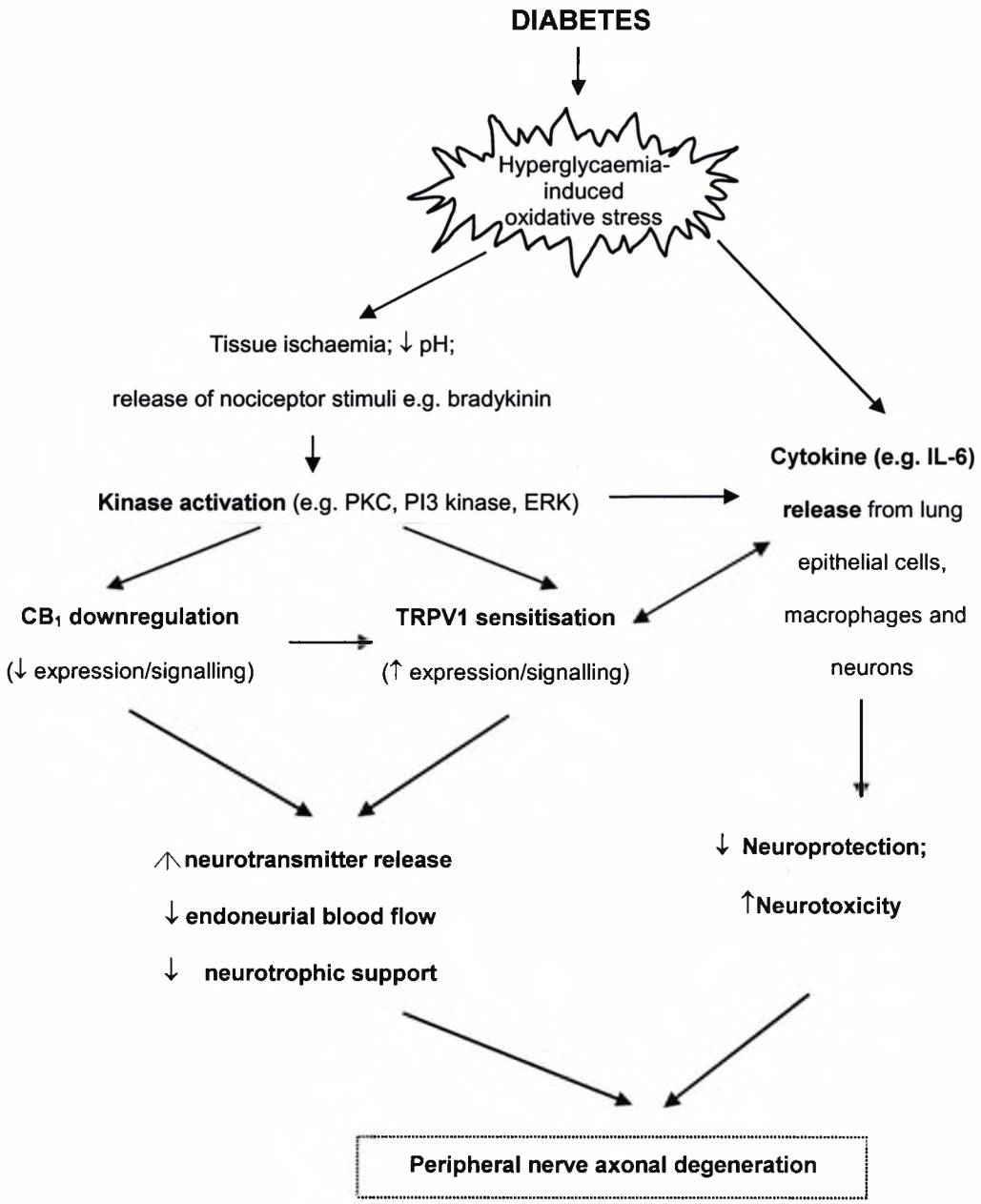


**Figure 7.2** Mechanisms involved in development and progression of diabetic neuropathy.

A major consequence of a decline in $CB_1$ expression is likely to be increased TRPV1 receptor signalling. Up-regulation of TRPV1 receptors on sensory nerves contributes to the thermal hyperalgesia and allodynia observed in diabetic mice (Kamei *et al.,* 2001b; Rashid *et al.,* 2003). In 2005, Hong and Wiley published data showing enhanced function of TRPV1 in diabetic rats, involving increased receptor phosphorylation via protein kinase C, oligomerization to active form, and recruitment to cell surface plasma membrane (Hong & Wiley, 2005).

Protein kinase C (PKC) activation in diabetes could result from the enhanced release of chemical mediators (e.g. bradykinin) under ischaemic conditions, following hyperglycaemia-induced oxidative stress. Indeed, inhibitors of PKC have been shown to decrease the hyperalgesia and C-fibre hyperexcitability found in diabetic rats (Ahlgren and Levine, 1994). Interestingly, whilst PKC can sensitize TRPV1 receptors, it down-regulates the activity of $CB_1$ receptors (Garcia *et al.,* 1998). Ellington and co-workers (2002) examined anandamide-induced inhibition of capsaicin-evoked CGRP release in rat paw skin from control and diabetic rats. They found anandamide inhibited CGRP release only in skin from control animals, and furthermore, actually stimulated CGRP release in skin from diabetic rats when tested at higher concentrations. These data suggest anandamide action at TRPV1 receptors overcomes the inhibitory actions mediated by $CB_1$ receptors in diabetes. Even if TRPV1 activation evokes synthesis and release of anandamide, as has been demonstrated in cultured rat neurons (Ahluwalia *et al.,* 2003), this will only serve to enhance TRPV1 signalling under conditions where $CB_1$ receptors are down-regulated. Thus, there would appear to be a differential regulation of $CB_1$ versus TRPV1 expression and/or function in diabetes.

Higher circulating endocannabinoid levels (anandamide and 2-AG) have been demonstrated in obese patients with type 2 diabetes (Matias *et al.,* 2006a), and the same authors report up-regulation of endocannabinoids in post-mortem eye tissues of patients with diabetic retinopathy (Matias *et al.,* 2006b). In obese postmenopausal women with fasting hyperinsulinaemia, elevated levels of anandamide and 2-AG were found to be associated with decreased $CB_1$ receptor expression in adipose tissue (Engeli *et al.,* 2005). The mechanistic link between glucose concentration and $CB_1$ receptors is likely to be oxidative stress. Obesity is strongly correlated with increased oxidative stress and, because high glucose enhances the production of cellular reactive oxygen species (Brownlee, 2001), the oxidative burden is even greater when obesity is coupled with insulin resistance (van Guilder *et al.,* 2006). Raised levels of endocannabinoids are likely to result from decreased enzymatic degradation, since Engeli and co-workers (2005) reported fatty acid amide hydrolase (FAAH) gene expression was down-regulated in adipocytes from obese women. In turn, the raised ligand concentrations may down-regulate $CB_1$ receptor expression via a negative feedback loop. As previously mentioned, a decline in $CB_1$ receptors in the presence of elevated endocannabinoid levels might tip the balance towards TRPV1 activation. Furthermore, FAAH can attenuate TRPV1 activation (Millns *et al.,* 2006), so any reduction in FAAH levels would further enhance signalling via TRPV1 receptors.

As mentioned above, low levels of IL-6 are neuroprotective. However, sustained high levels of IL-6 are neurotoxic. The resources contributing the high levels of IL-6 production come from not only the hyperglycaemia-induced oxidative stress (Gumieniczek *et al.,* 2006), but also other aberrant signal transducers, including activated PKC (Devaraj *et al.,* 2005) and TRPV1

receptors (Seki *et al.,* 2007, Nicol *et al.,* 1997). Furthermore, the over-expression of IL-6 may also contribute to the sensitization of TRPV1 receptors. Tamura and colleagues have demonstrated that oncostatin M, a member of the IL-6 family of cytokines, was expressed in both cell bodies and processes of nociceptive neurons in adult mice, which provided anatomical evidences that oncostatin M may affect the nociceptive function of the neurons through the modulation of TRPV1 receptors (Tamura *et al.,* 2003). Indeed, inflammatory cytokines as one of numerous inflammatory mediators can sensitize the response of TRPV1 receptors to noxious heat, protons and capsaicin, thus augmenting thermal hyperalgesia (Ma and Quirion, 2007).

In consequence, as suggested in Figure 7.2, TRPV1 sensitization could deprive sensory nerves of NGF and lead to axonal degeneration. This is based on the observation by Taylor and colleagues (1985) that capsaicin prevents retrograde axonal transport in rat sensory neurons (Taylor *et al.,* 1985). The tipped $CB_1$ and TRPV1 expression or signalling towards TRPV1 receptors leads to increased $Ca^{2+}$ signalling, neurotransmitter and neuropeptide release, decreased neurotrophic support and blood flow, and sustained inflammation, which all contribute the development and progression of diabetic neuropathy.

We demonstrated decreased neuronal expression of $CB_1$ receptors in *in vitro* and *in vivo* models of diabetic neuropathy (Chapter 4) (Zhang *et al.*, 2007), and hypothesized that such a decrease would result in attenuated nerve cell responses to a $CB_1$ agonist under hyperglycaemic conditions. At concentrations of the $CB_1$ agonist HU210 below 1mM we indeed observed a blunted inhibition of capsaicin-evoked calcium influx in PC12 cells cultured in high glucose in Chapter 5. However, at concentrations ≥1mM HU210, the

function of the $CB_1$ receptor is preserved, as evidenced by a similar degree of inhibition of capsaicin-evoked calcium influx in 5.5 and 50mM glucose conditions. These data actually draw a parallel with findings that the anti-nociceptive action of the mixed cannabinoid $CB_1/CB_2$ receptor agonist, WIN 55212-2, is preserved in diabetic mice (Dogrul *et al.,* 2004) and rats (Ulugol *et al.,* 2004). However, the results from these *in vivo* studies may involve non-CB receptor mechanisms. In 2006, Patwardhan and colleagues demonstrated that WIN 55,212-2 could inhibit capsaicin-evoked calcium currents in rat trigeminal neurons, via calcineurin-dependent dephosphorylation of TRPV1. This mechanism was independent of G-protein coupled CB receptors (Patwardhan *et al.,* 2006). We found that the inhibitory effect of HU210 on capsaicin-induced calcium influx could be blocked by the $CB_1$ antagonist AM251, as have others in rat DRG neurons (Millns *et al.*, 2001; Oshita *et al.*, 2005). This suggests the response is $CB_1$-dependent and, therefore, in our *in vitro* model of diabetic neuropathy, the enduring $CB_1$ receptors remain functional. The activation of PKC is involved in the development of diabetic neuropathy (Hong and Wiley, 2005; Ohsawa and Kamei, 1999), it may disrupt the cannabinoid neuro-protective action by phosphorylation of the $CB_1$ receptor (Garcia *et al.,* 1998). We, therefore, examined the phosphorylated $CB_1$ receptors to assess the remaining functional sites in hyperglycaemic cells. The results revealed that, although the active form of $CB_1$ receptors was indeed reduced in hyperglycaemic condition, the percentage out of the already reduced $CB_1$ receptor maintained unchanged, which may explain the $CB_1$ receptors remain functional although the expression is decreased.

Even so, the maintenance of receptor function following activation by concentrations of HU210 ≥1mM may reflect only the ability of *exogenous*

cannabinoids to activate the receptors. Critical to the link between decreased receptor expression and maintained function is the level of endocannabinoid $CB_1$ ligands. In obese patients with type 2 diabetes, higher circulating endocannabinoid levels (anandamide and 2-AG) have been demonstrated (Matias *et al.,* 2006a). Similarly elevated levels of anandamide and 2-AG were found to be associated with decreased $CB_1$ receptor expression in adipose tissue from obese postmenopausal women with fasting hyperinsulinaemia (Engeli *et al.,* 2005). The function of $CB_1$ receptors in these patients remains to be determined.

Considering $CB_1$ function still remains in hyperglycaemic conditions, we have investigated, in Chapter 6, the neuroprotective effect of the $CB_1$ agonist, H210, in the cell culture model of diabetic neuropathy, and whether the protection is through $CB_1$-dependent or $CB_1$- independent mechanism. In the present study, we have showed HU210 rescued neurite outgrowth in a concentration-dependent manner, and HU210 at the concentration 0.3-3μM fully restored the neurite outgrowth in hyperglycaemic cells to the degree comparable with the control cells. The rescue by HU210 is inhibited by the $CB_1$ agonist, but not the $CB_2$ agonist, suggesting that HU210 promotion of neurite outgrowth is mediated by the $CB_1$ receptor whilst the subsequent oxidative stress study suggests that the antioxidant effect of HU210 is largely independent of the $CB_1$ receptor. As already discussed in the chapter 6, the mechanism of HU210 regulating neurite outgrowth may involve the $CB_1$ receptor mediated Rap 1 activation via a convergent signal transducer and activator of (stat 3) dependent transcription process (He *et al.,* 2005; Vossler *et al.,* 1997). In addition, the antioxidant property of HU210 also plays an important part in facilitating neurite outgrowth in hyperglycaemic condition. It is well known that

oxidative stress is largely generated under diabetic states and it negatively affects mitochondrial function, endoneurial blood flow and neurotrophic support, all key elements influencing neuron function and survival. In PC12 cells, Rap1-STAT kinase activation is required for NGF signalling (Obara *et al.,* 2004), and it can be disrupted by oxidative stress (Kaur *et al.,* 2005). Therefore, like many other cannabinoids, HU210 acting as an antioxidant displays the neuroprotective property through a fully $CB_1$-independent mechanism (Hampson *et al.,* 1998; Marsicano *et al.,* 2002).

Further work must be conducted to determine the relative importance of $CB_1$ receptor mediated versus receptor-independent neuroprotective actions of natural and synthetic cannabinoids. A potential caveat in using $CB_1$ receptor agonists to prevent neurodegeneration in diabetes comes from a recent report revealing that administration of anandamide causes glucose intolerance in rats (Bermudez-Siva *et al.,* 2006). This appears to result from a reduction of glucose-dependent insulin secretion from the pancreas, which has implications in type 2 diabetes. Conversely, one must also consider the potential adverse effects on the nervous system if obese type 2 diabetics are prescribed the selective $CB_1$ antagonist SR141716 (rimonabant).

This is especially timely given the use of the selective $CB_1$ antagonist SR141716 (rimonabant) in patients with type 2 diabetes (Scheen *et al.,* 2006). Whilst Scheen and co-workers (2006) reported a reduction in bodyweight and improved metabolic risk factors in the treatment group, no data have yet been presented on nerve function in clinical trials of rimonabant. Considering the neuroprotective role cannabinoids play, there is potential for adverse effects on the nervous system in diabetics prescribed $CB_1$ antagonists. Early indications

from animal studies were that rimonabant administration caused hyperalgesia (Richardson *et al.,* 1997). This was attributed to tonic endocannabinoid production and activity on sensory neurons, a concept that has not been upheld (Beaulieu *et al.,* 2000). An alternative explanation is a possible inverse agonist action of SR141716 (Landsman *et al.,* 1997). More recently, researchers have found rimonabant confers analgesic and anti-inflammatory effects in lean and diet-induced obese arthritic female rats (Croci and Zarini, 2007). These apparently conflicting outcomes may be related to the timescale and conditions of the rodents used in the studies: acute versus chronic, healthy animals versus disease models. Clearly, the presence of excessive inflammation is significant, with analgesic actions of rimonabant being observed in models of neurogenic inflammatory pain (Costa *et al.,* 2005; Croci and Zarini, 2007). In their paper, Croci and Zarini (2007) state analgesia may not be due to $CB_1$–blockade per se, but rather a desensitization of TRPV1 receptors, or super-stimulation by endocannabinoids of $CB_2$ receptors which have potent anti-inflammatory actions, and have recently been shown to be present on neurons (Gong *et al.,* 2006) as well as immune cells. However, in 17 conditions such as diabetes, where TRPV1 receptors are up-regulated and sensitized, it is not clear whether anandamide – also being an endovanilloid (Zygmunt *et al.,* 1999) - would merely activate or desensitize the nociceptive pathway. We await the results of further clinical trials of rimonabant with interest.

In conclusion, in this project, we have demonstrated that the expression of $CB_1$ receptors is decreased in hyperglycaemic nerve cells and DRG neurons from diabetic rats. The loss of $CB_1$ receptors may contribute to the development of progression of diabetic neuropathy. However, the function of $CB_1$ receptors is still preserved in nerve cells when stimulated by high concentrations ($\geq 1\mu M$) of

exogenous agonists under conditions mimicking hyperglycaemia. High glucose impaired neurite outgrowth and produced oxidative stress in the cell culture model, which was counteracted by HU210 treatment through $CB_1$-dependent and $CB_1$-independent pathways, respectively. There is currently no single treatment for neuropathy that is effective in all diabetic patients. By virtue of their receptor-dependent and -independent neuroprotective actions, cannabinoids may be appropriate therapeutic agents in preventing the neurodegenerative process in diabetes.

## 7.2 Conclusions

In this thesis, we have investigated the expression of $CB_1$ receptors in an *in vitro* and *in vivo* model of diabetic neuropathy, and also an altered nerve cell response to $CB_1$ agonists resulting from the decreased $CB_1$ expression in hyperglycaemic conditions.

Firstly, we have validated PC12 cells being an *in vitro* cell model of diabetic neuropathy. PC12 cells were stimulated with NGF (50ng/ml) in the presence of increasing concentrations of glucose (5.5,10,20,30,40,50mM) to mimic hyperglycaemic conditions *in vivo*. The optimum length of time, 6 days, was determined by the observation of a maximal neurite outgrowth and difference between high glucose treatments and controls. On day 6 of culture, the result of total neurite length showed that high glucose (20-50mM) significantly attenuated the neurite outgrowth in PC12 cells. This inhibitory effect was due to high glucose as the osmotic control, mannitol (30 and 50mM), showed a similar level of neurite outgrowth to the control (glucose 5.5mM). Furthermore, the impaired neurite outgrowth in the presence of high glucose is associated with increased levels of oxidative stress and a glucose concentration-dependent increase in IL-6 production, thus producing some of the phenomena of diabetic neuropathy.

Secondly, we have examined the expression of $CB_1$ expression in PC12 cells cultured in high glucose. Increasing concentrations of glucose were found to decrease $CB_1$ expression at RNA and protein levels in PC12 cells. This result was corroborated in DRG neurons from diabetic rats, where the number of $CB_1$-positive neurons was decreased to approximately half that of control

animals, and the density of $CB_1$ receptors was reduced by 60% in diabetic versus control DRG.

Thirdly, we investigated whether the decreased expression of $CB_1$ receptors resulted in decreased function. Contrary to our hypothesis, we have found that $CB_1$ function is preserved at some agonist concentrations in PC12 cells cultured in high glucose. The capsaicin response study showed that capsaicin (50-700μM) stimulated a transient $Ca^{2+}$ influx in a concentration-dependent manner with the C50 value of 300μM. The application of capsaicin (300μM) evoked greater $Ca^{2+}$ influx in PC12 cells cultured in high glucose compared to the control and this response was significantly blocked by capsazepine (100μM) in both normal and high glucose conditions, confirming the response is mediated by TRPV1 receptors. The HU210 concentration-dependent (0.03, 0.3, 3, 30μM) inhibitory studies showed that the inhibition (%) curve generated from high glucose conditions shifted to the right compared with the control inhibition curve, indicating high glucose may slightly decrease $CB_1$ function. At higher concentration of 30μM, HU210 significantly inhibited capsaicin-evoked calcium entry by 80% and 77% in control and high glucose respectively. The lower HU210 (1μM) concentration showed a similar inhibitory effect by 43% and 40% correspondingly. The use of the $CB_1$ antagonist, AM251, and the $CB_2$ antagonist, AM630, strongly suggest that the inhibitory effect of TRPV1-mediated calcium entry is mediated by $CB_1$, not $CB_2$ receptors.

Finally, we have demonstrated that the $CB_1$ agonist, HU210 has neuroprotective effect in hyperglycaemic cells. The cell viability assay revealed that, on the day 6 of culture, apart from HU210 at 30μM where cells showed a significant death, the cell viability was not different in cells among other

concentrations (0.03μM-3μM) in both normal and high glucose conditions compared to controls. HU210 was found to rescue neurite outgrowth in PC12 cells cultured in 50mM glucose in a concentration-dependent manner (0.03μM-3μM) while there was no effect in the cells cultured in 5.5mM glucose. The $CB_1$ antagonist (AM251 1μM), but not the $CB_2$ antagonist (AM630 1μM), significantly attenuated the HU210 (0.3μM) mediated-neurite rescue, indicating a $CB_1$-mediated neuroprotective mechanism. In addition, HU210 at 0.03 and 0.3μM reduced the levels of oxidative stress in hyperglycaemic cells, which was not reversed by AM251. These results suggest that HU210 rescue neurite outgrowth via $CB_1$-dependent and $CB_1$-independent mechanisms.

In conclusion, we have demonstrated that despite a decrease in receptor expression, the function of the $CB_1$ receptor is preserved in nerve cells when stimulated by an exogenous agonist under conditions mimicking hyperglycaemia. High glucose impaired neurite outgrowth and enhanced oxidative stress was counteracted by HU210 treatment through $CB_1$-dependent and -independent pathways, respectively. Diabetic neuropathy affects at least 50% of diabetic patients and occurs with the same frequency in type 1 and type 2 diabetes; this number approaches 100% if subclinical non-symptomatic neuropathy is included (Vinik *et al.,* 2006). There is currently no single treatment for neuropathy that is effective in all diabetic patients. By virtue of their receptor-dependent and -independent neuroprotective actions, cannabinoids may be appropriate therapeutic agents in preventing the neurodegenerative process in diabetes.

## 7.3 Future studies

In the future, whether the $CB_1$ function is still preserved in hyperglycaemic conditions will be investigated in DRG neurons from diabetic rats using patch clamp technique. The example traces are showed in Figure 7.3. The capsaicin-evoked increased action potential from DRG neurons can be similarly conducted as displayed in Figure 7.3. The co-application of $CB_1$ agonists and antagonists with capsaicin will provide a clear answer whether the activation of $CB_1$ receptors can attenuate capsaicin-mediated response in hyperglycaemic neurons compared to controls.

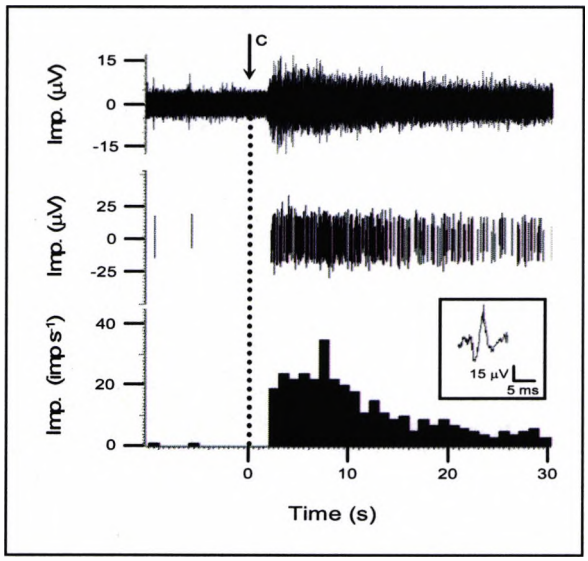


**Figure 7.3** Representative traces showing the increase in sensory discharge from perivascular nerves in response to capsaicin (c; 0.3 nmoles i.a.) in an anaesthetised rat. Top and middle traces = recorded action potentials (microvolts), unfiltered and filtered, respectively, and bottom trace = pooled discharge of individual action potentials recorded from the surface of the femoral artery (imp s-1). Inset = individual unit. (From supervisor: Dr Paula Smith, adapted from Smith & McQueen, 2001)

The level of endogenous cannabinoids can be measured in diabetic rats. If endogenous cannabinoids increase in response to hyperglycaemia, it may explain why the $CB_1$ function is still preserved whilst the expression is reduced.

Finally, the neuroprotective role of $CB_1$ agonists (HU210) can be studied in *ex in vivo* model, DRG neurons from diabetic rats. Also, the level of $CB_1$ receptors could be investigated after the treatment of $CB_1$ agonists. As the $CB_1$ receptor is a G protein-coupled receptor, an application of a $G_{i/o}$ protein inhibitor, or kinase pathway inhibitors, may be used to study the mechanism involved in the 'neurite rescue' by $CB_1$ agonists.

## REFERENCES


AHLGREN, S. C. & LEVINE, J. D. (1994) Protein kinase C inhibitors decrease hyperalgesia and C-fiber hyperexcitability in the streptozotocin-diabetic rat. *J Neurophysiol,* 72, 684-692.

AHLUWALIA, J., URBAN, L., BEVAN, S., CAPOGNA, M. & NAGY, I. (2002) Cannabinoid 1 receptors are expressed by nerve growth factor- and glial cell-derived neurotrophic factor-responsive primary sensory neurones. *Neuroscience,* 110, 747-753.

AHLUWALIA, J., URBAN, L., BEVAN, S. & NAGY, I. (2003) Anandamide regulates neuropeptide release from capsaicin-sensitive primary sensory neurons by activating both the cannabinoid 1 receptor and the vanilloid receptor 1 in vitro. *European Journal of Neuroscience,* 17, 2611-2618.

AHLUWALIA, J., URBAN, L., CAPOGNA, M., BEVAN, S. & NAGY, I. (2000) Cannabinoid 1 receptors are expressed in nociceptive primary sensory neurons. *Neuroscience,* 100, 685-688.

AKERBOOM, T. P. M. & SIES, H. (1981) Assay of glutathione, glutathione disulfide and glutathione mixed disulphides in biological samples. *Methods Enzymol*, 77, 373–382.

ALDRICH, M. (1997) History of therapeutic cannabis In: Mathre ML, (ed.). *Cannabis in medical practice: a legal, historical and pharmacological overview of the therapeutic use of marijuana.* Jefferson, North Carolina, US and London McFarland pp. 33-35.

ALONZI, T., MIDDLETON, G., WYATT, S., BUCHMAN, V., A. K. BETZ, U., MULLER, W., MUSIANI, P., POLI, V. & DAVIES, A. M. (2001) Role of STAT3 and PI 3-kinase/Akt in mediating the survival actions of cytokines on sensory neurons. *Molecular and Cellular Neuroscience,* 18, 270-282.

AMOS, A. F., MCCARTY, D. J. & ZIMMET, P. (1997) The rising global burden of diabetes and its complications: estimates and projections to the year 2010. *Diabet Med,* 14 Suppl 5, S1-S85.

ANDERSSON, U., LEIGHTON, B., YOUNG, M., BLOMSTRAND, E. & NEWSHOLME, E. (1998) Inactivation of aconitase and oxoglutarate dehydrogenase in skeletal muscle in vitro by superoxide anions and/or nitric oxide. *Biochem Biophys Res Commun* 249, 512-516.

ANDRIAMBELOSON, E., BAILLET, C., VITTE, P.-A., GAROTTA, G., DREANO, M. & CALLIZOT, N. (2006) Interleukin-6 attenuates the development of experimental diabetes-related neuropathy. *Neuropathology,* 26, 32-42.

ANNUNZIATO, L., AMOROSO, S., PANNACCIONE, A., CATALDI, M., PIGNATARO, G., D'ALESSIO, A., SIRABELLA, R., SECONDO, A., SIBAUD, L. & DI RENZO, G. F. (2003) Apoptosis induced in neuronal cells by oxidative stress: role played by caspases and intracellular calcium ions. *Toxicology Letters,* 139, 125-133.

ATKIN, S. L., MASSON, E. A. & WILCOX, D. (1996) An in vitro model of diabetes. *In Vitro Cell Dev Biol Anim,* 32, 379-381.

AVERILL, S., MCMAHON, S. B., CLARY, D. O., REICHARDT, L. F. & PRIESTLEY, J. V. (1995) Immunocytochemical localization of trkA receptors in chemically identified subgroups of adult rat sensory neurons. *Eur J Neurosci,* 7, 1484-1494.

AZAD, S. C., MARSICANO, G., EBERLEIN, I., PUTZKE, J., ZIEGLGANSBERGER, W., SPANAGEL, R. & LUTZ, B. (2001) Differential role of the nitric oxide pathway on delta(9)-THC-induced central nervous system effects in the mouse. *Eur J Neurosci,* 13, 561-568.

BAHR B.A., KARANIAN D.A., MAKANJI S.S. & MAKRIYANNIS A. (2006) Targeting the endocannabinoid system in treating brain disorders. *Expert Opin Investig Drugs* 15,351-365.

BARBER, A. J., LIETH, E., KHIN, S. A., ANTONETTI, D. A., BUCHANAN, A. G. & GARDNER, T. W. (1998) Neural apoptosis in the retina during experimental and human diabetes. Early onset and effect of insulin. *J Clin Invest,* 102, 783-791.

BASAVARAJAPPA, B. S., COOPER, T. B. & HUNGUND, B. L. (1998) Chronic ethanol administration down-regulates cannabinoid receptors in mouse brain synaptic plasma membrane. *Brain Res,* 793, 212-218.

BAUMGARTNER-PARZER, S. M., WAGNER, L., PETTERMANN, M., GRILLARI, J., GESSL, A. & WALDHAUSL, W. (1995) High-glucose--triggered apoptosis in cultured endothelial cells. *Diabetes,* 44, 1323-1327.

BEAULIEU, P., BISOGNO, T., PUNWAR, S., FARQUHAR-SMITH, W. P., AMBROSINO, G., DI MARZO, V. & RICE, A. S. C. (2000) Role of the endogenous cannabinoid system in the formalin test of persistent pain in the rat. *European Journal of Pharmacology,* 396, 85-92.

BELTRAMO, M., BERNARDINI, N., BERTORELLI, R., CAMPANELLA, M., NICOLUSSI, E., FREDDUZZI, S. & REGGIANI, A. (2006) $CB_2$ receptor-mediated antihyperalgesia: possible direct involvement of neural mechanisms. *European Journal of Neuroscience,* 23, 1530-1538.

BERMUDEZ-SIVA F.J., SERRANO A., DIAZ-MOLINA F.J., SANCHEZ VERA I., JUAN-PICO P., NADAL A., FUENTES E. AND RODRIGUEZ DE FONSECA, F. (2006) Activation of cannabinoid $CB_1$ receptors induces glucose intolerance in rats. *Eur J Pharmacol* 531:282-284.

BIERHAUS, A., HASLBECK, K.-M., HUMPERT, P. M., LILIENSIEK, B., DEHMER, T., MORCOS, M., SAYED, A. A. R., ANDRASSY, M., SCHIEKOFER, S., SCHNEIDER, J. G., SCHULZ, J. B., HEUSS, D., NEUNDORFER, B., DIERL, S., HUBER, J., TRITSCHLER, H., SCHMIDT, A.-M., SCHWANINGER, M., HAERING, H.-U., SCHLEICHER, E., KASPER, M., STERN, D. M., ARNOLD, B. & NAWROTH, P. P. (2004) Loss of pain perception in diabetes is dependent on a receptor of the immunoglobulin superfamily. *J. Clin. Invest.,* 114, 1741-1751.

BIERHAUS, A., HUMPERT, P. M., MORCOS, M., WENDT, T., CHAVAKIS, T., ARNOLD, B., STERN, D. M. & NAWROTH, P. P. (2005) Understanding RAGE, the receptor for advanced glycation end products. *J Mol Med,* 83, 876-886.

BISOGNO, T., KATAYAMA, K., MELCK, D., UEDA, N., DE PETROCELLIS, L., YAMAMOTO, S. & DI MARZO, V. (1998) Biosynthesis and degradation of bioactive fatty acid amides in human breast cancer and rat pheochromocytoma cells. Implications for cell proliferation and differentiation. *European Journal of Biochemistry,* 254, 634-642.

BISOGNO, T., MELCK, D., BOBROV, M., GRETSKAYA, N. M., BEZUGLOV, V. V., DE PETROCELLIS, L. & DI MARZO, V. (2000) N-acyl-dopamines: novel synthetic CB(1) cannabinoid-receptor ligands and inhibitors of anandamide inactivation with cannabimimetic activity in vitro and in vivo. *Biochem J,* 351 Pt 3, 817-824.

BOLEN, S., FELDMAN, L., VASSY, J., WILSON, L., YEH, H. C., MARINOPOULOS, S., WILEY, C., SELVIN, E., WILSON, R., BASS, E. B. & BRANCATI, F. L. (2007) Systematic review: comparative effectiveness and safety of oral medications for type 2 diabetes mellitus. *Ann Intern Med,* 147, 386-399.

BRIDGES, D., RICE, A. S. C., EGERTOVA, M., ELPHICK, M. R., WINTER, J. & MICHAEL, G. J. (2003) Localisation of cannabinoid receptor 1 in rat dorsal root ganglion using in situ hybridisation and immunohistochemistry. *Neuroscience,* 119, 803-812.

BRIDGES, R. J., KOH, J.-Y., HATALSKI, C. G. & COTMAN, C. W. (1991) Increased excitotoxic vulnerability of cortical cultures with reduced levels of glutathione. *European Journal of Pharmacology,* 192, 199-200.

BRILL, H. & NAHAS, G. (1984) Cannabis intoxication and mental illness. In: Nahas GG, (ed). *Marihuana in science and medicine.* . New York, Raven Press, p. 263-306.

BRONANDER, K. A. & BLOCH, M. J. (2007) Potential role of the endocannabinoid receptor antagonist rimonabant in the management of cardiometabolic risk: a narrative review of available data. *Vasc Health Risk Manag,* 3, 181-190.

BROWN, G. & BORUTAITE, V. (1999) Nitric oxide, cytochrome c and mitochondria. . *Biochem Soc Symp,* 66, 17-25.

BROWNLEE, M. (2001) Biochemistry and molecular cell biology of diabetic complications. *Nature,* 414, 813-820.

BUCK, S. H. & BURKS, T. F. (1986) The neuropharmacology of capsaicin: review of some recent observations. *Pharmacol Rev,* 38, 179-226.

BURNS, T. L. & INECK, J. R. (2006) Cannabinoid analgesia as a potential new therapeutic option in the treatment of chronic pain. *Ann Pharmacother,* 40, 251-260.

CALCUTT, N. A. (2004) Experimental models of painful diabetic neuropathy. *Journal of the Neurological Sciences,* 220, 137-139.

CALIGNANO, A., LA RANA, G., GIUFFRIDA, A. & PIOMELLI, D. (1998) Control of pain initiation by endogenous cannabinoids. *Nature,* 394, 277-281.

CAMPBELL, I. L., ABRAHAM, C. R., MASLIAH, E., KEMPER, P., INGLIS, J. D., OLDSTONE, M. B. A. & MUCKE, L. (1993) Neurologic disease induced in transgenic mice by cerebral overexpression of interleukin 6. *Proceedings of the National Academy of Sciences,* 90, 10061-10065.

CAMERON, N. E., COTTER, M. A. & MAXFIELD, E. K. (1993) Anti-oxidant treatment prevents the development of peripheral nerve dysfunction in streptozotocin-diabetic rats. *Diabetologia,* 36, 299-304.

CAMERON, N. E. & COTTER, M. A. (2007) The neurocytokine, interleukin-6, corrects nerve dysfunction in experimental diabetes. *Experimental Neurology,* 207, 23-29.

CAMERON, N. E., EATON, S. E., COTTER, M. A. & TESFAYE, S. (2001) Vascular factors and metabolic interactions in the pathogenesis of diabetic neuropathy. *Diabetologia,* 44, 1973-1988.

CATERINA, M. J., SCHUMACHER, M. A., TOMINAGA, M., ROSEN, T. A., LEVINE, J. D. & JULIUS, D. (1997) The capsaicin receptor: a heat-activated ion channel in the pain pathway. *Nature,* 389, 816-824.

CANTONI, O., SESTILI, P., CATTABENI, F., BELLOMO, G., POU, S., COHEN, M. & CERUTTI, P. (1989) Calcium chelator Quin 2 prevents hydrogen-peroxide-induced DNA breakage and cytotoxicity. *Eur J Biochem,* 182, 209-212.

CHAN, G. C., HINDS, T. R., IMPEY, S. & STORM, D. R. (1998) Hippocampal neurotoxicity of Delta9-tetrahydrocannabinol. *J Neurosci,* 18, 5322-5332.

CHAN, S.L. & MATTSON, M.P. (1999) Caspase and calpain substrates: roles in synaptic plasticity and cell death. *J Neurosci Res,* 58, 167-190.

CHARD, P. S., BLEAKMAN, D., SAVIDGE, J. R. & MILLER, R. J. (1995) Capsaicin-induced neurotoxicity in cultured dorsal root ganglion neurons: Involvement of calcium-activated proteases. *Neuroscience,* 65, 1099-1108.

CHEN, Y. & BUCK, J. (2000) Cannabinoids protect cells from oxidative cell death: a receptor-independent mechanism. *J Pharmacol Exp Ther,* 293, 807-812.

COLE, B. E. (2007) Diabetic peripheral neuropathic pain: recognition and management. *Pain Med,* 8 Suppl 2, S27-S32.

CONN, K., ULLMAN, M., EISENHAUER, P., FINE, R. & WELLS, J. (2001) Decreased expression of the NADH:ubiquinone oxidoreductase (complex I) subunit 4 in 1-methyl-4-phenylpyridinium-treated human neuroblastoma SH-SY5Y cells. *Neurosci Lett,* 306, 145-148.

COSTA, B., TROVATO, A. E., COLLEONI, M., GIAGNONI, G., ZARINI, E. & CROCI, T. (2005) Effect of the cannabinoid $CB_1$ receptor antagonist, SR141716, on nociceptive response and nerve demyelination in rodents with chronic constriction injury of the sciatic nerve. *Pain,* 116, 52-61.

CROCI, T. & ZARINI, E. (2007) Effect of the cannabinoid $CB_1$ receptor antagonist rimonabant on nociceptive responses and adjuvant-induced arthritis in obese and lean rats. *Br J Pharmacol,* 150, 559-566.

DAI, Y., IWATA, K., FUKUOKA, T., KONDO, E., TOKUNAGA, A., YAMANAKA, H., TACHIBANA, T., LIU, Y. & NOGUCHI, K. (2002) Phosphorylation of extracellular signal-regulated kinase in primary afferent neurons by noxious stimuli and its involvement in peripheral sensitization. *J. Neurosci.,* 22, 7737-7745.

DAGON, Y., AVRAHAM, Y., LINK, G., ZOLOTAREV, O., MECHOULAM, R. & BERRY, E. M. (2007) The synthetic cannabinoid HU-210 attenuates neural damage in diabetic mice and hyperglycemic pheochromocytoma PC12 cells. *Neurobiology of Disease,* 27, 174-181

DAJANI, E. Z., LARSEN, K. R., TAYLOR, J., DAJANI, N. E., SHAHWAN, T. G., NEELEMAN, S. D., TAYLOR, M. S., DAYTON, M. T. & MIR, G. N. (1999) 1',1'-Dimethylheptyl-delta-8-tetrahydrocannabinol-11-oic acid: a novel, orally effective cannabinoid with analgesic and anti-inflammatory properties. *J Pharmacol Exp Ther,* 291, 31-38.

DAS, K. P., FREUDENRICH, T. M. & MUNDY, W. R. (2004) Assessment of PC12 cell differentiation and neurite growth: a comparison of morphological and neurochemical measures. *Neurotoxicology and Teratology,* 26, 397-406.

DAVE, G. S. & KALIA, K. (2007) Hyperglycemia induced oxidative stress in type-1 and type-2 diabetic patients with and without nephropathy. *Cell Mol Biol (Noisy-le-grand),* 53, 68-78.

DE LA MONTE, S., GANJU, N., FEROZ, N., LUONG, T., BANERJEE, K., CANNON, J. & WANDS, J. (2000) Oxygen free radical injury is sufficient to

cause some Alzheimer-type molecular abnormalities in human CNS neuronal cells. *J Alzheimers Dis,* 2, 261–281.

DEDOV, V. N. & ROUFOGALIS, B. D. (1998) Rat dorsal root ganglion neurones express different capsaicin-evoked $Ca^{2+}$ transients and permeabilities to $Mn^{2+}$. *Neuroscience Letters,* 248, 151-154.

DERKINDEREN, P., VALJENT, E., TOUTANT, M., CORVOL, J. C., ENSLEN, H., LEDENT, C., TRZASKOS, J., CABOCHE, J. & GIRAULT, J. A. (2003) Regulation of extracellular signal-regulated kinase by cannabinoids in hippocampus. *J Neurosci,* 23, 2371-2782.

DENOVAN-WRIGHT, E. M. & ROBERTSON, H. A. (2000) Cannabinoid receptor messenger RNA levels decrease in a subset of neurons of the lateral striatum, cortex and hippocampus of transgenic Huntington's disease mice. *Neuroscience,* 98, 705-713.

DEVARAJ, S., VENUGOPAL, S. K., SINGH, U. & JIALAL, I. (2005) Hyperglycemia induces monocytic release of interleukin-6 via induction of protein kinase c-α and β. *Diabetes,* 54, 85-91.

DEVANE, W. A., DYSARZ, F. A. D., JOHNSON, M. R., MELVIN, L. S. & HOWLETT, A. C. (1988) Determination and characterization of a cannabinoid receptor in rat brain. *Mol Pharmacol,* 34, 605-613.

DEVANE, W. A., HANUS, L., BREUER, A., PERTWEE, R. G., STEVENSON, L. A., GRIFFIN, G., GIBSON, D., MANDELBAUM, A., ETINGER, A. & MECHOULAM, R. (1992) Isolation and structure of a brain constituent that binds to the cannabinoid receptor. *Science,* 258, 1946-1949.

DIAZ-LAVIADA, I. & RUIZ-LLORENTE, L. (2005) Signal transduction activated by cannabinoid receptors. *Mini Reviews in Medicinal Chemistry,* 5, 619-630.

DI WU, Q., WANG, J. H., FENNESSY, F., REDMOND, H. P. & BOUCHIER-HAYES, D. (1999) Taurine prevents high-glucose-induced human vascular endothelial cell apoptosis. *Am J Physiol Cell Physiol,* 277, C1229-C1238.

DOGRUL, A., GUL, H., AKAR, A., YILDIZ, O., BILGIN, F. & GUZELDEMIR, E. (2003) Topical cannabinoid antinociception: synergy with spinal sites. *Pain,* 105, 11-16.

DOGRUL, A., GUL, H., YILDIZ, O., BILGIN, F. & GUZELDEMIR, M. E. (2004) Cannabinoids blocks tactile allodynia in diabetic mice without attenuation of its antinociceptive effect. *Neuroscience Letters,* 368, 82-86.

DOMENICI, M. R., AZAD, S. C., MARSICANO, G., SCHIERLOH, A., WOTJAK, C. T., DODT, H.-U., ZIEGLGANSBERGER, W., LUTZ, B. & RAMMES, G. (2006) Cannabinoid receptor type 1 located on presynaptic terminals of principal neurons in the forebrain controls glutamatergic synaptic transmission. *J. Neurosci.,* 26, 5794-5799.

DOYLE, J. W., SMITH, R. M. & ROTH, T. P. (1997) The effect of hyperglycemia and insulin on the replication of cultured human microvascular endothelial cells. *Horm Metab Res,* 29, 43-45.

DRAY, A., BETTANEY, J. & FORSTER, P. (1989) Capsaicin desensitization of peripheral nociceptive fibres does not impair sensitivity to other noxious stimuli. *Neuroscience Letters,* 99, 50-54.

DUARTE, J. M. N., NOGUEIRA, C., MACKIE, K., OLIVEIRA, C. R., CUNHA, R. A. & KOFALVI, A. (2007) Increase of cannabinoid $CB_1$ receptor density in the hippocampus of streptozotocin-induced diabetic rats. *Experimental Neurology,* 204, 479-484.

DUBY, J. J., CAMPBELL, R. K., SETTER, S. M., WHITE, J. R. & RASMUSSEN, K. A. (2004) Diabetic neuropathy: an intensive review. *Am J Health Syst Pharm,* 61, 160-173.

DU TOIT, B. (1980) Cannabis in Africa. A survey of its distribution in Africa, and a study of cannabis use and users in multi-ethnic South Africa. Rotterdam: A. A. Balkema.

DVORAK, M., WATKINSON, A., MCGLONE, F. & RUKWIED, R. (2003) Histamine induced responses are attenuated by a cannabinoid receptor agonist in human skin. *Inflamm Res,* 52, 238-245.

DYCK, P.J., LAIS, A., KARNES, J.L., O'BRIEN, P., RIZZA, R. (1986) Fiber loss is primary and multifocal in sural nerves in diabetic polyneuropathy. *Annals of Neurology,* 19, 425-439.

DYSON, A., PEACOCK, M., CHEN, A., COURADE, J. P., YAQOOB, M., GROARKE, A., BRAIN, C., LOONG, Y. & FOX, A. (2005) Antihyperalgesic properties of the cannabinoid CT-3 in chronic neuropathic and inflammatory pain states in the rat. *Pain,* 116, 129-137.

EGERTOVA, M. & ELPHICK, M. R. (2000) Localisation of cannabinoid receptors in the rat brain using antibodies to the intracellular C-terminal tail of CB. *J Comp Neurol,* 422, 159-171.

ELLINGTON, H. C., COTTER, M. A., CAMERON, N. E. & ROSS, R. A. (2002) The effect of cannabinoids on capsaicin-evoked calcitonin gene-related peptide (CGRP) release from the isolated paw skin of diabetic and non-diabetic rats. *Neuropharmacology,* 42, 966-975.

ELLIS, J. L. & UNDEM, B. J. (1994) Inhibition by capsazepine of resiniferatoxin- and capsaicin-induced contractions of guinea pig trachea. *J Pharmacol Exp Ther,* 268, 85-89.

ENGELI, S., BOHNKE, J., FELDPAUSCH, M., GORZELNIAK, K., JANKE, J., BATKAI, S., PACHER, P., HARVEY-WHITE, J., LUFT, F. C., SHARMA, A. M. & JORDAN, J. (2005) Activation of the peripheral endocannabinoid system in human Obesity. *Diabetes,* 54, 2838-2843.

FANKHAUSER, M. (2002) History of cannabis in Western Medicine. In: Grotenhermen F, Russo E, (ed). *Cannabis and Cannabinoids.* New York, The Haworth Integrative Healing Press; Chapter 4. p. 37-51.

FARQUHAR-SMITH, W. P., EGERTOVA, M., BRADBURY, E. J., MCMAHON, S. B., RICE, A. S. & ELPHICK, M. R. (2000) Cannabinoid CB(1) receptor expression in rat spinal cord. *Mol Cell Neurosci,* 15, 510-521.

FELDMAN, E. L. (2003) Oxidative stress and diabetic neuropathy: a new understanding of an old problem. *J Clin Invest,* 111, 431-433.

FELDMAN, S. & QUENZER, F. (1984) *Fundamentals of neuropsychopharmacology,* Sunderland, Sinauer Associates press, Chapter 6.

FERGUSON, S. S. G. (2001) Evolving concepts in G protein-coupled receptor endocytosis: the role in receptor desensitization and signalling. *Pharmacol Rev,* 53, 1-24.

FILIP, M., GOLDA, A., ZANIEWSKA, M., MCCREARY, A. C., NOWAK, E., KOLASIEWICZ, W. & PRZEGALINSKI, E. (2006) Involvement of cannabinoid $CB_1$ receptors in drug addiction: effects of rimonabant on behavioral responses induced by cocaine. *Pharmacol Rep,* 58, 806-819.

FISCHBACH, T., GREFFRATH, W., NAWRATH, H. & TREEDE, R.-D. (2007) Effects of anandamide and noxious heat on intracellular calcium concentration in nociceptive DRG neurons of rats. *J Neurophysiol,* 98, 929-938.

FOX, A., KESINGLAND, A., GENTRY, C., MCNAIR, K., PATEL, S., URBAN, L. & JAMES, I. (2001) The role of central and peripheral Cannabinoid1 receptors in the antihyperalgesic activity of cannabinoids in a model of neuropathic pain. *Pain,* 92, 91-100.

GADIENT, R. A. & OTTEN, U. (1996) Postnatal expression of interleukin-6 (IL-6) and IL-6 receptor (IL-6R) mRNAs in rat sympathetic and sensory ganglia. *Brain Research,* 724, 41-46.

GAONI, Y. & MECHOULAM, R. (1964) Isolation structure and partial synthesis of an active constituent of hashish. *J Am Chem Soc.,* 86, 1646-1647.

GARCIA, D. E., BROWN, S., HILLE, B. & MACKIE, K. (1998) Protein kinase C disrupts cannabinoid actions by phosphorylation of the $CB_1$ cannabinoid receptor. *J. Neurosci.,* 18, 2834-2841.

GILLESPIE, K. M. (2006) Type 1 diabetes: pathogenesis and prevention. *CMAJ,* 175, 165-170.

GIULIETTI, A., VAN ETTEN, E., OVERBERGH, L., STOFFELS, K., BOUILLON, R. & MATHIEU, C. (2007) Monocytes from type 2 diabetic patients have a pro-inflammatory profile: 1,25-Dihydroxyvitamin D3 works as anti-inflammatory. *Diabetes Research and Clinical Practice,* 77, 47-57.

GLASS, M., DRAGUNOW, M. & FAULL, R. L. M. (2000) The pattern of neurodegeneration in Huntington's disease: a comparative study of cannabinoid, dopamine, adenosine and GABAA receptor alterations in the human basal ganglia in Huntington's disease. *Neuroscience,* 97, 505-519.

GLASS, M., FAULL, R. L. M. & DRAGUNOW, M. (1993) Loss of cannabinoid receptors in the substantia nigra in huntington's disease. *Neuroscience,* 56, 523-527.

GLASS, M., VAN DELLEN, A., BLAKEMORE, C., HANNAN, A. J. & FAULL, R. L. M. (2004) Delayed onset of huntington's disease in mice in an enriched environment correlates with delayed loss of cannabinoid $CB_1$ receptors. *Neuroscience,* 123, 207-212.

GONG, J.-P., ONAIVI, E. S., ISHIGURO, H., LIU, Q.-R., TAGLIAFERRO, P. A., BRUSCO, A. & UHL, G. R. (2006) Cannabinoid $CB_2$ receptors: Immunohistochemical localization in rat brain. *Brain Research,* 1071, 10-23.

GRAHAM, E. S., BALL, N., SCOTTER, E. L., NARAYAN, P., DRAGUNOW, M. & GLASS, M. (2006) Induction of Krox-24 by endogenous cannabinoid type 1 receptors in Neuro2A cells is mediated by the MEK-ERK MAPK pathway and is suppressed by the phosphatidylinositol 3-kinase pathway. *J Biol Chem,* 281, 29085-29095.

GREENE, L. A. & TISCHLER, A. S. (1976) Establishment of a noradrenergic clonal line of rat adrenal pheochromocytoma cells which respond to nerve growth factor. *Cell Biology,* 73, 2424-2428.

GRIFFIN, G., TAO, Q. & ABOOD, M. E. (2000) Cloning and pharmacological characterization of the rat CB(2) cannabinoid receptor. *J Pharmacol Exp Ther,* 292, 886-894.

GRUOL, D. L. & NELSON, T. E. (1997) Physiological and pathological roles of interleukin-6 in the central nervous system. *Mol Neurobiol,* 15, 307-339.

GUMIENICZEK, A., HOPKA, LSTROK, A, H., ROLI, NACUTE, SKI, J. & BOJARSKA-JUNAK, A. (2006) Interleukin-6 and oxidative stress in plasma of alloxan-induced diabetic rabbits after pioglitazone treatment. *Immunopharmacology and Immunotoxicology,* 28, 81-91.

GUSTAFSSON, K., CHRISTENSSON, B., SANDER, B. & FLYGARE, J. (2006) Cannabinoid receptor-mediated apoptosis induced by R(+)-methanandamide and Win55,212-2 is associated with ceramide accumulation and p38 activation in mantle cell lymphoma. *Mol Pharmacol,* 70, 1612-1620.

GUZMAN, M. (2003) Neurons on cannabinoids: dead or alive? *Br J Pharmacol,* 140, 439-440.

HAJOS, N., KATONA, I., NAIEM, S. S., MACKIE, K., LEDENT, C., MODY, I. & FREUND, T. F. (2000) Cannabinoids inhibit hippocampal GABAergic transmission and network oscillations. *European Journal of Neuroscience,* 12, 3239-3249.

HAKAK, Y., WALKER, J. R., LI, C., WONG, W. H., DAVIS, K. L., BUXBAUM, J. D., HAROUTUNIAN, V. & FIENBERG, A. A. (2001) Genome-wide expression analysis reveals dysregulation of myelination-related genes in chronic schizophrenia. *Proc Natl Acad Sci U S A,* 98, 4746-4751.

HAMANN, W. & DI VADI, P. P. (1999) Analgesic effect of the cannabinoid analogue nabilone is not mediated by opioid receptors. *Lancet,* 353, 560.

HAMPSON, A. J., GRIMALDI, M., AXELROD, J. & WINK, D. (1998) Cannabidiol and (-) Delta 9-tetrahydrocannabinol are neuroprotective antioxidants. *PNAS,* 95, 8268-8273.

HART, S., FISCHER, O. M. & ULLRICH, A. (2004) Cannabinoids induce cancer cell proliferation via tumor necrosis factor alpha-converting enzyme (TACE/ADAM17)-mediated transactivation of the epidermal growth factor receptor. *Cancer Res,* 64, 1943-1950.

HAYES, J. D. & MCLELLAN, L. I. (1999) Glutathione and glutathione-dependent enzymes represent a co-ordinately regulated defence against oxidative stress. *Free Radic Res,* 31, 273-300.

HE, J. C., GOMES, I., NGUYEN, T., JAYARAM, G., RAM, P. T., DEVI, L. A. & IYENGAR, R. (2005) The Gα(o/i)-coupled cannabinoid receptor-mediated neurite outgrowth involves Rap regulation of Src and Stat3. *J. Biol. Chem.,* 280, 33426-33434.

HEINRICH, P. C., BEHRMANN, I., HAAN, S., HERMANNS, H. M., MULLER-NEWEN, G. & SCHAPER, F. (2003) Principles of interleukin (IL)-6-type cytokine signalling and its regulation. *Biochem. J.,* 374, 1-20.

HERKENHAM, M., LYNN, A. B., JOHNSON, M. R., MELVIN, L. S., DE COSTA, B. R. & RICE, K. C. (1991) Characterization and localization of cannabinoid receptors in rat brain: a quantitative in vitro autoradiographic study. *J Neurosci,* 11, 563-583.

HERKENHAM, M., LYNN, A. B., LITTLE, M. D., JOHNSON, M. R., MELVIN, L. S., DE COSTA, B. R. & RICE, K. C. (1990) Cannabinoid receptor localization in brain. *Proc Natl Acad Sci U S A,* 87, 1932-1936.

HERMANN, H., MARSICANO, G. & LUTZ, B. (2002) Coexpression of the cannabinoid receptor type 1 with dopamine and serotonin receptors in distinct neuronal subpopulations of the adult mouse forebrain. *Neuroscience,* 109, 451-460.

HERZBERG, U., ELIAV, E., BENNETT, G. J. & KOPIN, I. J. (1997) The analgesic effects of R(+)-WIN 55,212-2 mesylate, a high affinity cannabinoid agonist, in a rat model of neuropathic pain. *Neuroscience Letters,* 221, 157-160.

HISSIN, P. J. & HILF, R. (1976) A fluorometric method for determination of oxidized and reduced glutathione in tissues. *Analytical Biochemistry,* 74, 214-226.

HOHMANN, A. G. & HERKENHAM, M. (1998) Localization of central cannabinoid $CB_1$ receptor messenger RNA in neuronal subpopulations of rat dorsal root ganglia: a double-label in situ hybridization study. *Neuroscience,* 90, 923-931.

HOHMANN, A. G. & HERKENHAM, M. (1999) Cannabinoid receptors undergo axonal flow in sensory nerves. *Neuroscience,* 92, 1171-1175.

HOLZER, P. (1991) Capsaicin: cellular targets, mechanisms of action, and selectivity for thin sensory neurons. *Pharmacol Rev,* 43, 143-201.

HONG, S. & WILEY, J. W. (2005) Early painful diabetic neuropathy is associated with differential changes in the expression and function of vanilloid receptor 1. *J. Biol. Chem.,* 280, 618-627.

HUSSAIN, M. J., PEAKMAN, M., GALLATI, H., LO, S. S., HAWA, M., VIBERTI, G. C., WATKINS, P. J., LESLIE, R. D. & VERGANI, D. (1996) Elevated serum levels of macrophage-derived cytokines precede and accompany the onset of IDDM. *Diabetologia,* 39, 60-69.

IKEDA, H., TOKITA, Y. & SUDA, H. (1997) Capsaicin-sensitive A delta fibers in cat tooth pulp. *J Dent Res,* 76, 1341-1349.

IZZO, A. A., FEZZA, F., CAPASSO, R., BISOGNO, T., PINTO, L., IUVONE, T., ESPOSITO, G., MASCOLO, N., DI MARZO, V. & CAPASSO, F. (2001) Cannabinoid $CB_1$-receptor mediated regulation of gastrointestinal motility in mice in a model of intestinal inflammation. *Br J Pharmacol,* 134, 563-570.

JAIN, S. K., KANNAN, K., LIM, G., MATTHEWS-GREER, J., MCVIE, R. & BOCCHINI, J. A., JR. (2003) Elevated blood interleukin-6 levels in hyperketonemic type 1 diabetic patients and secretion by acetoacetate-treated cultured U937 monocytes. *Diabetes Care,* 26, 2139-2143.

JAKOBSEN, J. & SIDENIUS, P. (1980) Decreased axonal transport of structural proteins in streptozotocin diabetic rats. *J Clin Invest,* 66, 292-297.

JEFFCOATE, W. J. & HARDING, K. G. (2003) Diabetic foot ulcers. *The Lancet,* 361, 1545-1551.

JIN, K. L., MAO, X. O., GOLDSMITH, P. C. & GREENBERG, D. A. (2000) $CB_1$ cannabinoid receptor induction in experimental stroke. *Ann Neurol,* 48, 257-261.

JORDAN, J. D., HE, J. C., EUNGDAMRONG, N. J., GOMES, I., ALI, W., NGUYEN, T., BIVONA, T. G., PHILIPS, M. R., DEVI, L. A. & IYENGAR, R. (2005) Cannabinoid receptor-induced neurite outgrowth is mediated by Rap1 activation through G(α)o/i-triggered proteasomal degradation of Rap1GAPII. *J. Biol. Chem.,* 280, 11413-11421.

JOSEPH, J., NIGGEMANN, B., ZAENKER, K. S. & ENTSCHLADEN, F. (2004) Anandamide is an endogenous inhibitor for the migration of tumor cells and T lymphocytes. *Cancer Immunol Immunother,* 53, 723-728.

JOY, E., WATSON, J. & BENSON, A. (1999) *Marijuana and Medicine: Assessing the Science Base,* Washington, DC, the National Academy of Science Chapter 2, p. 33-82.

JUNG, J., HWANG, S. W., KWAK, J., LEE, S.-Y., KANG, C.-J., KIM, W. B., KIM, D. & OH, U. (1999) Capsaicin binds to the intracellular domain of the capsaicin-activated ion channel. *J. Neurosci.,* 19, 529-538.

KAMEI, J., MIZOGUCHI, H., NARITA, M. & TSENG, L. F. (2001a) Therapeutic potential of PKC inhibitors in painful diabetic neuropathy. *Expert Opinion on Investigational Drugs,* 10, 1653-1664.

KAMEI, J., ZUSHIDA, K., MORITA, K., SASAKI, M. & TANAKA, S.-I. (2001b) Role of vanilloid VR1 receptor in thermal allodynia and hyperalgesia in diabetic mice. *European Journal of Pharmacology,* 422, 83-86.

KARASU, C., DEWHURST, M., STEVENS, E. J. & TOMLINSON, D. R. (1995) Effects of anti-oxidant treatment on sciatic nerve dysfunction in streptozotocin-diabetic rats; comparison with essential fatty acids. *Diabetologia,* 38, 129-134.

KARST, M., SALIM, K., BURSTEIN, S., CONRAD, I., HOY, L., SCHNEIDER, U. (2003) Analgesic effect of the synthetic cannabinoid CT-3 on chronic neuropathic pain: a randomized controlled trial. *The journal of the American Medical Association,* 290, 1757-1762.

KASSERRA, C. E., HARRIS, P., STENTON, G. R., ABRAHAM, W. & LANGLANDS, J. M. (2004) IPL576,092, a novel anti-inflammatory compound, inhibits leukocyte infiltration and changes in lung function in response to allergen challenge. *Pulm Pharmacol Ther,* 17, 309-318.

KATONA, I., SPERLAGH, B., MAGLOCZKY, Z., SANTHA, E., KOFALVI, A., CZIRJAK, S., MACKIE, K., VIZI, E. S. & FREUND, T. F. (2000) GABAergic interneurons are the targets of cannabinoid actions in the human hippocampus. *Neuroscience,* 100, 797-804.

KAUR, N., LU, B., R. K. M., WARD, S. M. & HALVORSEN, S. W. (2005) Inducers of oxidative stress block ciliary neurotrophic factor activation of Jak/STAT signalling in neurons. *J Neurochem,* 92, 1521-1530.

KELLY, S. & CHAPMAN, V. (2001) Selective cannabinoid $CB_1$ receptor activation inhibits spinal nociceptive transmission in vivo. *J Neurophysiol,* 86, 3061-3064.

KELLY, S., JHAVERI, M. D., SAGAR, D. R., KENDALL, D. A. & CHAPMAN, V. (2003) Activation of peripheral cannabinoid $CB_1$ receptors inhibits mechanically evoked responses of spinal neurons in noninflamed rats and rats with hindpaw inflammation. *Eur J Neurosci,* 18, 2239-2243.

KENNEDY, J. M. & ZOCHODNE, D. W. (2005) Impaired peripheral nerve regeneration in diabetes mellitus. *Journal of the Peripheral Nervous System,* 10, 144-157.

KENNEDY, W. R., WENDELSCHAFER-CRABB, G. & JOHNSON, T. (1996) Quantitation of epidermal nerves in diabetic neuropathy. *Neurology,* 47, 1042-1048.

KHASABOVA, I. A., SIMONE, D. A. & SEYBOLD, V. S. (2002) Cannabinoids attenuate depolarization-dependent $Ca^{2+}$ influx in intermediate-size primary afferent neurons of adult rats. *Neuroscience,* 115, 613-625.

KING, H. & REWERS, M. (1993) Global estimates for prevalence of diabetes mellitus and impaired glucose tolerance in adults. WHO Ad Hoc Diabetes Reporting Group. *Diabetes Care,* 16, 157-177.

KOSHIMURA, K., TANAKA, J., MURAKAMI, Y., KATO, Y. (2002) Involvement of nitric oxide in glucose toxicity on differentiated PC12 cells: prevention of glucose toxicity by tetrahydrobiopterin, a cofactor for nitric oxide synthase. *Neurosci Res,* 43, 31-38.

KRESS, M., REEH, P. W. & VYKLICKY, L. (1997) An interaction of inflammatory mediators and protons in small diameter dorsal root ganglion neurons of the rat. *Neuroscience Letters,* 224, 37-40.

LALLOO, U. G., FOX, A. J., BELVISI, M. G., CHUNG, K. F. & BARNES, P. J. (1995) Capsazepine inhibits cough induced by capsaicin and citric acid but not by hypertonic saline in guinea pigs. *J Appl Physiol,* 79, 1082-1087.

LANDER, H. M., TAURAS, J. M., OGISTE, J. S., HORI, O., MOSS, R. A. & SCHMIDT, A. M. (1997) Activation of the receptor for advanced glycation end products triggers a p21ras-dependent mitogen-activated protein kinase pathway regulated by oxidant stress. *J Biol Chem,* 272, 17810-17814.

LANDSMAN, R. S., BURKEY, T. H., CONSROE, P., ROESKE, W. R. & YAMAMURA, H. I. (1997) SR141716A is an inverse agonist at the human cannabinoid $CB_1$ receptor. *European Journal of Pharmacology,* 334, R1-R2.

LAWSON, S.N. (2002) Phenotype and function of somatic primary afferent nociceptive neurones with C-, Adelta- or Aalpha/beta-fibres. *Exp Physiol,* 87, 239-244.

LE FOLL, B. & GOLDBERG, S. R. (2005) Cannabinoid $CB_1$ receptor antagonists as promising new medications for drug dependence. *J Pharmacol Exp Ther,* 312, 875-883.

LEE, J., KOO, N. & MIN, D. B. (2003) Reactive oxygen species, aging, and antioxidative nutraceuticals. *Comprehensive Reviews In Food Science And Food Safety,* 3, 21-33.

LEE, L. Y. & LUNDBERG, J. M. (1994) Capsazepine abolishes pulmonary chemoreflexes induced by capsaicin in anesthetized rats. *J Appl Physiol,* 76, 1848-1855.

LELKES, E., UNSWORTH, B. R. & LELKES, P. I. (2001) Reactive oxygen species, apoptosis and altered NGF-induced signalling in PC12 pheochromocytoma cells cultured in elevated glucose: an in vitro cellular model for diabetic neuropathy. *Neurotox Res.,* 3, 189-203.

LI, W., WALUS, L., RABACCHI, S. A., JIRIK, A., CHANG, E., SCHAUER, J., ZHENG, B. H., BENEDETTI, N. J., LIU, B. P., CHOI, E., WORLEY, D., SILVIAN, L., MO, W., MULLEN, C., YANG, W., STRITTMATTER, S. M., SAH, D. W. Y., PEPINSKY, B. & LEE, D. H. S. (2004) A neutralizing anti-Nogo66 receptor monoclonal antibody reverses inhibition of neurite outgrowth by central nervous system myelin. *J. Biol. Chem.,* 279, 43780-43788.

LI, Z. G., ZHANG, W. & SIMA, A. A. (2003) C-peptide enhances insulin-mediated cell growth and protection against high glucose-induced apoptosis in SH-SY5Y cells. *Diabetes Metab Res Rev,* 19, 375-385.

LICHTMAN, A. H., PEART, J., POKLIS, J. L., BRIDGEN, D. T., RAZDAN, R. K., WILSON, D. M., POKLIS, A., MENG, Y., BYRON, P. R. & MARTIN, B. R. (2000) Pharmacological evaluation of aerosolized cannabinoids in mice. *European Journal of Pharmacology,* 399, 141-149.

LI, H. L. & LIN, H. (1974) An Archaeological and Historical Account of Cannabis in China. *Econ. Botany* 28 (4), 437-448.

LOW, P. A., NICKANDER, K. K. & TRITSCHLER, H. J. (1997) The roles of oxidative stress and antioxidant treatment in experimental diabetic neuropathy. *Diabetes,* 46.

LUNN, C. A., FINE, J. S., ROJAS-TRIANA, A., JACKSON, J. V., FAN, X., KUNG, T. T., GONSIOREK, W., SCHWARZ, M. A., LAVEY, B., KOZLOWSKI, J. A., NARULA, S. K., LUNDELL, D. J., HIPKIN, R. W. & BOBER, L. A. (2006) A novel cannabinoid peripheral cannabinoid receptor-selective inverse agonist blocks leukocyte recruitment in vivo. *J Pharmacol Exp Ther,* 316, 780-788.

MA, W. & QUIRION, R. (2007) Inflammatory mediators modulating the transient receptor potential vanilloid 1 receptor: therapeutic targets to treat inflammatory and neuropathic pain. *Expert Opinion on Therapeutic Targets,* 11, 307-320.

MACKIE, K. & HILLE, B. (1992) Cannabinoids inhibit N-type calcium channels in neuroblastoma-glioma cells. *Proc Natl Acad Sci U S A,* 89(9), 3825-3829.

MACKIE, K., LAI, Y., WESTENBROEK, R. & MITCHELL, R. (1995) Cannabinoids activate an inwardly rectifying potassium conductance and inhibit Q-type calcium currents in AtT20 cells transfected with rat brain cannabinoid receptor. *J. Neurosci.,* 15, 6552-6561.

MAILLEUX, P. & VANDERHAEGHEN, J. J. (1992) Localization of cannabinoid receptor in the human developing and adult basal ganglia. Higher levels in the striatonigral neurons. *Neurosci Lett,* 148, 173-176.

MAILLEUX, P. & VANDERHAEGHEN, J. J. (1993) Glucocorticoid regulation of cannabinoid receptor messenger RNA levels in the rat caudate-putamen. An in situ hybridization study. *Neurosci Lett,* 156, 51-53.

MALONE, J. I., LOWITT, S., KORTHALS, J. K., SALEM, A. & MIRANDA, C. (1996) The effect of hyperglycemia on nerve conduction and structure is age dependent. *Diabetes,* v45, p209(7).

MARSH, S. J., STANSFELD, C. E., BROWN, D. A., DAVEY, R. & MCCARTHY, D. (1987) The mechanism of action of capsaicin on sensory C-type neurons and their axons in vitro. *Neuroscience,* 23, 275-289.

MARSICANO, G. & LUTZ, B. (1999) Expression of the cannabinoid receptor $CB_1$ in distinct neuronal subpopulations in the adult mouse forebrain. *Eur J Neurosci,* 11, 4213-4225.

MARSICANO, G., MOOSMANN, B., HERMANN, H., LUTZ, B. & BEHL, C. (2002) Neuroprotective properties of cannabinoids against oxidative stress: role of the cannabinoid receptor $CB_1$. *Journal of Neurochemistry,* 80, 448-456.

MARTIN, B. R., MECHOULAM, R. & RAZDAN, R. K. (1999) Discovery and characterization of endogenous cannabinoids. *Life Sci,* 65, 573-595.

MARTIN, W. J., HOHMANN, A. G. & WALKER, J. M. (1996) Suppression of noxious stimulus-evoked activity in the ventral posterolateral nucleus of the thalamus by a cannabinoid agonist: correlation between electrophysiological and antinociceptive effects. *J. Neurosci.,* 16, 6601-6611.

MARZ, P., OTTEN, U. & ROSE-JOHN, S. (1999) Neural activities of IL-6-type cytokines often depend on soluble cytokine receptors. *European Journal of Neuroscience,* 11, 2995-3004.

MATIAS, I., GONTHIER, M.-P., ORLANDO, P., MARTIADIS, V., DE PETROCELLIS, L., CERVINO, C., PETROSINO, S., HOAREAU, L., FESTY, F., PASQUALI, R., ROCHE, R., MAJ, M., PAGOTTO, U., MONTELEONE, P. & DI MARZO, V. (2006a) Regulation, function, and dysregulation of

endocannabinoids in models of adipose and β-pancreatic cells and in obesity and hyperglycemia. *J Clin Endocrinol Metab,* 91, 3171-3180.

MATIAS, I., WANG, J. W., MORIELLO, A. S., NIEVES, A., WOODWARD, D. F. & DI MARZO, V. (2006b) Changes in endocannabinoid and palmitoylethanolamide levels in eye tissues of patients with diabetic retinopathy and age-related macular degeneration. *Prostaglandins, Leukotrienes and Essential Fatty Acids,* 75, 413-418.

MATSUDA, L. A., LOLAIT, S. J., BROWNSTEIN, M. J., YOUNG, A. C. & BONNER, T. I. (1990) Structure of a cannabinoid receptor and functional expression of the cloned cDNA. 346, 561-564.

MCCROSKERY, S., CHAUDHRY, A., LIN, L. & DANIELS, M. P. (2006) Transmembrane agrin regulates filopodia in rat hippocampal neurons in culture. *Molecular and Cellular Neuroscience,* 33, 15-28.

MCHUGH, J. F. & MCHUGH, W. B. (2004) Diabetes and peripheral sensory neurons: what we don't know and how it can hurt us. *AACN Clin Issues. ,* 15, 136-149.

MCTERNAN, C. L., MCTERNAN, P. G., HARTE, A. L., LEVICK, P. L., BARNETT, A. H. & KUMAR, S. (2002) Resistin, central obesity, and type 2 diabetes. *The Lancet,* 359, 46-47.

MECHOULAM, R., PANIKASHVILI, D. & SHOHAMI, E. (2002) Cannabinoids and brain injury: therapeutic implications. *Trends in Molecular Medicine,* 8, 58-61.

MELTZER, H. Y., ARVANITIS, L., BAUER, D. & REIN, W. (2004) Placebo-controlled evaluation of four novel compounds for the treatment of schizophrenia and schizoaffective disorder. *Am J Psychiatry,* 161, 975-984.

METODIEWA, D. & KOSKA, C. (2000) Reactive oxygen species and reactive nitrogen species: relevance to cyto(neuro)toxic events and neurologic disorders. An overview. *Neurotox Res* 1, 197-233.

MICHAEL, M. D., KULKARNI, R. N., POSTIC, C., PREVIS, S. F., SHULMAN, G. I., MAGNUSON, M. A. & KAHN, C. R. (2000) Loss of insulin signalling in hepatocytes leads to severe insulin resistance and progressive hepatic dysfunction. *Mol Cell,* 6, 87-97.

MIKURIYA, T. H. (1969) Marijuana in medicine: past, present and future. *Calif Med,* 110, 34-40.

MILLNS, P. J., CHAPMAN, V. & KENDALL, D. A. (2001) Cannabinoid inhibition of the capsaicin-induced calcium response in rat dorsal root ganglion neurones. 132, 969-971.

MILLNS, P. J., CHIMENTI, M., ALI, N., RYLAND, E., DE LAGO, E., FERNANDEZ-RUIZ, J., CHAPMAN, V. & KENDALL, D. A. (2006) Effects of inhibition of fatty acid amide hydrolase vs. the anandamide membrane transporter on TRPV1-mediated calcium responses in adult DRG neurons; the role of CB receptors. *Eur J Neurosci,* 24, 3489-3495.

MITCHELL, V. A., ASLAN, S., SAFAEI, R. & VAUGHAN, C. W. (2005) Effect of the cannabinoid ajulemic acid on rat models of neuropathic and inflammatory pain. *Neuroscience Letters,* 382, 231-235.

MOLDRICH, G. & WENGER, T. (2000) Localization of the $CB_1$ cannabinoid receptor in the rat brain. An immunohistochemical study*. *Peptides,* 21, 1735-1742.

MOREAU, J. (1845) *Du Hachisch et de l'Alienation Mentale: Etudes Psychologiques,* Paris: Librarie de Fortin Mason (English edition: New York, Raven Press; 1972).

MOREIRA, F. A., AGUIAR, D. C. & GUIMARAES, F. S. (2007) Anxiolytic-like effect of cannabinoids injected into the rat dorsolateral periaqueductal gray. *Neuropharmacology,* 52, 958-965.

MORISSET, V., AHLUWALIA, J., NAGY, I. & URBAN, L. (2001) Possible mechanisms of cannabinoid-induced antinociception in the spinal cord. *Eur J Pharmacol,* 429, 93-100.

MUKHOPADHYAY, S., SHIM, J.-Y., ASSI, A.-A., NORFORD, D. & HOWLETT, A. C. (2002) $CB_1$ cannabinoid receptor-G protein association: a possible mechanism for differential signalling. *Chemistry and Physics of Lipids,* 121, 91-109.

MUNRO, S., THOMAS, K. L. & ABU-SHAAR, M. (1993) Molecular characterization of a peripheral receptor for cannabinoids. *Nature,* 365, 61-65.

NAGAYAMA, T., SINOR, A. D., SIMON, R. P., CHEN, J., GRAHAM, S. H., JIN, K. & GREENBERG, D. A. (1999) Cannabinoids and Neuroprotection in Global and Focal Cerebral Ischemia and in Neuronal Cultures. *J. Neurosci.,* 19, 2987-2995.

NEW, D. C. & WONG, Y. H. (2003) BML-190 and AM251 act as inverse agonists at the human cannabinoid $CB_2$ receptor: signalling via cAMP and inositol phosphates. *FEBS Letters,* 536, 157-160.

NICOL, G. D., LOPSHIRE, J. C. & PAFFORD, C. M. (1997) Tumor necrosis factor enhances the capsaicin sensitivity of rat sensory neurons. *J. Neurosci.,* 17, 975-982.

NUMAZAKI, M., TOMINAGA, T., TOYOOKA, H. & TOMINAGA, M. (2002) Direct phosphorylation of capsaicin receptor vr1 by protein kinase cepsilon and identification of two target serine residues. *J. Biol. Chem.,* 277, 13375-13378.

OBARA, Y., LABUDDA, K., DILLON, T. J. & STORK, P. J. S. (2004) PKA phosphorylation of Src mediates Rap1 activation in NGF and cAMP signalling in PC12 cells. *Journal of Cell Science,* 117, 6085-6094.

OHSAWA, M. & KAMEI, J. (1999a) Possible involvement of spinal protein kinase C in thermal allodynia and hyperalgesia in diabetic mice. *European Journal of Pharmacology,* 372, 221-228.

OHSAWA, M. & KAMEI, J. (1999b) Role of intracellular calcium in thermal allodynia and hyperalgesia in diabetic mice. *Brain Research,* 833, 278-281.

OHUCHI, T., MARUOKA, S., SAKUDO, A. & ARAI, T. (2002) Assay-based quantitative analysis of PC12 cell differentiation. *Journal of Neuroscience Methods,* 118, 1-8.

ONG, W. Y. & MACKIE, K. (1999) A light and electron microscopic study of the $CB_1$ cannabinoid receptor in primate brain. *Neuroscience,* 92, 1177-1191.

ORTIZ, A., ZIYADEH, F. N. & NEILSON, E. G. (1997) Expression of apoptosis-regulatory genes in renal proximal tubular epithelial cells exposed to high ambient glucose and in diabetic kidneys. *J Investig Med,* 45, 50-56.

OSHITA, K., INOUE, A., TANG, H.-B., NAKATA, Y., KAWAMOTO, M., YUGE, O. & YUGE, O. (2005) $CB_1$ cannabinoid receptor stimulation modulates transient receptor potential vanilloid receptor 1 activities in calcium influx and substance P Release in cultured rat dorsal root ganglion cells. *Journal of Pharmacological Sciences,* 97, 377-385.

OTTEN, U., MARZ, P., HEESE, K., HOCK, C., KUNZ, D. & ROSE-JOHN, S. (2000) Cytokines and neurotrophins interact in normal and diseased states. *Ann NY Acad Sci,* 917, 322-330.

PACHER, P., BATKAI, S. & KUNOS, G. (2006) The endocannabinoid system as an emerging target of pharmacotherapy. *Pharmacol Rev,* 58, 389-462.

PASCHEN, W., MENGESDORF, T., ALTHAUSEN, S. & HOTOP, S. (2001) Peroxidative stress selectively down-regulates the neuronal stress response activated under conditions of endoplasmic reticulum dysfunction. *J Neurochem,* 76, 1916–1924.

PATWARDHAN, A. M., JESKE, N. A., PRICE, T. J., GAMPER, N., AKOPIAN, A. N. & HARGREAVES, K. M. (2006) The cannabinoid WIN 55,212-2 inhibits transient receptor potential vanilloid 1 (TRPV1) and evokes peripheral

antihyperalgesia via calcineurin. *Proceedings of the National Academy of Sciences,* 103, 11393-11398.

PERRAS, C. (2005) Sativex for the management of multiple sclerosis symptoms. *Issues Emerg Health Technol*, 1-4.

PERTWEE, R. G. (1988) The central neuropharmacology of psychotropic cannabinoids. *Pharmacol Ther,* 36, 189-261.

PERTWEE, R. G., GIBSON, T. M., STEVENSON, L. A., ROSS, R. A., BANNER, W. K., SAHA, B., RAZDAN, R. K. & MARTIN, B. R. (2000) O-1057, a potent water-soluble cannabinoid receptor agonist with antinociceptive properties. *Br J Pharmacol,* 129, 1577-1584.

PIERCE, K. L., LUTTRELL, L. M. & LEFKOWITZ, R. J. (2001) New mechanisms in heptahelical receptor signalling to mitogen activated protein kinase cascades. *Oncogene,* 20, 1532-1539.

PIPER, A. S., YEATS, J. C., BEVAN, S. & DOCHERTY, R. J. (1999) A study of the voltage dependence of capsaicin-activated membrane currents in rat sensory neurones before and after acute desensitization. *J Physiol,* 518, 721-733.

PI-SUNYER, F. X., ARONNE, L. J., HESHMATI, H. M., DEVIN, J. & ROSENSTOCK, J. (2006) Effect of rimonabant, a cannabinoid-1 receptor blocker, on weight and cardiometabolic risk factors in overweight or obese patients: RIO-North America: a randomized controlled trial. *Jama,* 295, 761-775.

POP-BUSUI, R., KIRKWOOD, I., SCHMID, H., MARINESCU, V., SCHROEDER, J., LARKIN, D., YAMADA, E., RAFFEL, D. M. & STEVENS, M. J. (2004) Sympathetic dysfunction in type 1 diabetes: association with impaired myocardial blood flow reserve and diastolic dysfunction. *J Am Coll Cardiol. ,* 44, 2368-2374.

PORCELLA, A., MAXIA, C., GESSA, G. L. & PANI, L. (2001) The synthetic cannabinoid WIN55212-2 decreases the intraocular pressure in human glaucoma resistant to conventional therapies. *Eur J Neurosci,* 13, 409-412.

PREMKUMAR, L. S. & AHERN, G. P. (2000) Induction of vanilloid receptor channel activity by protein kinase C. *Nature,* 408, 985-990.

PUGAZHENTHI, S., NESTEROVA, A., JAMBAL, P., AUDESIRK, G., KERN, M., CABELL, L., EVES, E., ROSNER, M., BOXER, L. & REUSCH, J. (2003) Oxidative stress-mediated down-regulation of bcl-2 promoter in hippocampal neurons. *J Neurochem* 84, 982-996.

PURVES, T., MIDDLEMAS, A., AGTHONG, S., JUDE, E. B., BOULTON, A. J. M., FERNYHOUGH, P. & TOMLINSON, D. R. (2001) A role for mitogen-activated protein kinases in the etiology of diabetic neuropathy. *FASEB J.,* 15, 2508-2514.

RALEVIC, V. (2003) Cannabinoid modulation of peripheral autonomic and sensory neurotransmission. *European Journal of Pharmacology,* 472, 1-21.

RASHID, M. H., INOUE, M., BAKOSHI, S. & UEDA, H. (2003) Increased expression of vanilloid receptor 1 on myelinated primary afferent neurons contributes to the antihyperalgesic effect of capsaicin cream in diabetic neuropathic pain in mice. *J Pharmacol Exp Ther,* 306, 709-717.

RATAN, R. R., MURPHY, T. H. & BARABAN, J. M. (1994) Oxidative stress induces apoptosis in embryonic cortical neurons. *Journal of Neurochemistry,* 62, 376-379.

REENSTRA, W. R., HUSNI, N., DITTMER, C., ORLOW, D. L. & BURAS, J. A. (1999) Skin dermal fibroblasts from donors with diabetes proliferate slower and express less growth factor receptors than non-diabetic controls. *Acad Emerg Med,* 6, 494.

RICHARDSON, J. D., AANONSEN, L. & HARGREAVES, K. M. (1997) SR 141716A, a cannabinoid receptor antagonist, produces hyperalgesia in untreated mice. *European Journal of Pharmacology,* 319, R3-R4.

RICHARDSON, J. D., AANONSEN, L. & HARGREAVES, K. M. (1998a) Antihyperalgesic effects of spinal cannabinoids. *European Journal of Pharmacology,* 345, 145-153.

RICHARDSON, J. D., KILO, S. & HARGREAVES, K. M. (1998b) Cannabinoids reduce hyperalgesia and inflammation via interaction with peripheral $CB_1$ receptors. *Pain,* 75, 111-119.

RICHFIELD, E. K. & HERKENHAM, M. (1994) Selective vulnerability in Huntington's disease: preferential loss of cannabinoid receptors in lateral globus pallidus. *Ann Neurol,* 36, 577-584.

ROMERO, F. J., MONSALVE, E., HERMENEGILDO, C., PUERTAS, F. J., HIGUERAS, V., NIES, E., SEGURA-AGUILAR, J. & ROMA, J. (1991) Oxygen toxicity in the nervous tissue: comparison of the antioxidant defense of rat brain and sciatic nerve. *Neurochem Res,* 16, 157-161.

ROTHWELL, N. J. & RELTON, J. K. (1993) Involvement of cytokines in acute neurodegeneration in the CNS. *Neuroscience & Biobehavioral Reviews,* 17, 217-227.

RUSSELL, J. W. & FELDMAN, E. L. (1999) Insulin-like growth factor-I prevents apoptosis in sympathetic neurons exposed to high glucose. *Horm Metab Res,* 31, 90-96.

RUSSELL, J. W., GOLOVOY, D., VINCENT, A. M., MAHENDRU, P. I. A., OLZMANN, J. A., MENTZER, A. & FELDMAN, E. L. (2002) High glucose-induced oxidative stress and mitochondrial dysfunction in neurons. *FASEB J.,* 16, 1738-1748.

RUSSELL, J. W., SULLIVAN, K. A., WINDEBANK, A. J., HERRMANN, D. N. & FELDMAN, E. L. (1999) Neurons undergo apoptosis in animal and cell culture models of diabetes. *Neurobiology of Disease,* 6, 347-363.

RYBERG, E., LARSSON, N., SJOGREN, S., HJORTH, S., HERMANSSON, N. O., LEONOVA, J., ELEBRING, T., NILSSON, K., DRMOTA, T. & GREASLEY, P. J. (2007) The orphan receptor GPR55 is a novel cannabinoid receptor. *Br J Pharmacol,* 152, 1092-1101.

SAID, G. (2007) Diabetic neuropathy--a review. *Nat Clin Pract Neurol,* 3, 331-340.

SAID, G., SLAMA, G. & SELVA, J. (1983) Progressive centripetal degeneration of axons in small fibre diabetic polyneuropathy. *Brain,* 106 (Pt 4), 791-807.

SANCHEZ, J. F., KRAUSE, J. E. & CORTRIGHT, D. N. (2001) The distribution and regulation of vanilloid receptor VR1 and VR1 5' splice variant RNA expression in rat. *Neuroscience,* 107, 373-381.

SANGER, G. J. & ANDREWS, P. L. R. (2006) Treatment of nausea and vomiting: Gaps in our knowledge. *Autonomic Neuroscience,* 129, 3-16.

SARKER, K. P., OBARA, S., NAKATA, M., KITAJIMA, I. & MARUYAMA, I. (2000) Anandamide induces apoptosis of PC-12 cells: involvement of superoxide and caspase-3. *FEBS Letters,* 472, 39-44.

SCHEEN, A. J., FINER, N., HOLLANDER, P., JENSEN, M. D. & VAN GAAL, L. F. (2006) Efficacy and tolerability of rimonabant in overweight or obese patients with type 2 diabetes: a randomised controlled study. *The Lancet,* 368, 1660-1672.

SCHMEICHEL, A. M., SCHMELZER, J. D. & LOW, P. A. (2003) Oxidative injury and apoptosis of dorsal root ganglion neurons in chronic experimental diabetic neuropathy. *Diabetes,* 52, 165-171.

SEKI, N., SHIRASAKI, H., KIKUCHI, M. & HIMI, T. (2007) Capsaicin induces the production of IL-6 in human upper respiratory epithelial cells. *Life Sciences,* 80, 1592-1597.

SEMRA, Y. K., SMITH, N. C. E. & LINCOLN, J. (2004) Comparative effects of high glucose on different adult sympathetic neurons in culture. *Neuroreport.,* 15, 2321-2325.

SHARKEY, K. A., CRISTINO, L., OLAND, L. D., VAN SICKLE, M. D., STAROWICZ, K., PITTMAN, Q. J., GUGLIELMOTTI, V., DAVISON, J. S. & DI MARZO, V. (2007) Arvanil, anandamide and N-arachidonoyl-dopamine (NADA) inhibit emesis through cannabinoid $CB_1$ and vanilloid TRPV1 receptors in the ferret. *European Journal of Neuroscience,* 25, 2773-2782.

SHEEHAN, J., EISCHEID, A., SAUNDERS, R., POURATIAN, N. & POURATIAN, N. (2006) Potentiation of neurite outgrowth and reduction of apoptosis by immunosuppressive agents: implications for neuronal injury and transplantation. *Neurosurgical focus,* 20, E9.

SHEN, M. & THAYER, S. A. (1998) The cannabinoid agonist Win55,212-2 inhibits calcium channels by receptor-mediated and direct pathways in cultured rat hippocampal neurons. *Brain Research,* 783, 77-84.

SHEU, M. L., HO, F. M., YANG, R. S., CHAO, K. F., LIN, W. W., LIN-SHIAU, S. Y. & LIU, S.-H. (2005) High glucose induces human endothelial cell apoptosis through a phosphoinositide 3-kinase-regulated cyclooxygenase-2 pathway. *Arterioscler Thromb Vasc Biol,* 25, 539-545.

SHIN, E.-Y., LEE, C.-S., CHO, T. G., KIM, Y. G., SONG, S., JUHNN, Y.-S., PARK, S. C., MANSER, E. & KIM, E.-G. (2006) βPak-interacting exchange factor-mediated Rac1 activation requires smgGDS guanine nucleotide exchange factor in basic fibroblast growth factor-induced neurite outgrowth. *J. Biol. Chem.,* 281, 35954-35964.

SHINDO H., THOMAS T.P., LARKIN D.D., KARIHALOO A.K., INADA H., ONAYA T., STEVENS M.J. & GREENE D.A. (1996) Modulation of basal nitric

oxide-dependent cyclic-GMP production by ambient glucose, myo-inositol, and protein kinase C in SH-SY5Y human neuroblastoma cells. *J Clin Invest* 97,736-745.

SHIRE, D., CALANDRA, B., RINALDI-CARMONA, M., OUSTRIC, D., PESSEGUE, B., BONNIN-CABANNE, O., LE FUR, G., CAPUT, D. & FERRARA, P. (1996a) Molecular cloning, expression and function of the murine $CB_2$ peripheral cannabinoid receptor. *Biochimica et Biophysica Acta (BBA) - Gene Structure and Expression,* 1307, 132-136.

SHOWALTER, V. M., COMPTON, D. R., MARTIN, B. R. & ABOOD, M. E. (1996) Evaluation of binding in a transfected cell line expressing a peripheral cannabinoid receptor ($CB_2$): identification of cannabinoid receptor subtype selective ligands. *J Pharmacol Exp Ther,* 278, 989-999.

SIC L. CHAN, M. P. M. (1999) Caspase and calpain substrates: Roles in synaptic plasticity and cell death. *Journal of Neuroscience Research,* 58, 167-190.

SIEGLING, A., HOFMANN, H. A., DENZER, D., MAULER, F. & DE VRY, J. (2001) Cannabinoid CB(1) receptor upregulation in a rat model of chronic neuropathic pain. *Eur J Pharmacol,* 415, R5-R7.

SIEMIONOW, M. & DEMIR, Y. (2004) Diabetic neuropathy: pathogenesis and treatment. *J Reconstr Microsurg. ,* 20, 241-252.

SILVERDALE, M. A., MCGUIRE, S., MCINNES, A., CROSSMAN, A. R. & BROTCHIE, J. M. (2001) Striatal cannabinoid $CB_1$ receptor mRNA expression is decreased in the reserpine-treated rat model of Parkinson's disease. *Experimental Neurology,* 169, 400-406.

SIMA, A. A. F. (2003) New insights into the metabolic and molecular basis for diabetic neuropathy. *Cellular and Molecular Life Sciences (CMLS),* 60, 2445-2464.

SINK, K. S., VEMURI, V. K., OLSZEWSKA, T., MAKRIYANNIS, A. & SALAMONE, J. D. (2008) Cannabinoid $CB_1$ antagonists and dopamine antagonists produce different effects on a task involving response allocation and effort-related choice in food-seeking behavior. *Psychopharmacology (Berl)*, 196, 565-574.

SKUNDRIC, D. F. & LISAK, R. P. (2003) Role of neuropoietic cytokines in development and progression of diabetic polyneuropathy: from glucose metabolism to neurodegeneration. *Exp Diabesity Res.,* 4, 303-312.

SMITH, P. F. (2002) Cannabinoids in the treatment of pain and spasticity in multiple sclerosis. *Curr Opin Investig Drugs,* 3, 859-864.

SMITH, P. J. & MCQUEEN, D. S. (2001) Anandamide induces cardiovascular and respiratory reflexes via vasosensory nerves in the anaesthetized rat. *Br J Pharmacol,* 134, 655-663.

SODERSTROM, K. & JOHNSON, F. (2000) $CB_1$ cannabinoid receptor expression in brain regions associated with zebra finch song control. *Brain Res,* 857, 151-157.

SOMEYA, A., KUNIEDA, K., AKIYAMA, N., HIRABAYASHI, T., HORIE, S. & MURAYAMA, T. (2004) Expression of vanilloid VR1 receptor in PC12 cells. *Neurochemistry International,* 45, 1005-1010.

SOTELO, J. R., HORIE, H., ITO, S., BENECH, C., SANGO, K. & TAKENAKA, T. (1991) An in vitro model to study diabetic neuropathy. *Neuroscience Letters,* 129, 91-94.

SRIVASTAVA, A. K. (2002) High glucose-induced activation of protein kinase signalling pathways in vascular smooth muscle cells: a potential role in the pathogenesis of vascular dysfunction in diabetes (review). *Int J Mol Med,* 9, 85-89.

STAMER, W. D., GOLIGHTLY, S. F., HOSOHATA, Y., RYAN, E. P., PORTER, A. C., VARGA, E., NOECKER, R. J., FELDER, C. C. & YAMAMURA, H. I.

(2001) Cannabinoid CB(1) receptor expression, activation and detection of endogenous ligand in trabecular meshwork and ciliary process tissues. *Eur J Pharmacol,* 431, 277-286.

STANDER, S., SCHMELZ, M., METZE, D., LUGER, T. & RUKWIED, R. (2005) Distribution of cannabinoid receptor 1 ($CB_1$) and 2 ($CB_2$) on sensory nerve fibers and adnexal structures in human skin. *Journal of Dermatological Science,* 38, 177-188.

STANSBERRY, K. B., PEPPARD, H. R., BABYAK, L. M., POPP, G., MCNITT, P. M. & VINIK, A. I. (1999) Primary nociceptive afferents mediate the blood flow dysfunction in non-glabrous (hairy) skin of type 2 diabetes: a new model for the pathogenesis of microvascular dysfunction. *Diabetes Care,* 22, 1549-1554.

STEINER, H., BONNER, T. I., ZIMMER, A. M., KITAI, S. T. & ZIMMER, A. (1999) Altered gene expression in striatal projection neurons in $CB_1$ cannabinoid receptor knockout mice. *Proc Natl Acad Sci U S A,* 96, 5786-5790.

STRANGMAN, N. M., PATRICK, S. L., HOHMANN, A. G., TSOU, K. & WALKER, J. M. (1998) Evidence for a role of endogenous cannabinoids in the modulation of acute and tonic pain sensitivity. *Brain Research,* 813, 323-328.

STRITTMATTER, S. M. & FISHMAN, M. C. (1991) The neuronal growth cone as a specialized transduction system. *Bioessays,* 13, 127-134.

STRITTMATTER, S. M., FISHMAN, M. C. & ZHU, X. P. (1994) Activated mutants of the alpha subunit of G(o) promote an increased number of neurites per cell. *J. Neurosci.,* 14, 2327-2338.

STRITTMATTER, S. M., VALENZUELA, D., KENNEDY, T. E., NEER, E. J. & FISHMAN, M. C. (1990) Go is a major growth cone protein subject to regulation by GAP-43. *Nature,* 344, 836-841.

STUMVOLL, M., GOLDSTEIN, B. J. & VAN HAEFTEN, T. W. (2005) Type 2 diabetes: principles of pathogenesis and therapy. *The Lancet,* 365, 1333-1346.

SUGIURA, T., TOMINAGA, M., KATSUYA, H. & MIZUMURA, K. (2002) Bradykinin lowers the threshold temperature for heat activation of vanilloid receptor 1. *J Neurophysiol,* 88, 544-548.

SULLIVAN, K. A. & FELDMAN, E. L. (2005) New developments in diabetic neuropathy. *Curr Opin Neurol.,*18, 586-590.

SUN, Y., ALEXANDER, S. P. H., GARLE, M. J., GIBSON, C. L., HEWITT, K., MURPHY, S. P., KENDALL, D. A. & BENNETT, A. J. (2007) Cannabinoid activation of PPAR[alpha]; a novel neuroprotective mechanism. *Br J Pharmacol,* 152, 734-743.

SZALLASI, A. & BLUMBERG, P. M. (1990) Specific binding of resiniferatoxin, an ultrapotent capsaicin analog, by dorsal root anglion membranes. *Brain Research,* 524, 106-111.

SZOLCSANYI, J. (1977) A pharmacological approach to elucidation of the role of different nerve fibres and receptor endings in mediation of pain. *J Physiol (Paris),* 73, 251-259.

SZOLCSANYI, J. & JANCSO-GABOR, A. (1976) Sensory effects of capsaicin congeners. Part II: Importance of chemical structure and pungency in desensitizing activity of capsaicin-type compounds. *Arzneimittelforschung,* 26, 33-37.

SZOLCSANYI, J., JANCSO-GABOR, A. & JOO, F. (1975) Functional and fine structural characteristics of the sensory neuron blocking effect of capsaicin. *Naunyn Schmiedebergs Arch Pharmacol,* 287, 157-169.

TAGA, T. & KISHIMOTO, T. (1997) Gp130 and the interleukin-6 family of cytokines. *Annual Review of Immunology,* 15, 797-819.

TAMURA, S., MORIKAWA, Y., MIYAJIMA, A. & SENBA, E. (2003) Expression of oncostatin M receptor beta in a specific subset of nociceptive sensory neurons. *European Journal of Neuroscience,* 17, 2287-2298.

TARGHER, G., ZENARI, L., BERTOLINI, L., MUGGEO, M. & ZOPPINI, G. (2001) Elevated levels of interleukin-6 in young adults with type 1 diabetes without clinical evidence of microvascular and macrovascular complications. *Diabetes Care,* 24, 956-957.

TAYLOR, D. C., PIERAU, F. K. & SZOLCSANYI, J. (1985) Capsaicin-induced inhibition of axoplasmic transport is prevented by nerve growth factor. *Cell Tissue Res,* 240, 569-573.

THORNALLEY, P. J. (2002) Glycation in diabetic neuropathy: characteristics, consequences, causes, and therapeutic options. *Int Rev Neurobiol,* 50, 37-57.

TOTH, C., BRUSSEE, V., CHENG, C. & ZOCHODNE, D. W. (2004) Diabetes mellitus and the sensory neuron. *Journal of Neuropathology and Experimental Neurology,* 63, 561-573.

TOUW, M. (1981) The religious and medicinal uses of Cannabis in China, India and Tibet. *J Psychoactive Drugs,* 13, 23-34.

TSOU, K., BROWN, S., SANUDO-PENA, M. C., MACKIE, K. & WALKER, J. M. (1997) Immunohistochemical distribution of cannabinoid $CB_1$ receptors in the rat central nervous system. *Neuroscience,* 83, 393-411.

TSOU, K., LOWITZ, K. A., HOHMANN, A. G., MARTIN, W. J., HATHAWAY, C. B., BEREITER, D. A. & WALKER, J. M. (1996) Suppression of noxious stimulus-evoked expression of fos protein-like immunoreactivity in rat spinal cord by a selective cannabinoid agonist. *Neuroscience,* 70, 791-798.

TWITCHELL, W., BROWN, S. & MACKIE, K. (1997) Cannabinoids Inhibit N- and P/Q-Type Calcium Channels in Cultured Rat Hippocampal Neurons. *J Neurophysiol,* 78, 43-50.

UEDA, H., HOWSON, J. M. M., ESPOSITO, L., HEWARD, J., SNOOK, CHAMBERLAIN, G., RAINBOW, D. B., HUNTER, K. M. D., SMITH, A. N., DI GENOVA, G., HERR, M. H., DAHLMAN, I., PAYNE, F., SMYTH, D., LOWE, C., TWELLS, R. C. J., HOWLETT, S., HEALY, B., NUTLAND, S., RANCE, H. E.,

EVERETT, V., SMINK, L. J., LAM, A. C., CORDELL, H. J., WALKER, N. M., BORDIN, C., HULME, J., MOTZO, C., CUCCA, F., HESS, J. F., METZKER, M. L., ROGERS, J., GREGORY, S., ALLAHABADIA, A., NITHIYANANTHAN, R., TUOMILEHTO-WOLF, E., TUOMILEHTO, J., BINGLEY, P., GILLESPIE, K. M., UNDLIEN, D. E., RONNINGEN, K. S., GUJA, C., IONESCU-TIRGOVISTE, C., SAVAGE, D. A., MAXWELL, A. P., CARSON, D. J., PATTERSON, C. C., FRANKLYN, J. A., CLAYTON, D. G., PETERSON, L. B., WICKER, L. S., TODD, J. A. & GOUGH, S. C. L. (2003) Association of the T-cell regulatory gene CTLA4 with susceptibility to autoimmune disease. *Nature,* 423, 506-511.

ULUGOL, A., KARADAG, H. C., IPCI, Y., TAMER, M. & DOKMECI, I. (2004) The effect of WIN 55,212-2, a cannabinoid agonist, on tactile allodynia in diabetic rats. *Neuroscience Letters,* 371, 167-170.

VALLANO, M. L., BEAMAN-HALL, C. M., BUI, C. J. & MIDDLETON, F. A. (2006) Depolarization and $Ca^{2+}$ downregulate $CB_1$ receptors and $CB_1$-mediated signalling in cerebellar granule neurons. *Neuropharmacology,* 50, 651-660.

VAN DAM, P. S., VAN ASBECK, B. S., ERKELENS, D. W., MARX, J. J., GISPEN, W. H. & BRAVENBOER, B. (1995) The role of oxidative stress in neuropathy and other diabetic complications. *Diabetes Metab Rev,* 11, 181-192.

VAN DER STELT, M. & DI MARZO, V. (2005) Cannabinoid receptors and their role in neuroprotection. *Neuromolecular Med* 7, 37-50.

VAN DER STELT, M., VELDHUIS, W. B., BAR, P. R., VELDINK, G. A., VLIEGENTHART, J. F. G. & NICOLAY, K. (2001) Neuroprotection by Δ9-tetrahydrocannabinol, the main active compound in marijuana, against ouabain-induced in vivo excitotoxicity. *J. Neurosci.,* 21, 6475-6479.

VAN DER STELT, M., VELDHUIS, W. B., MACCARRONE, M., BAR, P. R., NICOLAY, K., VELDINK, G. A., DI MARZO, V. & VLIEGENTHART, J. F. (2002) Acute neuronal injury, excitotoxicity, and the endocannabinoid system. *Mol Neurobiol,* 26, 317-346.

VAN GUILDER, G. P., HOETZER, G. L., GREINER, J. J., STAUFFER, B. L. & DESOUZA, C. A. (2006) Influence of metabolic syndrome on biomarkers of oxidative stress and inflammation in obese adults. *Obesity (Silver Spring),* 14, 2127-2131.

VANEY, C., HEINZEL-GUTENBRUNNER, M., JOBIN, P., TSCHOPP, F., GATTLEN, B., HAGEN, U., SCHNELLE, M. & REIF, M. (2004) Efficacy, safety and tolerability of an orally administered cannabis extract in the treatment of spasticity in patients with multiple sclerosis: a randomized, double-blind, placebo-controlled, crossover study. *Mult Scler,* 10, 417-424.

VELLANI, V., MAPPLEBECK, S., MORIONDO, A., DAVIS, J. B. & MCNAUGHTON, P. A. (2001) Protein kinase C activation potentiates gating of the vanilloid receptor VR1 by capsaicin, protons, heat and anandamide. *J Physiol,* 534, 813-825.

VERONESI, B., CARTER, J. D., DEVLIN, R. B., SIMON, S. A. & OORTGIESEN, M. (1999) Neuropeptides and capsaicin stimulate the release of inflammatory cytokines in a human bronchial epithelial cell line. *Neuropeptides,* 33, 447-456.

VINCENT, A. M., BROWNLEE, M. & RUSSELL, J. W. (2002) Oxidative stress and programmed cell death in diabetic neuropathy. *Ann NY Acad Sci,* 959, 368-383.

VINCENT, A. M., RUSSELL, J. W., LOW, P. & FELDMAN, E. L. (2004) Oxidative stress in the pathogenesis of diabetic neuropathy. *Endocr Rev,* 25, 612-628.

VINCENT, A. M., STEVENS, M. J., BACKUS, C., MCLEAN, L. L. & FELDMAN, E. L. (2005) Cell culture modeling to test therapies against hyperglycemia-mediated oxidative stress and injury. *Antioxid Redox Signal,* 7, 1494-1506.

TRISCHITTA, V., FRITTITTA, L., VIGNERI, R. (1997) Early molecular defects in human insulin resistance: studies in healthy subjects with low insulin sensitivity. *Diabetes / Metabolism Reviews,* 13, 147-162.

VINIK, A., ULLAL, J., PARSON, H. K. & CASELLINI, C. M. (2006) Diabetic neuropathies: clinical manifestations and current treatment options. *Nat Clin Pract Endocrinol Metab.* , 2, 269-281.

VINIK, A. I. (2004) Diabetic neuropathies. *Medical Clinics of North America,* 88, 947-999.

VINIK, A. I. (1999) Diabetic neuropathy: pathogenesis and therapy. *Am J Med,* 107, 17S-26S.

VIVIANI, B., BARTESAGHI, S., CORSINI, E., GALLI, C. L. & MARINOVICH, M. (2004) Cytokines role in neurodegenerative events. *Toxicology Letters,* 149, 85-89.

VOSSLER, M. R., YAO, H., YORK, R. D., PAN, M.-G., RIM, C. S. & STORK, P. J. S. (1997) cAMP activates MAP kinase and Elk-1 through a B-Raf- and Rap1-dependent pathway. *Cell,* 89, 73-82.

VRIENS, J., JANSSENS, A., PRENEN, J., NILIUS, B. & WONDERGEM, R. (2004) TRPV channels and modulation by hepatocyte growth factor/scatter factor in human hepatoblastoma (HepG2) cells. *Cell Calcium,* 36, 19-28.

WALKER, J. M. & HUANG, S. M. (2002) Cannabinoid analgesia. *Pharmacology & Therapeutics,* 95, 127-135.

WALKER, K., PERKINS, M. & DRAY, A. (1995) Kinins and kinin receptors in the nervous system. *Neurochemistry International,* 26, 1-16.

WALPOLE, C. & WRIGGLESWORTH, R. (1993) *Capsaicin in the study of pain (Wood JN ed),* San Diego, CA, Academic Press.

WARDLE, K. A., FUREY, G. & SANGER, G. J. (1996) Pharmacological characterization of the vanilloid receptor in the rat isolated vas deferens. *J Pharm Pharmacol,* 48, 285-291.

WARDLE, K. A., RANSON, J. & SANGER, G. J. (1997) Pharmacological characterization of the vanilloid receptor in the rat dorsal spinal cord. *Br J Pharmacol,* 121, 1012-1016.

WATSON, R. T. & PESSIN, J. E. (2001) Intracellular organization of insulin signalling and GLUT4 translocation. *Recent Prog Horm Res,* 56, 175-194.

WAUTIER, J. L., WAUTIER, M. P., SCHMIDT, A. M., ANDERSON, G. M., HORI, O., ZOUKOURIAN, C., CAPRON, L., CHAPPEY, O., YAN, S. D., BRETT, J. & ET AL. (1994) Advanced glycation end products (AGEs) on the surface of diabetic erythrocytes bind to the vessel wall via a specific receptor inducing oxidant stress in the vasculature: a link between surface-associated AGEs and diabetic complications. *Proc Natl Acad Sci U S A,* 91, 7742-7746.

WILD, S., ROGLIC, G., GREEN, A., SICREE, R. & KING, H. (2004) Global prevalence of diabetes: estimates for the year 2000 and projections for 2030. *Diabetes Care,* 27, 1047-1053.

WILKINSON, J. D. & WILLIAMSON, E. M. (2007) Cannabinoids inhibit human keratinocyte proliferation through a non-$CB_1$/$CB_2$ mechanism and have a potential therapeutic value in the treatment of psoriasis. *Journal of Dermatological Science,* 45, 87-92.

WILLIAMSON, E. M. & EVANS, F. J. (2000) Cannabinoids in clinical practice. *Drugs,* 60, 1303-1314.

WINTER, J. (1987) Characterization of capsaicin-sensitive neurones in adult rat dorsal root ganglion cultures. *Neuroscience Letters,* 80, 134-140.

WINTER, J., DRAY, A., WOOD, J. N., YEATS, J. C. & BEVAN, S. (1990) Cellular mechanism of action of resiniferatoxin: a potent sensory neuron excitotoxin. *Brain Research,* 520, 131-140.

WINTER, J., FORBES, C. A., STERNBERG, J. & LINDSAY, R. M. (1988) Nerve growth factor (NGF) regulates adult rat cultured dorsal root ganglion neuron responses to the excitotoxin capsaicin. *Neuron,* 1, 973-981.

WISE, L. E., IREDALE, P. A., STOKES, R. J. & LICHTMAN, A. H. (2007) Combination of rimonabant and donepezil prolongs spatial memory duration. *Neuropsychopharmacology,* 32, 1805-1812.

YAGIHASHI, S., YAMAGISHI, S.-I. & WADA, R. (2007) Pathology and pathogenetic mechanisms of diabetic neuropathy: correlation with clinical signs and symptoms. *Diabetes Res Clin Pract.* , 77 Suppl 1, S184-S189.

YOSHIHARA, S., MORIMOTO, H., OHORI, M., YAMADA, Y., ABE, T. & ARISAKA, O. (2006) Cannabinoid receptor agonists inhibit Ca(2+) influx to synaptosomes from rat brain. *Pharmacology,* 76, 157-162.

ZARUBA, R., EPSTEIN, P. & CARR, P. (2007) Hyperglycemia alters enzyme activity and cell number in spinal sensory ganglia. *Journal of Brachial Plexus and Peripheral Nerve Injury,* 2, 11.

ZHANG, F., HONG, S., STONE, V. & SMITH, P. J. (2007) Expression of cannabinoid $CB_1$ receptors in models of diabetic neuropathy. *J Pharmacol Exp Ther,* 323, 508-515.

ZIEGLER, D. (1999) Cardiovascular autonomic neuropathy: clinical manifestations and measurement. *Diabetes Rev.,* 7, 342-357.

ZHUANG, S., KITTLER, J., GRIGORENKO, E. V., KIRBY, M. T., SIM, L. J., HAMPSON, R. E., CHILDERS, S. R., DEADWYLER, S.A. (1998) Effects of long-term exposure to delta9-THC on expression of cannabinoid receptor ($CB_1$) mRNA in different rat brain regions. *Brain Res Mol Brain Res*, 62, 141-149.

ZOCHODNE, D. W., VERGE, V. M. K., CHENG, C., SUN, H. & JOHNSTON, J. (2001) Does diabetes target ganglion neurones?: Progressive sensory neurone involvement in long-term experimental diabetes. *Brain,* 124, 2319-2334.

ZUARDI, A. W. (2006) History of cannabis as a medicine: a review. *Revista Brasileira de Psiquiatria,* 28, 153-157.

ZYGMUNT, P. M., PETERSSON, J., ANDERSSON, D. A., CHUANG, H., SORGARD, M., DI MARZO, V., JULIUS, D. & HOGESTATT, E. D. (1999) Vanilloid receptors on sensory nerves mediate the vasodilator action of anandamide. *Nature,* 400**,** 452-457.

Campbell IW & Song S, Diabetes Overview, netdoctor. http://www.netdoctor.co.uk/diseases/facts/diabetes.htm (accessed at 27.09.2007)

NHS Diabetes foot guide http://www.diabetes.nhs.uk/downloads/NDST_Diabetic_Foot_Guide.pdf (accessed at 18.09.2007)

Mathur R., Diabetes Mellitus, in Medical Revision, eds: William C. Shiel. Medicinenet http://www.medicinenet.com/diabetes_mellitus/article.htm (accessed at 27.09.2007)

Votey S.R. & Anne L Peters. Diabetes Mellitus Type 1- A Review, 2005 http://www.emedicine.com/EMERG/topic133.htm (accessed at 27.09.2007)

Votey S.R. & Anne L Peters. Diabetes Mellitus Type 2- A Review, 2005 http://www.emedicine.com/EMERG/topic134.htm (accessed at 27.09.2007)

**APPENDIX**

PUBLICATIONS

ZHANG, F., HONG, S.G., STONE, V. & SMITH, P. J. W. (2007) Expression of cannabinoid $CB_1$ receptors in models of diabetic neuropathy. *Journal of Pharmacology and Experimental Therapeutics*, 323(2):508-515

ZHANG F., STONE V. & SMITH P. J. W. (2007) The protective effect of a cannabinoid $CB_1$ receptor agonist on neurite outgrowth in a cell model of diabetic neuropathy. Abstract C461, published in *the Proceeding of Life Sciences 2007*.

ZHANG F., STONE V. & SMITH P. J. W. (2007) Function of cannabinoid $CB_1$ receptors in cell culture models of diabetic neuropathy. Abstract published in *the Proceeding of Focused Meeting - 3rd European Workshop on Cannabinoid Research.*

ZHANG F., STONE V. & SMITH P. J. W. (2006) Expression of cannabinoid $CB_1$ receptors in cell culture models of diabetic neuropathy. Abstract A004.20, published in *FENS Forum Abstracts, vol. 3*.

# PUBLISHED PAPER(S) NOT INCLUDED WITH THESIS